
Photoresponsive Azobenzene/Cyclodextrin Supramolecular Systems: From UV-Light-Responsive to Visible-Light-Responsive

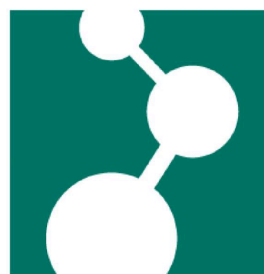
Dissertation

Zur Erlangung des Grades

Doktor der Naturwissenschaften

am Fachbereich Chemie, Pharmazie und Geowissenschaften

der Johannes Gutenberg-Universität Mainz



von

Dongsheng Wang

geboren in Sichuan, P.R. China

Mainz, März 2017

Tag der Prüfung: 19. April 2017

Dekan:

1. Berichterstatter:

2. Berichterstatter:

Dissertation an der Universität Mainz (D77)

Table of Contents

Abstract.....	1
Chapter 1 Introduction and Motivation.....	5
1.1 Supramolecules.....	5
1.2 Photoresponsive azobenzene/cyclodextrin supramolecular host-guest complex.....	6
1.2.1 Azobenzene.....	7
1.2.1.1 Isomerization mechanism.....	8
1.2.1.2 Molecular properties switching by light.....	10
1.2.2 Cyclodextrin.....	10
1.2.3 Azo/CD host-guest complexes.....	12
1.2.3.1 Hydrophobic effects.....	12
1.2.3.2 Association and dissociation of Azo/CD host-guest complexes.....	14
1.2.4 Host-guest interaction determinations.....	16
1.2.4.1 Benesi-Hildebrand method.....	16
1.2.4.2 Isothermal titration calorimetry.....	18
1.2.4.3 Atomic Force Microscopy.....	20
1.3 Applications based on Azo/CD host-guest complexes.....	22
1.3.1 Drug delivery systems.....	22
1.3.2 Hydrogel.....	25
1.3.3 Surface.....	28
1.3.4 Micro/nano-particles self-assembly.....	29
1.4 Visible/NIR-light-responsive Azobenzene.....	31

1.4.1 Upconversion.....	32
1.4.2 Two-photon process.....	33
1.4.3 Chemical modification.....	35
1.4.3.1 Electron donating.....	35
1.4.3.2 Electron withdrawing.....	37
1.4.3.3 BF ₂ -coordination.....	38
1.5 Motivation.....	39
1.5.1 Red-light-responsive Azo/CD host-guest complex.....	40
1.5.2 Red-light-responsive biomacromolecules and drug delivery systems.....	41
1.5.3 Further increasing molecular scale of Azo.....	42
1.5.4 Photoresponsive orthogonal supramolecular system.....	42
Chapter 2 Supramolecular Hydrogels Constructed by Red-Light-Responsive Host-Guest Interactions for Photo-Controlled Protein Release in Deep Tissue.....	59
2.1 Introduction.....	61
2.2 Photoresponse of tetra-ortho-methoxy-substituted azobenzene.....	64
2.3 Red-light-responsive supramolecular interactions.....	64
2.4 Red-light-responsive sol-gel transition systems.....	67
2.5 Red-light-controlled protein release.....	69
2.6 Conclusion.....	72
Supporting Information.....	74
Chapter 3 Red-light-responsive Supramolecular Valves for Photo-controlled Drug Release From Mesoporous Nanoparticles.....	103
3.1 Introduction.....	105
3.2 Photoresponsiveness of mAzo-Si.....	107
3.3 Preparation and characterization of MSNs, MSNs-Azo and MSNs-Azo/DOX/CD.....	108
3.4 Red-light-induced drug release.....	111

3.5 Conclusion.....	113
Supporting Information.....	117
Chapter 4 A Photoresponsive Orthogonal Supramolecular Complex based on Host-guest Interactions.....	129
4.1 Introduction.....	131
4.2 Photoisomerization of ipAzo-Py.....	133
4.3 Host-guest Interaction between ipAzo-Py and γ -CD.....	135
4.4 Photoresponsive orthogonal supramolecular system.....	137
4.5 Conclusions.....	140
Supporting Information.....	145
Chapter 5 Conclusion and Outlook.....	193
Acknowledgement.....	195
Curriculum vitae.....	197
Affidavit.....	199

Abstract

As a typical photoresponsive supramolecular host-guest pair, azobenzene (Azo) and cyclodextrin (CD) has been widely investigated with applications spanning biomedicine and shape memory or self-healing materials. In this system, *trans* Azo enters the hydrophobic cavity of α or β -CD and forms a strong 1:1 host-guest complex, which is dissembled after UV-light-induced *trans*-to-*cis* isomerization. However, the UV-light-responsiveness of the traditional Azo/CD host-guest complex limits its applications, especially on biomedical field, due to the harm and poor penetrability of UV light to human tissue.

Here, to solve the problem, we synthesized a tetra-ortho-methoxy-substituted Azo (mAzo), which showed *trans*-to-*cis* isomerization under red light irradiation, and *cis*-to-*trans* isomerization under blue light irradiation. A strong 1:1 host-guest complex was formed between *trans* mAzo and β -CD, while the host-guest interaction between *cis* mAzo and β -CD was weak. Based on the red-light-responsive mAzo/ β -CD host-guest complex, supramolecular hydrogels and mesoporous silica nanoparticles (MSNs) were prepared for the red-light-induced biomacromolecules and drug delivery in deep tissue. Red light irradiation induced a gel-to-sol transition of the hydrogel as a result of the disassembly of the mAzo/ β -CD complex, and further triggered the loaded protein release. Nanovalves constructed by mAzo/ β -CD host-guest complex were immobilized on MSNs surface, and red light could open the nanovalves and induced the loaded drug release. Both the delivery systems could be applied in deep tissue, and red light with extremely low intensity was needed to trigger the cargo release.

Afterward, another red-light-responsive Azo, tetra-ortho-isopropoxy-substituted Azo (ipAzo) was synthesized. A novel ipAzo/ γ -CD supramolecular host-guest complex was demonstrated. Opposite to the traditional Azo/ α -CD complex, γ -CD formed a strong 1:1 host-guest complex with *cis* ipAzo, rather than *trans* ipAzo. DFT calculated molecular models revealed that this behavior derives from a difference in the size of *trans* and *cis* ipAzo relative to γ -CD. By combining the red-light-responsive ipAzo/ γ -CD and UV-light-responsive Azo/ α -CD host-guest complexes, a photoresponsive orthogonal supramolecular system was demonstrated for the first time. This new discovery is helpful to be applied in the future to prepare photoresponsive orthogonal supramolecular materials, which are intelligent and multifunctional under complex stimuli.

Zusammenfassung

Als typisches photoreaktives supramolekulares Wirt-Gast-Paar wurde Azobenzol (Azo) und Cyclodextrin (CD) weitgehend mit Anwendungen untersucht, die Biomedizin und Formgedächtnis oder selbstheilende Materialien umfassen. In diesem System tritt *trans* Azo in den hydrophoben Hohlraum von α - oder β -CD ein und bildet einen starken 1:1-Wirt-Gast-Komplex, der nach UV-Licht-induzierter *trans*-zu-*cis*-Isomerisierung dissoziiert. Allerdings beschränkt die UV-Licht-Empfindlichkeit des traditionellen Azo/CD-Wirt-Gast-Komplexes seine Anwendungen, insbesondere im biomedizinischen Feld, da UV-Licht menschliches Gewebe schädigt und schlecht durchdringen kann.

Um dieses Problem zu lösen, haben wir ein tetra-ortho-methoxysubstituiertes Azo (mAzo) synthetisiert, das eine *trans*-zu-*cis*-Isomerisierung unter roter Lichtbestrahlung und eine *cis*-zu-*trans*-Isomerisierung unter blauer Lichtbestrahlung zeigte. Zwischen *trans* mAzo und β -CD wurde ein starker 1:1-Wirt-Gast-Komplex gebildet, während die Wirt-Gast-Interaktion zwischen *cis*-mAzo und β -CD schwach war. Basierend auf dem rotlichtempfindlichen mAzo/ β -CD-Wirt-Gast-Komplex wurden supramolekulare Hydrogele und mesoporöse Siliciumdioxid-Nanopartikel (MSNs) für die rotlichtinduzierte Biomakromolekül- und Arzneimittelabgabe in tiefem Gewebe hergestellt. Die Rotlichtbestrahlung induzierte einen Gel-zu-Sol-Übergang des Hydrogels als Folge der Demontage des mAzo/ β -CD-Komplexes und löste ferner die Proteinfreisetzung aus. Nanoventile, die durch den mAzo/ β -CD-Wirt-Gast-Komplex konstruiert wurden, wurden auf der MSNs-Oberfläche immobilisiert. Rotes Licht konnte die Nanoventile öffnen und die

Arzneimittelfreisetzung induzieren. Die Abgabesysteme könnten in tiefem Gewebe angewendet werden, und es wurde rotes Licht mit extrem geringer Intensität benutzt, um die Ladungsfreigabe auszulösen.

Danach wurde ein weiteres rotlichtempfindliches Azo, tetra-ortho-isopropoxysubstituiertes Azo (ipAzo) synthetisiert. Ein neuartiger ipAzo/ γ -CD-supramolekularer Wirt-Gast-Komplex wurde nachgewiesen. Gegenüber dem traditionellen Azo/ α -CD-Komplex bildete γ -CD einen starken 1:1-Wirt-Gast-Komplex mit *cis* ipAzo anstatt *trans* ipAzo. DFT-berechnete, molekulare Modelle zeigten, dass dieses Verhalten von einem Unterschied in der Größe von *trans* und *cis* ipAzo relativ zu γ -CD stammt. Durch die Kombination der auf den rotlichtempfindlichen ipAzo/ γ -CD und UV-lichtempfindlichen Azo/ α -CD-Wirt-Gast-Komplexe wurde erstmals ein lichtempfindliches, orthogonales, supramolekulares System nachgewiesen. Diese neue Entdeckung ist hilfreich, um in der Zukunft in lichtempfindlichen, orthogonalen, supramolekularen Materialien angewendet zu werden, die intelligent und multifunktionell unter komplexen Reizen sind.

Chapter 1

Introduction and Motivation

1.1 Supramolecules

Supramolecules, defined as the complexes formed in two or more molecules which are not covalently bonded ^[1], was firstly introduced by Karl Lothar Wolf in 1937 to describe hydrogen-bonded acetic acid dimers ^[2]. In the following 50 years, the supramolecular chemistry was gradually developed and the supramolecular structures were understood in gradually more detail, including the understanding of the hierarchical structure of proteins and the double helical structure of DNA. The importance of supramolecular chemistry was noticed by the Nobel Prize for Chemistry in 1987, which was awarded to Donald J. Cram, Jean-Marie Lehn and Charles J. Pedersen in recognition of their work in the area. From the 1990s, more and more researches turned the focus to design supramolecular systems and their functionality ^[3-10]. Till now, supramolecular materials have been widely studied and applied in various fields, including catalysis ^[11-13], medicine ^[14-17], soft materials ^[18-20], nanotechnology ^[21-25], shape-memory materials ^[26-28], surface functionalization ^[29-32] and polymerization ^[33-37].

The key of supramolecular chemistry is the intermolecular noncovalent interaction in the chemical species (building blocks), which is much weaker than the intramolecular covalent interaction. Therefore, the supramolecular structures are

always dynamic, and are strongly correlated with the environment. In fact, the formation of the supramolecular structure is the equilibrant state of the dynamic process. The dynamic process in supramolecular chemistry is more like a biological process. For now the complex self-assembly process has been recognized to play an important role in different elements of the origin of life ^[38].

Due to the dynamic property and weak interactions of supramolecules, the supramolecular systems are mostly stimuli-responsive (stimuli-responsibility is an important factor of life) ^[39-42]. It illustrates the supramolecular systems are potential to be applied for designing intelligent devices. Till now, the supramolecular systems responsive to various stimuli have been developed, including pH ^[43-47], heat ^[48-50], light ^[51-55], chemical ^[56-59], ultrasonic ^[60-63], and reduction/oxidation ^[64-67]. Supramolecular machines and nano-robots could be fabricated responsive to external stimulus, which won the nobel prize of 2016, indicating that supramolecules take a really important part in humans' life ^[68-70].

1.2 Photoresponsive azobenzene/cyclodextrin supramolecular host-guest complex

Light as a clean, efficient and precise external stimulus has been extensively used to control processes and functions in chemistry, biology and materials science. Photoresponsive supramolecular materials have been designed for various applications spinning biomedicine and shape memory or self-healing materials.

A chromophore responsive to external light irradiation is the key to design photoresponsive materials. Till now, various molecules have been reported for the photo-induced isomerization, cyclo-opening, and cyclo-addition (**Figure 1.1**), including azobenzene, coumarin, spiropyran and diarylethene ^[71-74]. Among these molecules, azobenzene meets the most investigation and application, especially in the field of photoresponsive supramolecular systems.

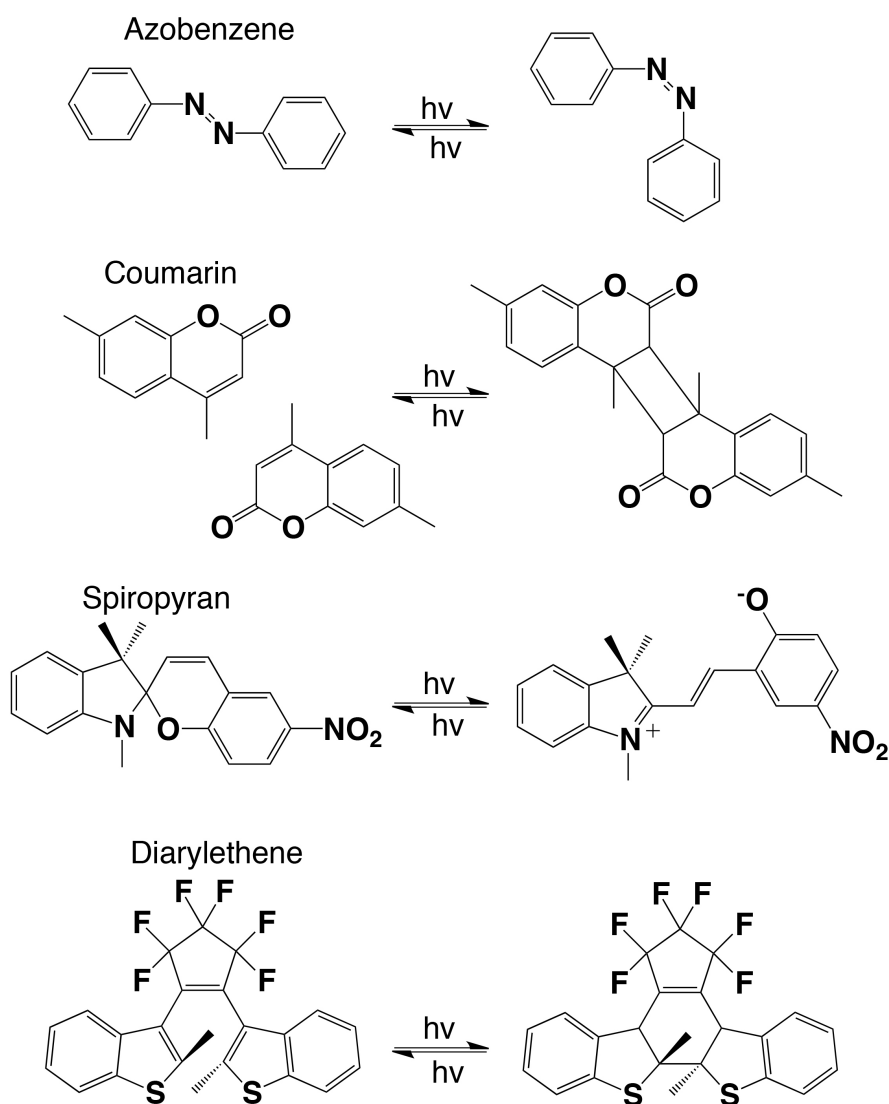


Figure 1.1 Photoresponsive molecules, including Azo, coumarin, spiropyran, and diarylethene.

1.2.1 Azobenzene

Azobenzene (Azo) is well-known for the *trans*-to-*cis* isomerization under UV light irradiation (320~380 nm), while the *cis*-to-*trans* isomerization could be induced by heating or visible light irradiation (430~530 nm) (**Figure 1.2**)^[75].

Azo was firstly introduced by Mitscherlich in 1834^[76], and investigated by Nobel in 1856 as “yellowish-red crystalline flakes”^[77]. As a well-known

photoresponsive molecule, the light-induced *trans*-to-*cis* isomerization of Azo was firstly reported by Hartley in 1937^[78]. Strong sunlight was used as the irradiation source by Hartley, and ~27% of *cis* Azo could be obtained. A much higher content (>95%) of *cis* Azo could be obtained by applying UV light (365 nm) as the triggered light source^[79]. The *cis* Azo could be isolated and form small, bright red crystals^[80]. The *trans* Azo, which is more thermal stable, could be obtained from *cis* Azo by heating or visible light irradiation.

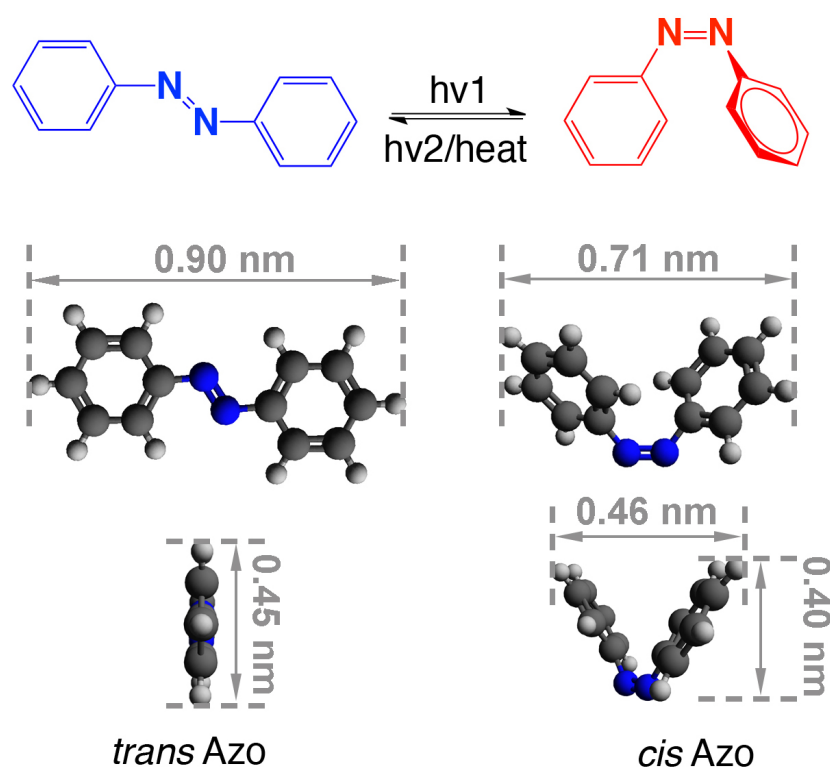


Figure 1.2 Molecular structure and DFT calculated model of *trans* and *cis* Azo.

1.2.1.1 Isomerization mechanism

There are four mechanisms have been supposed as possible pathways for Azo photoisomerization, including rotation, inversion, concerted inversion, and inversion-assisted rotation^[75] (**Figure 1.3**).

- (i) For the rotation mechanism, the N=N double bond is ruptured, which

allows free rotation of the N-N bond. The C-N-N-C dihedral angle is changed by rotating while the N-N-C angle remains $\sim 120^\circ$ [81].

- (ii) For the inversion mechanism, the N=N double bond is not broken. One N=N-C angle increases from $\sim 120^\circ$ to 180° while the other N=N-C angle remains $\sim 120^\circ$. The C-N=N-C dihedral angle remain fixed at 0° during the process.
- (iii) For the concerted inversion mechanism, both N=N-C bond increase to 180° and generate a linear transition state. The C-N=N-C dihedral angle remain 0° during the process.
- (iv) For the inversion-assisted rotation mechanism, the C-N=N-C dihedral angle and N=N-C angles change simultaneously.

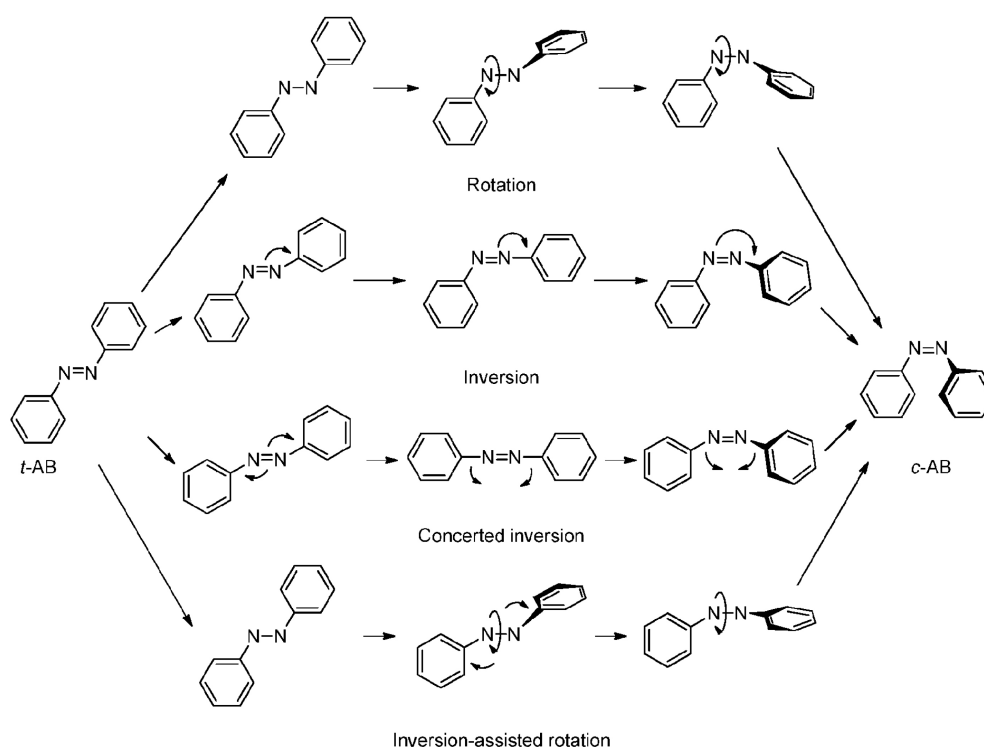


Figure 1.3 The supposed rotation, inversion, concerted inversion and inversion-assisted rotation pathways. Copyright 2011 Royal Society of Chemistry.

Relaxation from all these four transition states can generate either the *trans* or *cis* isomer. To explain experimental observations, multiple isomerization pathways are

often invoked^[82].

1.2.1.2 Molecular properties switching by light

The *trans* Azo showed a nearly planar structure with the dihedral angle between two benzene rings of $\sim 0^\circ$, the dipole moment of the *trans* Azo is therefore 0 D. After treating with UV light, the *cis* isomer shows non-planar structure with the dihedral angle between two benzene rings of $\sim 60^\circ$, which increases the dipole moment to 3 D.

Compare with *trans* Azo, which shows molecular length and width of 9.0 Å and 4.5 Å, *cis* Azo is more compact in 2D, with the molecular length and width of 7.1 Å and 4.0 Å. However, *cis* Azo extends on the 3rd dimension, due to the $\sim 60^\circ$ dihedral angle between the two benzene rings. The side view of *cis* Azo is like a closed equilateral triangle with two interlaced benzene rings. The thickness of *cis* Azo is calculated to be 4.6 Å (Figure 1.2).

1.2.2 Cyclodextrin

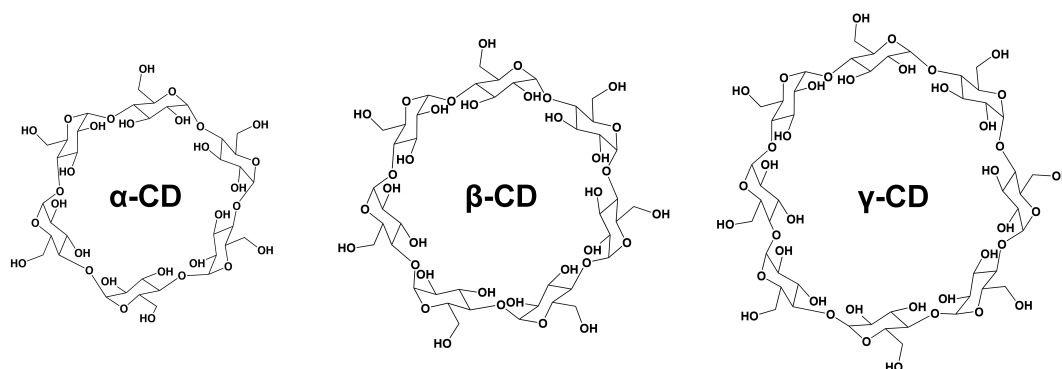


Figure 1.4 Molecular structures of α , β , and γ -CD.

Cyclodextrin (CD), also known as cycloamylose, cyclomaltose or Schardinger dextrin, is cyclic oligosaccharide composed of D-glucose units that are joined by α -1,4-glucosidic linkages^[83].

As a molecule has been known for over 120 years, CD was firstly found by the pharmacist and chemist A. Villiers in 1891 ^[84]. In the early 1890s, Villiers was investigating the degradation and reduction of carbohydrates under the action of ferments. Some unexpeted crystals were noticed, which were the first CD molecules. After several months research, Villiers described the chemical composition of the crystalline carbohydrate as a multiple of the formular $[(C_6H_{10}O_5)_2+3H_2O]$, and proposed the name “cellulosine” due to the similarities with cellulose ^[85]. By manipulating the experimental processes, Villiers obtained two distinct crystallized cellulosines, which might be α -CD and β -CD. The Austrian chemist and bacteriologist F. Schardinger took over Villiers’s work on CDs after he switching the focus to alkaloids. The first detailed preparation, separation and purification of the two cellulosines reported by Villiers were described between 1905 and 1911 ^[86-88]. The chemical behavior in the presence of alcohols, chloroform, ether, and iodine solutions were investigated during the same time. Schardinger is the first researcher to characterize and describe the fundamental properties of the two cellulosines, and he indeed became known as the “Founding Father” of cyclodextrin chemistry. He also hypothesized the molecular structure of the cellulosines were cyclic “polysaccharides”. In the year of 1911, Schardinger decided to call the cellulosines crystalline α -dextrin and crystalline β -dextrin, which are also called “Schardinger dextrans” in his honor ^[88].

The molecular structures of Schardinger dextrans were further investigated in 1930s, the German scientist K. J. Freudenberg investigated the glycosidic bonds rotation and reducing power of the Schardinger dextrin using rigid Kekulé models, and found that the dextrans and starch showed closely parallel rotation-time curves ^[89, 90]. While the rigid Kekulé models did not allow free roation of the individual bonds, Freudenberg hypothesized that Schardinger dextrans have a cyclic structure, which was demonstrated a few years later by him using optical activity data ^[91]. During the same period, Kratky, Schneidmesser and Borchert confirmed the cyclic structure of

Schardinger dextrans by X-ray crystallography ^[92, 93]. In 1948, a larger molecule γ -dextrin was discovered and characterized by Freudenberg ^[94].

The detail molecular structure of dextrans was further demonstrated by D. French using the X-ray diffraction technique and crystal density measurements ^[95]. He reported that Schardinger dextrans were cyclic oligosaccharides, formed from starch polysaccharide, and were nonreducing D-glucopyranosyl polymers containing 6, 7, or 8 monomers linked by α -1,4-glucosidic linkages (**Figure 1.4**).

In the late 1940s, F. Cramer began to study the inclusion properties of Schardinger dextrans. He was the first to use the word “cyclodextrins (CDs)” to define these molecules, which was even the title of his doctoral thesis (PhD in 1949 under the supervision of Freudenberg) ^[96].

Till now, CDs have been widely studied and applied in supramolecular chemistry, biomedicine, electrophoresis, and chromatography.

1.2.3 Azo/CD host-guest complexes

The CD structure can be seemed as a truncated cone in aqueous solution. The hydroxyl groups of the CDs are located at the outer surface of the molecules, which makes CDs water-soluble but simultaneously generates a relatively hydrophobic inner cavity. The outside-hydrophilic and inside-hydrophobic property makes CDs potential to be host molecules for some hydrophobic guest molecules. Hydrophobic molecules including Azo, adamantane, ferrocene, viologen and C_{60} are able to enter the hydrophobic cavity of CDs to form the host-guest complex ^[97-100]. Actually, the first host-guest complex between CD and hydrophobic guests was announced in 1952 by F. Cramer, which is between aromatic compounds and β -CD ^[101].

1.2.3.1 Hydrophobic effects

Hydrophobic effects are normally seemed as the driving force for the formation

of host-guest complexes between CDs and hydrophobic guests. Hydrophobic effects are occasionally mistaken for a force, and generally relate to the exclusion from polar solvents, particularly water in CD case, of large particles or molecules those are weakly solvated (e.g. via hydrogen bonds or dipolar interactions). Essentially, the water molecules are interacted strongly each other resulting in a natural agglomeration of other species (such as nonpolar organic molecules), as they are squeezed out of the way of the strong intersolvent interactions. This can produce effects resembling attraction between one organic molecule and another, although there are some other interactions between the organic molecules themselves, including van der Waals and π - π stacking attractions. Hydrophobic effects may be divided into two energetic components: enthalpic and entropic [102].

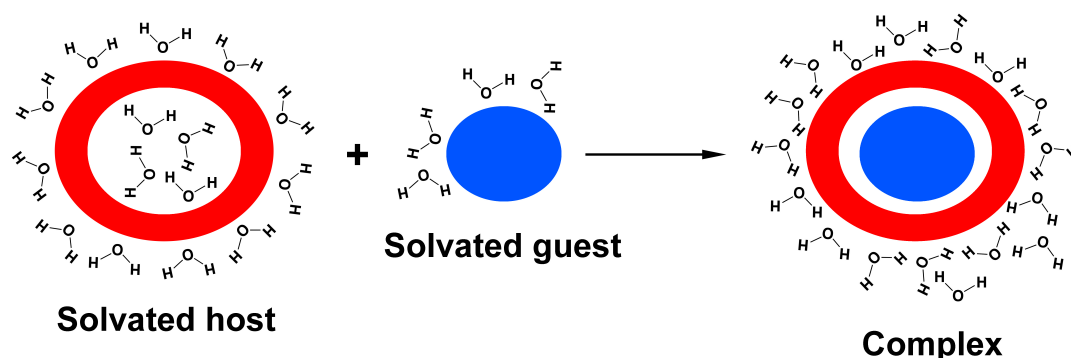


Figure 1.5 Hydrophobic binding of host and guest molecules in aqueous solution.

The enthalpic hydrophobic effect involves the stabilisation of water molecules driven from host molecule cavity upon guest binding. The host cavities are often hydrophobic (e.g. CD), the intracavity water cannot bind strongly with the host walls and is therefore of high energy. Upon release into the bulk solvent, the intracavity water molecules are stabilised by interactions with other water molecules.

The entropic hydrophobic effect arises from the fact that the presence of host and guest molecules in solution (often water) creates two "holes" in the structure of bulk water. Combining host and guest to form a complex results in less disruption to the solvent structure and hence an entropic gain (resulting in a decrease of overall free

energy) (Figure 1.5).

1.2.3.2 Association and dissociation of Azo/CD host-guest complexes

Photoresponsive Azo/CD host-guest complexes were firstly introduced by Osa's group in 1983^[103]. Azo could form host-guest complex with γ -CD in presence of some other guest molecules, including cyclodextranol, anisole, benzyl alcohol, (+) – fenchone, and (–) – borneol. However, for the very early Azo/ γ -CD host-guest system, light could not really control the assembly and disassembly of the complex. In 1991, after changing the host molecule to β -CD, Osa's group firstly reported the photoresponsive 1:1 Azo/ β -CD host-guest complex^[104]. Azo-modified- β -CD could form a supramolecular dimer based on the Azo/ β -CD complex, which dissociated into monomers after UV light irradiation, due to the weak interaction between *cis* Azo and β -CD. The photoresponsive Azo/ α -CD host-guest complex was demonstrated by Nakashima in 1997^[105], which was similar to the Azo/ β -CD complex.

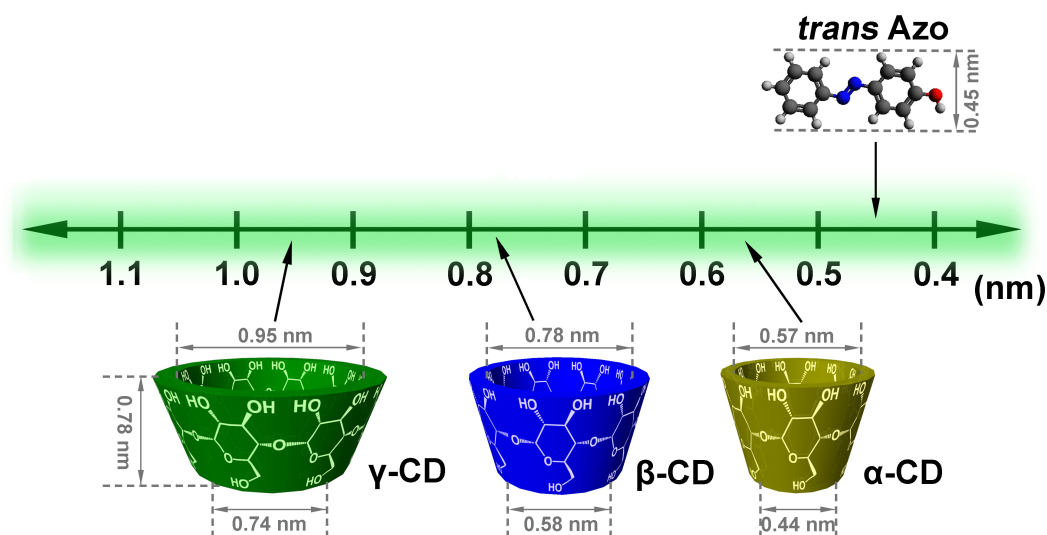


Figure 1.6 Molecular scale relationships between *trans* Azo and CDs. Dimension informations of CDs are from literatures^[83].

Actually, *trans* Azo is believed to enter the hydrophobic cavity of α or β -CD to form a strong 1:1 host-guest complex, while *cis* Azo slides out of the hydrophobic

cavity (**Figure 1.6**)^[106-108]. The host-guest interaction between Azo and CD is generally considered to be strong only in aqueous environment. The hydrophobic *trans* Azo is hidden in the hydrophobic CD cavity to minimize the system energy.

The formation of the Azo/CD host-guest complex is highly related to the molecular scale of Azo and CD. As mentioned before, α , β and γ -CD show different scales of the hydrophobic cavity due to the various repeated D-glucos units numbers. If the cavity is too small, the Azo molecule cannot enter deeply to form strong complex. In contrast, if the cavity is too large, although the Azo molecule can easily enter the hydrophobic cavity, it can also slide out easily, and strong host-guest complex can not form. For both *trans* and *cis* Azo, α , β and γ -CD are large enough. α , β and γ -CD show the same molecular height, which is 0.78 nm. For the γ -CD, both the min and max cavity diameter are larger than α and β -CD (**Figure 1.6**). While α and β -CD are slightly larger than *trans* Azo, γ -CD is too large for *trans* Azo. Actually, the *trans* Azo/ α -CD complex is reported to be stronger than *trans* Azo/ β -CD, due to the fact that α -CD cavity fits *trans* Azo better than β -CD.

After UV light irradiation, *cis* Azo is obtained, which slides out of the hydrophobic cavity of CD, and further induces the Azo/CD host-guest complex dissociation. There are two main reasons for the disassembly of the Azo/CD complex after treating with UV light:

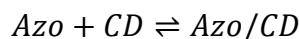
- (i) Compare with the *trans* Azo, *cis* Azo is more hydrophilic. The hydrophobic effect in Azo/CD system as the driving force is therefore weaker. The results make the *cis* Azo/CD complex unstable in the same environment, which is easily dissociated to the fragments.
- (ii) The molecular scale of *cis* Azo is different to *trans* Azo and does not fit the hydrophobic cavity. Compare with *trans* Azo, which is nearly planar structure, *cis* Azo shows the dihedral angle between two benzene rings of $\sim 60^\circ$. These induced geometric unfitting of *cis* Azo to the CD cavity. However, for now, the relationship between *cis* Azo and CD cavity (too

large or too small) are still in debating.

1.2.4 Host-guest interaction determinations

To determine how “strong” is the complex formed between Azo and CD, the host-guest interaction can be quantitatively investigated by measuring the binding constant (K_a).

For the Azo/CD host-guest systems, due to the known 1:1 stoichiometry, the equilibrium equation can be written as:



The K_a can be defined as:

$$K_a = \frac{[Azo/CD]_{eq}}{[Azo]_{eq}[CD]_{eq}}$$

where $[Azo]_{eq}$, $[CD]_{eq}$, and $[Azo/CD]_{eq}$ are the concentrations of Azo, CD, and Azo/CD complex when the system is in equilibrium.

Thermodynamically speaking, for the Azo and CD system, the overall Gibbs free energy decrease is favourable for the formation of Azo/CD host-guest complex. The change in Gibbs free energy, ΔG , is a function of the K_a ,

$$\Delta G = RT \ln K_a$$

where R is the gas constant, and T is the absolute temperature (in K).

The dependency of ΔG on the macroscopic terms of enthalpy, ΔH , and entropy, ΔS can be written as follows:

$$\Delta G = \Delta H - T\Delta S$$

Therefore, the K_a can also be determined through thermodynamic methods.

1.2.4.1 Benesi-Hildebrand method

As a mathematical approach for the determination of binding constant and

stoichiometry of weak complexes, the Benesi-Hildebrand method has been typically applied to reaction equilibria those form one-to-one complexes, such as charge-transfer complexes and host-guest complexes^[109-111].

This method was firstly introduced to measure the interaction between iodine and aromatic hydrocarbons in 1949^[112], while an UV/vis spectrophotometer was used. After more than half-century development, the Benesi-Hildebrand method has been widely applied to determine the binding constants of 1:1 host-guest systems, while UV/vis spectrophotometer, fluorescence spectrophotometer, and nuclear magnetic resonance (NMR) could be used for calculation^[113-116].

The theoretical foundation of this method is to assume that one of the reactants (host or guest) presents in an excess amount over the other reactant. For the Azo/CD system, when the system is determined by an UV/vis spectrophotometer, the observed absorbance is:

$$A_{obs} = A_{Azo} + A_{CD} + A_{Azo/CD}$$

Assume the initial concentration of CD is much larger than the initial concentration of Azo, the absorption from Azo should be therefore negligible:

$$A_{obs} = A_{CD} + A_{Azo/CD}$$

The difference of the absorbance before and after adding CD is:

$$\Delta A = A_{obs} - A_0 = A_{CD} + A_{Azo/CD} - A_{Azo_0} - A_{CD_0}$$

Using the Beer-Lambert law, The equation can be rewritten as:

$$\Delta A = \epsilon^{CD}[CD]b + \epsilon^{Azo/CD}[Azo/CD]b - \epsilon^{Azo}[Azo_0]b - \epsilon^{CD}[CD_0]b$$

Due to the previous assumption that $[CD_0] \gg [Azo_0]$, $[CD] = [CD_0]$ and $[Azo/CD] = [Azo_0]$ can be expected. Therefore, the equation can be rewritten as:

$$\Delta A = \Delta\epsilon[Azo/CD]b$$

where $\Delta\epsilon$ is the difference between $\epsilon_{Azo/CD}$ and ϵ_{Azo} .

The binding constant (K_a) could be written as:

$$K_a = \frac{[Azo/CD]}{\{[Azo_0] - [Azo/CD]\}[CD]}$$

Therefore, the equation can be rewritten as:

$$[Azo/CD] = \frac{K_a[Azo_0][CD_0]}{1 + K_a[CD_0]}$$

and

$$\Delta A = b\Delta\epsilon \frac{K_a[Azo_0][CD_0]}{1 + K_a[CD_0]}$$

The equation can be further rewritten as a double reciprocal form:

$$\frac{1}{\Delta A} = \frac{1}{bK_a\Delta\epsilon[Azo_0][CD_0]} + \frac{1}{b\Delta\epsilon[Azo_0]}$$

Therefore, by adding various amounts of CD in an Azo aqueous solution, the obtained plots can be fitted in straight line, and the K_a can be thus calculated.

Till now, the Benesi-Hildebrand method has been used by many groups to determine the host-guest interaction between Azo and CD. The results obtained from UV/vis spectra and NMR is similar (**Table 1.1**). The calculated binding constants between *trans* Azo and α -CD are much higher than those between *cis* Azo and α -CD [107, 117-120].

Table 1.1 Calculated binding constants between Azo and α -CD by Benesi-Hildebrand method via UV/vis spectrophotometer and NMR.

K_a (M^{-1})	UV/vis		NMR	
	<i>trans</i> Azo	<i>cis</i> Azo	<i>trans</i> Azo	<i>cis</i> Azo
α -CD	1.2×10^4	-	1.1×10^3	4.1

1.2.4.2 Isothermal titration calorimetry

Isothermal titration calorimetry (ITC) is used to determine the thermodynamic parameters (binding constant, enthalpy changes, entropy changes, and stoichiometry) of interactions between two or more molecules in solution [121].

For the ITC equipment, two identical cells made of highly efficient thermally conducting and chemically inert material are included, one is reference cell and the

other is sample cell. Temperature differences between the reference cell and sample cell are detected by sensitive thermopile/thermocouple circuits (**Figure 1.7**) ^[122]. During the measurement, one of the component solutions is titrating to the other component, and induces the temperature change in the sample cell. The heater in the reference cell then activates to make the reference cell temperature the same to the sample cell. Measurements consist of the time-dependent input of power required to maintain equal temperatures between the sample and reference cells.

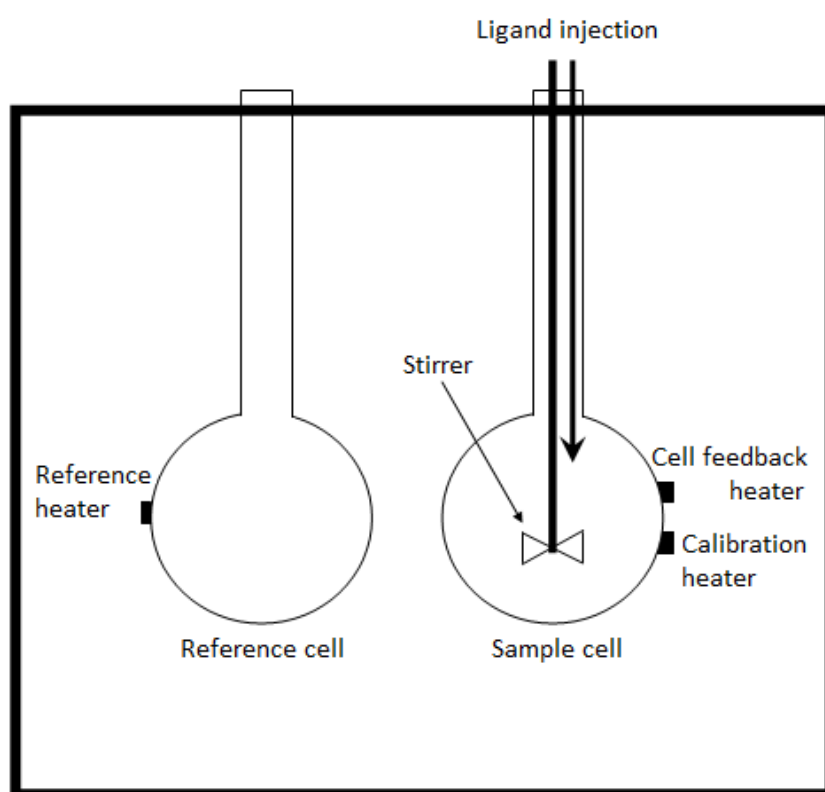


Figure 1.7 Working mechanism of ITC. Copyright www.wikipedia.org.

The heat transfer during the host-guest complex formation process can be therefore used to calculate the K_a between the host and guest molecules, according to the equations mentioned before (section 1.2.4).

There have been many examples to determine the host-guest interaction between Azo and CD by ITC, while the data are essentially similar to the results obtained by

Benesi-Hildebrand method. However, one thing should be concerned during the determination of host-guest interaction by ITC. Since the ITC measurement is based on thermal change, while the Azo molecule used is amphiphilic, the self-assembly of Azo in aqueous solution can affect the fitting data, which may cause the experimental error ^[123].

1.2.4.3 Atomic Force Microscopy

Compared with the Benesi-Hildebrand method and ITC, atomic force microscopy (AFM) could be seemed as a direct way to measure the interaction between host and guest molecules ^[124].

AFM or scanning-force microscopy (SFM) is a type of scanning probe microscopy, with a demonstrated resolution on the order of fractions of nanometer, more than 1000 times smaller than the optical diffraction limit. The surface information is gathered by “feeling” or “touching” the surface with a mechanical probe. After invented by IBM scientists in 1982, AFM obtained highly attention in the following 30 years for the surface imaging. The precursor to AFM, the scanning tunneling microscope, developed by G. Binnig and H. Rohrer in the early 1980s, won the Nobel Prize for Physics in 1986. The first experimental implementation of AFM was made by Binnig, Quate, and Gerber in the same year, and the first commercially available AFM was introduced in 1989.

The working mechanism of a typical AFM can be briefly described in **Figure 1.8**. While the tip on cantilever is scanning on sample surface, the cantilever can be displaced due to the interaction with the surface. The laser beam on the cantilever can be reflected to the photo detector (e.g. photodiode, linear position sensitive device, and array detector), which is used to detect the motion of the cantilever. The displacement of the cantilever induces the displacement of the laser beam reflection on the detector, which can therefore obtain the information on the sample surface.

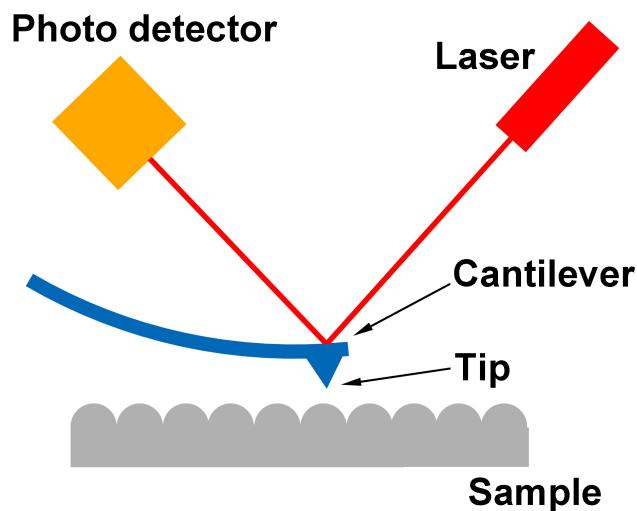


Figure 1.8 Working mechanism of AFM.

Besides imaging the surface there is another major application of AFM, force spectroscopy, which is also important for the host-guest interaction investigation ^[125, 126]. The force spectroscopy is a direct measurement of tip-sample interaction as a function of the gap between the tip and sample (the result is called a force-distance curve or force spectra). For the measurement, host (or guest) molecules are grafted onto flat substrate surface, while the other molecules are grafted onto the tip of AFM (**Figure 1.9**) ^[127]. The molecules on AFM tip are brought into contact with the grafted molecules on substrate surface, and the force spectra are measured during the detachment of the AFM tip from the surface. A force-distance profile interrelated to the host-guest interaction can be therefore obtained. However, it is difficult to control the grafted densities of the molecules on AFM tip and surface. Moreover, the AFM is easily affected by unspecific interactions. Therefore, this method is normally used in the multivalent binding situations.

For the host-guest interactions based on hydrophobic driving forces (like Azo/CD host-guest interaction), the force spectra are needed to be measured in water environment, which makes it even more difficult to determine the Azo/CD host-guest

interaction accurately. Moreover, the moving speed of AFM tip, the chain length between AFM tip and functional groups, and the surface morphology also affect the testing results. Therefore, there are still not many examples to investigate the host-guest interaction between Azo and CD by AFM. However, the totally different mechanism of the AFM method to Benesi-Hildebrand and ITC methods makes the AFM interesting and necessary for the host-guest interaction investigation.

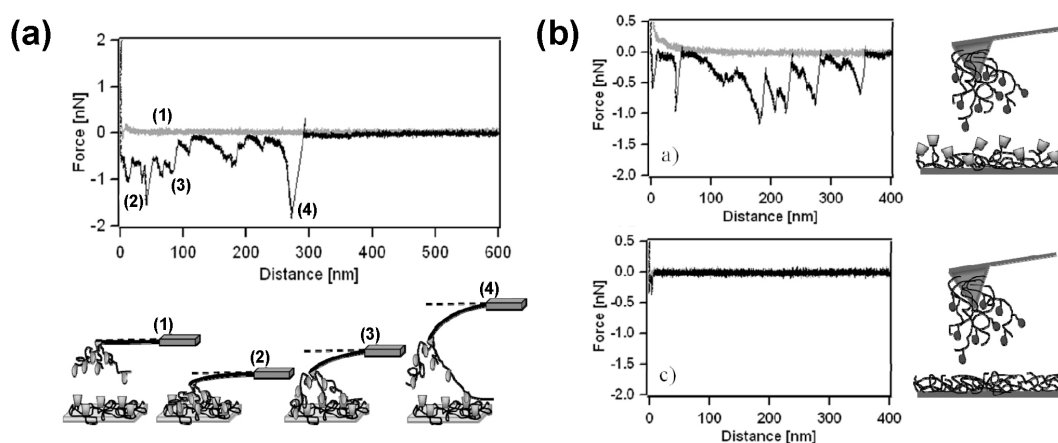


Figure 1.9 Force spectra measured by AFM can be used to determine the supramolecular interaction between host and guest molecules. (a) Guest molecules modified AFM tip is contacting the host molecules modified substrate surface, force spectra are recorded in different processes; (b) Force spectra obtained between modified AFM tip and modified (up) or unmodified (down) substrate surface. Copyright 2004 American Chemical Society.

1.3 Applications based on Azo/CD host-guest complexes

The photoresponsive Azo/CD host-guest complexes have been applied in various fields, including drug delivery, hydrogel, functional surface, and macroscopic self-assembly.

1.3.1 Drug delivery systems

Drug delivery systems have been widely studied for reducing drug toxicity and enhancing therapeutic efficiency [128, 129]. In fact, CD itself has been reported to fabricate drug carriers for some hydrophobic drugs. The outside-hydrophilic and inside-hydrophobic property helps the hydrophobic drugs hiding in the hydrophobic cavity of CD and penetrating through the cell membrane easily [130].

Combining with photoresponsive Azo/CD host-guest complexes endues drug delivery systems responsive to external irradiations. Photoresponsive drug carriers can be thus fabricated; and light can be applied to control the drug delivery precisely *in vitro* or *in vivo* [131]. Azo/CD based photoresponsive drug delivery systems can be designed in various forms, including hard silica nanoparticle, soft self-assembly, hybrid nanoparticle and microgel [132-138].

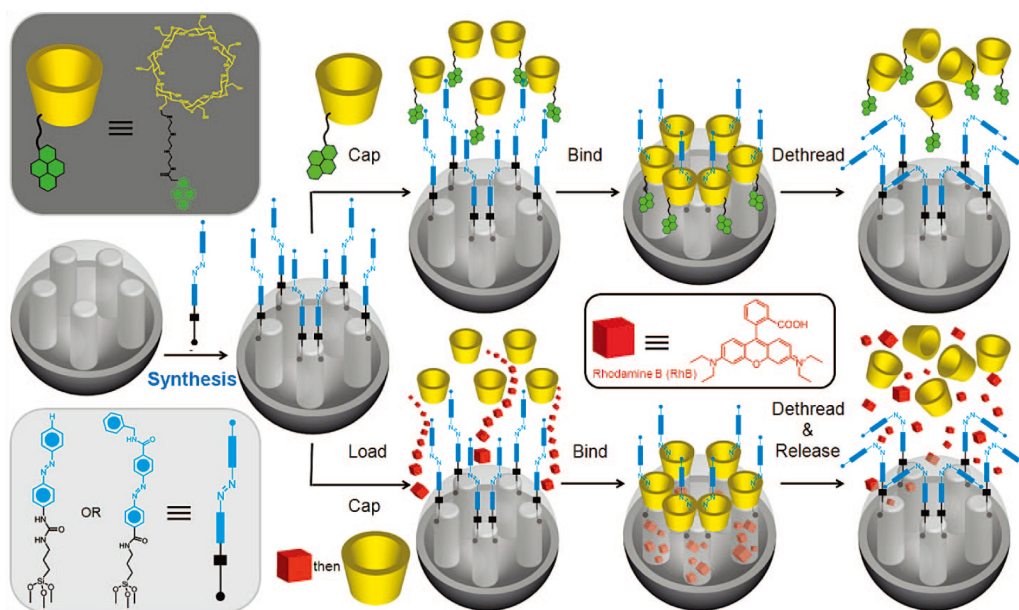


Figure 1.10 Photoresponsive drug delivery MSNs prepared based on Azo/β-CD host-guest complex. Copyright 2009 American Chemical Society.

Mesoporous silica nanoparticles (MSNs) have been investigated for long time as photoresponsive drug carriers. Zink's group grafted Azo onto MSNs' surface, and used β-CD as the nano-valve to control the loaded drug delivery (**Figure 1.10**) [139]. The β-CD was immobilized on MSNs surface in dark due to the Azo/β-CD host-guest

interaction, and the drug molecules were therefore locked in the nano pores of MSNs. After UV light irradiation, the Azo/ β -CD host-guest complex was collapsed, inducing the nano-valve open and further drug release. However, the potentiality of MSNs to induce blood-brain-barrier is needed to be concerned ^[140].

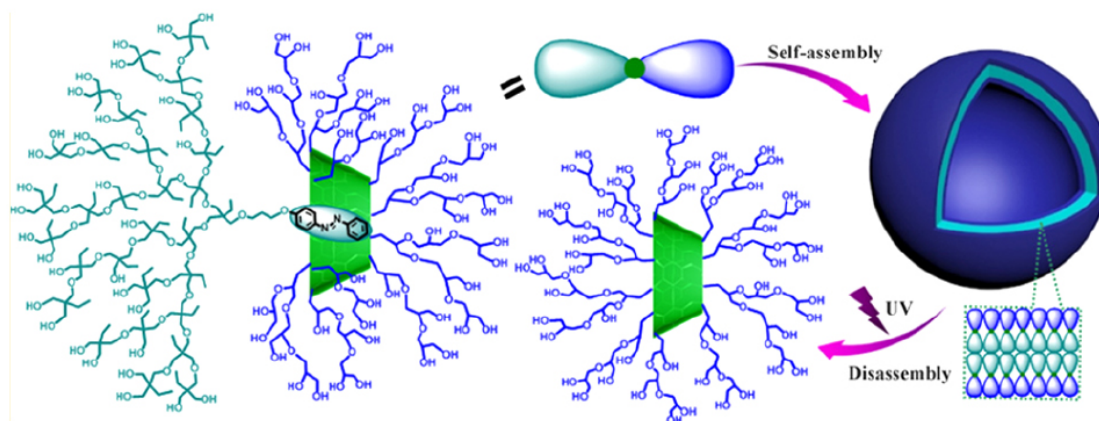


Figure 1.11 Janus dendrimer formed by Azo/ β -CD host-guest complex, the dendrimer can further self-assemble to vesicles, which can be disassembled after UV light irradiation. Copyright 2013 American Chemical Society.

Soft nano self-assemblies are also important drug carriers. The soft nanoparticles, including micelles, vesicles, and capsules, are normally fabricated by self-assembly of amphiphilic molecules, dendrimers or polymers ^[141-144]. Photoresponsive self-assemble nanoparticles could be prepared by the host-guest interaction between Azo and CD and applied in drug delivery systems. A typical method to fabricate photoresponsive self-assemble nanoparticles is by applying the Azo/CD host-guest complex as a joint to connect the hydrophilic and hydrophobic part to form amphiphilic building blocks ^[145]. Yan's group reported a supramolecular Janus hyperbranched amphiphilic polymer formed from Azo and β -CD connected dendrimers, and the further hierarchically self-assemble to vesicles from the hyperbranched polymer ^[146]. The vesicles could be deformed under UV light irradiation due to the *trans*-to-*cis* photoisomerization and the dissociation of the Azo/ β -CD host-guest complex (**Figure 1.11**). Moreover, Azo contained co-polymers

have been reported for the preparation of nano-polymersomes. Two hydrophobic segments (one is Azo part) were included in the polymer blocks. While CD could swallow the *trans* Azo and change the segment hydrophilic, the amphiphilic co-polymers could be therefore formed and further self-assembled to nano-polymersomes^[147, 148].

Light as a non-contact, clean, and effective external stimulus, has been widely studied for the preparation of controllable drug delivery systems. Actually, besides the photoresponsive drug delivery systems, photothermal and photodynamic systems are widely investigated for phototherapy^[149-152]. We believe the photoresponsive drug delivery systems will someday find the applications in clinic.

1.3.2 Hydrogel

A hydrogel is a network of hydrophilic polymer chains, sometimes found as a colloidal gel while water is the dispersion phase. A hydrogel is highly absorbent to water (it can contain >90% of water), and shows a degree of flexibility very similar to nature tissue. Due to the high content of water in the polymer network, the first appearance of the term “hydrogel” in literature was in 1894^[153]. Till now, hydrogels have been deeply investigated on their chemical and mechanical properties, and are widely applied in the fields of drug delivery, tissue engineering, intelligent systems, and self-healing materials [154-157].

A sol-gel transtion (also known as gelation) can be defined as a change from a liquild state (sol) to a gel state, this is different to the definition of sol-gel process. In the liquid state, components are dispersed well in the liquid and are relatively free to move. In the gel state, the components bond together to form a network extending throughout the whole substance, which provides the material an elasticity.

By applying the Azo/CD host-guest complex as photoresponsive crosslinker, the hydrogels can be prepared with controllable stiffness and rheology, which has been

reported as photoresponsive sol-gel transition systems ^[158, 159].

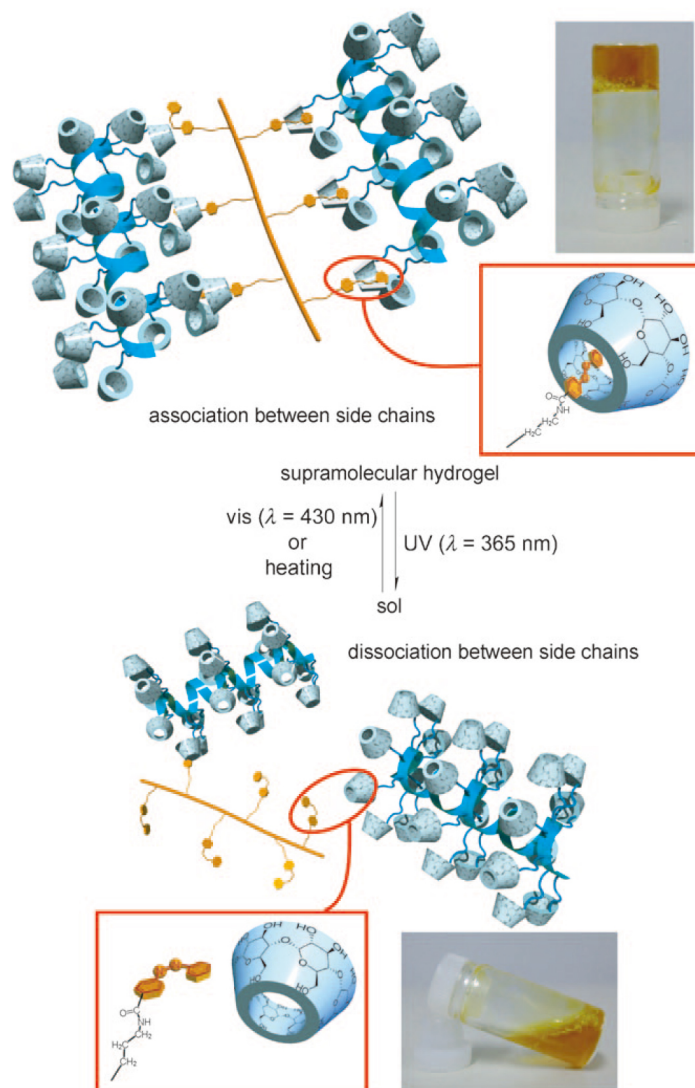


Figure 1.12 Photoresponsive sol-gel transition system formed by Azo/ α -CD host-guest complex. Copyright 2010 Wiley-VCH Verlag GmbH & Co. KGaA.

Harada's group has a lot of works on photoresponsive sol-gel transition. Azo and α -CD were grafted on poly acrylic acid (PAA) and curdlan (CUR) as side chains. Hydrogel could be formed after mixing the PAA-Azo and CUR- α -CD in aqueous solution (**Figure 1.12**) ^[117]. After treating with UV light irradiation, the gel switched to sol due to the dissociation of the Azo/ α -CD complex. The sol could be transformed back to gel form after blue light irradiation. Actually, the photoresponsive sol-gel

transition material could also be fabricated via a supramolecular competition system. It's well-known that α -CD can form a hydrogel with poly ether glycol (PEG), because the PEG molecule enters the α -CD cavity and forms a pseudopolyrotaxane^[160-162]. Jiang's group designed a photoresponsive sol-gel transition system based on the PEG/ α -CD hydrogel, while an Azo contained competitive guest Azo-C1-N⁺ was used (**Figure 1.13**). The system was UV and blue light responsive and was in an opposite way to Harada's system^[163].

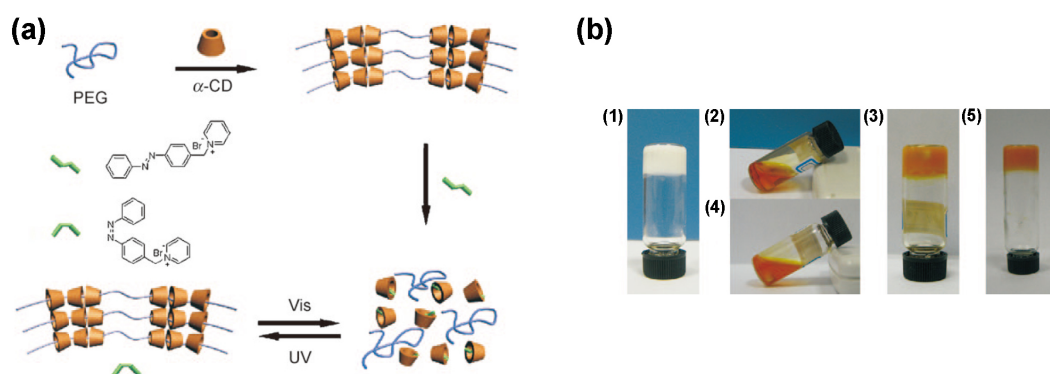


Figure 1.13 (a) Cartoon of an opposite photoresponsive sol-gel transition system. Hydrogel is formed between α -CD and PEG, and Azo-C1-N⁺ is used as supramolecular competitor. (b) Photos of Azo/PEG supramolecular hydrogel (1), after adding Azo competitor (2), after UV light irradiation (3), after visible light irradiation (4), and after adding equivalent α -CD (5). Copyright 2010 Wiley-VCH Verlag GmbH & Co. KGaA.

Hydrogels were also investigated in photoresponsive macroscopic assembly. Harada's group prepared PAA-Azo and PAA- α -CD hydrogels, and investigated their macroscopic assemblies. The PAA-Azo and PAA- α -CD hydrogels stack together under dark while floating on water. UV light irradiation could induce the disassembly of the hydrogels due to the weak interaction between PAA-*cis* Azo and PAA- α -CD hydrogels^[118].

1.3.3 Surface

Functional surfaces have been widely studied in the fields of biomaterials, molecular imprinting, and solar energy [164-168]. For many functional materials, the main working part is surface or closed to surface. Therefore, modifying material surface is convenient and efficient to prepare functional materials [169-171].

Photoresponsive functional surface could be designed using the Azo/CD host-guest complex as a linker to immobilize the functional group or polymer on surface. Zhang's group reported a substrate surface with the photo-controllable hydrophobicity/hydrophilicity [172]. A fluorinated Azo based self-assembled monolayer was prepared on gold substrate surface, which was hydrophobic. The CF_3 -group could hide in α -CD cavity when the Azo was in trans form, and further induced the surface hydrophilicity increasing. After treating with UV light irradiation, the Azo/ α -CD complex on surface was dissociated, inducing the appearance of CF_3 -group, which further triggered the surface hydrophilicity decreasing (**Figure 1.14**).

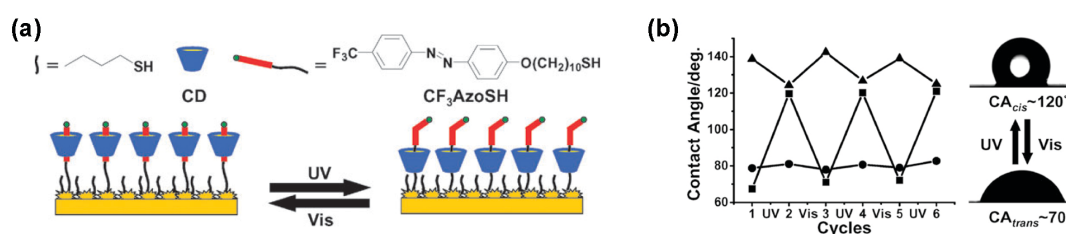


Figure 1.14 (a) Photoresponsive surface based on Azo/ α -CD host-guest complex. (b) The hydrophilicity/hydrophobicity of the surface could be controlled by UV and visible light. Copyright 2008 Royal Society of Chemistry.

Functional polymers have been widely applied to fabricate functional surfaces. Besides the well-know “graft from” and “graft to” methods, by immobilizing the polymers onto surfaces via Azo/CD host-guest complex, the surface function could be possibly switched by light. Zhao's group reported a silicon wafer substrate surface modified with β -CD monolayer [173]. Functional polymers with an Azo head group

could be immobilized onto the substrate surface due to the host-guest interaction between Azo and β -CD. The surface function could be switched by irradiating with UV light and treating with another functional Azo-headed polymer (**Figure 1.15**). This method is convenient and efficient, while the silicon wafer substrate is recyclable during the measurement and applying.

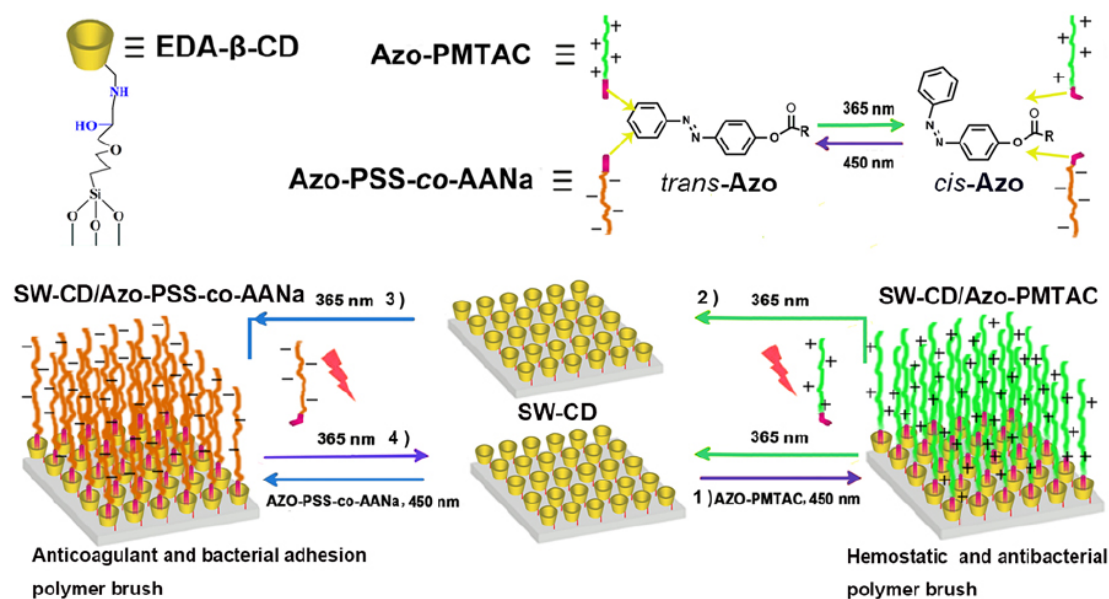


Figure 1.15 Functional polymer brush can be immobilized on substrate surface by Azo/ β -CD host-guest complex. The functionality of surface can be controlled by UV light and visible light. Copyright 2014 American Chemical Society.

1.3.4 Micro/nano-particles self-assembly

Micro or nano sized particles can play the role as self-assembly building blocks. While weak interactions induce the particles aggregation, they can self-assemble into huge aggregates ^[174-175], raspberry-like structures ^[176] and special self-assemblies ^[177-180].

Host-guest interaction between Azo and CD is strong enough to trigger micro/nano-particles self-assembly. Ravoo's group demonstrated a serial of photoresponsive huge aggregates self-assembled by nanoparticles, including silica

nanoparticles and CD based vesicles ^[181]. Azo-linkers and β -CD grafted silica nanoparticles were fabricated. In *trans* form, the Azo-linkers could induce the β -CD silica nanoparticles aggregation (**Figure 1.16**). After treating with UV light, the huge aggregates formed by β -CD silica nanoparticles were disassembled, due to the weak host-guest interaction between *cis* Azo-linker and β -CD.

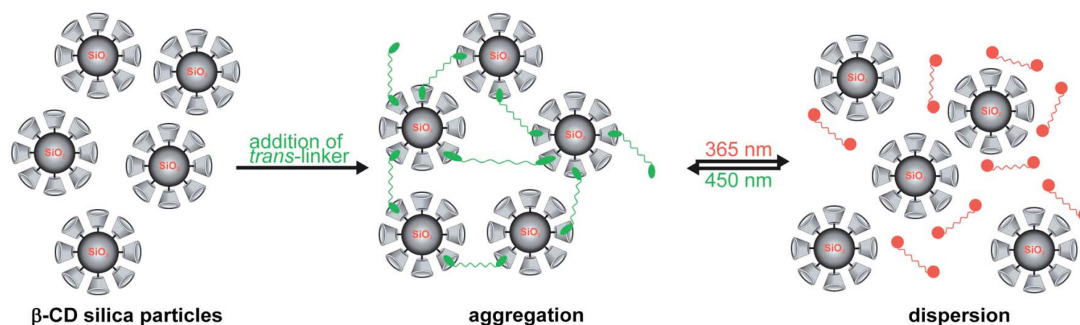


Figure 1.16 Photoresponsive aggregation and dispersion of β -CD silica nanoparticles with Azo-linkers. Copyright 2014 Royal Society of Chemistry.

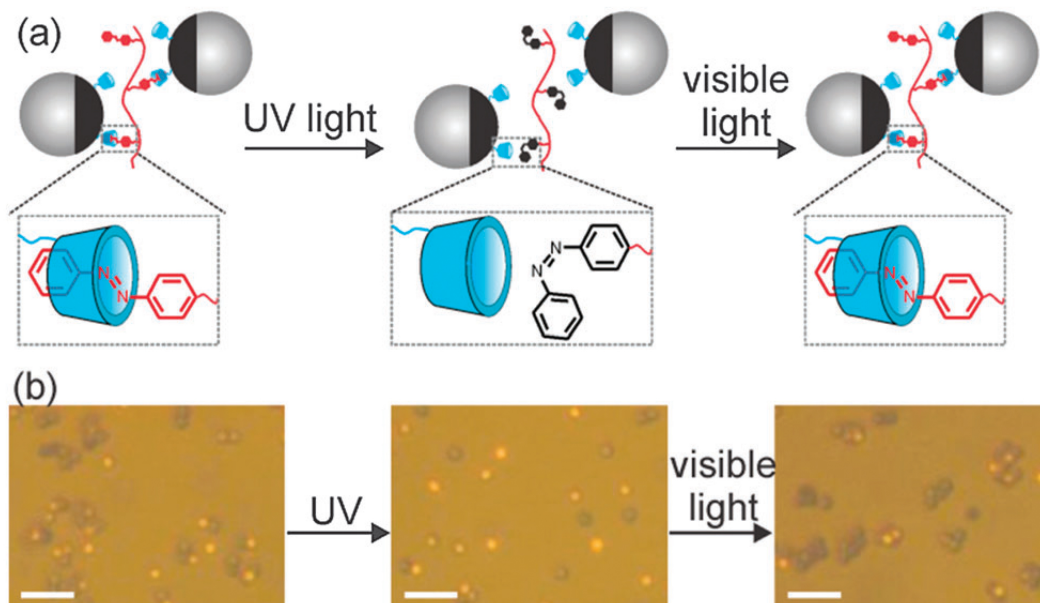


Figure 1.17 Schematic illustration (a) and optical microscopy images (b) of photoinduced assembly and disassembly of β -CD modified Janus microparticles in the presence of pAzo. Copyright 2015 Royal Society of Chemistry.

Wu's group reported a photoresponsive self-assembly in Janus microparticles

based on Azo/ β -CD host-guest interaction^[182]. Janus microparticles were prepared by grafting β -CD onto half of silica microparticles. A hydrophilic Azo-containing polymer pAzo was used as the photoresponsive multi-linker. Aggregation of the Janus microparticles could be observed after introducing pAzo in dark or visible light. UV light irradiation could induce the Janus microparticles disassembly (**Figure 1.17**).

1.4 Visible/NIR-light-responsive Azobenzene

Although Azo/CD photoresponsive host-guest system has been widely investigated, the UV-light-responsive property of Azo still hinders the system application, especially for the *in vivo* applications. UV light shows strong toxicity to cells and tissues, and is difficult to penetrate deep tissues and induce photoreactions or photoisomerization *in vivo*^[183-185].

The penetrability of light is proportional to the light wavelength (**Figure 1.18**)^[186], therefore, to solve the problem of UV-light-responsive Azo/CD host-guest system, making Azo responsive to the light with longer wavelength is necessary.

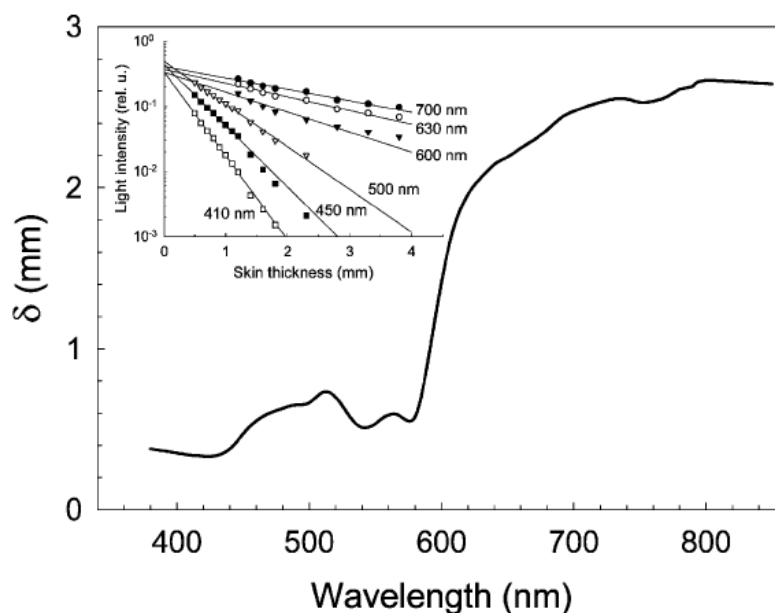


Figure 1.18 Penetrability of light with different wavelengths to tissue. Copyright 2002 Royal Society of Chemistry.

1.4.1 Upconversion

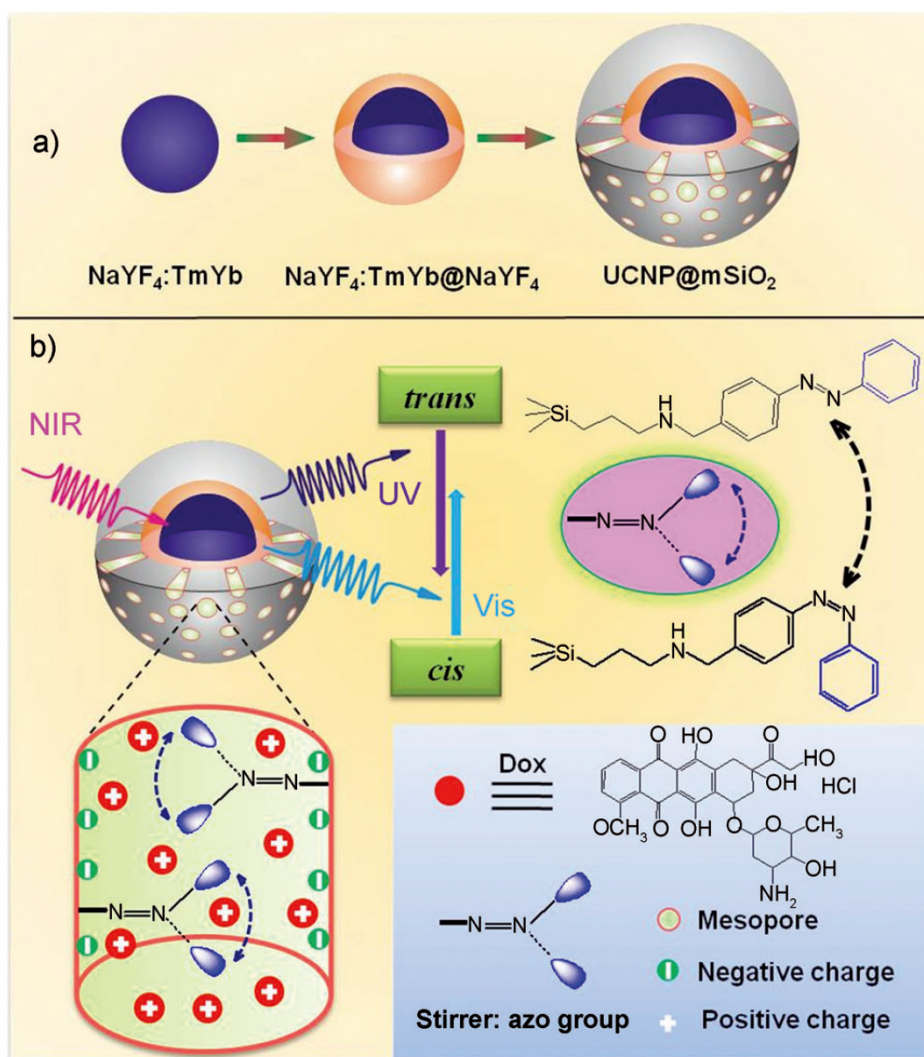


Figure 1.19 Cartoon of preparation of upconverting nanoparticles with mesoporous shell (a) and release mechanism of loaded drug (b). Copyright 2013 Wiley-VCH Verlag GmbH & Co. KGaA.

Upconversion is a photon process in which the sequential absorption of two or more photons leads to the emission of light with shorter wavelength than the excitation wavelength, which is an anti-Stokes type emission^[187-188]. With the help of up-converting nanoparticles, the system can convert the infrared excitation light to UV and visible light, which can trigger the photoisomerization of Azo.

Shi's group reported a NIR-light-triggered drug delivery system by upconverting nanoparticles with Azo impellers for cancer therapy ^[189]. NaYF₄:TmYb@NaYF₄ upconverting nanoparticles convert the 980 nm NIR light to UV and visible light, which induce the fast *trans*-to-*cis* and *cis*-to-*trans* photoisomerization of Azo impellers, and further trigger the loaded drug release (**Figure 1.19**). However, the heat induced by NIR light may also trigger the loaded drug release, which was demonstrated by Zink's group ^[190]. Recently, Ravoo's group reported a NIR-light-responsive Azo/CD host-guest complex by upconversion technique ^[191]. *Trans*-to-*cis* isomerization of Azo can be induced by 980 nm NIR light, which further trigger the disassembly of Azo/CD complex on nanoparticle surface.

Upconversion is a helpful technique to apply UV-light-responsive molecules in biomedical field. However, the upconverted efficiency is low, which makes the high power laser necessary during the therapy process. Burning and harming of skin tissue are therefore needed to be considered ^[192, 193]. Moreover, the overlapping of emission spectra of upconverting nanoparticles and absorption spectra of photoresponsive molecules are important for the upconverted efficiency.

1.4.2 Two-photon process

Two-photon process is the simultaneous absorption of two photons by a molecule, which excites the molecule from one state to a higher energy electronic state ^[194-196]. The energy difference between the two states is equal to the sum of the energies of the two photons. The two-photon process is a nonlinear optical process, which is several orders of magnitude weaker than linear optical process at low light intensities. However, at high light intensities, the nonlinear process can dominate over the linear absorption.

A lot of works have been done to photo-control the isomerization of Azo by NIR light via a two-photon process. Gorostiza's group and Isacoff's group reported a

series of Azo contained molecules, which could be controlled by NIR light with the wavelength longer than 820 nm ^[197, 198]. Hsiao's group reported a fluorene-bridged Azo which was responsive to NIR light with the wavelength of 800 nm ^[199].

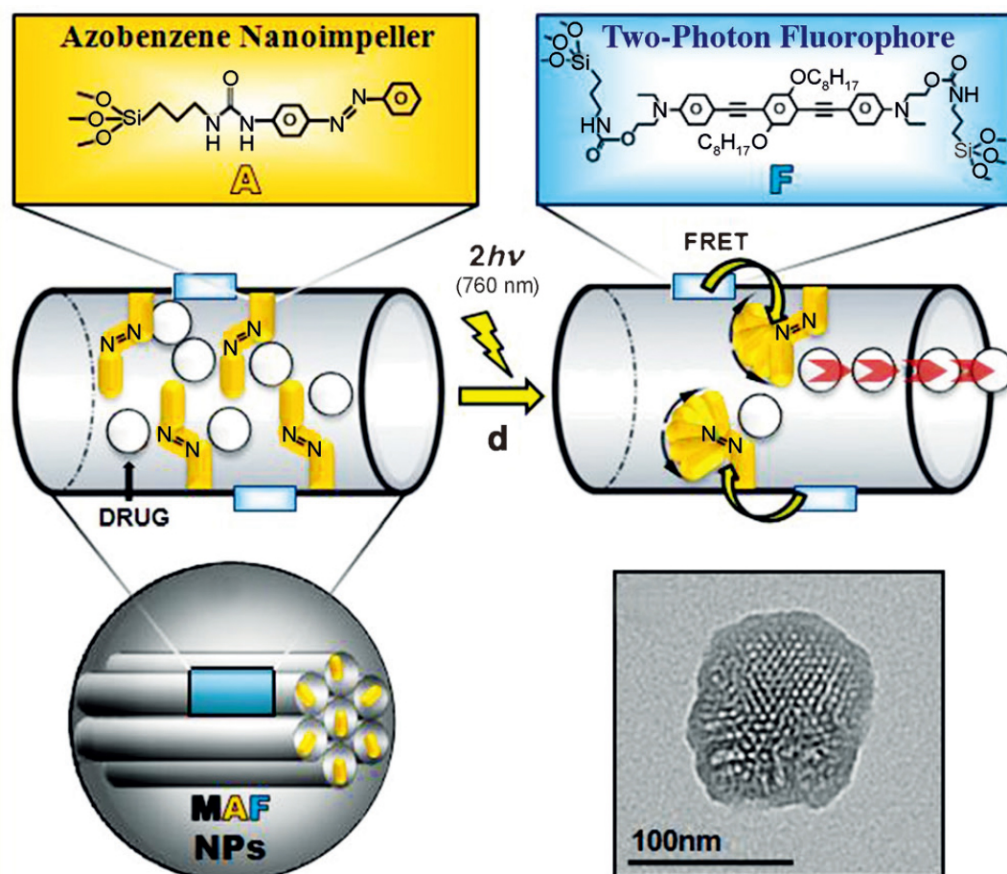


Figure 1.20 Photoresponsive drug delivery mesoporous silica nanoparticles based on two-photon absorption and FRET process, Azo is used as nanoimpeller in the system, which can induce drug release from the carrier. Copyright 2013 Wiley-VCH Verlag GmbH & Co. KGaA.

Zink's group designed a combinative drug delivery system based on two-photon process and Förster resonance energy transfer (FRET) process ^[200]. An Azo based impeller was grafted inside the nanopores of MSNs, while a two-photon fluorophore was included to absorb the NIR light. Fast *trans*-to-*cis* and *cis*-to-*trans* photoisomerization of Azo impeller was induced via FRET process, and further triggered the drug release (**Figure 1.20**).

Photocontrolling Azo molecules via two-photon process can naturally develop the applications of Azo systems in biomedical region, however, the two photon process needs femtosecond laser with very high light intensity. The small laser beam area and extremely high laser intensity still limit the application of two-photon absorption in Azo based systems.

1.4.3 Chemical modification

Besides the “indirect” way such as upconversion and two-photon process to make the Azo molecules responsive to NIR light by additional equipment, a “direct” way to prepare red or NIR-light-responsive Azo could be defined as making the Azo molecules intrinsically responsive to light with the long wavelength.

Since the last century there have been researches about tuning the absorption spectra of Azo molecules by chemical modifying the benzene rings with electron donating or electron withdrawing groups ^[201, 202]. The π - π^* and n- π^* absorption bands of Azo can obviously shift depends on the electron density and distribution on the Azo molecule, which is tightly related to the molecule’s photoresponsive property. Actually, till now, there have been plenty of examples to red-shift the responsive light of Azo molecules to red or even NIR light region, which makes the Azo based systems better suited to be applied in biomedical region.

1.4.3.1 Electron donating

In the year of 2011, Woolley’s group firstly reported a tetra-ortho-methoxy-substituted Azo (mAzo), and found that the mAzo showed *trans*-to-*cis* isomerization under green light irradiation (530-560 nm), while the *cis*-to-*trans* isomerization occurred after heating or blue light irradiation (450-460 nm) ^[203]. The *trans* mAzo showed a large n- π^* absorption band which extended to red light region (>600 nm).

After green light irradiation, the $n\text{-}\pi^*$ absorption band of *cis* mAzo blue shifted and was separated from that of *trans* mAzo in green light region (**Figure 1.21**). Therefore, green light could induce the $n\text{-}\pi^*$ absorption band of *trans* mAzo and further triggered the *trans*-to-*cis* isomerization. The *cis* mAzo showed a much longer half-time than *cis* Azo in dark and room temperature (53 h vs ~12 min), which was also positive for the application. Another paper about mAzo was published by Woolley's group in 2013, mAzo was demonstrated to show *trans*-to-*cis* photoisomerization under red light irradiation (635 nm). Although the *trans* mAzo showed trace absorption in the deep red light region, the red light could still astonishingly induce this part and further trigger the photoisomerization ^[204].

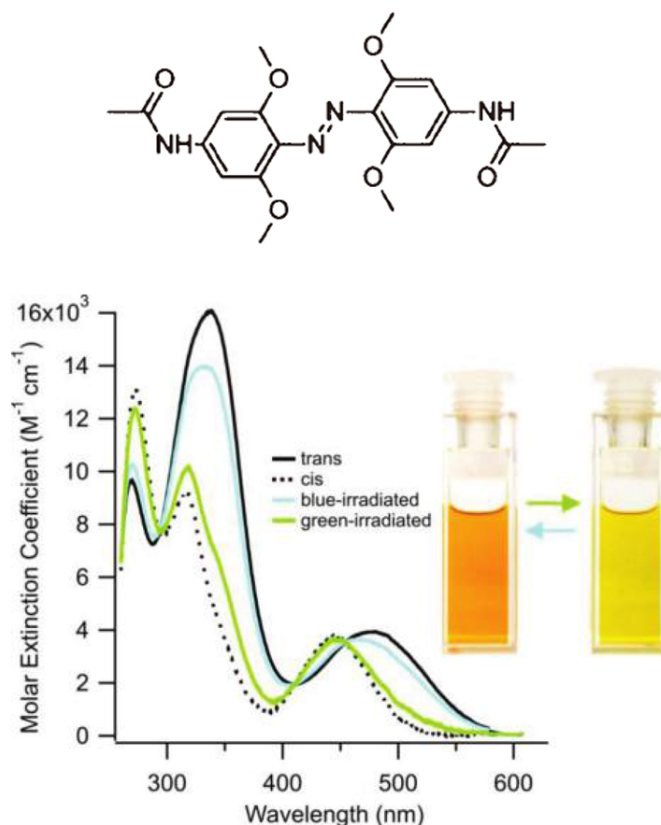


Figure 1.21 Molecular structure and UV/vis spectra of mAzo. Copyright 2011 American Chemical Society.

The successful synthesis of red-light-responsive mAzo certainly develops the

application of Azo systems in biomedical region. Actually, there have been many works published about the mAzo applications in the fields of biomaterials, energy, and optical materials ^[205-207].

1.4.3.2 Electron withdrawing

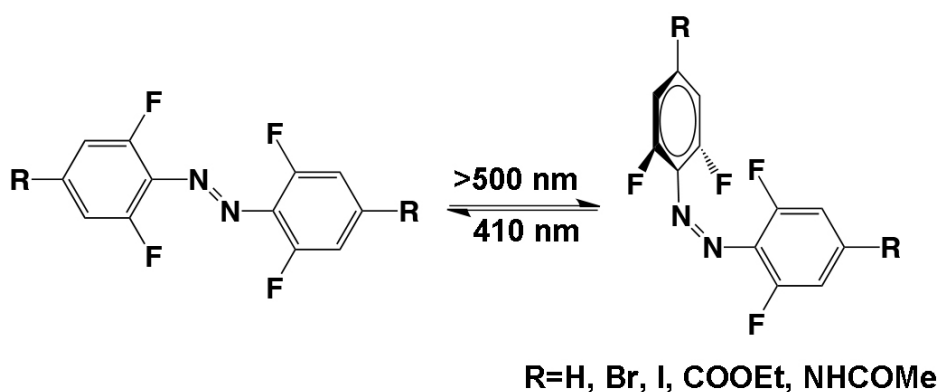


Figure 1.22 Molecular structure of *trans* and *cis* fAzo.

Another method to synthesize Azo molecules responsive to light with long wavelengths is by grafting electron withdrawing groups on the benzene rings. Hecht's group synthesized a tetra-ortho-fluoro-substituted Azo (fAzo), which showed *trans*-to-*cis* isomerization under green light irradiation (>500 nm), and *cis*-to-*trans* isomerization under blue light irradiation (410 nm) ^[208]. The photoresponsive properties could be further tuned by introducing different para-substituents on benzene rings. Approximately 97% of *cis* fAzo could be obtained by green light irradiating, which is higher than mAzo (~80%) (**Figure 1.22**). The half-life of *cis* fAzo is ca. 700 d at room temperature, which is 2 orders of magnitude longer than that of *cis* mAzo. The super-long half-life of *cis* fAzo makes the *cis* fAzo possible to be applied as a material. However, due to the contained fluorine in fAzo, it may meet some problems when applies in biomedical region ^[209-211].

1.4.3.3 BF₂-coordination

Actually, besides the modification with electron donating and electron withdrawing groups, BF₂-coordination is also an important method to synthesize red or NIR-light-responsive Azo molecules.

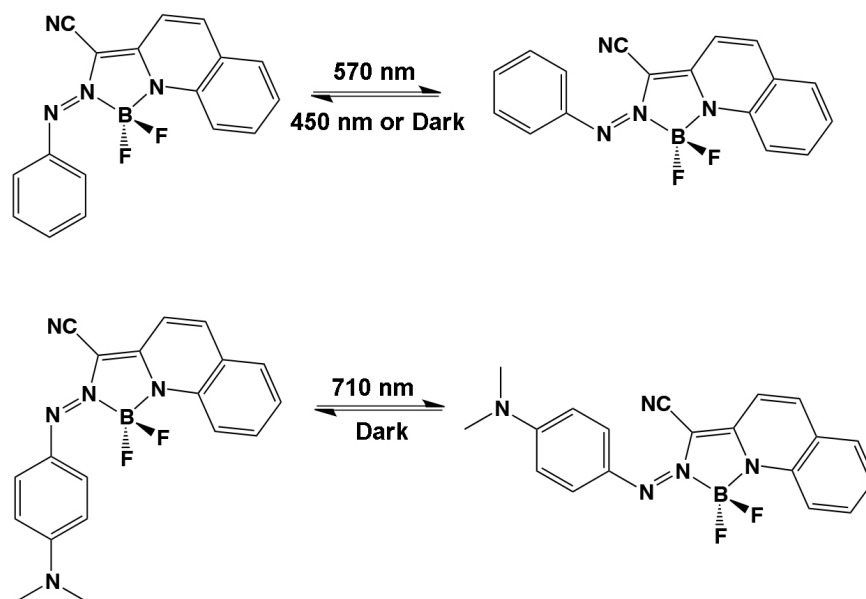


Figure 1.23 Molecular structure of BF₂-coordinated Azo.

Aprahamina's group synthesized a BF₂-coordinated Azo compound in the year of 2012 ^[212]. The complex structure showed *trans*-to-*cis* isomerization under the irradiation with a 570 nm yellow light, while the *cis*-to-*trans* isomerization occurred under the irradiation of a 450 nm blue light (**Figure 1.23**). The *cis* BF₂-coordinated Azo also had a long half-life in dark and under room temperature (~12.5 h).

A series of BF₂-coordinated Azo were reported by Aprahamina's group in 2014 ^[213]. One Azo molecule really responsive to NIR light (710 nm) was synthesized. Unfortunately, the *cis* isomer was very unstable under dark in room temperature (with a half-life of only 250 s), which limited the application of the NIR-light-responsive Azo (**Figure 1.23**). Anyway, this amazing synthesis and modification still point out

the future of NIR-light-responsive Azo molecules.

Actually, in the mentioned mAzo, fAzo, and BF₂-coordinated Azo above, only mAzo is easily applied for the investigation of red-light-responsive host-guest supramolecular systems with CD molecules. Both fAzo and BF₂-coordinated Azo contain fluorine in the molecule, which may form strong hydrogen bonds with the hydroxyl groups on CD molecules ^[214]. The strong unspecific interaction may invalidate the photoresponsive host-guest complex.

1.5 Motivation

As a typical photoresponsive host-guest supramolecular system, Azo/CD has been widely investigated and applied in the fields of nanomaterial, hydrogel, and functional interface. UV light (~365 nm) and blue light (~470 nm) can precisely and efficiently control the association and dissociation of the Azo/CD host-guest complex. However, the requirement of UV light strongly hinders the application and development of Azo/CD based supramolecular systems on biomedical field, including drug delivery, tissue engineering, and cell culture. Therefore, investigations on visible or NIR-light-responsive Azo/CD host-guest systems are urgent and necessary. While the supramolecular systems can be controlled by low intensity visible or NIR light, the systems are potential to be applied in deep tissue for drug delivery or tissue engineering. Moreover, visible light accounts for about 43% of the incoming solar energy, which is far beyond UV light (~4%) ^[215]. The results indicate the possibility to control photoresponsive supramolecular systems by sunlight. Furthermore, UV-light-responsive and visible-light-responsive supramolecular systems may be combined to design novel photoresponsive systems. Lights with various wavelengths are potential to control the supramolecular systems orthogonally. The photoresponsive orthogonal supramolecular systems can be further applied to fabricate intelligent photoresponsive materials, which are active even under complex

external stimuli. These may be helpful to design reflex arc in robots in the future.

With the help of synthesizing visible or NIR-light-responsive Azo, the Azo/CD host-guest complex is potential to be controlled by light with long wavelengths (section 2.1). Afterwards, the new Azo/CD host-guest system can be applied for preparing red-light-responsive biomacromolecules and drug delivery systems (section 2.2). Moreover, by further modifying the benzene rings on Azo with bulky electron donating groups may bring some new photoresponsive and supramolecular properties, the investigation on this region will help us to understand the Azo/CD host-guest interaction deeply (section 2.3). Finally, visible-light-responsive Azo/CD host-guest supramolecular system is not only applicable in biomedical field. Some novel photoresponsive supramolecular systems can be further designed (section 2.4).

1.5.1 Red-light-responsive Azo/CD host-guest complex

Although UV-light-responsive Azo/CD host-guest supramolecular system has met widely investigation and application, the requirement of UV light as induced irradiation still hinders the development of the system in biomedical field. To extend the induced irradiation to visible or NIR light region (biomedical window) is therefore necessary ^[216].

There have been several “indirect” methods to red-shift the induced light of Azo, including upconversion and two-photon absorption. NIR light is thus able to be used to induce the *trans*-to-*cis* isomerization of Azo, and further trigger the dissociation of the Azo/CD host-guest complex. However, for the upconversion and two-photon absorption based methods, there are still some problems needed to be concerned. High laser intensity and upconverting nanoparticles are needed for the upconversion method, while a femtosecond laser with extremely high light intensity is needed for the two-photon absorption method. Both of them will make the design of photoresponsive supramolecular system more complicated. Therefore, a “direct” way

to obtain visible-light-responsive Azo/CD host-guest supramolecular system is urgently needed.

The successful synthesis of mAzo, which shows *trans*-to-*cis* isomerization under red light (~635 nm), and *cis*-to-*trans* isomerization under blue light (~470 nm), makes us considering the possibility to design red-light-responsive mAzo/CD host-guest complex. Different to the fluorine-contained fAzo and BF₂-coordinated Azo, the unspecific interaction between mAzo and CD molecules could not be strong, which makes the mAzo/CD host-guest complex potential to be photoresponsive.

In chapter 2, I focused on investigating the red-light-responsive host-guest interaction between mAzo and different CD molecules. Pyridium was grafted on mAzo with a 6-carbon spacer in between (mAzo-Py) to increase the hydrophilicity of the whole molecule. ¹H NMR and two-dimensional nuclear Overhauser effect spectroscopy (2D NOESY) were used to demonstrate the formation of photoresponsive host-guest complex. Moreover, mAzo was grafted on poly acrylic acid (PAA) chains to form PAA-mAzo, which was also used for the determination of red-light-responsive host-guest supramolecular interaction. Traditional UV-light-responsive Azo/CD host-guest complex was investigated simultaneously, and compared with the mAzo/CD host-guest complex.

1.5.2 Red-light-responsive biomacromolecules and drug delivery systems

Red light (>600 nm) shows a much stronger penetrability to human tissue than UV light (<400 nm), which makes the red-light-responsive supramolecular system potential to be applied in deep tissue. Therefore, in chapter 2 and chapter 3, I designed two red-light-responsive delivery systems used for biomacromolecules and small molecular drug. Red light with the wavelength of 625 nm was expected to penetrate deep tissue and trigger the loaded biomacromolecules or drug release. Due to the fact

that the photoisomerization of mAzo is a linear optical process, a LED with extremely low light intensity (60 mW/cm^2) is enough to trigger the cargo release in deep tissue, which is helpful for the tumor phototherapy in deep.

1.5.3 Further increasing molecular scale of Azo

Till now, only Azo/ α -CD and Azo/ β -CD complexes have been reported to be photoresponsive in the traditional host-guest supramolecular systems formed between Azo and CD. It could be interesting and attractive to enrich the photoresponsive host-guest supramolecular family.

The host-guest interaction between *trans* Azo and α -CD is stronger than that between *trans* Azo and β -CD (K_a (*trans* Azo/ α -CD)= 2000 M^{-1} , K_a (*trans* Azo/ β -CD)= 770 M^{-1}), while the host-guest interaction between *cis* Azo and α - or β -CD are very weak (K_a (*cis* Azo/ α -CD)= 35 M^{-1} , K_a (*cis* Azo/ β -CD)= 280 M^{-1}) [118]. The result is attributed to the larger hydrophobic cavity of β -CD than α -CD, while *trans* Azo well fits the α -CD cavity, the β -CD cavity is too large for the *trans* Azo.

Besides red-shifting the induced light of photoisomerization, modifying the benzene rings of Azo with bulky electron donating groups also increase the molecular scale, which may change the supramolecular property. In chapter 4, I focused on further increasing the molecular scale of Azo by introducing bulky electron donating groups. Tetra-ortho-isopropoxy-substituted Azo (ipAzo) with four larger substituent groups than mAzo was synthesized. Pyridium was grafted on ipAzo with a 6-carbon spacer in between to prepare hydrophilic ipAzo-Py, which was further used for the investigation of photoresponsive host-guest interaction.

1.5.4 Photoresponsive orthogonal supramolecular system

Red-light-responsive Azo has been reported to be applied in biomedical region,

due to the good tissue penetrability and biocompatibility of red light with the wavelength longer than 600 nm. However, besides the biomedical field, we are still searching for some other applications of red-light-responsive Azo.

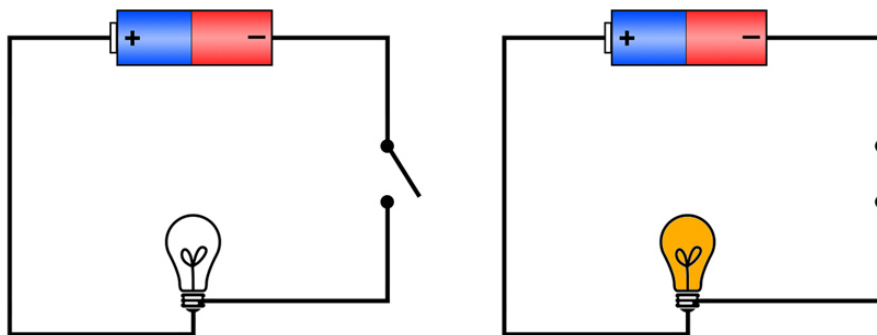


Figure 1.24 Electric circuit with one switch, there are only two states (“on” and “off”) for the system.

Most photoresponsive systems are based on only one photoresponsive chromophore, just like an electric circuit with one switch (**Figure 1.24**). External photoirradiation can only switch the system between two states (“on” and “off” in electric circuit). By introducing two or more photoresponsive chromophores in one photoresponsive system, it’s potential to control the system in several photostationary states by different external irradiations (**Figure 1.25**). The photoresponsive chromophores should be orthogonal to each other in photoswitching step.

In chapter 4, we try to realize the orthogonal photo-controlling by introducing two Azo molecules in one photoresponsive system. Combing with CD molecules used as hosts, the photoresponsive orthogonal supramolecular system can be therefore prepared.

The photoresponsive orthogonal supramolecular system can be controlled by up to 4 different external irradiations. The derivative materials can be therefore photo-controlled to switch in up to 4 different states. The results make the photoresponsive materials multifunctional, and more intelligent.

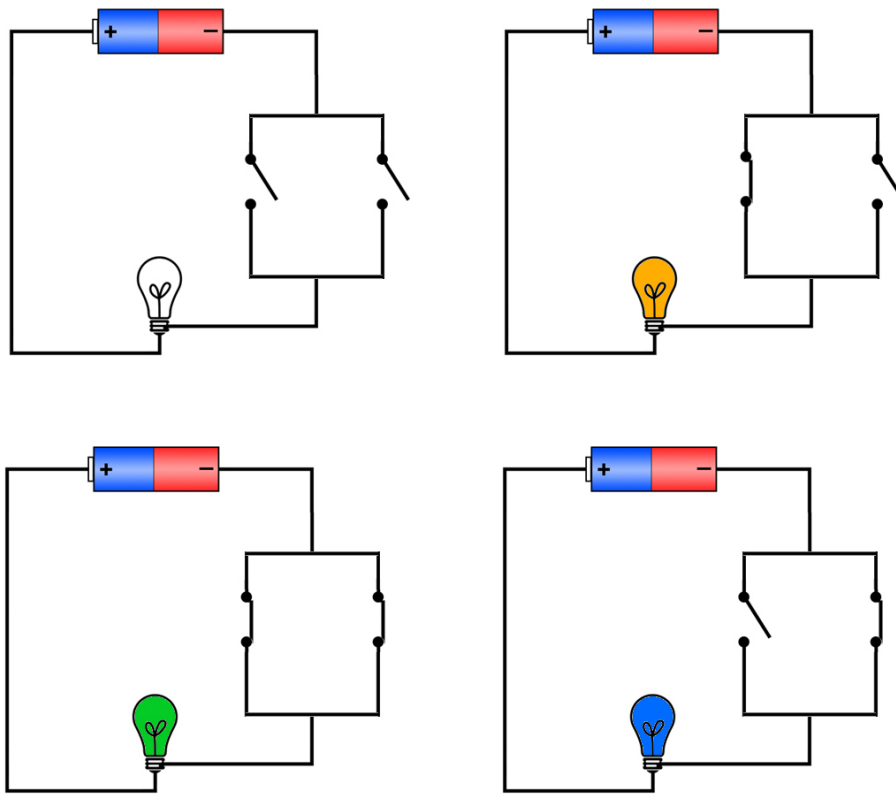


Figure 1.25 Electric circuit with two switches, there are four states for the system.

References

1. Lehn, J. -M. *Supramolecular Chemistry: Concepts and Perspectives*; John Wiley & Sons, Inc, Weinheim, **1995**.
2. Wolf, K. L.; Frahm, H.; Harms, H. *Phys, Chem. Abt. B*, **1937**, *36*, 237-287.
3. Palmer, L. C.; Stupp, S. I. *Acc. Chem. Res.*, **2008**, *41*, 1674-1684.
4. Bottari, G.; Torre, G.; Torres, T. *Acc. Chem. Res.*, **2015**, *48*, 900-910.
5. Zhao, Y.; Gohy, J. -F. *Chem. Soc. Rev.*, **2013**, *42*, 7117-7129.
6. Feiters, M. C.; Rowan, A. E.; Nolte, R. J. M. *Chem. Soc. Rev.*, **2000**, *29*, 375-384.
7. Balzani, V.; Credi, A.; Raymo, F. M.; Stoddart, J. F. *Angew. Chem. Int. Ed.*, **2000**, *39*, 3348-3391.
8. Diederich, F.; Gómez-López, M. *Chem. Soc. Rev.*, **1999**, *28*, 263-277.
9. Benniston, A. C. *Chem. Soc. Rev.*, **1996**, *25*, 427-435.
10. Fabbrizzi, L.; Poggi, A. *Chem. Soc. Rev.*, **1995**, *24*, 197-202.
11. Zheng, L.; Sonzini, S.; Ambarwati, M.; Rosta, E.; Scherman, O. A.; Herrmann, A. *Angew. Chem. Int. Ed.*, **2015**, *54*, 13007-13011.
12. Liu, Y.; Pauloehrl, T.; Presolski, S. I.; Albertazzi, L.; Palmans, A. R. A.; Meijer, E. *W. J. Am. Chem. Soc.*, **2015**, *137*, 13096-13105.
13. Dong, R.; Preffermann, M.; Liang, H.; Zheng, Z.; Zhu, X.; Zhang, J.; Feng, X. *Angew. Chem. Int. Ed.*, **2015**, *54*, 12058-12063.
14. Aznar, E.; Marcos, M. D.; Martínez-Máñez, R.; Sancrnón, F.; Soto, J.; Amorós, P.; Guillem, C. *J. Am. Chem. Soc.*, **2009**, *131*, 6833-6843.
15. Blasco, E.; Schmidt, B. V. K. J.; Barner-Kowollik, C.; Piñol, M.; Oriol, L. *Macromolecules*, **2014**, *47*, 3693-3700.
16. Cao, Z.; Wu, H.; Dong, J.; Wang, G. *Macromolecules*, **2014**, *47*, 8777-8783.
17. Yuan, Q.; Zhang, Y.; Chen, T.; Lu, D.; Zhao, Z.; Zhang, X.; Li, Z.; Yan, C. -H.; Tan, W. *ACS Nano.*, **2012**, *6*, 6337-6344.
18. Zhang, Q.; Qu, D. -H.; Ma, X.; Tian, H. *Chem. Commun.*, **2013**, *49*, 9800-9802.
19. Guan, Y.; Zhao, H.; Yu, L.; Cheng, S.; Wang, Y. *RSC Adv.*, **2014**, *4*, 4955-4959.

20. Liu, Z.; Feng, Y.; Yan, Z.; He, Y.; Liu, C.; Fan, Q. *Chem. Mater.*, **2012**, *24*, 3751-3757.
21. Liu, Y.; Yu, C.; Jin, H.; Jiang, B.; Zhu, X.; Zhou, Y.; Lu, Z.; Yan, D. *J. Am. Chem. Soc.*, **2013**, *135*, 4765-4770.
22. Achilleos, D. S.; Hatton, T. A.; Vamvakaki, M. *J. Am. Chem. Soc.*, **2012**, *134*, 5726-5729.
23. Duan, Y.; Yan, S.; Zhou, X.; Xu, W.; Xu, H.; Liu, Z.; Zhang, L.; Zhang, C.; Cui, G.; Yao, L. *Chem. Commun.*, **2014**, *50*, 8335-8338.
24. Jin, H.; Zheng, Y.; Liu, Y.; Cheng, H.; Zhou, Y.; Yan, D. *Angew. Chem. Int. Ed.*, **2011**, *50*, 10352-10356.
25. Lee, S.; Oh, S.; Lee, J.; Malpani, Y.; Jung, Y.; Kang, B.; Lee, J. Y.; Ozasa, K.; Isoshima, T.; Lee, S. Y.; Hara, M.; Hashizume, D.; Kim, J. *Langmuir*, **2013**, *29*, 5869-5877.
26. Li, G.; Wu, J.; Wang, B.; Yan, S.; Zhang, K.; Ding, J.; Yin, J. *Biomacromolecules*, **2015**, *16*, 3508-3518.
27. Kashif, M.; Chang, Y. *Eur. Polymer. J.*, **2015**, *70*, 306-316.
28. Miyamae, K.; Nakahata, M.; Takashima, Y.; Harada, A. *Angew. Chem. Int. Ed.*, **2015**, *54*, 8984-8987.
29. Kumar, S.; Dory, Y. L.; Lepage, M.; Zhao, Y. *Macromolecules*, **2011**, *44*, 7385-7393.
30. Wan, P.; Jiang, Y.; Wang, Y.; Wang, Z.; Zhang, X. *Chem. Commun.*, **2008**, *44*, 5710-5712.
31. Xu, B.; Zhou, X.; Stains, C. I. *J. Am. Chem. Soc.*, **2015**, *137*, 14252-14255.
32. Wang, D.; Xie, D.; Shi, W.; Sun, S.; Zhao, C. *Langmuir*, **2013**, *29*, 8311-8319.
33. Yang, L.; Tan, X.; Wang, Z.; Zhang, X. *Chem. Rev.*, **2015**, *115*, 7196-7239.
34. Weng, W.; Beck, J. B.; Jamieson, A. M.; Rowan, S. J. *J. Am. Chem. Soc.*, **2006**, *128*, 11663-11672.
35. Ogawa, K.; Kobuke, Y. *Angew. Chem. Int. Ed.*, **2000**, *39*, 4070-4073.

-
36. Bodenthin, Y.; Pietsch, U.; Möhwald, H.; Kurth, D. G. *J. Am. Chem. Soc.*, **2005**, *127*, 3110-3114.
37. Del Barrio, J.; Horton, P. N.; Lairez, D.; Lloyd, G. O.; Toprakcioglu, C.; Scherman, O. A. *J. Am. Chem. Soc.*, **2013**, *135*, 11760-11763.
38. Xu, L.; Liu, Y.; Zhang, X. *Nanoscale*, **2011**, *3*, 4901-4915.
39. Albertazzi, L.; Veeken, N. V. D.; Baker, M. B.; Palmans, A. R. A.; Meijer, E. W. *Chem. Commun.*, **2015**, *51*, 16166-16168.
40. Li, D.; Chen, X.; Ren, K.; Ji, J. *Chem. Commun.*, **2015**, *51*, 1576-1578.
41. Wang, K.; Chen, Y.; Liu, Y. *Chem. Commun.*, **2015**, *51*, 1647-1649.
42. Guo, M.; Pitet, L. M.; Wyss, H. M.; Vos, M.; Dankers, P. Y. W.; Meijer, E. W. *J. Am. Chem. Soc.*, **2014**, *136*, 6969-6977.
43. Liang, S.; Zhao, Y.; Adronov, A. *J. Am. Chem. Soc.*, **2014**, *136*, 970-977.
44. Jiang, X.; Ge, Z.; Xu, J.; Liu, H.; Liu, S. *Biomacromolecules*, **2007**, *8*, 3184-3192.
45. Zhao, Y.; Li, Z.; Kabehie, S.; Botros, Y. Y.; Stoddart, J. F.; Zink, J. I. *J. Am. Chem. Soc.*, **2010**, *132*, 13016-13025.
46. Liu, R.; Zhang, Y.; Zhao, X.; Agarwal, A.; Mueller, L. J.; Feng, P. *J. Am. Chem. Soc.*, **2010**, *132*, 1500-1501.
47. Kuan, S. L.; Ng, D. Y. W.; Wu, Y.; Förtsch, C.; Barth, H.; Doroshenko, M.; Koynov, K.; Meier, C.; Weil, T. *J. Am. Chem. Soc.*, **2013**, *135*, 17254-17257.
48. Cakir, N.; Hizal, G.; Becer, C. R. *Polym. Chem.*, **2015**, *6*, 6623-6631.
49. Brassinne, J.; Bourgeois, J.; Fustin, C.; Gohy, J. *Soft. Matter.*, **2014**, *10*, 3086-3092.
50. Zou, H.; Guo, W.; Yuan, W. *J. Mater. Chem. B*, **2013**, *1*, 6235-6244.
51. Fu, S.; Sun, H.; Li, J.; Bai, Y.; Luo, Q.; Dong, Z.; Xu, J.; Liu, J. *RSC Adv.*, **2015**, *5*, 101894-101899.
52. Martinez-Cuezva, A.; Valero-Moya, S.; Alajarin, M.; Berna, J. *Chem. Commun.*, **2015**, *51*, 14051-14504.
53. Ye, L.; Liu, X.; Ito, K.; Feng, Z. *J. Mater. Chem. B*, **2014**, *2*, 5746-5757.

-
54. Saiz, L. M.; Oyanguren, P. A.; Galante, M. J.; Zucchi, I. A. *Nanotechnology*, **2014**, *25*, 065601.
55. Moulin, E.; Cid, J.; Giuseppone, N. *Adv. Mater.*, **2013**, *25*, 477-487.
56. Chi, X.; Xue, M. *Chem. Commun.*, **2014**, *50*, 13754-13756.
57. Chen, L.; Zhao, X.; Lin, Y.; Su, Z.; Wang, Q. *Polym. Chem.*, **2014**, *5*, 6754-6760.
58. Chi, X.; Xue, M.; *RSC Adv.* **2014**, *4*, 37786-37789.
59. Yan, X.; Wu, X.; Wei, P.; Zhang, M.; Huang, F. *Chem. Commun.*, **2012**, *48*, 8201-8203.
60. Liang, B.; Tong, R.; Wang, Z.; Guo, S.; Xia, H. *Langmuir*, **2014**, *30*, 9524-9532.
61. Shigemitsu, H.; Hisaki, I.; Senga, H.; Yasumiya, D.; Thakur, T. S.; Saeki, A.; Seki, S.; Tohnai, N.; Miyata, M. *Chem. Asian. J.*, **2013**, *8*, 1372-1376.
62. Lee, S.; Zhu, X.; Wang, Y. J.; Xuan, S.; You, Q.; Chan, W.; Wong, C.; Wang, F.; Yu, J. C.; Cheng, C. H. K.; Leung, K. C. F. *ACS Appl. Mater. Interfaces.*, **2013**, *5*, 1566-1574.
63. Pappas, C. G.; Frederix, P. W. J. M.; Mutasa, T.; Fleming, S.; Abul-Haija, Y. M.; Kelly, S. M.; Gachagan, A.; Kalafatovic, D.; Trevino, J.; Ulijn, R. V.; Bai, S. *Chem. Commun.*, **2015**, *51*, 8465-8468.
64. Chi, X.; Yu, G.; Ji, X.; Li, Y.; Tang, G.; Huang, F. *ACS Macro. Lett.*, **2015**, *4*, 996-999.
65. Zhou, Y.; Jie, K.; Shi, B.; Yao, Y. *Chem. Commun.*, **2015**, *51*, 11112-11114.
66. Wang, K.; Hu, Q.; Zhu, W.; Zhao, M.; Ping, Y.; Tang, G. *Adv. Funct. Mater.*, **2015**, *25*, 3380-3392.
67. Peng, L.; Zhang, H.; Feng, A.; Huo, M.; Wang, Z.; Hu, J.; Gao, W.; Yuan, J. *Polym. Chem.*, **2015**, *6*, 3652-3659.
68. Noorden, R. V.; Castelvechi, D. *Nature*, **2016**, *538*, 152-153.
69. Stoddart, J. F. *Chem. Soc. Rev.*, **2009**, *38*, 1802-1820.
70. Koumura, N.; Zijlstra, R. W. J.; Delden, R. A. V.; Harada, N.; Feringa, B. L. *Nature*, **1999**, *401*, 152-155.

-
71. Ercole, F.; Davis, T. P.; Evans, R. A. *Poly. Chem.*, **2010**, *1*, 37-54.
72. Brimioulle, R.; Bauer, A.; Bach, T. *J. Am. Chem. Soc.*, **2015**, *137*, 5170-5176.
73. Piantek, M.; Schulze, G.; Koch, M.; Franke, K. J.; Leyssner, F.; Krüger, A.; Navío, C.; Miguel, J.; Bernien, M.; Wolf, M.; Kuch, W.; Tegeder, P.; Pascual, J. I. *J. Am. Chem. Soc.*, **2009**, *131*, 12729-12735.
74. Uchida, K.; Yamanoi, Y.; Yonezawa, T.; Nishihara, H. *J. Am. Chem. Soc.*, **2011**, *133*, 9239-9241.
75. Bandara, H. M. D.; Burdette, S. C. *Chem. Soc. Rev.*, **2012**, *41*, 1809-1825.
76. Mitscherlich, E. *Ann. Pharm.*, **1834**, *12*, 311-314.
77. Nobel, A. *Annalen der Chemie und Pharmacie*, **1856**, *98*, 253-256.
78. Hartley, G. S. *Nature*, **1937**, *140*, 281-281.
79. Zhou H.; Xue, C.; Weis, P.; Suzuki, Y.; Huang, S.; Koynov, K.; Auernhammer, G. K.; Berger, R.; Butt, H.-J.; Wu, S. *Nat. Chem.*, **2017**, *9*, 145-151.
80. Hartley, G. S. *J. Chem. Soc.*, **1938**, *1*, 633-642
81. Magee, J. L.; Jr. Shand, W.; Eyring, H. *J. Am. Chem. Soc.*, **1941**, *63*, 677-688.
82. Fujino, T.; Arzhantsev, S. Y.; Tahara, T. *J. Phys. Chem. A.*, **2001**, *105*, 8123-8129.
83. Manakker, F. V. D.; Vermonden, T.; Nostrum, C. F. V.; Hennink, W. E. *Biomacromolecules*, **2009**, *10*, 3157-3175.
84. Villiers, A. *Bull. Soc. Chim. Paris.*, **1891**, *45*, 468.
85. Villiers, A. *C. R. Acad. Sci.* **1891**, *CXII*, 536.
86. Schardinger, F. *Zentralbl. Bakteriол., Parasitenkd., Infektionskrankh. Hyg., Abt. 2* **1905**, *XIV*, 772.
87. Schardinger, F. *Zentralbl. Bakteriол., Parasitenkd., Infektionskrankh. Hyg., Abt. 2* **1907**, *XIX*, 161.
88. Schardinger, F. *Zentralbl. Bakteriол., Parasitenkd., Infektionskrankh. Hyg., Abt. 2* **1911**, *29*, 188.
89. Freudenberg, K.; Blomqvist, G.; Ewald, L.; Soff, K. *Ber. Dtsch. Chem. Ges.*, **1936**,

- 69, 1258.
90. Freudenberg, K.; Rapp, W. *Ber. Dtsch. Chem. Ges.*, **1936**, 69, 2041.
91. Freudenberg, K.; Cramer, F. *Z. Naturforsch. B.*, **1948**, 3, 464.
92. Kratky, O.; Schneidmesser, B. *Ber. Dtsch. Chem. Ges.*, **1938**, 71, 1413.
93. Borchert, W. *Z. Naturforsch. B.*, **1948**, 3, 464.
94. Freudenberg, K.; Cramer, F. *Z. Naturforsch. B.*, **1948**, 3, 464.
95. French, D.; Rundle, R. E. *J. Am. Chem. Soc.*, **1942**, 64, 1651.
96. Cramer, F. Die cyclodextrine aus Stärke. *Dissertation*, Heidelberg, **1949**.
97. Yu, G.; Jie, K.; Huang, F. *Chem. Rev.*, **2015**, 115, 7240-7303.
98. Crini, G. *Chem. Rev.*, **2014**, 114, 10940-10975.
99. Harada, A.; Takashima, Y. Nakahata, M. *Acc. Chem. Res.*, **2014**, 47, 2128-2140.
100. Ikeda, A.; Aono, R.; Maekubo, N.; Katao, S.; Kikuchi, J.; Akiyama, M. *Chem. Commun.*, **2011**, 47, 12795-12797.
101. Cramer, F. *Angew. Chem.* **1952**, 64, 136.
102. Steed, J. W.; Atwood, J. L. *Supramolecular chemistry*. John Wiley & Sons, Ltd, Baffins Lane, Chichester, **2000**.
103. Ueno, A.; Tomita, Y.; Osa, T. *Tetrahedron. Lett.*, **1983**, 24, 5245-5248.
104. Fukushima, M.; Osa, T.; Ueno, A. *J. Chem. Soc., Chem. Commun.*, **1991**, 15-17.
105. Murakami, H.; Kawabuchi, A.; Kotoo, K. *J. Am. Chem. Soc.*, **1997**, 119, 7605-7606.
106. Jog, P. V.; Gin, M. S. *Org. Lett.*, **2008**, 10, 3693-3696.
107. Wang, Y.; Ma, N.; Wang, Z.; Zhang, X. *Angew. Chem.*, **2007**, 119, 2881-2884.
108. Zheng, X.; Wang, D.; Shuai, Z.; Zhang, X. *J. Phys. Chem. B*, **2012**, 116, 823-832.
109. Orojloo, M.; Amani, S. *Talanta*, **2016**, 159, 292-299.
110. Pouliquen, G.; Amiel, C.; Tribet, C. *J. Phys. Chem. B*, **2007**, 111, 5587-5595.

-
111. Maafi, M.; Mahedero, M. C.; Aaron, J. *Talanta*, **1997**, *44*, 2193-2199.
112. Benesi, H. A.; Hildebrand, J. H. *J. Am. Chem. Soc.*, **1949**, *71*, 2703-2707.
113. Samanta, A.; Guchhait, N.; Bhattacharya, S. C. *J. Phys. Chem. B*, **2014**, *118*, 13279-13289.
114. Sahana, A.; Banerjee, A.; Lohar, S.; Chottapadhyay, A.; Mukhopadhyay, S. K.; Das, D. *RSC Adv.*, **2013**, *3*, 14044-14047.
115. Indirapriyadharshini, V. K.; Karunanithi, P.; Ramamurthy, P. *Langmuir*, **2001**, *17*, 4056-4060.
116. Zhang, G.; Wang, L.; Cai, X.; Zhang, L.; Yu, J.; Wang, A. *Dyes. Pigm.*, **2013**, *98*, 232-237.
117. Tamesue, S.; Takashima, Y.; Yamaguchi, H.; Shinkai, S.; Harada, A. *Angew. Chem. Int. Ed.*, **2010**, *49*, 7461-7464.
118. Takashima, Y.; Hatanaka, S.; Otsubo, M.; Nakahata, M.; Kakuta, T.; Hashidzume, A.; Yamaguchi, H.; Harada, A. *Nat. Commun.*, **2012**, *3*, 1270.
119. Wang, M.; Zhang, X.; Li, L.; Wang, J.; Wang, J.; Ma, J.; Yuan, Z.; Lincoln, S. F.; Guo, X. *Macromol. Mater. Eng.*, **2016**, *301*, 191-198.
120. Tomatsu, I.; Hashidzume, A.; Harada, A. *J. Am. Chem. Soc.*, **2006**, *128*, 2226-2227.
121. Pierce, M. M.; Raman, C. S.; Nall, B. T. *Methods*, **1999**, *19*, 213-221.
122. https://en.wikipedia.org/wiki/Isothermal_titration_calorimetry
123. Wang, D.; Wagner, M.; Saydjari, A. K.; Mueller, J.; Winzen, S.; Butt, H.-J.; Wu, S. *Chem. Eur. J.*, **2017**, *23*, 2628-2634.
124. Auletta, T.; Jong, M. R. D.; Mulder, A.; Veggel, F. C. J. M. V.; Huskens, J.; Reinhoudt, D. N.; Zou, S.; Zapotoczny, S.; Schönherr, H.; Vancso, G. J.; Kuipers, L. *J. Am. Chem. Soc.*, **2004**, *126*, 1577-1584.
125. Ptak, A.; Kappl, M.; Butt, H.-J. *Appl. Phys. Lett.*, **2006**, *88*, 263109.
126. Butt, H.-J.; Cappella, B.; Kappl, M. *Surf. Sci. Rep.*, **2005**, *59*, 1-152.
127. Kaftan, O.; Tumbiolo, S.; Dubreuil, F.; Auzély-Velty, R.; Fery, A.;

- Papastavrou, G. *J. Phys. Chem. B*, **2011**, *115*, 7726-7735.
128. Zhang, Y.; Yu, J.; Bomba, H. N.; Zhu, Y.; Gu, Z. *Chem. Rev.*, **2016**, *116*, 12536-12563.
129. Ulbrich, K.; Holá, K.; Šubr, V.; Bakandritsos, A.; Tuček, J.; Zbořil, R. *Chem. Rev.*, **2016**, *116*, 5338-5431.
130. Ghosh, I.; Nau, W. M. *Adv. Drug. Delivery. Rev.*, **2012**, *64*, 764-783.
131. Park, C.; Lee, K.; Kim, C. *Angew. Chem. Int. Ed.*, **2009**, *48*, 1275-1278.
132. Luo, G.; Chen, W.; Jia, H.; Sun, Y.; Cheng, H.; Zhuo, R.; Zhang, X. *Nano. Res.*, **2015**, *8*, 1893-1905.
133. Gohy, J.; Zhao, Y. *Chem. Soc. Rev.*, **2013**, *42*, 7117-7129.
134. Zhao, Q.; Lian, Z.; Gao, X.; Yan, Y.; Huang, J. *Langmuir*, **2016**, *32*, 11973-11979.
135. Yao, H.; Qi, M.; Liu, Y.; Tian, W. *Chem. Eur. J.*, **2016**, *22*, 8508-8519.
136. Zhu, L.; Zhao, C.; Zhang, J.; Gong, D. *RSC Adv.*, **2015**, *5*, 84263-84268.
137. Zhang, H.; Xin, Y.; Yan, Q.; Zhou, L.; Peng, L.; Yuan, J. *Macromol. Rapid. Commun.*, **2012**, *33*, 1952-1957.
138. Li, J.; Zhou, Z.; Ma, L.; Chen, G.; Li, Q. *Macromolecules*, **2014**, *47*, 5739-5748.
139. Ferris, D. P.; Zhao, Y.; Khashab, N. M.; Khatib, H. A.; Stoddart, J. F.; Zink, J. I. *J. Am. Chem. Soc.*, **2009**, *131*, 1686-1688.
140. DOI: 10.1371/journal.pone.0160705
141. Zhang, X.; Huang, Y.; Ghazwani, M.; Zhang, P.; Li, J.; Thorne, S. T.; Li, S. *ACS Macro. Lett.*, **2015**, *4*, 620-623.
142. Duan, Q.; Cao, Y.; Li, Y.; Hu, X.; Xiao, T.; Lin, C.; Pan, Y.; Wang, L. *J. Am. Chem. Soc.*, **2013**, *135*, 10542-10549.
143. Kauscher, U.; Samanta, A.; Ravoo, B. J. *Org. Biomol. Chem.*, **2014**, *12*, 600-606.
144. Grolman, J. M.; Inci, B.; Moore, J. S. *ACS Macro. Lett.*, **2015**, *4*, 441-445.

-
145. Wang, J.; Wang, X.; Yang, F.; Shen, H.; You, Y.; Wu, D. *Langmuir*, **2014**, *30*, 13014-13020.
146. Liu, Y.; Yu, C.; Jin, H.; Jiang, B.; Zhu, X.; Zhou, Y.; Lu, Z.; Yan, D. *J. Am. Chem. Soc.*, **2013**, *135*, 4765-4770.
147. Tong, Z.; Wang, R.; Huang, J.; Xu, J.; Fan, Z. *Polym. Chem.*, **2015**, *6*, 2214-2225.
148. Wang, S.; Shen, Q.; Nawaz, M. H.; Zhang, W. *Polym. Chem.*, **2013**, *4*, 2151-2157.
149. Cheng, L.; Wang, C.; Feng, L.; Yang, K.; Liu, Z. *Chem. Rev.*, **2014**, *114*, 10869-10939.
150. Pitsillides, C. M.; Joe, E. K.; Wei, X.; Anderson, R. R.; Lin, C. P. *Biophys. J.*, **2003**, *84*, 4023-4032.
151. Vivero-Escoto, J. L.; Huxford-Phillips, R. C.; Lin, W. B. *Chem. Soc. Rev.*, **2012**, *41*, 2673-2685.
152. Couleaud, P.; Morosini, V.; Frochot, C.; Richeter, S.; Raehm, L.; Durand, J. *O. Nanoscale*, **2010**, *2*, 1083-1095.
153. *Zeitschrift für Chemie und Industrie der Kolloide*, **1907**, *1*, 213-214.
154. Verhulsel, M.; Vignes, M.; Descroix, S.; Malaquin, L.; Vignjevic, D. M.; Viovy, J. *Biomaterials*, **2014**, *35*, 1816-1832.
155. Billiet, T.; Vandenhaute, M.; Schelfhout, J.; Vlierberghe, S. V.; Dubruel, P. *Biomaterials*, **2012**, *33*, 6020-6041.
156. Smith, M. H.; Lyon, L. A. *Acc. Chem. Res.*, **2012**, *45*, 985-993.
157. Park, M. H.; Joo, M. K.; Choi, B. G.; Jeong, B. *Acc. Chem. Res.*, **2012**, *45*, 424-433.
158. Chen, X.; Liu, Z.; Parker, S. G.; Zhang, X.; Gooding, J. J.; Ru, Y.; Liu, Y.; Zhou, Y. *ACS Appl. Mater. Interfaces.*, **2016**, *8*, 15857-15863.
159. Guan, Y.; Zhao, H.; Yu, L.; Chen, S.; Wang, Y. *RSC Adv.*, **2014**, *4*, 4955-4959.

160. Li, Z.; Zheng, Z.; Su, S.; Yu, L.; Wang, X. *Soft. Matter.*, **2016**, *12*, 7089-7101.
161. Liu, K. L.; Zhu, J.; Li, J. *Soft. Matter.*, **2010**, *6*, 2300-2311.
162. Li, Z.; Zheng, Z.; Su, S.; Yu, L.; Wang, X. *Macromolecules*, **2016**, *49*, 373-386.
163. Liao, X.; Chen, G.; Liu, X.; Chen, W.; Chen, F.; Jiang, M. *Angew. Chem. Int. Ed.*, **2010**, *49*, 4409-4413.
164. Kolind, K.; Leong, K. W.; Besenbacher, F.; Foss, M. *Biomaterials*, **2012**, *33*, 6626-6633.
165. Shin, H.; Jo, S.; Mikos, A. G. *Biomaterials*, *24*, 4353-4364.
166. Yoshikawa, M.; Tharpa, K.; Dima, S. *Chem. Rev.*, **2016**, *116*, 11500-11528.
167. Chen, L.; Wang, X.; Lu, W.; Wu, X.; Li, J. *Chem. Soc. Rev.*, **2016**, *45*, 2137-2211.
168. Chen, K.; Song, S.; Liu, F.; Xue, D. *Chem. Soc. Rev.*, **2015**, *44*, 6230-6257.
169. Nie, C.; Cheng, C.; Ma, L.; Deng, J.; Zhao, C. *Langmuir*, **2016**, *32*, 5955-5965.
170. Ma, L.; Cheng, C.; Nie, C.; He, C.; Deng, J.; Wang, L.; Xia, Y.; Zhao, C. *J. Mater. Chem. B*, **2016**, *4*, 3203-3215.
171. Deng, J.; Liu, X.; Zhang, S.; Cheng, C.; Nie, C.; Zhao, C. *Langmuir*, **2015**, *31*, 9665-9674.
172. Wan, P.; Jiang, Y.; Wang, Y.; Wang, Z.; Zhang, X. *Chem. Commun.*, **2008**, *44*, 5710-5712.
173. Deng, J.; Liu, X.; Shi, W.; Cheng, C.; He, C.; Zhao, C. *ACS Macro. Lett.*, **2014**, *3*, 1130-1133.
174. Manna, D.; Udayabhaskararao, T.; Zhao, H.; Klajn, R. *Angew. Chem. Int. Ed.*, **2015**, *54*, 12394-12397.
175. Ryu, Y.; Jin, Z.; Lee, J.; Noh, S.; Shin, T.; Jo, S.; Choi, J.; Park, H.; Cheon, J.; Kim, H. *Angew. Chem. Int. Ed.*, **2015**, *54*, 923-926.

-
176. Lan, Y.; Wu, Y.; Karas, A.; Scherman, O. A. *Angew. Chem. Int. Ed.*, **2014**, *53*, 2166-2169.
177. Pyun, J. *Angew. Chem. Int. Ed.*, **2012**, *51*, 12408-12409.
178. Chen, Q.; Bae, S.; Granick, S. *Nature*, **2011**, *469*, 381-385.
179. Zhang, J.; Yan, J.; Granick, S. *Angew. Chem. Int. Ed.*, **2016**, *55*, 5166-5169.
180. Yan, J.; Bae, S.; Granick, S. *Adv. Mater.*, **2015**, *27*, 874-879.
181. Krings, J. A.; Vönhören, B.; Tegeder, P.; Siozios, V.; Peterlechner, M.; Ravoo, B. J. *J. Mater. Chem. A*, **2014**, *2*, 9587-9593.
182. Zhou, Y.; Wang, D.; Huang, S.; Auernhammer, G.; He, Y.; Butt, H.-J.; Wu, S. *Chem. Commun.*, **2015**, *51*, 2725-2727.
183. Vrouwe, M. G.; Pines, A.; Overmeer, R. M.; Hanada, K.; Mullenders, L. H. F. *J. Cell. Sci.*, **2010**, *124*, 435-446.
184. Banerjee, G.; Gupta, N.; Kapoor, A.; Raman, G. *Cancer. Lett.*, **2005**, *223*, 275-284.
185. Wang, Z.; Johns, V. K.; Liao, Y. *Chem. Eur. J.*, **2014**, *20*, 14637-14640.
186. Juzenas, P.; Juzeniene, A.; Kaalhus, O.; Iani, V.; Moan, J. *Photochem. Photobiol. Sci.*, **2002**, *1*, 745-748.
187. Huang, X.; Han, S.; Huang, W.; Liu, X. *Chem. Soc. Rev.*, **2013**, *42*, 173-201.
188. Wu, H.; Ying, L.; Yang, W.; Cao, Y. *Chem. Soc. Rev.*, **2009**, *38*, 3391-3400.
189. Liu, J.; Bu, W.; Pan, L.; Shi, J. *Angew. Chem. Int. Ed.*, **2013**, *52*, 4375-4379.
190. Dong, J.; Zink, J. I. *Small*, **2015**, *11*, 4165-4172.
191. Möller, N.; Hellwig, T.; Stricker, L.; Engel, S.; Fallnich, C.; Ravoo, B. J. *Chem. Commun.*, **2017**, *53*, 240-243.
192. He, S.; Krippes, K.; Ritz, S.; Chen, Z.; Best, A.; Butt, H.-J.; Mailänder, V.; Wu, S. *Chem. Commun.*, **2015**, *51*, 431-434.
193. Chen, Z.; Sun, W.; Butt, H.-J.; Wu, S. *Chem. Eur. J.*, **2015**, *21*, 9165-9170.
194. Shen, Y.; Shuhendler, A. J.; Ye, D.; Xu, J.; Chen, H. *Chem. Soc. Rev.*, **2016**, *45*, 6725-6741.

-
195. Xing, J.; Zheng, M.; Duan, X. *Chem. Soc. Rev.*, **2015**, *44*, 5031-5039.
196. Kneipp, J.; Kneipp, H.; Kneipp, K. *Chem. Soc. Rev.*, **2008**, *37*, 1052-1060.
197. Izquierdo-Serra, M.; Gascón-Moya, M.; Hirtz, J. J.; Pittolo, S.; Poskanzer, K. E.; Ferrer, E.; Alibés, R.; Busqué, F.; Yuste, R.; Hernando, J.; Gorostiza, P. *J. Am. Chem. Soc.*, **2014**, *136*, 8693-8701.
198. Carroll, E. C.; Berlin, S.; Levitz, J.; Kienzler, M. A.; Yuan, Z.; Madsen, D.; Larsen, D. S.; Isacoff, E. Y. *Proc. Natl. Acad. Sci.*, **2015**, *112*, 776-785.
199. Chu, C.; Chang, Y.; Tsai, B.; Lin, T.; Lin, J.; Hsiao, V. K. S. *Chem. Asian. J.*, **2014**, *9*, 3390-3396.
200. Croissant, J.; Maynadier, M.; Gallud, A.; N'Dongo, H. P.; Nyalosaso, J. L.; Derrien, G.; Charnay, C.; Durand, J.; Raehm, L.; Serein-Spirau, F.; Cheminet, N.; Jarrosson, T.; Mongin, O.; Blanchard-Desce, M.; Gary-Bobo, M.; Garcia, M.; Lu, J.; Tamanoi, F.; Tarn, D.; Guardado-Alvarez, T. M.; Zink, J. I. *Angew. Chem. Int. Ed.*, **2013**, *52*, 13813-13817.
201. Forber, C. L.; Kelusky, E. C.; Bunce, N. J.; Zerner, M. C. *J. Am. Chem. Soc.*, **1985**, *107*, 5884-5890.
202. Bunce, N. J.; Ferguson, G.; Forber, C. L.; Stachnyk, G. J. *J. Org. Chem.*, **1987**, *52*, 394-398.
203. Beharry, A. A.; Sadovski, O.; Woolley, G. A. *J. Am. Chem. Soc.*, **2011**, *133*, 19684-19687.
204. Samanta, S.; Beharry, A. A.; Sadovski, O.; McCormick, T. M.; Babalhavaeji, A.; Tropepe, V.; Woolley, G. A. *J. Am. Chem. Soc.*, **2013**, *135*, 9777-9784.
205. Velema, W. A.; Szymanski, W.; Feringa, B. L. *J. Am. Chem. Soc.*, **2014**, *136*, 2178-2191.
206. Wegner, H. A. *Angew. Chem. Int. Ed.*, **2012**, *51*, 4787-4788.
207. Weis, P.; Wang, D.; Wu, S. *Macromolecules*, **2016**, *49*, 6368-6373.
208. Bléger, D.; Schwarz, J.; Brouwer, A. M.; Hecht, S. *J. Am. Chem. Soc.*, **2012**, *134*, 20597-20600.

-
209. Movsisyan, M.; Delbeke, E. I. P.; Berton, J. K. E. T.; Battilocchio, C.; Ley, S. V.; Stevens, C. V. *Chem. Soc. Rev.*, **2016**, *45*, 4892-4928.
210. Shao, X.; Xu, C.; Lu, L.; Shen, Q. *Acc. Chem. Res.*, **2015**, *48*, 1227-1236.
211. Mercey, G.; Verdelet, T.; Renou, J.; Kliachyna, M.; Baati, R.; Nachon, F.; Jean, L.; Renard, P. *Acc. Chem. Res.*, **2012**, *45*, 756-766.
212. Yang, Y.; Hughes, R. P.; Aprahamian, I. *J. Am. Chem. Soc.*, **2012**, *134*, 15221-15224.
213. Yang, Y.; Hughes, R. P.; Aprahamian, I. *J. Am. Chem. Soc.*, **2014**, *136*, 13190-13193.
214. Zhang, L.; Zhang, H.; Gao, F.; Peng, H.; Ruan, Y.; Xu, Y.; Weng, W. *RSC Adv.*, **2015**, *5*, 12007-12014.
215. Dong, R.; Hu, Y.; Wu, Y.; Gao, W.; Ren, B.; Wang, Q.; Cai, Y. *J. Am. Chem. Soc.*, **2017**, *139*, 1722-1725.
216. Kalka, K.; Merk, H.; Mukhtar, H. *J. Am. Acad. Dermatol.*, **2000**, *42*, 389-413.

Supramolecular Hydrogels Constructed by Red-Light-Responsive Host-Guest Interactions for Photo-Controlled Protein Release in Deep Tissue

Reprinted with permission from:

Wang, D.; Wagner, M.; Butt, H. -J.; Wu, S. *Soft. Matter.*, **2015**, *11*, 7656-7662.

Copyright (2015) by the Royal Society of Chemistry.

Statement of Contribution

convinced the idea.

led this work.

and D. Wang designed the experiment.

measured the NMR.

D. Wang did the synthesis and other measurements.

D. Wang and wrote the manuscript.

Abstract

We report a novel red-light-responsive supramolecule. The tetra-ortho-methoxy-substituted azobenzene (mAzO) and β -cyclodextrin (β -CD) spontaneously formed a supramolecular complex. The substituted methoxy groups shifted the responsive wavelength of the azo group to the red light region, which is in the therapeutic window and desirable for biomedical applications. Red light induced the isomerization of mAzO and the disassembly of the mAzO/ β -CD supramolecular complex. We synthesized a mAzO-functionalized polymer and a β -CD-functionalized polymer. Mixing the two polymers in an aqueous solution generated a supramolecular hydrogel. Red light irradiation induced a gel-to-sol transition as a result of the disassembly of the mAzO/ β -CD complexes. Proteins were loaded in the hydrogel. Red light could control protein release from the hydrogel in tissue due to its deep

penetration depth in tissue. We envision the use of red-light-responsive supramolecules for deep-tissue biomedical applications.

Chapter 2

Supramolecular Hydrogels Constructed by Red-Light-Responsive Host-Guest Interactions for Photo-Controlled Protein Release in Deep Tissue

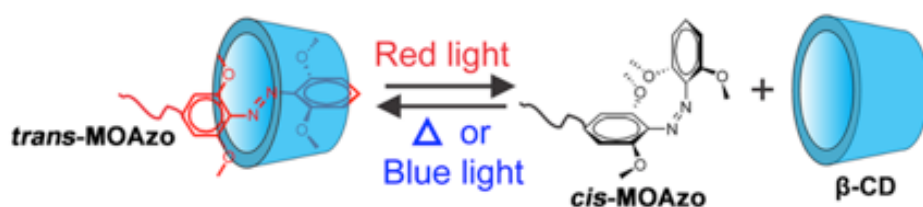
2.1 Introduction

Supramolecular interactions are non-covalent interactions between two or more molecules. Due to their moderate bond strength and reversibility, supramolecular interactions are usually responsive to external stimuli, such as light, pH, and redox [1-16]. Supramolecular interactions can be used to construct stimuli-responsive materials for various applications.¹ Photoresponsive supramolecular materials, for example, exhibit numerous biomedical applications, including drug delivery, photo-controlled protein adsorption and cell adhesion [17-19]. Currently, most photoresponsive supramolecules efficiently absorb UV light and are thus controlled by UV light. However, UV light is problematic in biomedical applications. Compared with UV light, red and near-infrared (NIR) light in the therapeutic window (600-900 nm) are better suited for biomedical applications because they cause less photodamage and can penetrate deeper into tissue. Therefore, red- or NIR-light-responsive supramolecules are desirable for biomedical applications.

One approach to design red- or NIR-light-responsive supramolecules is based on

simultaneous two-photon absorption. However, this method is inefficient even when high-intensity femtosecond lasers are used. Another approach to achieve red- or NIR-light-responsive supramolecules is by coupling UV-responsive supramolecules with upconverting nanoparticles. However, photon upconversion requires high-intensity lasers that may cause overheating problems and photodamage to biomaterials [20-22].

Red-shifting the responsive wavelength of photoresponsive supramolecules is an approach to prepare intrinsic red- or NIR-light-responsive supramolecules. This approach should be more efficient than nonlinear optical processes such as two photon absorption and photon upconversion because red or NIR light are directly absorbed by supramolecules. To construct red- or NIR-light-responsive supramolecules, we may red-shift the responsive wavelength of UV-responsive supramolecules. It is well-known that *trans* azobenzene can spontaneously form supramolecular complexes with α - or β -cyclodextrin (CD) [1-10, 17-19]. UV irradiation can induce *trans*-to-*cis* isomerization of azobenzene, which leads to the disassembly of the supramolecular complexes [1-10, 17-19]. Recently, new azo derivatives have been synthesized to red-shift the responsive wavelength of the azo group [23-27]. In particular, some azo derivatives are responsive to red or NIR light [28, 29]. However, the feasibility of using the azo derivatives to construct red- or NIR-light-responsive supramolecules has not been explored. Moreover, no attention has been focused on constructing intrinsic red- or NIR-light-responsive supramolecules.



Scheme 2.1 Schematic illustration of the supramolecular interaction between mAzo and β -CD. Red light irradiation triggers the disassembly of the mAzo/ β -CD complex; blue light irradiation or heating triggers the reassembly of the complex.

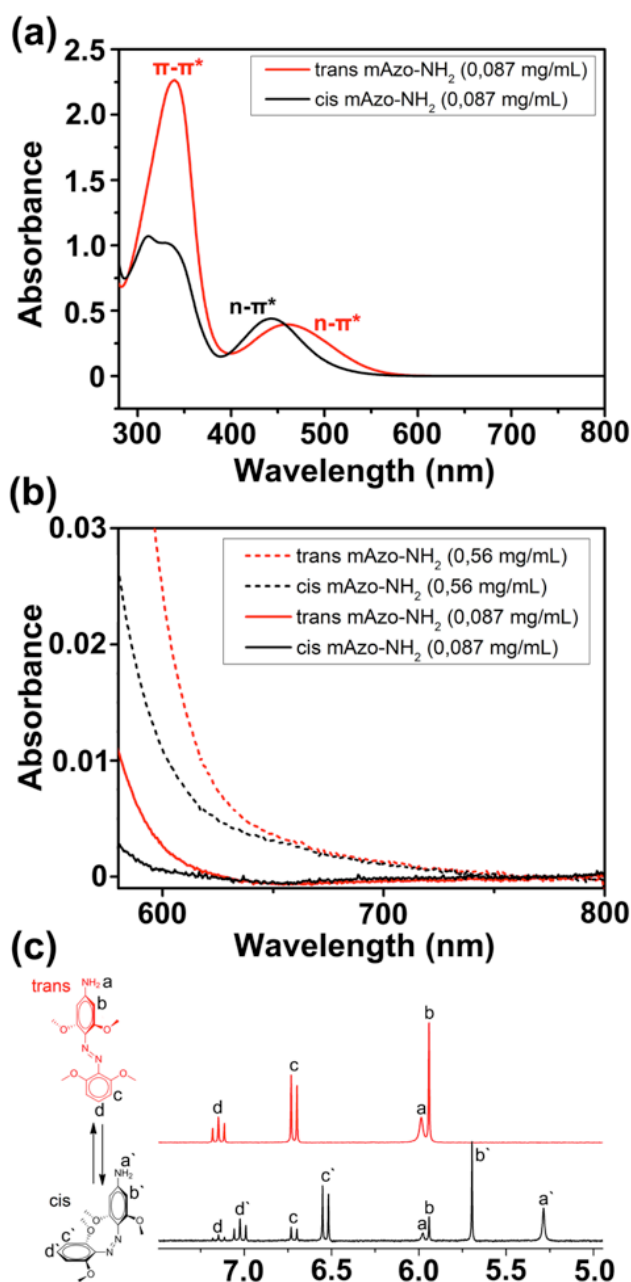


Figure 2.1 (a) UV/vis absorption spectra of mAzo-NH₂ (0.087 mg/mL in DMSO) before and after the 625-nm red light irradiation (60 mW/cm², 30 min). (b) Enlarged absorption spectra of mAzo-NH₂ in the red-light region. mAzo-NH₂ solutions with low (0.087 mg/mL) and high (0.56 mg/mL) concentrations are measured. The $n-\pi^*$ band of the trans isomer extends to the red-light region. (c) ¹H-NMR spectra (250 MHz in DMSO-d₆ at 298 K) of mAzo-NH₂ before (red) and after (black) red light irradiation (625 nm, 60 mW/cm², 30 min)

Here, we fabricate red-light-responsive supramolecules using tetra-ortho-methoxy-substituted azobenzene (mAzo) and β -CD (**Scheme 2.1**). Based on the red-light-responsive supramolecules, we prepared a responsive hydrogel that showed a gel-to-sol transition under red light irradiation. The hydrogel was used as a protein carrier. Red light was demonstrated to be able to control protein release from the hydrogel even in deep tissue. Compared with the conventional UV-responsive supramolecular interaction of azobenzene and CD, the new red-light-responsive supramolecular interaction reported in this paper is more suitable for biomedical applications.

2.2 Photoresponse of tetra-ortho-methoxy-substituted azobenzene

We synthesized mAzo-NH₂ and studied its red-light-induced isomerization by ¹H-NMR and UV/Vis absorption spectroscopy (**Figure 2.1**). The $n\text{-}\pi^*$ transition band of *trans* mAzo-NH₂ extended to the red-light region and was separated from that of *cis* mAzo-NH₂ (**Figure 2.1a**). Thus, red light could excite *trans* mAzo-NH₂ and induce *trans*-to-*cis* isomerization [27-29]. Approximately 85% of the *trans* isomers switched to *cis* isomers after 625 nm red light irradiation for 30 min (60 mW/cm²) (**Figure 2.1c**). The *cis* mAzo-NH₂ could change back to *trans* isomers by heating or blue light irradiation.

2.3 Red-light-responsive supramolecular interactions

To investigate the supramolecular interactions between mAzo and CDs in aqueous solutions, the hydrophilic compound mAzo-Py was synthesized by grafting mAzo-NH₂ with pyridinium (**Figure 2.2, S2.1**). Red light could still induce isomerization of mAzo-Py in the presence of CDs (**Figure S2.5**). The supramolecular interactions between mAzo-Py and β -CD in D₂O were studied by NMR spectroscopy

Figure 2.2, S2.6, S2.7). In two-dimensional nuclear Overhauser effect spectroscopy (2D NOESY), the correlation between the protons of *trans* mAzo-Py (Proton 1 and 2) and the inner proton of β -CD (Proton f) demonstrated the host-guest interaction between *trans* mAzo-Py and β -CD (**Figure 2.2**, left). Moreover, adding *trans* mAzo-Py to the solution of β -CD caused the shift of the signals of the inner protons of β -CD (**Figure S2.6**), suggesting that *trans* mAzo-Py entered the cavity of β -CD. Furthermore, the correlation between the carbons of *trans* mAzo-Py and the inner protons of β -CD also proved the host-guest interaction between *trans* mAzo-Py and β -CD (**Figure S2.7**). To study the interaction between *cis* mAzo-Py and β -CD, *trans* mAzo-Py was converted to *cis* mAzo-Py by red light irradiation. No dipole-dipole (2D NOESY) correlation between the protons of *cis* mAzo-Py (Proton 3 and 4) and the inner protons of β -CD indicated that red light irradiation triggered the disassembly of the host-guest complex (**Figure 2.2**, right). Thus, the supramolecular interaction between mAzo-Py and β -CD was red-light-responsive.

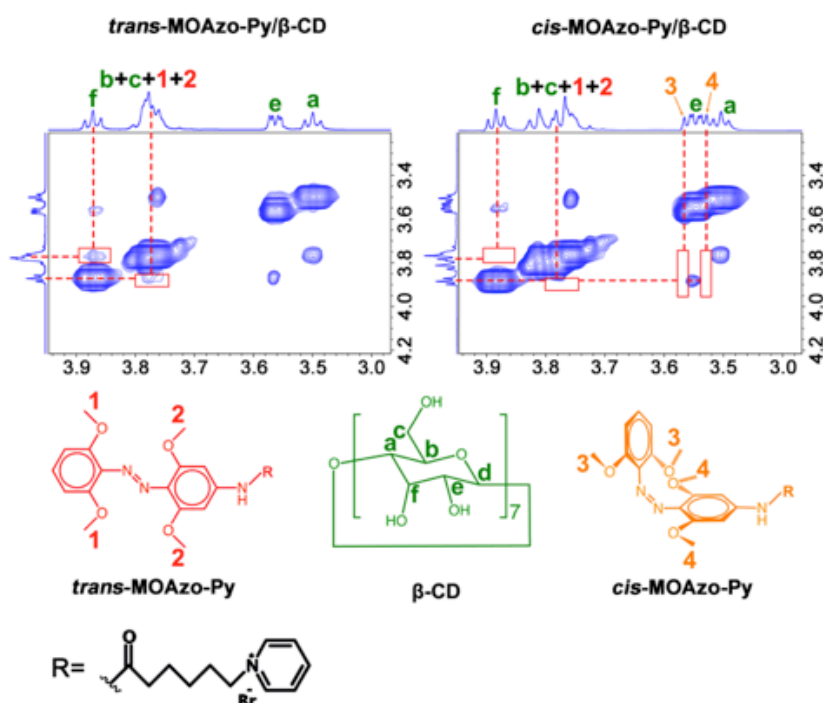


Figure 2.2 2D NOESY spectra (700 MHz in D₂O at 298 K) of *trans* mAzo-Py/ β -CD (left) and *cis* mAzo-Py/ β -CD (right). Corresponding protons in the spectra are shown

on the chemical structures of *trans* mAzo-Py, β -CD and *cis* mAzo-Py. The red rectangles in the spectra show whether there are correlation peaks between the protons of mAzo and the protons of β -CD. The concentration of β -CD is 1.67 mg/mL. The molar ratio of mAzo-Py/ β -CD is 1/1

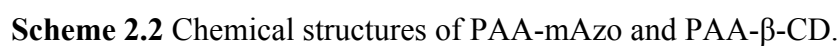
Table 2.1. Association constants (K_a) between α -CD or β -CD and the tetra-ortho-methoxy-substituted azobenzene (mAzo) group or the normal azobenzene group.^a

Host	Guest	K_a (M^{-1})
α -CD	<i>trans</i> mAzo	145.2
α -CD	<i>cis</i> mAzo	66.9
α -CD	<i>trans</i> azobenzene	1744.7
α -CD	<i>cis</i> azobenzene	11.9
β -CD	<i>trans</i> mAzo	1546
β -CD	<i>cis</i> mAzo	82.1
β -CD	<i>trans</i> azobenzene	892.1
β -CD	<i>cis</i> azobenzene	363.4

^aThe details for measuring K_a are provided in the Supporting Information (Equation S1 and **Figure S2.14-S2.19**)

The association constants between the mAzo group and CDs were measured by 1H -NMR spectroscopy to quantify the supramolecular interactions (**Figure S2.8-S2.12, S2.14-S2.18**). The association constants between the normal azobenzene group and CDs were also measured for comparison (**Figure S2.19**). The association constants are listed in **Table 2.1**. For normal azobenzene, both α - and β -CDs had high association constants with the *trans* isomer and low association constants with the *cis* isomer. Thus, both the azobenzene/ α -CD and azobenzene/ β -CD supramolecules were

2.4 Red-light-responsive sol-gel transition systems



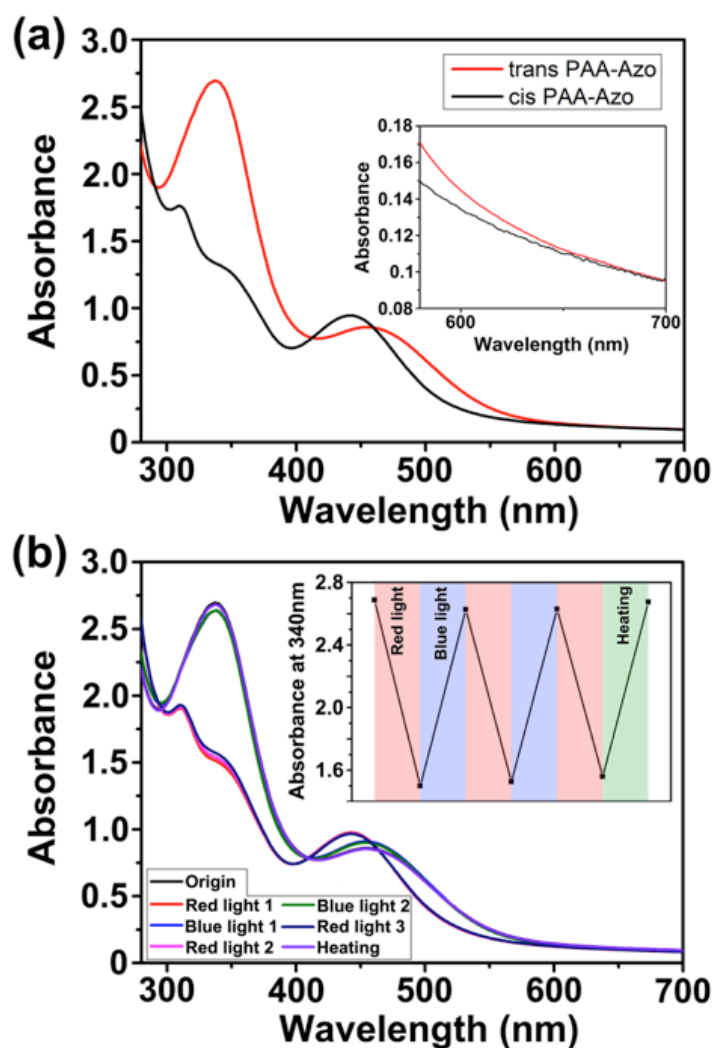


Figure 2.3 UV-vis absorption spectra of PAA-mAzo (1.43 mg/mL in H₂O) before and after red light irradiation (60 mW/cm², 30 min). The inset shows the enlarged absorption spectra of PAA-mAzo in the red-light region. (b) UV-vis spectra of the PAA-mAzo after alternate red/blue light irradiation (60 mW/cm², 30 min) and heating (60 °C, 10 h). The inset shows the changes of absorbance at 340 nm.

To demonstrate the potential applications of the mAzo/ β -CD interaction in stimuli-responsive materials, we fabricated supramolecular hydrogels. The gelators PAA-mAzo and PAA- β -CD were synthesized by grafting poly(acrylic acid) with mAzo and β -CD moieties, respectively (**Scheme 2.2**, **Figure S2.2**, **S2.3**). Similar to

mAzo-NH₂ and mAzo-Py, PAA-mAzo showed red-light-induced isomerization (**Figure 2.3a**). Red light induced *trans*-to-*cis* isomerization of PAA-mAzo because the n- π^* band of the *trans* isomer extended to the red-light region. Both blue light and heating can induce *cis*-to-*trans* isomerization. Approximately 95% of *trans* PAA-mAzo was obtained after *cis* PAA-mAzo was irradiated by blue light for 1 min (60 mW/cm²). Approximately 100% of *trans* PAA-mAzo could be obtained after *cis* PAA-mAzo was heated at 60 °C for 10 h. The isomerization can be switched reversibly for many times (**Figure 2.3b**).

Supramolecular hydrogels were prepared by mixing *trans* PAA-mAzo and PAA- β -CD in PBS buffer in the dark (ESI). Gelation occurred because the mAzo/ β -CD supramolecular complexes cross-linked the polymers (**Figure 2.4a**). Red light irradiation (625 nm, 60 mW/cm², 30 min) triggered the disassembly of the supramolecular complexes and a gel-to-sol transition (**Figure 2.4b**). The gel-to-sol transition was reversible. Blue light irradiation or heating could induce the sol-to-gel transition. Our red-light-responsive hydrogel is better suited for biomedical applications than the conventional UV-responsive hydrogel because red light can penetrate deeper into tissue and cause less photodamage to biomaterials [14, 15]. Thus, it pushes photoresponsive hydrogels one step further toward biomedical applications.

2.5 Red-light-controlled protein release

The red-light-responsive supramolecular hydrogel was applied as a platform for controlled release of proteins (**Scheme 2.3**). Fluorescently labeled bovine serum albumin (BSA) was loaded in the supramolecular hydrogel (ESI). Red light irradiation induced the collapse of the hydrogel and the release of BSA (**Figure 2.5a**). The amounts of released BSA under different irradiation conditions were quantified by fluorescence spectroscopy (**Figure 2.5b**, **S2.20**, **S2.21**). Only 9% BSA was released when the BSA-loaded hydrogel was kept in the dark for 60 min. Blue light

irradiation (470 nm, 60 mW/cm²) for 60 min induced the release of only 15% BSA. Approximately 45% BSA was released after red light irradiation (625 nm, 15 mW/cm²) for 60 min. The release rate increased, and ~83% BSA was released after higher-intensity (60 mW/cm²) red light irradiation for 60 min. We could also control the protein release kinetics “on-demand” via alternating red and blue light irradiation (Figure 2.5c).

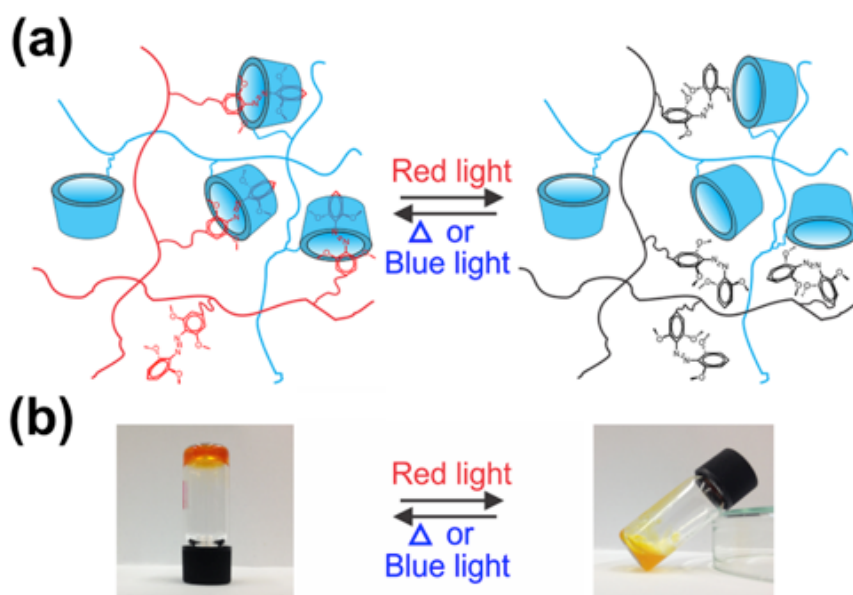
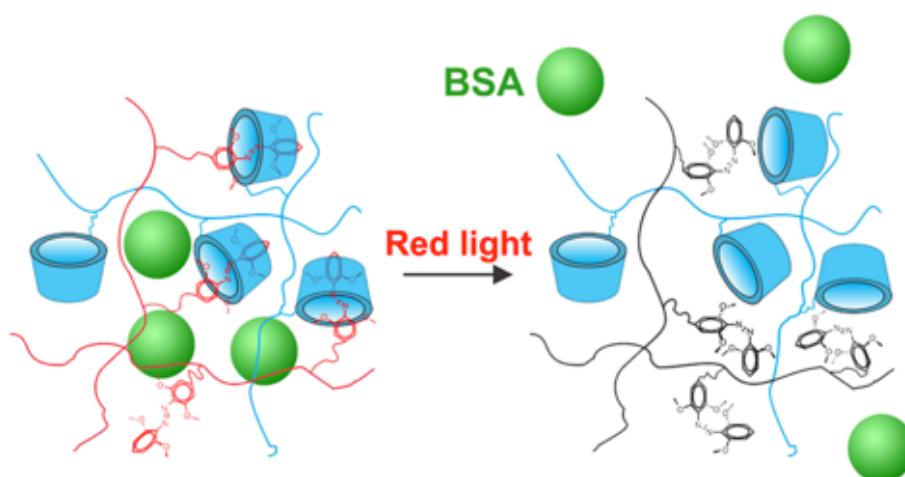


Figure 2.4 Schematic model (a) and photographs (b) of the reversible sol-gel transition of the PAA-mAzo/PAA-β-CD mixture.



Scheme 2.3 Schematic illustration of red-light-induced protein release from the PAA-mAzo/PAA-β-CD hydrogel.

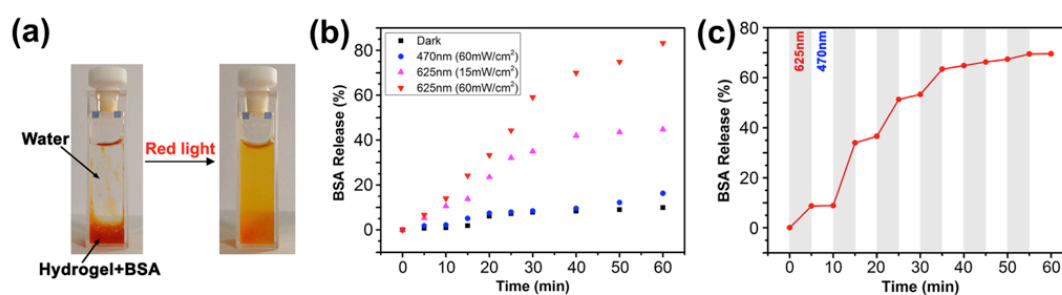


Figure 2.5 (a) Photographs of red-light-induced protein release from the PAA-mAzo/PAA- β -CD hydrogel. The BSA-loaded hydrogel at the bottom of the cuvette was irradiated by red light (625 nm, 60 mW/cm²) for 30 min. (b) Protein release profiles for BSA-loaded PAA-mAzo/PAA- β -CD hydrogel in the dark, upon blue light irradiation (470 nm, 60 mW/cm²) and red light irradiation (625 nm, 15 mW/cm² or 60 mW/cm²). (c) “On-demand” release of BSA from the hydrogel by alternating red (625 nm, 60 mW/cm²) and blue light (470 nm, 60 mW/cm²) irradiation.

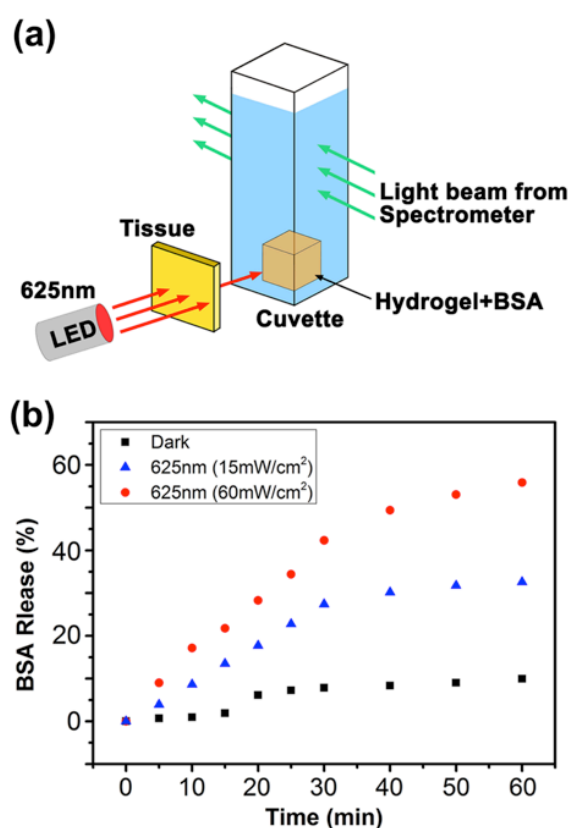


Figure 2.6 Experimental setup (a) and protein release profiles (b) when a 2-mm-thick

tissue sample was placed between the light source and the BSA-loaded hydrogel.

To test whether the supramolecular hydrogel maintained the red light responsiveness in deep tissue, a piece of pork tissue was placed between the light source and the sample (**Figure 2.6a**). Red light (625 nm, 15 or 60 mW/cm²) still induced protein release after passing through the tissue (**Figure 2.6b**). Importantly, the light intensity used in this experiment (15 and 60 mW/cm²) was an order of magnitude lower than the maximum permissible exposure of skin at 625 nm (200 mW/cm²) [30, 31]. This light intensity was also much lower than that for upconverting-nanoparticle-assisted photochemistry [20-22]. Therefore, photodamage to the tissue was prevented (**Figure S2.22**).

2.6 Conclusion

In summary, we demonstrated the red-light-responsive supramolecular interaction between mAzo and β -CD. Supramolecular hydrogels were prepared by mixing the mAzo-functionalized polymer and the β -CD-functionalized polymer in an aqueous solution. Red light irradiation induced the disassembly of the mAzo/ β -CD complexes and a gel-to-sol transition. The supramolecular hydrogel was used as a protein carrier. Red light could precisely control the protein release from the hydrogel. The red-light-responsive supramolecules exhibited several advantages over the conventional UV-responsive supramolecules for biomedical applications: (i) they could be controlled in deep tissue; (ii) controlling the supramolecules using low-intensity red light prevented photodamage to the biomaterials. We expect the mAzo/ β -CD interaction to be useful not only for constructing hydrogels but also for constructing red-light-responsive supramolecular surfaces, polymers, colloids and macroscopic assemblies. Additionally, we expect that not only azo derivatives but also other visible- or NIR-light-responsive compounds should be suitable for

constructing supramolecular assemblies via rational design [32-36]. We envision using red- or NIR-light-responsive supramolecules for drug delivery, protein therapy, optogenetics, and control adhesion and migration of cells.

References

1. in *Supramolecular Chemistry: Concepts and Perspectives*, ed. J.-M. Lehn, Wiley-VCH Verlag GmbH & Co. KGaA, Weinheim, 2006.
2. Cheng, M.; Shi, F.; Li, J.; Lin, Z.; Jiang, C.; Xiao, M.; Zhang, L.; Yang, W.; Nishi, T. *Adv. Mater.*, **2014**, *26*, 3009-3013.
3. Cheng, M.; Liu, Q.; Xian, Y.; Shi, F. *ACS Appl. Mater. Interfaces.*, **2014**, *6*, 7572-7578.
4. Zhou, Y.; Wang, D.; Huang, S.; Auernhammer, G.; He, Y.; Butt, H.-J.; Wu, S. *Chem. Commun.*, **2015**, *51*, 2725-2727.
5. Wang, D.; Xie, D.; Shi, W.; Sun, S.; Zhao, C. *Langmuir*, **2013**, *29*, 8311-8319.
6. Takashima, Y.; Hatanaka, S.; Otsubo, M.; Nakahata, M.; Kakuta, T.; Hashidzume, A.; Yamaguchi, H.; Harada, A. *Nat. Commun.*, **2012**, *3*, 1270.
7. Zhang, B.; Liang, Y.; Yang, W.; Yang, Y.; Wu, L. *Chem. Commun.*, **2014**, *50*, 10823-10826.
8. Yue, L.; Ai, H.; Yang, Y.; Lu, W.; Wu, L. *Chem. Commun.*, **2013**, *49*, 9770-9772.
9. Zhao, Q.; Wang, Y.; Yan, Y.; Huang, J. *ACS Nano.*, **2014**, *11*, 11341-11349.
10. Jiang, L.; Yan, Y.; Huang, J. *Adv. Colloid. Interface. Sci.*, **2011**, *169*, 13-25.
11. Tan, L.; Wu, H.; Yang, M.; Liu, C.; Zhuo, R. *RSC Adv.*, **2015**, *5*, 10393-10399.
12. Wu, S.; Duan, S.; Lei, Z.; Su, W.; Zhang, Z.; Wang, K.; Zhang, Q. *J. Mater. Chem.*, **2010**, *20*, 5202-5209.
13. Wu, S.; Bubeck, C. *Macromolecules*, **2013**, *46*, 3512-3518.
14. Tamesue, S.; Takashima, Y.; Yamaguchi, H.; Shinkai, S.; Harada, A. *Angew. Chem. Int. Ed.*, **2010**, *49*, 7461-7464.
15. Liao, X.; Chen, G.; Liu, X.; Chen, W.; Chen, F.; Jiang, M. *Angew. Chem. Int. Ed.*, **2010**, *49*, 4409-4413.
16. Deng, J.; Liu, X.; Shi, W.; Cheng, C.; He, C.; Zhao, C. *ACS Macro. Lett.*, **2014**, *3*, 1130-1133.
17. Wan, P. B.; Wang, Y. P.; Jiang, Y. G.; Xu, H. P.; Zhang, X. *Adv. Mater.*, **2009**, *21*,

- 4362-4365.
18. Samanta, A.; Stuart, M. C.; Ravoo, B. J. *J. Am. Chem. Soc.*, **2012**, *134*, 19909-19914.
19. Gong, Y.-H.; Yang, J.; Cao, F.-Y.; Zhang, J.; Cheng, H.; Zhuo, R.-X.; Zhang, X.-Z. *J. Mater. Chem. B.*, **2013**, *1*, 2013-2017.
20. He, S.; Krippes, K.; Ritz, S.; Chen, Z.; Best, A.; Butt, H.-J.; Mailänder, V.; Wu, S. *Chem. Commun.*, **2015**, *51*, 431-434.
21. Chen, Z.; He, S.; Butt, H.-J.; Wu, S. *Adv. Mater.*, **2015**, *27*, 2203-2206.
22. Chen, Z.; Sun, W.; Butt, H.-J.; Wu, S. *Chem. Eur. J.*, **2015**, *21*, 9165-9170.
23. Siewertsen, R.; Neumann, H.; Buchheim-Stehn, B.; Herges, R.; Näther, C.; Renth, F.; Temps, F. *J. Am. Chem. Soc.*, **2009**, *131*, 15594-15595.
24. Venkataramani, S.; Jana, U.; Dommaschk, M.; Sönnichsen, F. D.; Tuczek, F.; Herges, R. *Science*, **2011**, *331*, 445-448.
25. Yang, Y.; Hughes, R. P.; Aprahamian, I. *J. Am. Chem. Soc.*, **2012**, *134*, 15221-15224.
26. Beharry, A. A.; Sadovski, O.; Woolley, G. A. *J. Am. Chem. Soc.*, **2011**, *133*, 19684-19687.
27. Bléger, D.; Schwarz, J.; Brouwer, A. M.; Hecht, S. *J. Am. Chem. Soc.*, **2012**, *134*, 20597-20600.
28. Samanta, S.; Beharry, A. A.; Sadovski, O.; McCormick, T. M.; Babalhavaeji, A.; Tropepe, V.; Woolley, G. A. *J. Am. Chem. Soc.*, **2013**, *135*, 9777-9784.
29. Yang, Y.; Hughes, R. P.; Aprahamian, I. *J. Am. Chem. Soc.*, **2014**, *136*, 13190-13193.
30. *American National Standard for safe use of lasers*, ed. Laser Institute of America, Orlando, FL, 2000.
31. *Laser safety handbook*, ed. Northwestern University, Evanston, IL, 2011.
32. Kawai, H.; Kanegae, T.; Christensen, S.; Kiyosue, T.; Sato, Y.; Imaizumi, T.; Kadota, A.; Wada, M. *Nature*, **2003**, *421*, 287-290.

33. Levskaya, A.; Weiner, O. D.; Lim, W. A.; Voigt, C. A. *Nature*, **2009**, *461*, 997-1001.
34. Shi, Z. Peng, P.; Strohecker, D.; Liao, Y. *J. Am. Chem. Soc.*, **2011**, *133*, 14699-14703.
35. Johns, V. K.; Peng, P.; Dejesus, J.; Wang, Z.; Liao, Y. *Chem. Eur. J.*, **2014**, *20*, 689-692.
36. Wang, Z.; Johns, V. K.; Liao, Y. *Chem. Eur. J.*, **2014**, *20*, 14637-14640.

Supporting Information

1. Synthesis

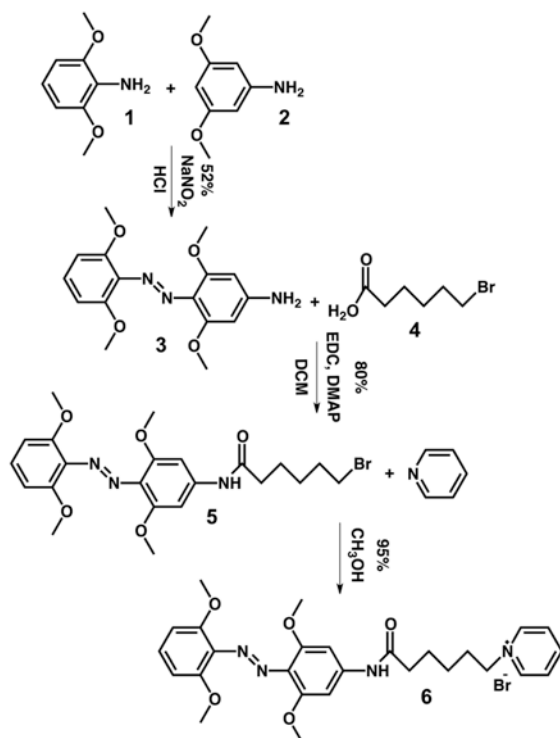


Figure S2.1 Route for the synthesis of 6 (mAzo-Py).

Synthesis of 3 (mAzo-NH₂). 2, 6-Dimethoxy-aniline (1 in **Figure S2.1**) (0.459 g, 3.00 mmol) was dissolved in the mixture of 0.56 mL of H_2O and 0.73 mL of HCl (37 wt. %). After the solution was cooled to 0~5 °C, NaNO_2 (0.207 g, 3.00 mmol) in 2 mL H_2O was added slowly. The solution was stirred for 20 min and the temperature of the solution was kept at 0~5 °C. The diazonium salt was then slowly added to a suspension of 3,5-dimethoxy-aniline (0.459 g, 3.00 mmol) in 20 mL of H_2O at 0~5 °C. The pH of the mixture was adjusted to 8~9 by adding saturated sodium bicarbonate solution and the mixture was stirred overnight. The red solid was filtered and purified by chromatography using 1/1 methanol/ethyl acetate as eluent to get the product 3. Yield: 52%. $^1\text{H-NMR}$ ($\text{DMSO-}d_6$, 250 MHz): δ =7.15 (t, J =8.3 Hz, 1H; Ar-H), δ =6.71 (d, J =8.4 Hz, 2H; Ar-H), δ =5.99 (s, 2H; Ar-NH₂), δ =5.94 (s, 2H; Ar-H), δ =3.67 (ds,

12H; -OCH₃). ¹³C-NMR (DMSO-*d*₆, 63 MHz): δ=156.1 (Ar-C), δ=153.4 (Ar-C), δ=151.0 (Ar-C), δ=126.6 (Ar-C), δ=123.4 (Ar-C), δ=105.3 (Ar-C), δ=89.9 (Ar-C), δ=55.9 (-OMe), δ=55.4 (-OMe). MS m/z=317.2.

Synthesis of 5. 4 (0.246g, 1.26 mmol), EDC (0.253g, 1.32 mmol) and DMAP (0.020g, 0.16 mmol) were dissolved into 60 mL of dichloromethane (DCM) and the mixture was stirred for 10 min. Then, 3 (0.420 g, 1.32 mmol) was added into the solution. The reaction was kept at room temperature for 24 h. The result solution was purified by chromatography using DCM as eluent to get the product 5. Yield: 80%. ¹H-NMR (DMSO-*d*₆, 250MHz): δ=10.14 (s, 1H; -CO-NH-), δ=7.24 (t, J=8.3 Hz, 1H; Ar-H), δ=7.15 (s, 2H; Ar-H), δ=6.78 (d, J=8.4 Hz, 2H; Ar-H), δ=3.72 (ds, 12H; -OCH₃), δ=3.55 (t, J=6.7 Hz, 2H; -CH₂-Br), δ=2.37 (t, J=7.2 Hz, 2H; -CH₂-CO-), δ=1.95-1.35 (m, 6H; -CH₂-). ¹³C-NMR (DMSO-*d*₆, 63 MHz): δ=171.6 (-NH-CO-), δ=153.0 (Ar-C), δ=151.2 (Ar-C), δ=141.7 (Ar-C), δ=133.9 (Ar-C), δ=128.6 (Ar-C), δ=105.3 (Ar-C), δ=95.6 (Ar-C), δ=56.1 (-OMe), δ=55.9 (-OMe), δ=36.4 (-CH₂-CONH-), δ=35.0 (-CH₂-Br-), δ=32.0, 27.2, 24.1 (-CH₂-). MS m/z=493.1.

Synthesis of 6 (mAzo-Py). 5 (0.080g, 0.16 mmol) was dissolved in THF (20 mL). Then, pyridine (20 mL) was added. The reaction mixture was stirred overnight at 60 °C under Ar. The solvents were removed by rotated evaporation. The obtained red solid was dissolved in methanol. The solution was added stepwise with stirring to plenty of petroleum ether, and the red precipitate was filtered and dried under vacuum to get the 6. Yield: 95%. ¹H-NMR (D₂O-*d*₂, 250MHz): δ=8.82 (d, J=7.0 Hz, 2H; Py-H), δ=8.51 (t, J=7.8 Hz, 1H; Py-H), δ=8.03 (t, J=7.2 Hz, 2H; Py-H), δ=7.42 (t, J=8.5 Hz, 1H; Ar-H), δ=6.91 (s, 2H; Ar-H), δ=6.87 (d, J=8.5 Hz, 2H; Ar-H), δ=4.61 (t, J=7.2 Hz, 2H; -CH₂-Py), δ=3.85 (ds, 12H; -OCH₃), δ=2.41 (t, J=7.2 Hz, 2H; -CH₂-CO-), δ=2.12-1.30 (m, 6H; -CH₂-).

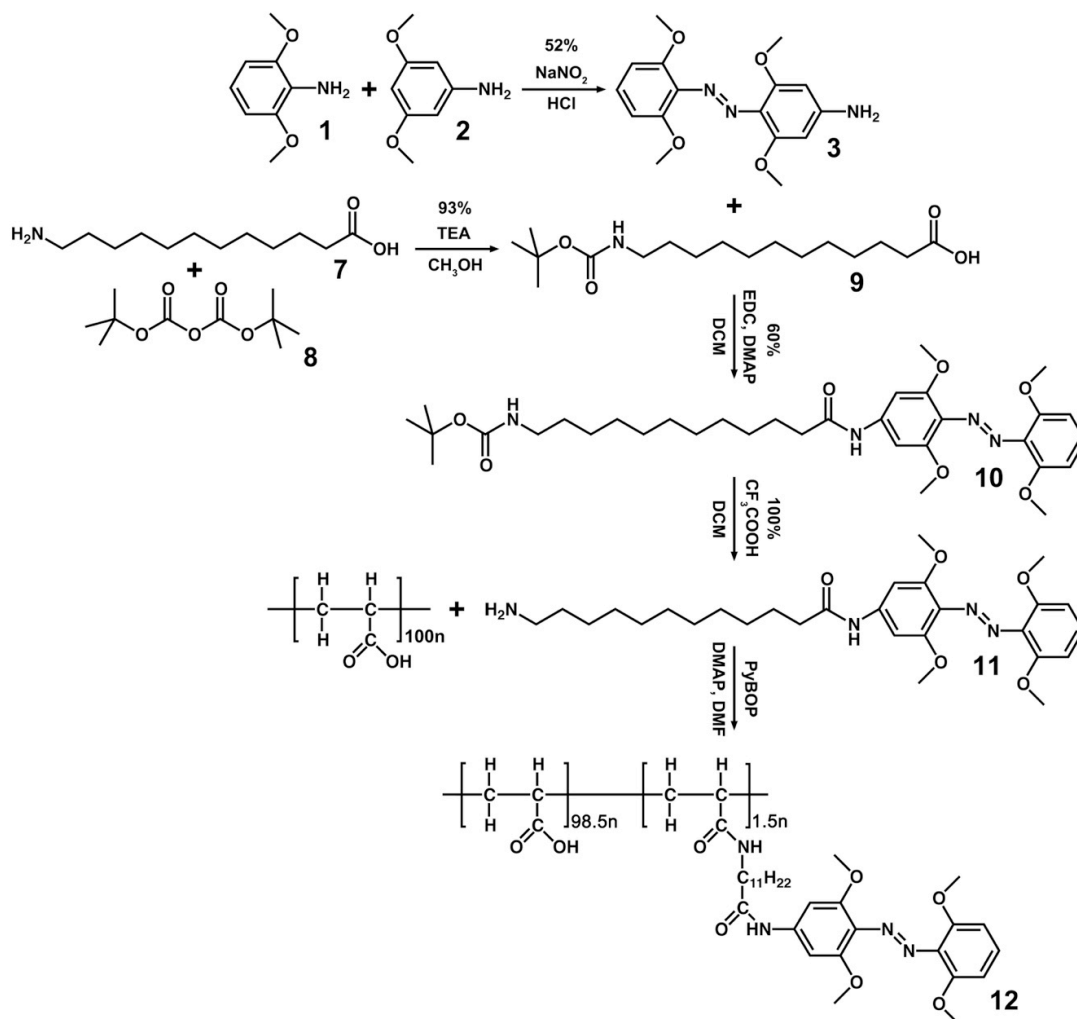


Figure S2.2. Route for the synthesis of 12 (PAA-mAzo).

Synthesis of 9. 12-Aminododecanoic acid (**7** in **Figure S2.2**) (1.000 g, 4.65 mmol), di-tert-butyl dicarbonate (**8** in **Figure S2**) (1.010 g, 4.65 mmol) and triethylamine (TEA) (0.775 mL, 5.58 mmol) were dissolved into 15 mL of methanol. The reaction was kept 60 °C overnight. After removing the solvent using a rotary evaporator, the obtained solid was dissolved in ethyl acetate, and washed with HCl solution (0.25 M) twice. The white solid was then dried in a vacuum oven to obtain the product (**9**). Yield: 93%. $^1\text{H-NMR}$: $\delta=11.98$ (s, 1H; -COOH), $\delta=6.76$ (t, $J=5.6$ Hz, 1H; -CO-NH-), $\delta=2.89$ (q, $J=6.5$ Hz, 2H; -CH₂-), $\delta=2.19$ (t, $J=7.3$ Hz, 2H; -CH₂-), $\delta=1.49$ (t, $J=7.1$ Hz,

4H; -CH₂-), δ =1.38 (s, 9H; -CH₃), δ =1.24 (s, 14H; -CH₂-). ¹³C-NMR: δ =174.4 (-COOH), δ =155.5 (-CO-NH-), δ =77.2 (Me₃-C-), δ =33.6, 29.4, 29.0, 28.9, 28.7, 28.5, 28.2, 26.2 (-CH₂-), δ =24.5 (-CH₃). MS m/z=315.2.

Synthesis of 10. Compound 9 (0.157 g, 0.50 mmol), EDC (0.096 g, 0.50 mmol) and DMAP (0.020 g, 0.16 mmol) were dissolved in 10 mL of DCM at room temperature. The mixture was stirred for 20 min. Then, 3 (0.159 g, 0.50 mmol) was added into the solution. The reaction was kept at room temperature for 24 h. Then, the result solution was purified by chromatography using 1/2 acetone/ethyl acetate as eluent to get the product 10. Yield: 60%. ¹H-NMR: δ =7.29 (t, J=8.3 Hz, 1H; Ar-H), δ =7.18 (s, 3H; Ar-H and O=C-NH-Ar), δ =6.90-6.70 (m, 3H; Ar-H and O=C-NH-C), δ =3.75 (d, J=2.0 Hz, 12H; -OCH₃), δ =2.92 (q, J=6.5 Hz, 2H; -CH₂-), δ =2.32 (t, J=7.3 Hz, 2H; -CH₂-), δ =1.66 (t, J=7.1 Hz, 4H; -CH₂-), δ =1.41 (s, 9H; -CH₃), δ =1.30 (s, 14H; -CH₂-). ¹³C-NMR: δ =179.8 (-CO-NH-Ar), δ =156.6 (Ar-C), δ =156.1 (-CO-NH-), δ =151.1 (Ar-C), δ =149.4 (Ar-C), δ =128.4 (Ar-C), δ =125.5 (Ar-C), δ =104.1 (Ar-C), δ =91.5 (Ar-C), δ =71.0 (Me₃-C-), δ =55.1 (-OMe), δ =54.8 (-OMe), δ =33.3, 29.4, 29.0, 28.9, 28.8, 28.7, 28.2 25.3 (-CH₂-), δ =24.4 (-CH₃). MS m/z=614.7.

Synthesis of 11. Compound 10 (0.179 mg, 0.30 mmol) and 3 mL of CF₃COOH were dissolved in 10 mL of DCM. The mixture was stirred at room temperature for 1 h. The resulted solution was washed using saturated Na₂CO₃ solution. Then, the residual DCM was removed using a rotary evaporator. The dark red solid was further washed by water for several times to obtain the Compound 11. Yield: >99%. ¹H-NMR: δ =7.29 (t, J=8.3 Hz, 1H; Ar-H), δ =7.18 (s, 2H; Ar-H), δ =6.80 (d, J=8.4 Hz, 2H; Ar-H), δ =6.17 (s, 2H; -NH₂), δ =3.74 (d, J=2.1 Hz, 12 H; -OCH₃), δ =2.92 (q, J=6.5 Hz, 2H; -CH₂-), δ =2.37 (t, J=7.3 Hz, 2H; -CH₂-), δ =1.66 (t, J=7.1 Hz, 4H; -CH₂-), δ =1.88-1.48 (m, 4H; -CH₂-), δ =1.30 (s, 14H; -CH₂-). ¹³C-NMR: δ =179.6 (-CO-NH-Ar), δ =152.9 (Ar-C), δ =151.1 (Ar-C), δ =145.1 (Ar-C), δ =127.2 (Ar-C), δ =122.4 (Ar-C), δ =105.3 (Ar-C), δ =95.6 (Ar-C), δ =56.0 (-OCH₃), δ =55.8 (-OCH₃), δ =33.3, 29.7, 29.0, 28.9, 28.8, 28.7, 28.2, 26.1 (-CH₂-). MS m/z=515.6.

Synthesis of 12 (PAA-mAzo). To prepare PAA-mAzo (12 in **Figure S2.2**), PAA (0.288 g, 4.00 mmol of the repeat unit), PyBOP (0.062 g, 0.12 mmol), DMAP (0.015 g, 0.12 mmol) and 11 (0.062 g, 0.12 mmol) were dissolved in 20 mL of DMF at room temperature. The reaction was kept at room temperature for 24 h. The product was purified by dialysis using a dialysis tube (cut-off molecular weight: 7000). The grafting density determined by $^1\text{H-NMR}$ is 1.5%.

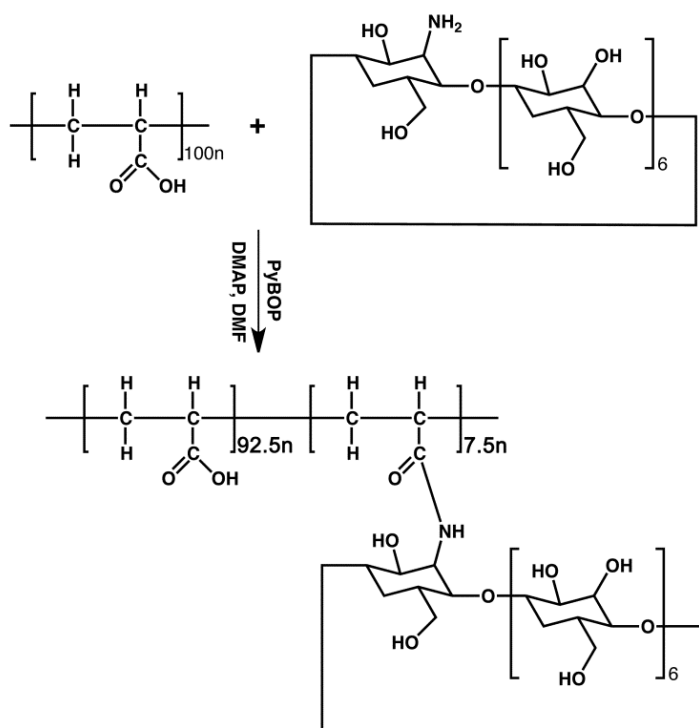


Figure S2.3. Route for the synthesis of PAA- β -CD.

Synthesis of PAA- β -CD. PAA (0.288 g, 4.00 mmol of the repeat unit), PyBOP (0.208 g, 0.40 mmol), DMAP (0.015 g, 0.12 mmol) and NH_2 - β -CD (0.453 g, 0.40 mmol) were dissolved into 20 mL of DMF. The reaction mixture was kept at room temperature for 24 h. The product was purified by dialysis using a dialysis tube (cut-off molecular weight: 7000). The grafting density determined by $^1\text{H-NMR}$ is 7.5%.

2. Photoisomerization of mAzo and host-guest interactions between mAzo and β -CD

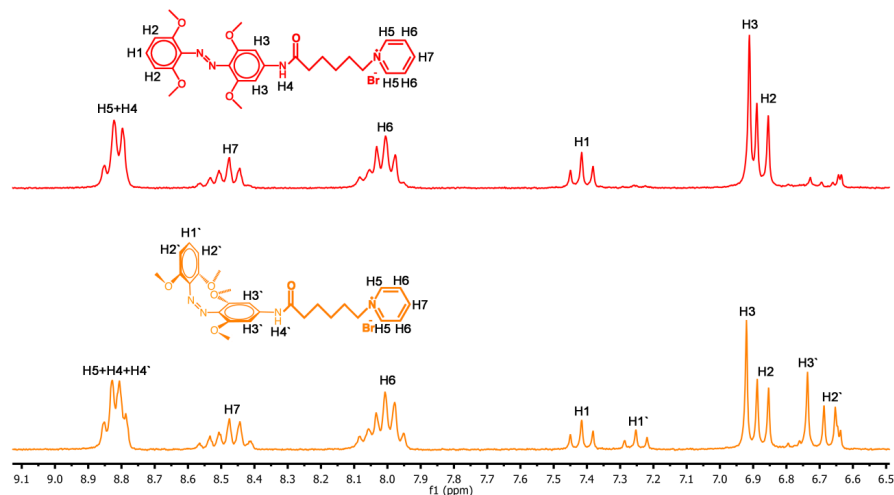


Figure S2.4. ^1H -NMR (250 MHz, D_2O , 298K) spectra of mAzo-Py before (red) and after (orange) 625-nm light irradiation. Photoisomerization of mAzo-Py can be induced by red light.

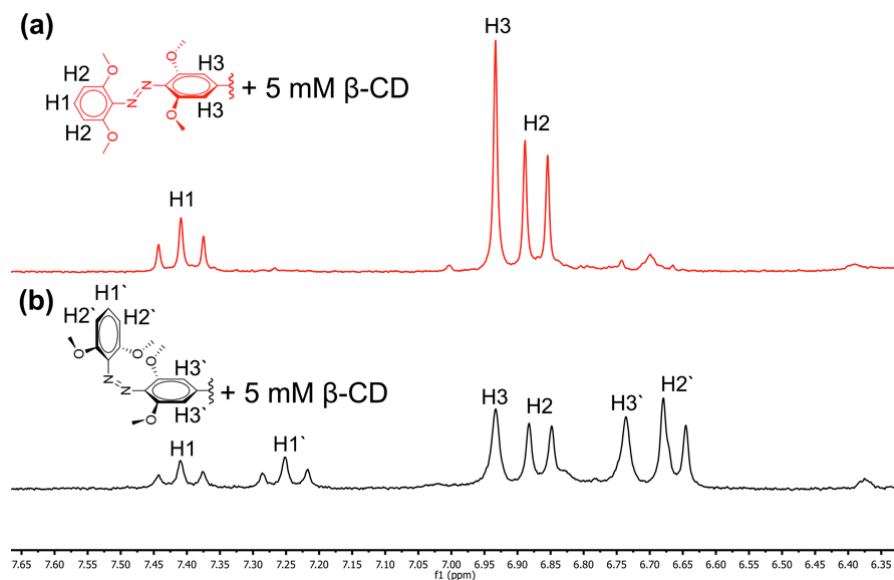


Figure S2.5. ^1H -NMR (250 MHz, D_2O , 298K) spectra of mAzo-Py/ β -CD (1:5) before (a) and after (b) 625-nm light irradiation. Red light can induce the photoisomerization of mAzo-Py in the presence of β -CD. The concentration of mAzo-Py is 1 mM.

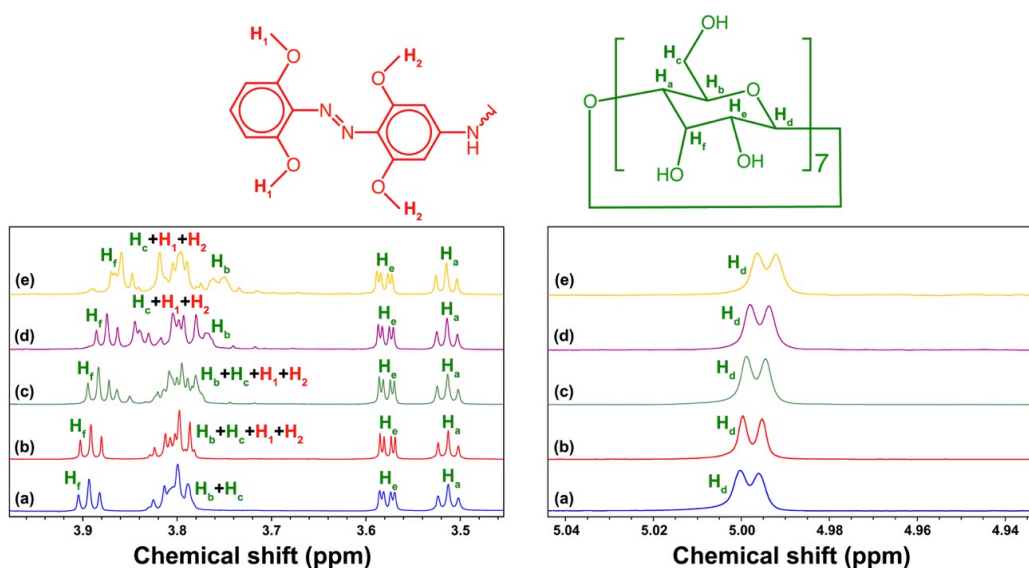


Figure S2.6. ^1H -NMR (700MHz, 298K) spectra of *trans* mAzo-Py and its mixtures with β -CD in D_2O : *trans* mAzo-Py: β -CD=0:1 (a), *trans* mAzo-Py: β -CD=0.5:1 (b), *trans* mAzo-Py: β -CD=1:1 (c), *trans* mAzo-Py: β -CD=2:1 (d) and *trans* mAzo-Py: β -CD=4:1 (e). The concentration of β -CD is 1.67 mg/mL.

H_b , H_d and H_f are protons inside the cavity of β -CD. As the ratio of *trans* mAzo-Py in mAzo-Py/ β -CD increases, the signals of H_b , H_d and H_f shift, indicating *trans* mAzo-Py enters the cavity of β -CD. The other protons are outside or at the edge of the cavity of β -CD. As the ratio of *trans* mAzo-Py in mAzo-Py/ β -CD increases, the signals of the outer protons of β -CD have no or only slight shift. The result suggests that *trans* mAzo has stronger interactions with inner protons of β -CD. Thus, this experiment confirms the host-guest interaction between *trans* mAzo and β -CD.

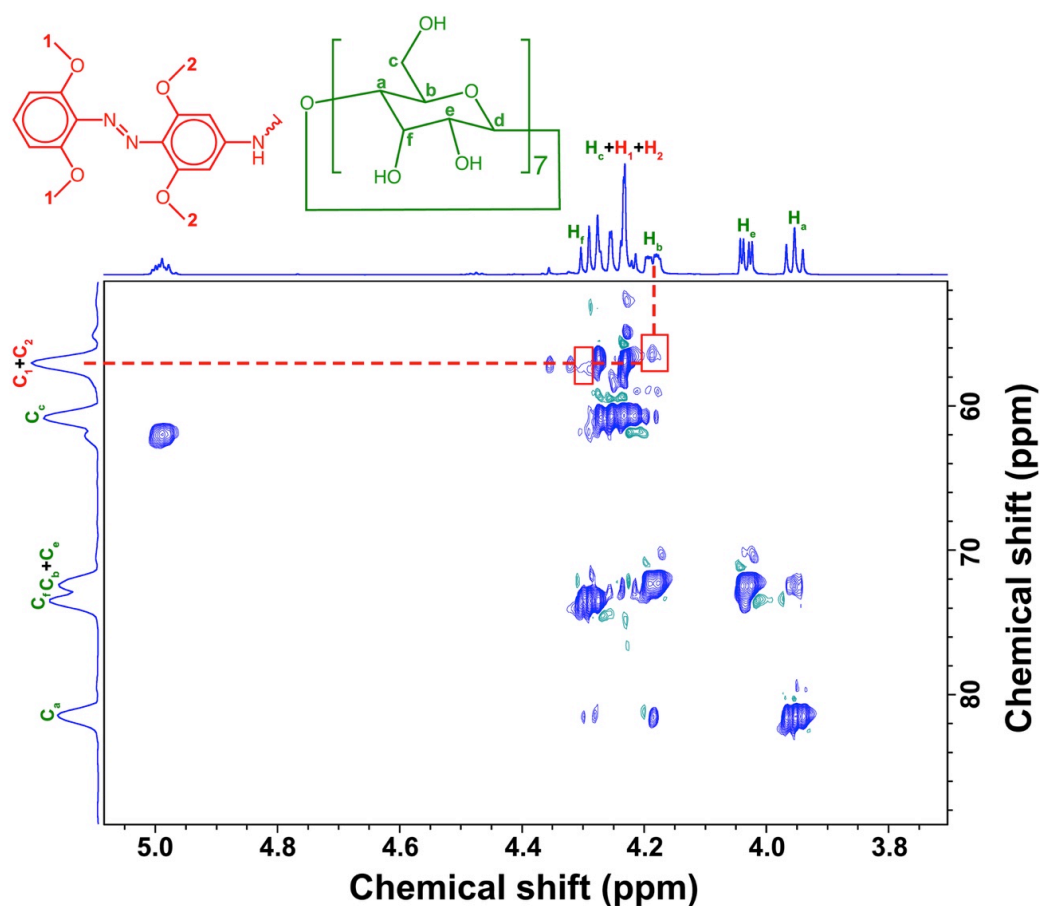


Figure S2.7. 2D HSQC-NOESY spectrum (700MHz, 298K) of *trans* mAzo-Py/β-CD (2/1 in molar ratio) in D₂O. The concentration of β-CD is 1.67 mg/mL.

The correlation peaks between the carbons of *trans* mAzo-Py (C₁ and C₂) and the inner protons of β-CD (H_b and H_f) shows the host-guest interaction between *trans* mAzo-Py and β-CD. Additionally, there is no correlation peak between the carbons of *trans* mAzo-Py (C₁ and C₂) and the outer protons of β-CD (H_a and H_e). Thus, *trans* mAzo strongly interact with the inner protons of β-CD. These results indicate that *trans* mAzo-Py enters the cavity of β-CD.

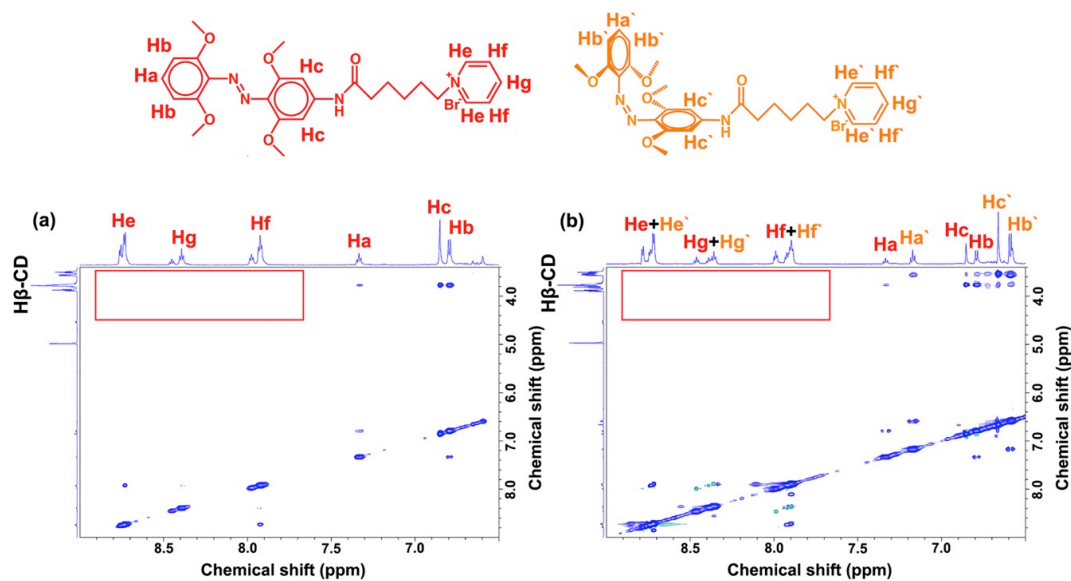


Figure S2.8. 2D NOESY spectra (700 MHz in D₂O at 298 K) of *trans* mAzo-Py/β-CD (a) and *cis* mAzo-Py/β-CD (b). No corresponding proton was found between pyridine and β-CD (red rectangles) in both of the spectra. The concentration of β-CD is 1.67 mg/mL. The molar ratio of mAzo-Py/β-CD is 1/1.

3. Association constants between mAzo-Py and CDs

^1H NMR was used to measure the association constants (K_a) between mAzo-Py and α -CD or β -CD. mAzo-Py and CDs were dissolved in D_2O . The concentration of mAzo-Py was kept as 1.0 mM. The concentrations of CDs were 5, 10, 15 and 20 mM, respectively. ^1H NMR spectra of mAzo-Py/CD mixtures in D_2O were measured. Due to the host-guest interaction between mAzo and CDs, the signals of protons will shift. A modified Benesi-Hildebrand equation^[2] was used for the calculation of the association constants between mAzo-Py and CDs.

$$\frac{1}{\Delta\delta_{obs}} = \frac{1}{K_a\Delta\delta C_{CD}} + \frac{1}{\Delta\delta} \quad (\text{S1})$$

where $\Delta\delta_{obs}$ is the observed shifts of the peaks; K_a is the association constant; $\Delta\delta$ is a constant correlated to the concentration of the mAzo-Py; C_{CD} is the concentration of the CD.

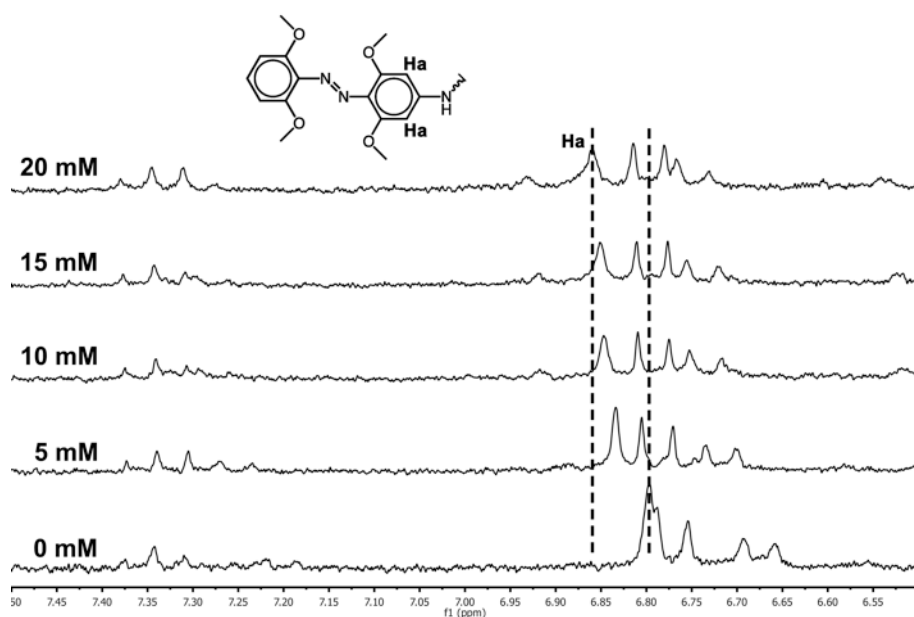


Figure S2.9. ¹H-NMR (250 MHz, 298K) spectra of *trans* mAzo-Py with different concentrations of α-CD (0, 5, 10, 15 and 20 mM) in D₂O. The concentration of mAzo-Py is 1 mM.

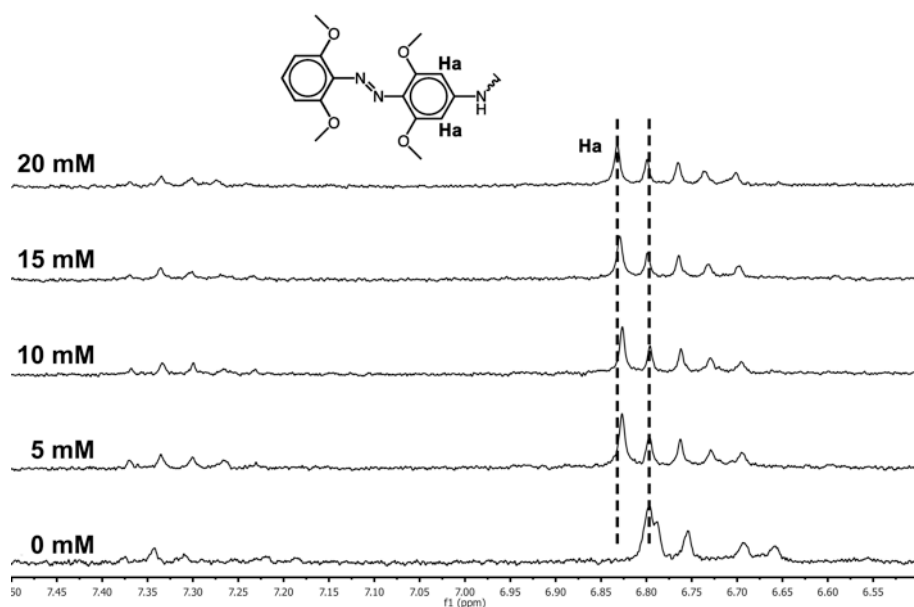


Figure S2.10. ¹H-NMR (250 MHz, 298K) spectra of *trans* mAzo-Py with different concentrations of β-CD (0, 5, 10, 15 and 20 mM) in D₂O. The concentration of mAzo-Py is 1 mM.

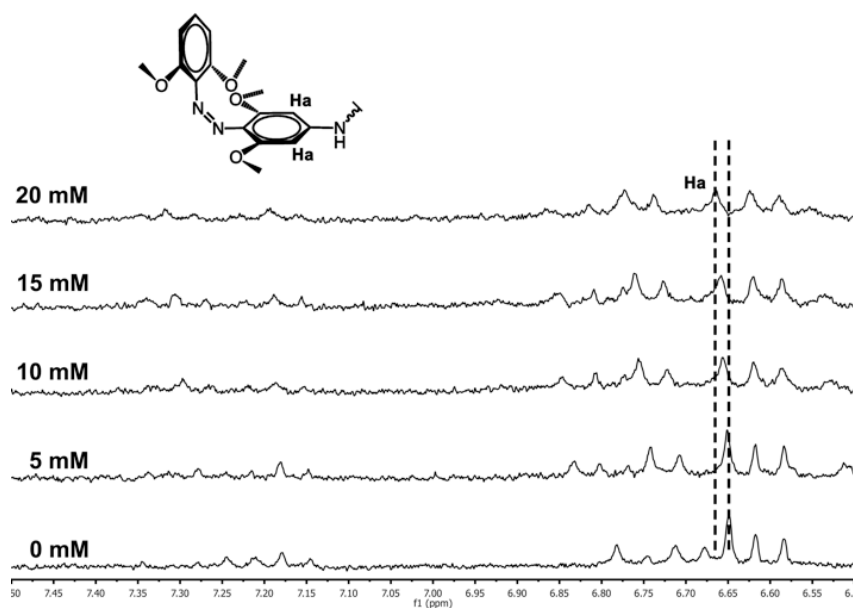


Figure S2.11. ¹H-NMR (250 MHz, 298K) spectra of *cis* mAzo-Py with different concentrations of α-CD (0, 5, 10, 15 and 20 mM) in D₂O. The concentration of mAzo-Py is 1 mM.

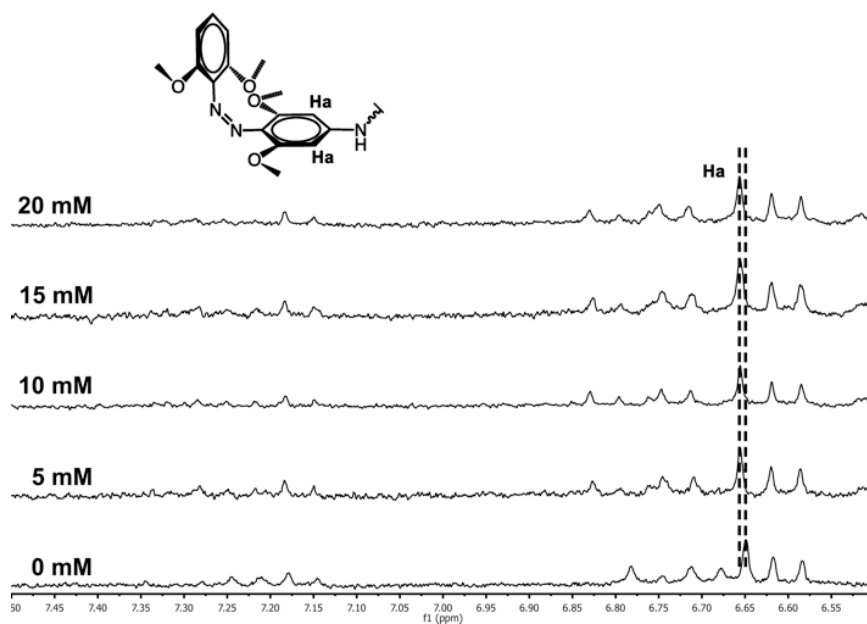


Figure S2.12. ¹H-NMR (250 MHz, 298K) spectra of *cis* mAzo-Py with different concentrations of β-CD (0, 5, 10, 15 and 20 mM) in D₂O. The concentration of mAzo-Py is 1 mM.

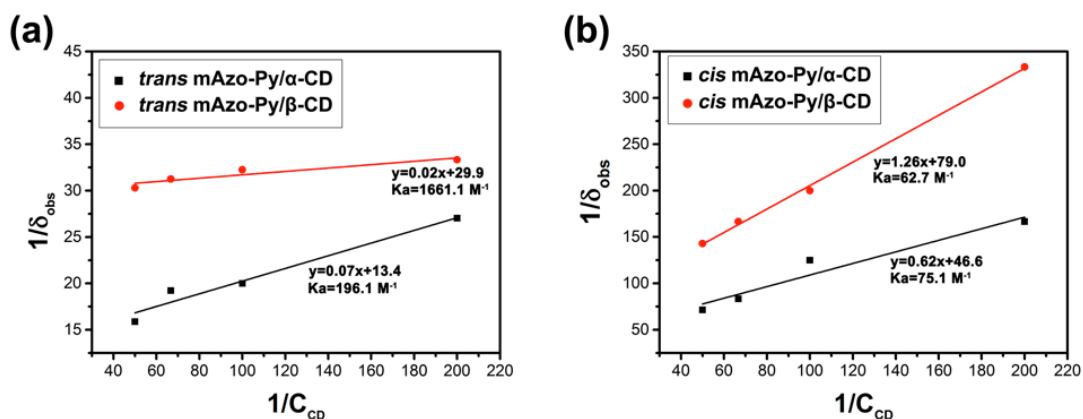


Figure S2.13. (a) Association constants (K_a) between *trans* mAzo-Py and CDs. The data for calculating the association constants were obtained from **Figure S2.9** and **S2.10**. (b) Association constants (K_a) between *cis* mAzo-Py and CDs. The data for calculating the association constants were obtained from **Figure S2.11** and **S2.12**. Equation S1 was used to calculate the association constants.

4. Photoresponse of PAA-mAzo

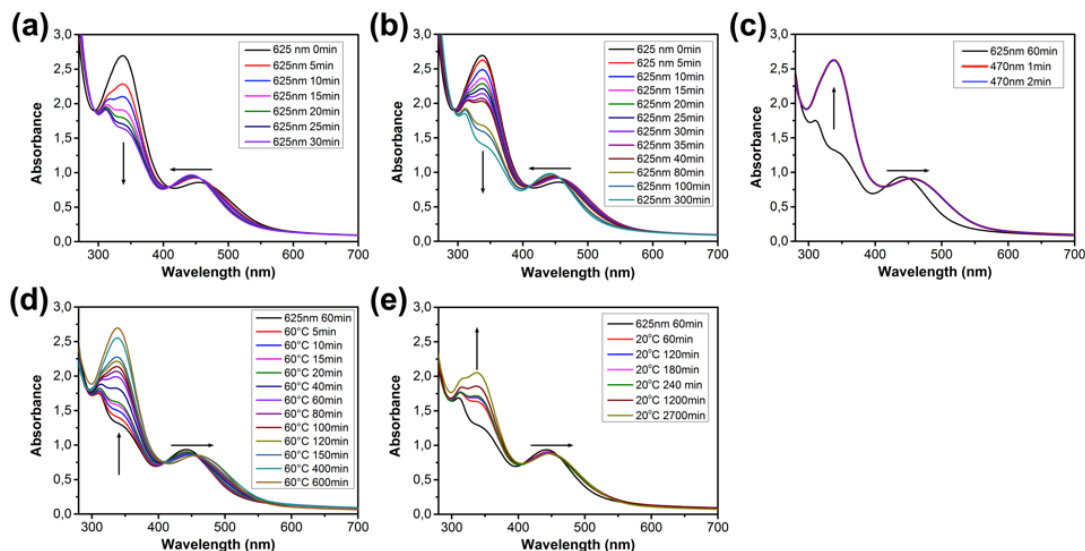


Figure S2.14. UV/Vis absorption spectra of *trans* PAA-mAzo after 60 mW/cm² (a) and 15 mW/cm² (b) 625-nm red light irradiation for different time. (c) UV/Vis absorption spectra of *cis* PAA-mAzo after 60 mW/cm² 470-nm blue light irradiation for different time. The *cis*-to-*trans* isomerization was completed in 1 min. UV/Vis absorption spectra of *cis* PAA-mAzo kept at 60 °C (d) and 20 °C (e) for different time. Cis-to-trans isomerization could be induced thermally. The half-lives of *cis* isomer at 60 °C and 20 °C are 60 min and 34 h, respectively.

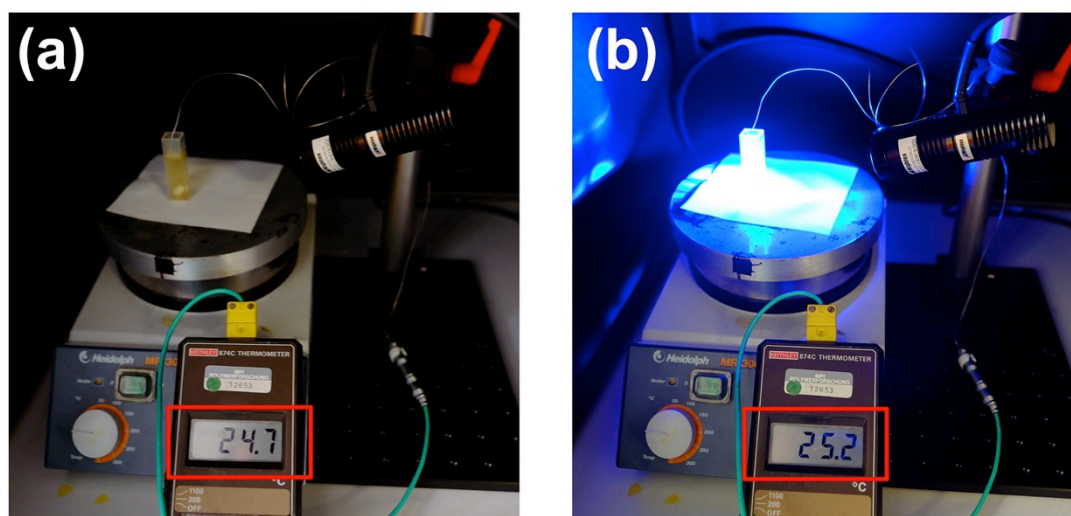


Figure S2.15. Photos for measuring the photothermal effect caused by 470 nm blue light by using the Keithley 874C thermometer. The temperature of the PAA-mAzo solution (1.43 mg/mL in H₂O) before irradiating is 24.7 °C (a), and increases to 25.2 °C after blue light irradiation (60 mW/cm², 10 min). The measurement demonstrates that the cis-to-trans isomerization under the blue light is mainly a photoreaction.

5. Association constants between PAA-mAzo and CDs

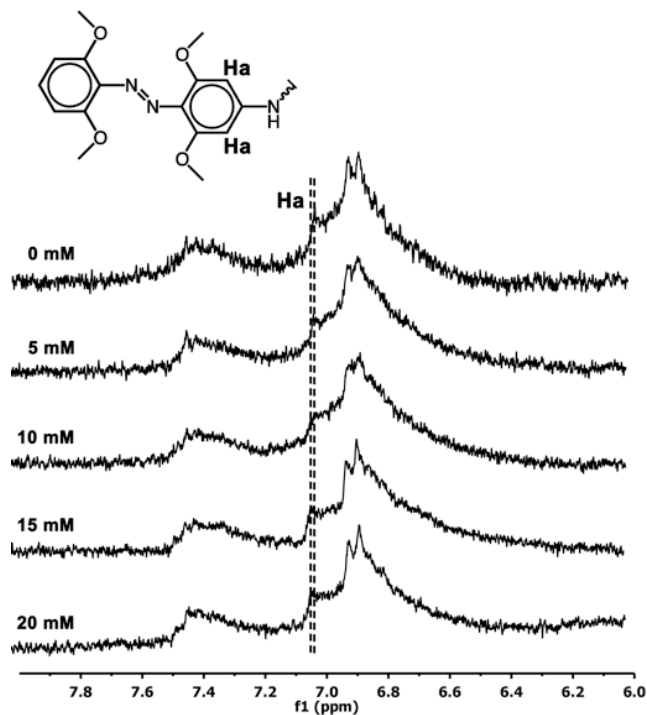


Figure S2.16. ^1H -NMR (250 MHz, 298K) spectra of *trans* PAA-mAzo (1 mM of mAzo groups) with different concentrations (0, 5, 10, 15, 20 mM) of α -CD in D_2O .

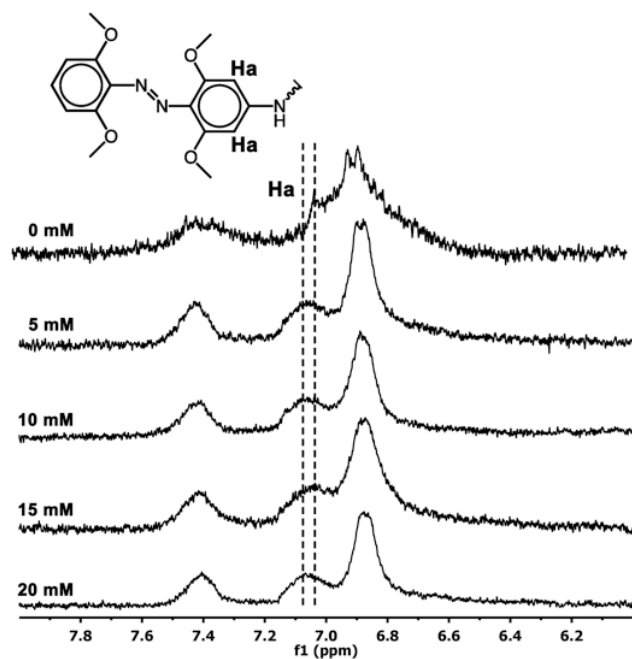


Figure S2.17. ^1H -NMR (250 MHz, 298K) spectra of *trans* PAA-mAzo (1 mM of mAzo group) with different concentrations (0, 5, 10, 15, 20 mM) of β -CD in D_2O .

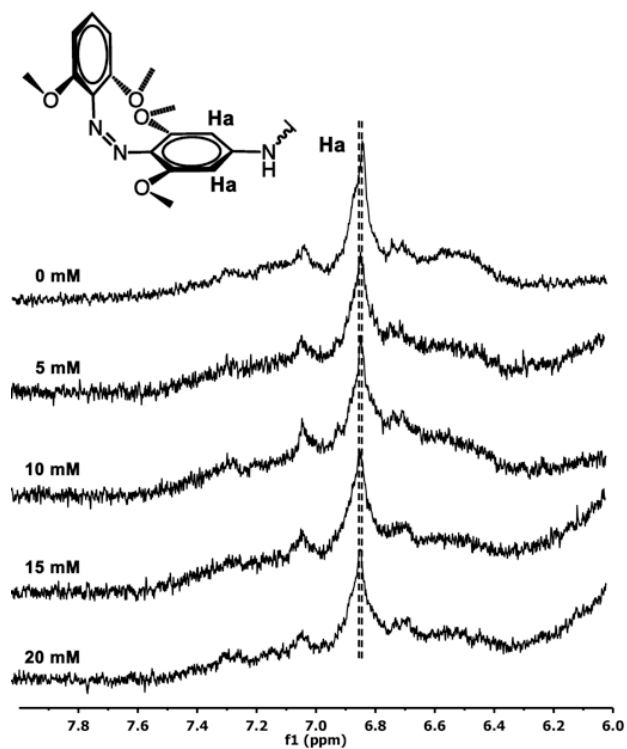


Figure S2.18. ^1H -NMR (250 MHz, 298K) spectra of *cis* PAA-mAzo (1 mM of mAzo group) with different concentrations (0, 5, 10, 15, 20 mM) of α -CD in D_2O .

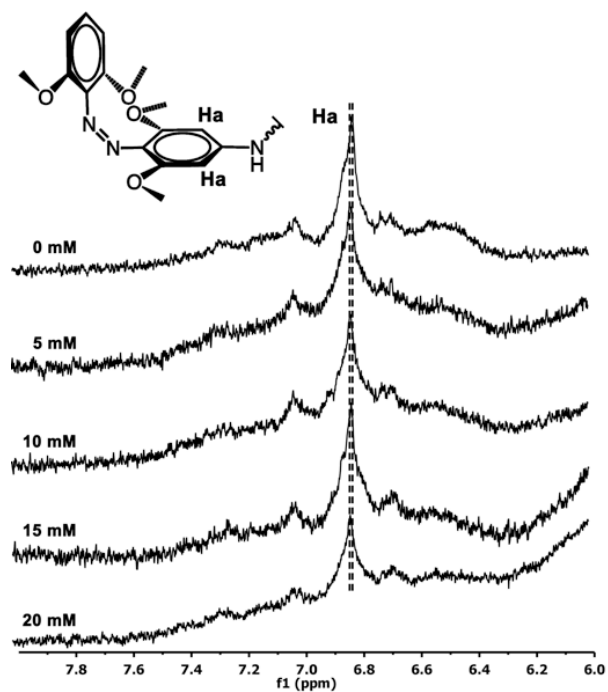


Figure S2.19. ^1H -NMR (250 MHz, 298K) spectra of *cis* PAA-mAzo (1 mM of mAzo group) with different concentrations (0, 5, 10, 15, 20 mM) of β -CD in D_2O .

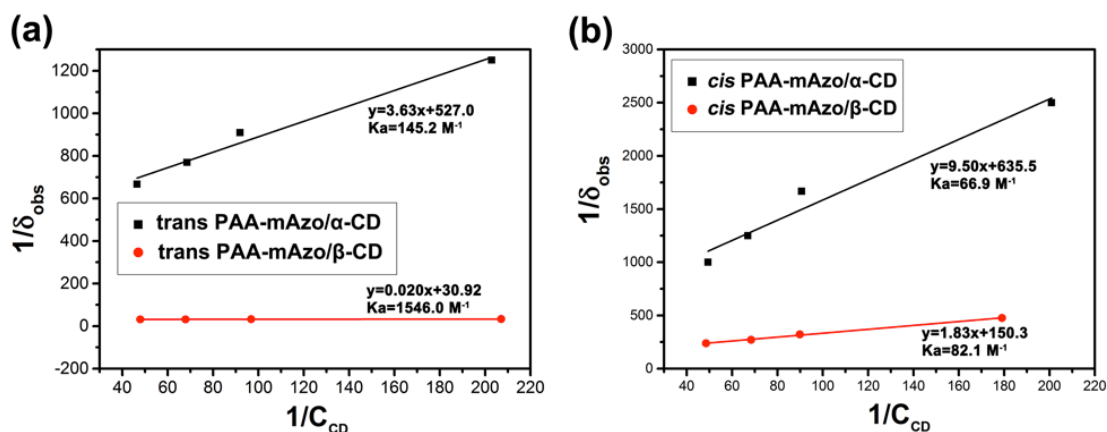


Figure S2.20. (a) Association constants (K_a) between *trans* PAA-mAzo and CDs. The data for calculating the association constants were taken from **Figure S2.16** and **S2.17**. (b) Association constants (K_a) between *cis* PAA-mAzo and CDs. The data for calculating the association constants were taken from **Figure S2.18** and **S2.19**. Equation S1 was used to calculate the association constants. The mAzo/CD association constants measured using PAA-mAzo is similar to those measured using mAzo-Py (**Figure S2.13**).

6. Association constants between PAA-Azo and CDs

PAA-Azo is used for control experiments (Figure S2.21). It contains normal azobenzene groups. In our previous work, we synthesized PAA-Azo and studied the host-guest interactions between PAA-Azo and CDs.^[3]

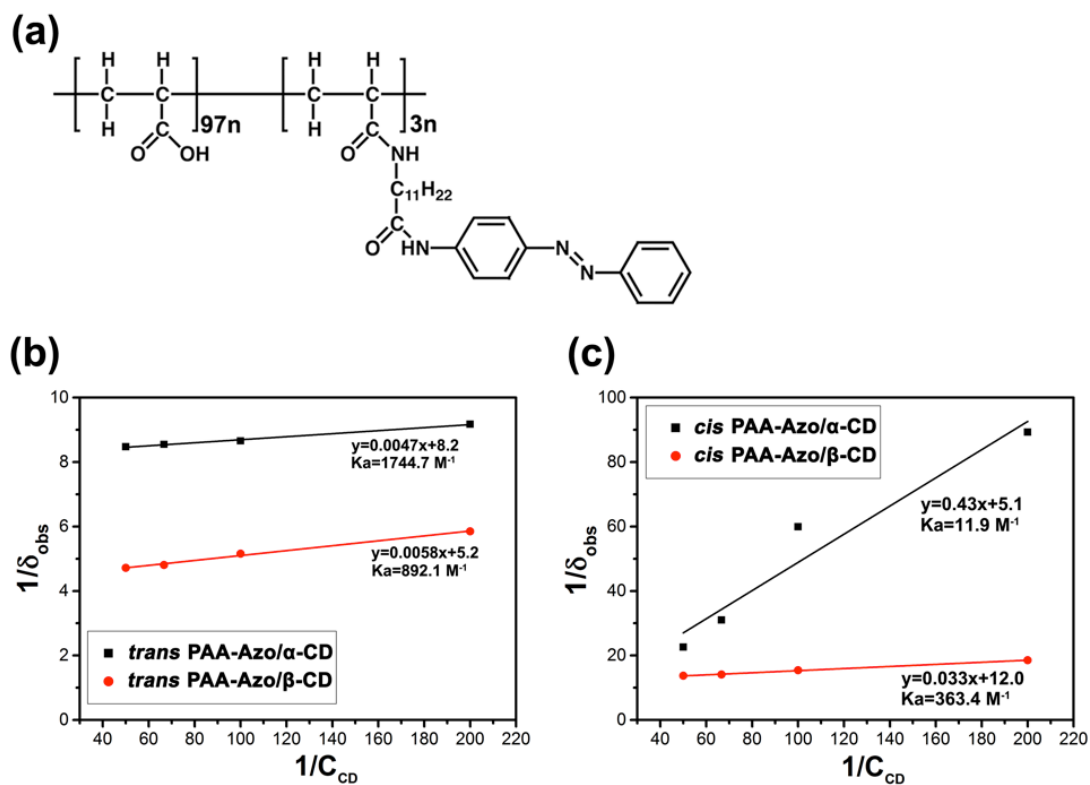


Figure S2.21. (a) Chemical structure of PAA-Azo. (b) Association constants between *trans* PAA-Azo and CDs. (c) Association constants between *cis* PAA-Azo and CDs.

7. Red-light-responsive hydrogels

Hydrogel preparation. Solutions of PAA-mAzo (0.27 mL, 3 wt% in PBS buffer, pH 8) and PAA- β -CD (0.1 mL, 3 wt% in PBS buffer, pH 8) were mixed in the dark. The supramolecular hydrogel was formed spontaneously within 10 min.

Loading BSA into the hydrogel and red-light-controlled BSA release. As shown in **Figure S3.29**, the BSA loaded supramolecular hydrogel was prepared at the bottom of the cuvette. BSA was dissolved in PBS buffer (pH=8) with the concentration of 1 mg/mL. PAA-mAzo and PAA- β -CD solutions were prepared as mentioned above. Then, 135 μ L of PAA-mAzo, 50 μ L of PAA- β -CD and 15 μ L of BSA solutions were mixed at the bottom of the cuvette in the dark. BSA-loaded supramolecular hydrogel was formed spontaneously within 10 min. The BSA loaded hydrogel was washed with PBS buffer for several times to remove non-trapped proteins.

For the photo-controlled protein release, 3.5 mL of PBS solution (pH=8) was added into the cuvette. The hydrogel was irradiated by the LEDs from the side of the cuvette (**Figure S2.22 (a)**). The concentration of the released BSA was monitored using fluorescence spectroscopy (**Figure S2.22 (b)-(f)**). The red-light-controlled BSA release in deep tissue was investigated by placing a piece of pork tissue between the light source and the cuvette (**Figure S2.23**).

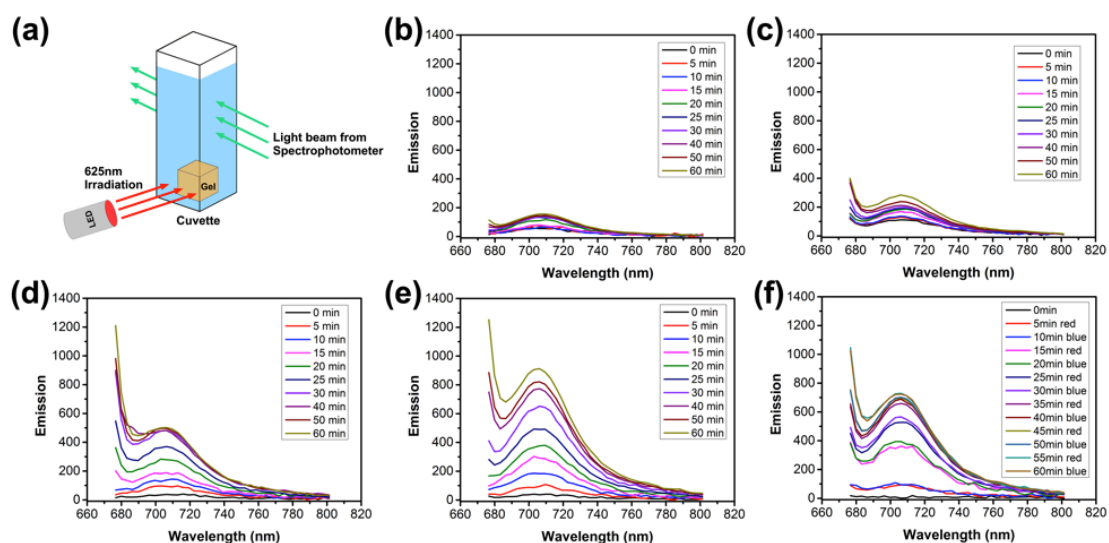


Figure S2.22. (a) Schematic illustration of red-light-induced protein release. Fluorescence spectra ($\lambda_{\text{ex}} = 640 \text{ nm}$) of the BSA-loaded hydrogel in the dark (b), under 60 mW/cm^2 470-nm blue light (c), 15 mW/cm^2 625-nm red light (d) and 60 mW/cm^2 625-nm red light (e) irradiation for different time. The amount of released BSA is shown in Figure 3c in the main manuscript. (f) Fluorescence spectra ($\lambda_{\text{ex}} = 640 \text{ nm}$) of the BSA-loaded hydrogel under alternate 625-nm red light (60 mW/cm^2) and 470-nm blue light (60 mW/cm^2) irradiation for different time. The amount of released BSA is shown in **Figure 3.5** in the main manuscript.

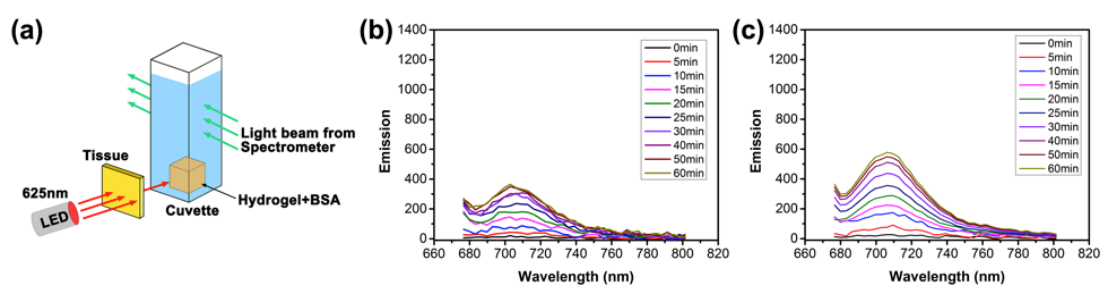


Figure S2.23. (a) Schematic illustration of red-light-induced BSA release in deep tissue. Fluorescence spectra ($\lambda_{\text{ex}} = 640 \text{ nm}$) of the BSA-loaded hydrogel under 15 mW/cm^2 (b) and 60 mW/cm^2 (c) 625-nm red light irradiation for different time when a piece of tissue was placed between the hydrogel and the LED. The amount of released BSA is shown in **Figure 2.6** in the main manuscript.

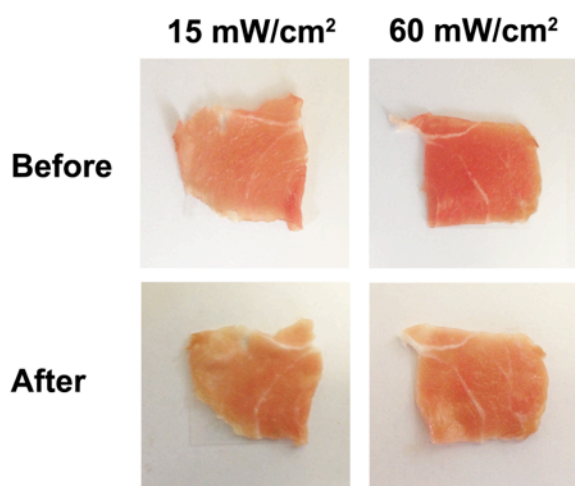


Figure S2.24. Tissue before and after red light irradiation for 60 min. The used light intensity is much lower than the maximum permissible exposure of skin at 625 nm (200 mW/cm^2). No burn wound was observed. The obvious burn wound is reported by our former researches.^[4]

8. NMR spectra of new compounds

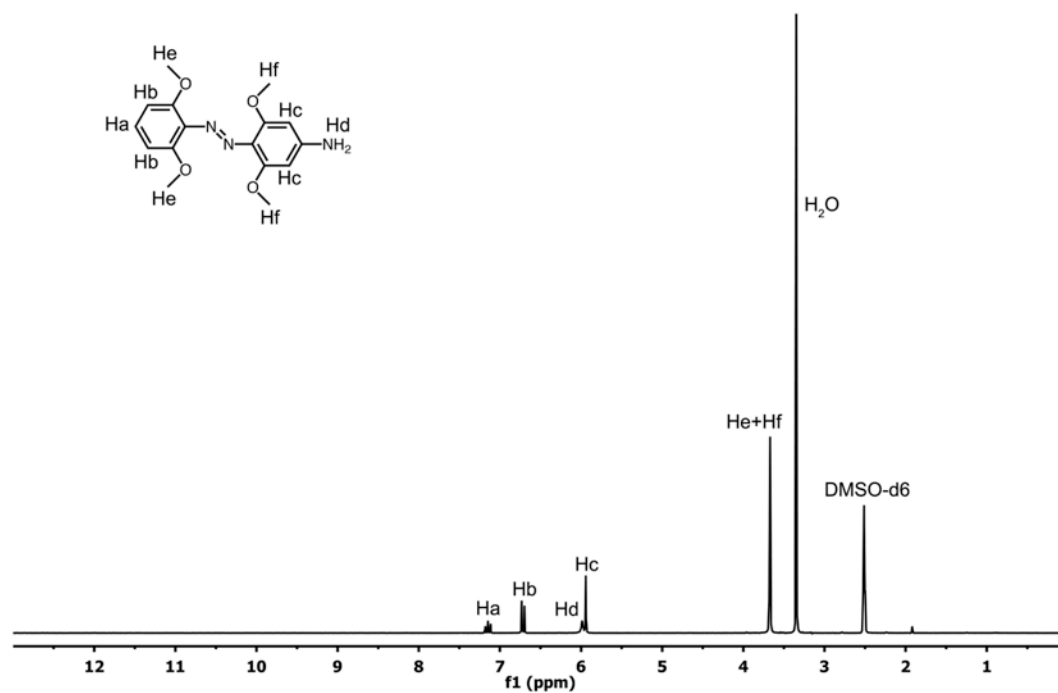


Figure S2.25. ^1H -NMR (250 MHz, 298K, DMSO- d_6) spectrum of 3.

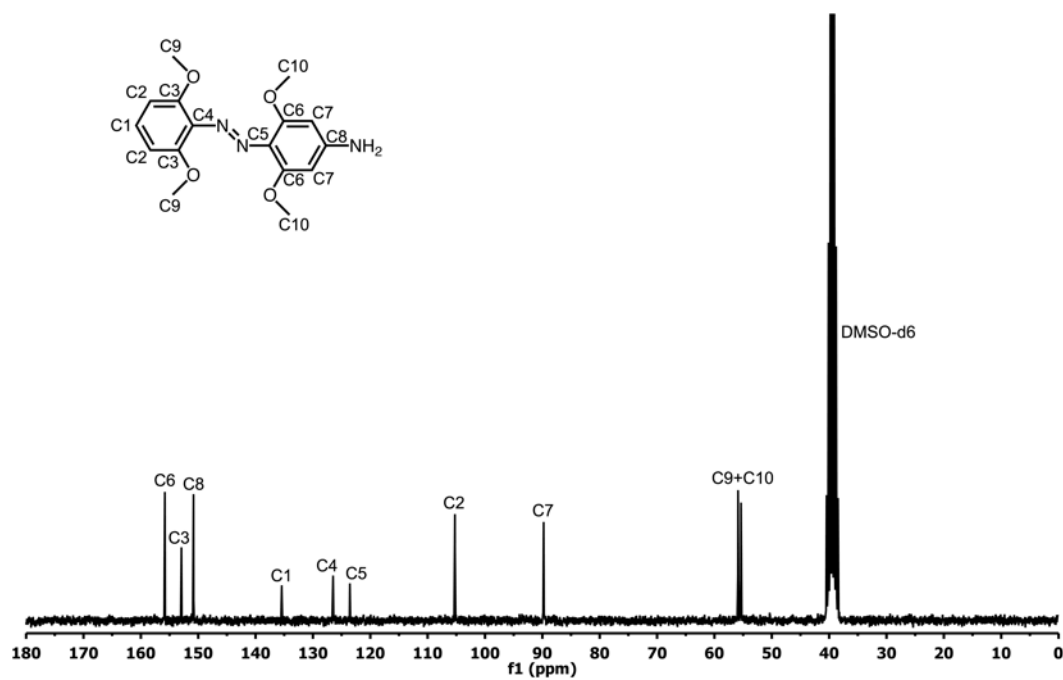


Figure S2.26. ^{13}C -NMR (63 MHz, 298K, DMSO- d_6) spectrum of 3.

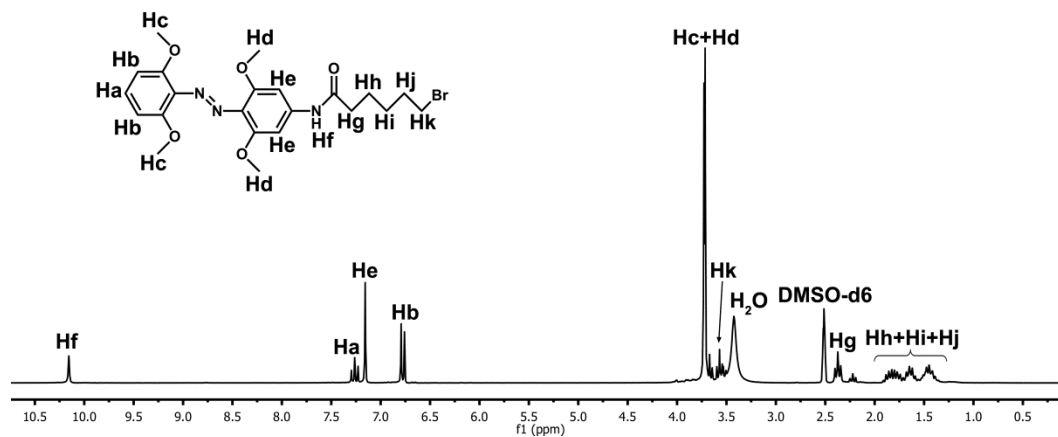


Figure S2.27. ^1H -NMR (250 MHz, 298K, DMSO- d_6) spectrum of 5.

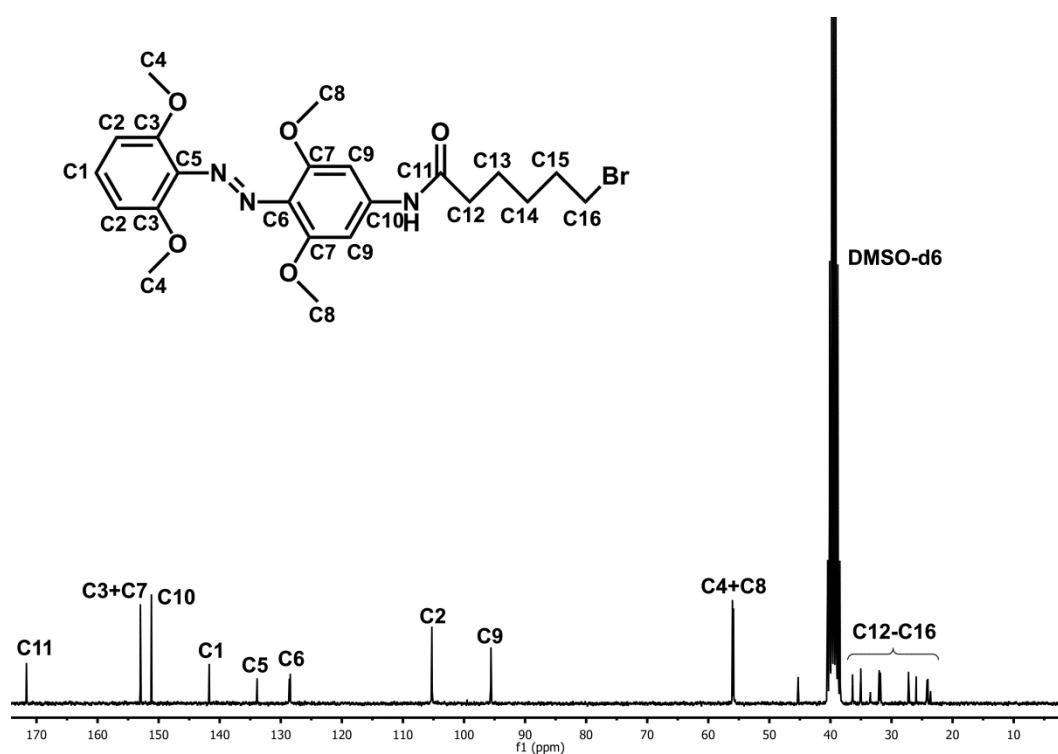


Figure S2.28. ^{13}C -NMR (63 MHz, 298K, DMSO- d_6) spectrum of 5.

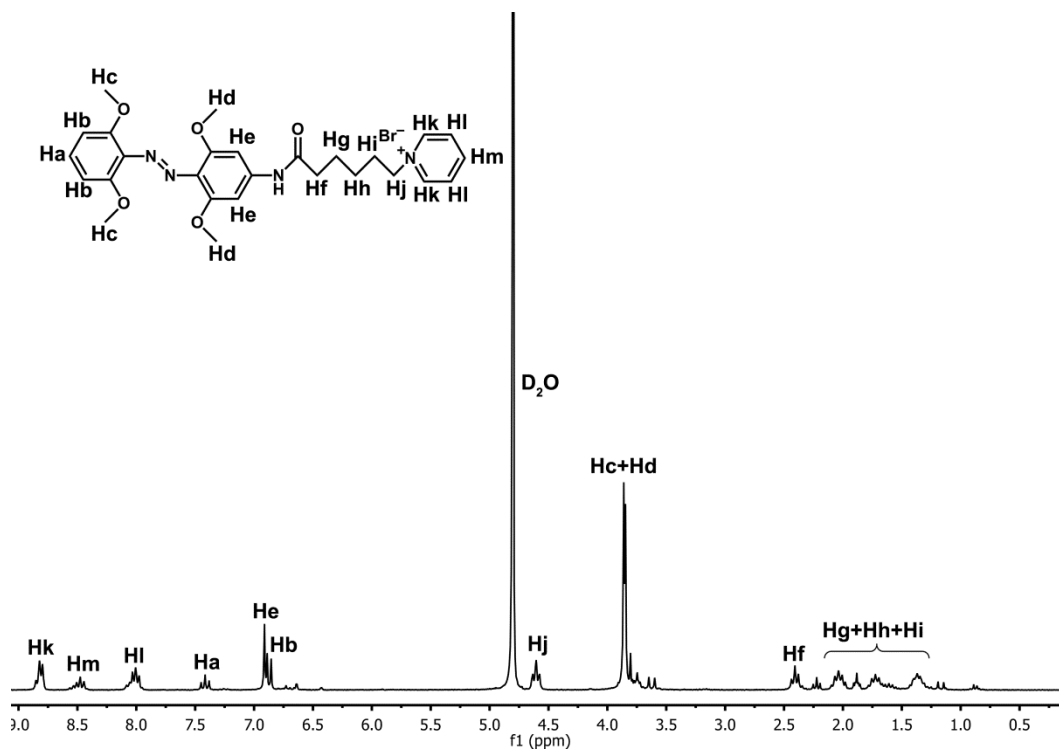


Figure S2.29. ^1H -NMR (250 MHz, 298K, D_2O) spectrum of mAzo-Py.

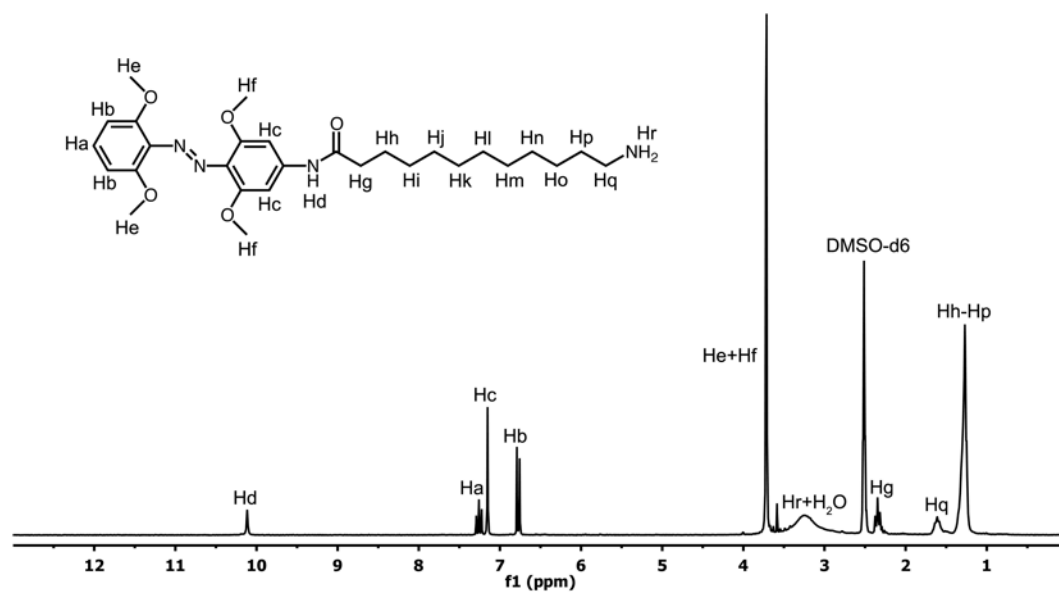


Figure S2.30. ^1H -NMR (250 MHz, 298K, DMSO-d_6) spectrum of 11.

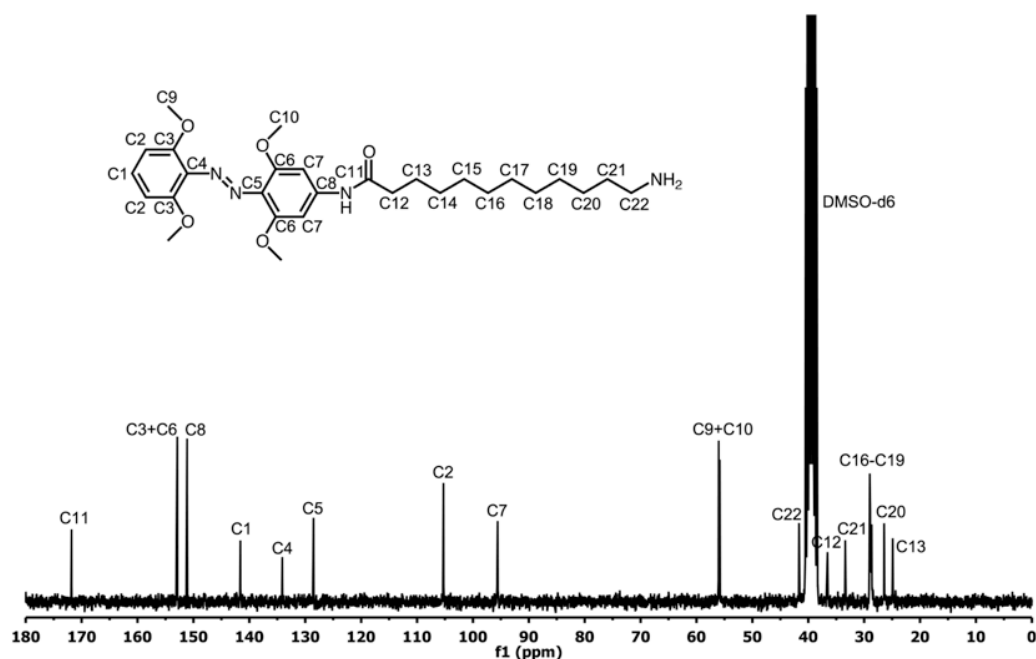


Figure S2.31. ^{13}C -NMR (63 MHz, 298K, DMSO-d_6) spectrum of 11.

References

- [1] a) A. A. Beharry, O. Sadvski, G. A. Woolley, *J. Am. Chem. Soc.* **2011**, *133*, 19684-19687; b) D. Bléger, J. Schwarz, A. M. Brouwer, S. Hecht, *J. Am. Chem. Soc.* **2012**, *134*, 20597-20600; c) S. Samanta, A. A. Beharry, O. Sadvski, T. M. McCormick, A. Babalhavaeji, V. Tropepe, G. A. Woolley, *J. Am. Chem. Soc.* **2013**, *135*, 9777-9784; d) W. A. Velema, W. Szymanski, B. L. Feringa, *J. Am. Chem. Soc.* **2014**, *136*, 2178-2191.
- [2] S. Tamesue, Y. Takashima, H. Yamaguchi, S. Shinkai, A. Harada, *Angew. Chem. Int. Ed.* **2010**, *49*, 7461-7464.
- [3] Y. Zhou, D. Wang, S. Huang, G. Auernhammer, Y. He, H.-J. Butt, S. Wu, *Chem. Commun.* **2015**, *51*, 2725-2727.
- [4] Z. Chen, W. Sun, H.-J. Butt, S. Wu, *Chem. Eur. J.* **2015**, *21*, 1-7.

Red-light-responsive supramolecular valves for photo-controlled drug release from mesoporous nanoparticles

Reprinted with permission from:

Wang, D.; Wu, S. *Langmuir*, **2016**, 32, 632-636. Copyright (2015) by the American Chemical Society.

Statement of Contribution

D. Wang convinced the idea.

led this work.

and D. Wang designed the experiment.

D. Wang did the synthesis and measurements.

D. Wang and wrote the manuscript.

Abstract

Red-light-responsive supramolecular valves constructed by tetra-ortho-methoxy-substituted azobenzene (mAzo) and β -cyclodextrin (β -CD) were used to control drug release from mesoporous silica nanoparticles (MSNs). Doxorubicin (DOX) was used as a model drug and loaded into nanopores of mAzo modified MSNs. β -CD formed supramolecular valves with mAzo by host-guest interaction and closed the nanopores. Red light was able to open the supramolecular valves and induce DOX release even in deep tissue.

Chapter 3

Red-light-responsive supramolecular valves for photo-controlled drug release from mesoporous nanoparticles

3.1 Introduction

Drug delivery systems have been widely studied for reducing drug toxicity and enhancing therapeutic efficacy. External stimuli, including light, pH, temperature and redox, can potentially control drug release at target sites of diseases.¹⁻⁵ Among these stimuli, light is a clean, non-invasive and efficient stimulus that is able to control drug delivery with high spatial and temporal resolution. For photo-controlled drug delivery, light induces photoreactions, which trigger drug release from the drug delivery systems.⁶⁻⁹ Most photoreactions used in drug delivery were induced by UV light, which limits the applications of photoresponsive drug delivery systems due to the poor tissue penetrability of UV light and the photodamage to biological systems caused by UV light.¹⁰⁻¹² Compared to UV light, red and near-infrared (NIR) light in the therapeutic window (600-900 nm) are better suited for biomedical applications.^{13, 14} Therefore, the investigations of red- or NIR-light-responsive drug delivery systems are urgently needed.

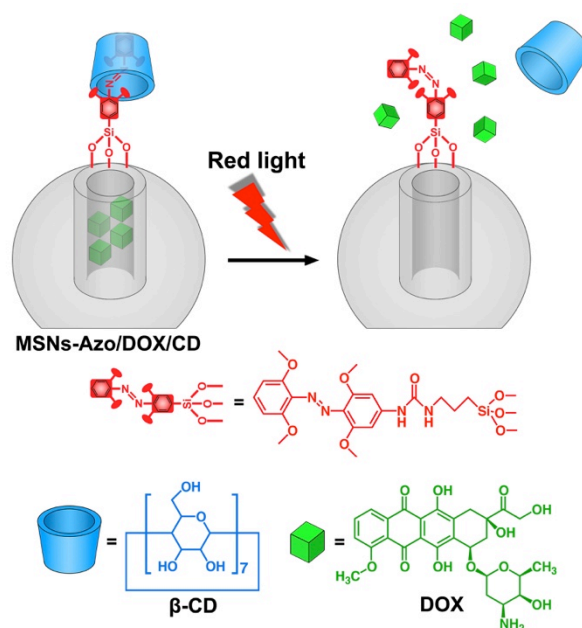
Till now, two main approaches to design red- or NIR-light-responsive drug

delivery systems are based on simultaneous two-photon absorption and photon upconversion.¹⁵⁻¹⁸ However, both the approaches are based on nonlinear optical processes that require high-intensity lasers, which may cause overheating problems and photodamage to biological components.^{19, 20} Furthermore, light intensity will be significantly decreased after passing through tissue because tissue strongly scatters incident light. The obtained light intensity in deep tissue might be insufficient to trigger two-photon absorption or photon upconversion.

Red-shifting the responsive wavelength of photoresponsive materials is an alternative way to design red- or NIR-light-responsive drug delivery systems. Avoiding the simultaneous two-photon absorption and upconversion processes, the intrinsic red- or NIR-light-responsive drug delivery systems may require lower light intensity.

Tetra-ortho-methoxy-substituted azobenzene (mAzo) is a novel red-light-responsive molecule. Different with the normal UV-light-responsive azobenzene, mAzo shows trans-to-cis isomerization under red light irradiation; cis-to-trans isomerization can be induced by heat or blue light.²¹⁻²⁵ In our previous study, the red-light-responsive supramolecular complex between mAzo and β -cyclodextrin (β -CD) was demonstrated. The association constant between *trans* mAzo and β -CD is 1546.0 M^{-1} , while it is only 82.1 M^{-1} between *cis* mAzo and β -CD. Therefore, a strong host-guest complex was formed between the *trans* mAzo and β -CD, and was able to be dissociated after red light irradiation.²⁶

Mesoporous silica nanoparticles (MSNs) with high surface area exhibit excellent biocompatibility, mechanical and chemical stability, and have been widely studied as drug carriers for the designing of drug delivery systems²⁷⁻²⁹. MSNs are easy to be post-modified, which makes them potential to be decorated by different stimuli-responsive groups. Therefore, MSNs can be applied to design stimuli-responsive drug delivery systems.^{30, 31}



Scheme 3.1 Cartoon of the red-light-responsive drug delivery system constructed by mesoporous silica nanoparticles (MSNs) modified with mAzo/β-CD supramolecular valves.

Herein, we fabricated red-light-responsive mesoporous silica nanoparticles for drug delivery using mAzo/β-CD as supramolecular valves (**Scheme 3.1**). Doxorubicin (DOX) was used as model drug and loaded into nanopores of the MSNs. Red light was able to control DOX release from the MSNs even in deep tissue. Red light with moderate intensity from LEDs is sufficient to induce drug delivery from the MSNs.

3.2 Photoresponsiveness of mAzo-Si

The photoresponsiveness of mAzo-Si was investigated by UV/vis absorption spectroscopy and ^1H NMR (**Figure 3.1**). The $n\text{-}\pi^*$ transition band of trans mAzo-Si extended to the red light region and was stronger than that of cis mAzo-Si (**Figure 3.1a**). Thus, trans mAzo-Si could be excited by red light and switched to the cis form. Approximately 85% of cis mAzo-Si was obtained after irradiating with 625 nm red light for 30 min (60 mW/cm^2) (**Figure 3.1b**, calculated from the peak areas of Ha and

Ha`)). The mAzo-Si solution changed from orange to yellow after red light irradiation. Cis mAzo-Si could be switched back to trans isomer by heating or blue light irradiation (Figure S3.2).

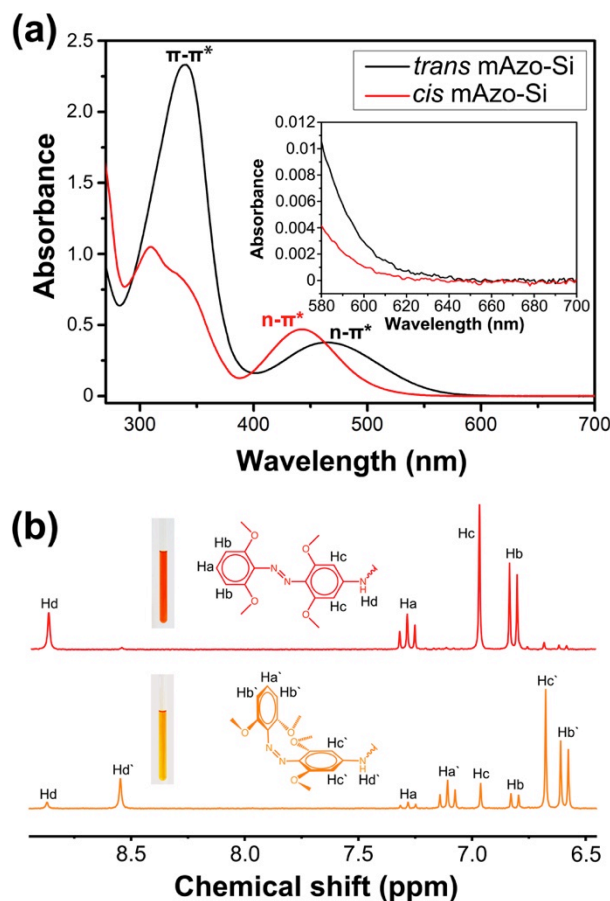
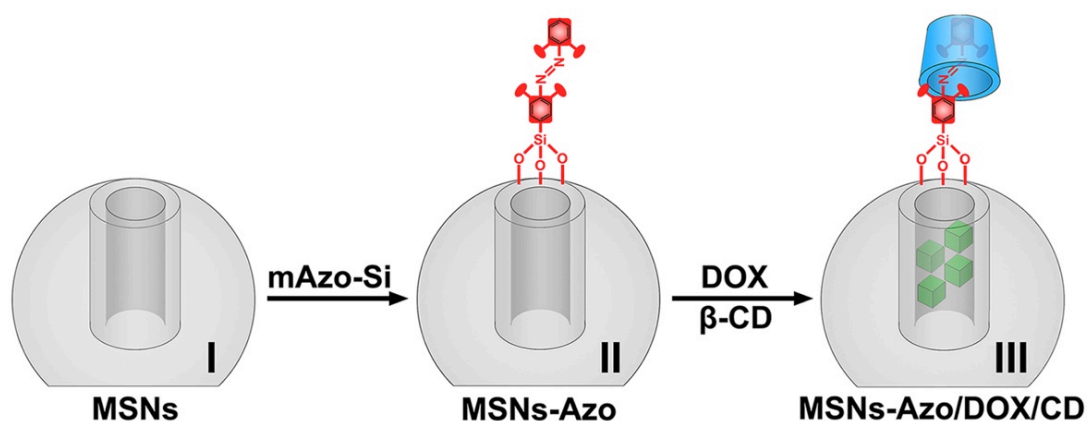


Figure 3.1 UV/vis (a) and ^1H NMR (b) spectra of mAzo-Si before and after red light irradiation (625 nm, 60 mW/cm², 30 min). The inset in (a) shows the enlarged absorption spectra of mAzo-Si in the red light region. The insets in (b) are photographs of *trans* and *cis* mAzo-Si.

3.3 Preparation and characterization of MSNs, MSNs-Azo and MSNs-Azo/DOX/CD



Scheme 3.2 Preparation of MSNs (I), MSNs-Azo (II) and MSNs-Azo/DOX/CD (III), I-II: mAzo-Si was grafted onto the MSNs surface; II-III: DOX was loaded into the nanopores of MSNs-Azo, and β -CD was capped onto the MSNs-Azo surface via host-guest interaction.

To prepare the drug delivery system, MSNs were synthesized as drug carriers (SI). mAzo-Si was then grafted on MSNs to prepare MSNs-Azo (**Scheme 3.2**). DOX was loaded into the nanopores, and β -CD was then capped onto the nanoparticles surface to form supramolecular valves with the grafted mAzo-Si to close the pores (MSNs-Azo/DOX/CD, **Scheme 3.2**). The DOX loading efficiency measured by UV/vis spectroscopy was 3.21 wt. % (**Figure S3.4**).

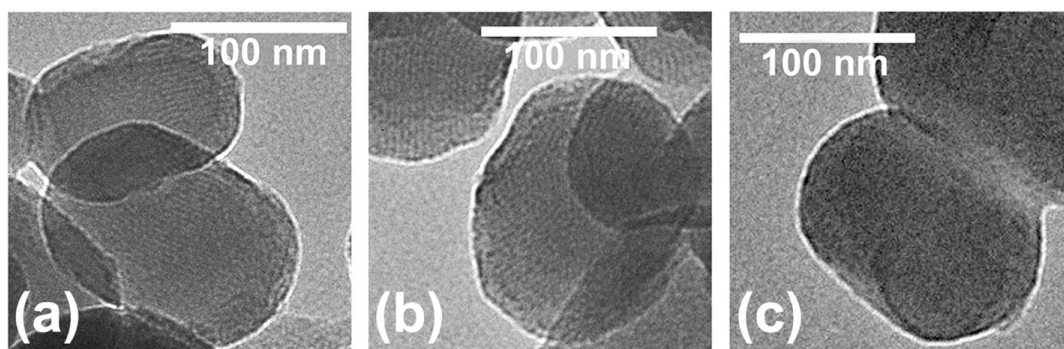


Figure 3.2 TEM images of MSNs (a), MSNs-Azo (b) and MSNs-Azo/DOX/CD (c).

Transmission electron microscopy (TEM) images showed that MSNs,

MSNs-Azo and MSNs-Azo/DOX/CD were elliptical nanoparticles with the length and width of ~ 200 and ~ 150 nm, respectively (**Figure 3.2**). The pore size of the mesoporous structures in MSNs and MSNs-Azo was ~ 2.8 nm. MSNs-Azo/DOX/CD did not exhibit any mesoporous structure in the TEM image (**Figure 3.2c**), indicating that DOX occupied the nanopores of the MSNs-Azo/DOX/CD.

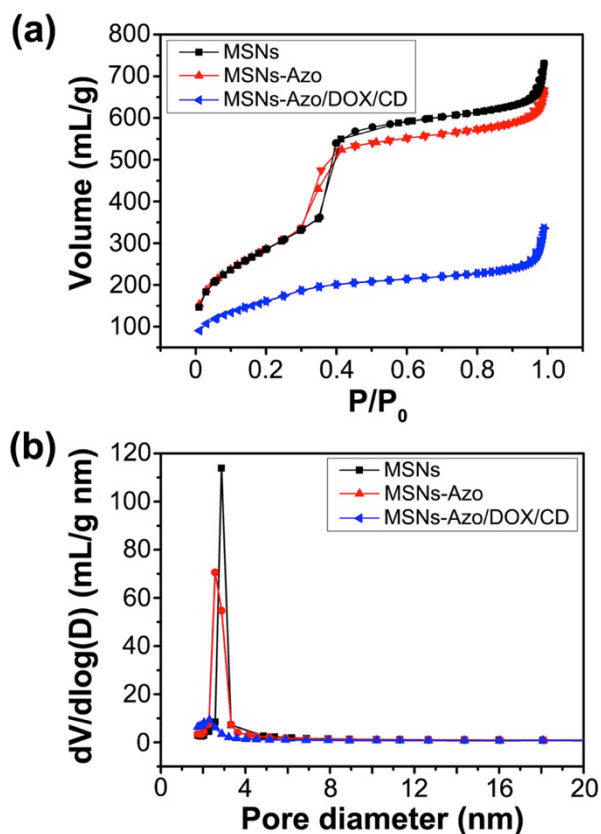


Figure 3.3 Nitrogen adsorption-desorption isotherms (a) and BJH pore size distribution (b) of MSNs, MSNs-Azo and MSNs-Azo/DOX/CD.

The N_2 adsorption-desorption isotherms were measured to investigate the mesoporous structures of MSNs, MSNs-Azo and MSNs-Azo/DOX/CD (**Figure 3.3a**). MSNs showed typical H1-hysteresis loops, indicating MSNs are mesoporous materials. The Brunauer-Emmett-Teller (BET) surface area of MSNs was $\sim 1045 \pm 20$ m^2/g ($n=3$). The N_2 adsorption-desorption isotherms of MSNs-Azo were similar to those of MSNs, and the BET surface area of MSNs-Azo (1044 ± 20 m^2/g) was almost

the same as that of MSNs. After loading with DOX, much weaker N_2 absorption was observed for the MSNs-Azo/DOX/CD. The BET surface area of the MSNs-Azo/DOX/CD decreased to $576 \pm 11 \text{ m}^2/\text{g}$, indicating the successful loading of DOX. The Barrett-Joyner-Halanda (BJH) pore sizes of the MSNs and MSNs-Azo were similar (2.5 to 3.3 nm) to those measured using TEM (**Figure 3.3b**). For the MSNs-Azo/DOX/CD, the peak of BJH pore size distribution was weak, which was coincided to the TEM and BET results.

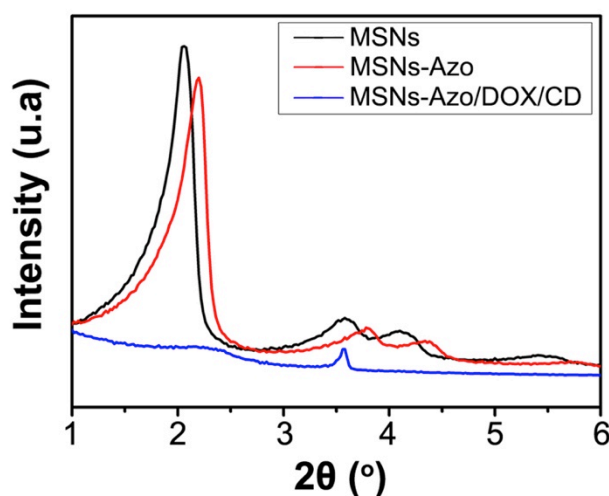


Figure 3.4 XRD patterns of MSNs, MSNs-Azo and MSNs-Azo/DOX/CD.

Moreover, the mesoporous structure was investigated by X-ray diffraction (XRD). A typical MCM-41 structure of the MSNs was observed in the XRD patterns (**Figure 3.4**). After the mAzo-Si modification, the MSNs-Azo still showed the ordered mesoporous structure, suggesting that mAzo-Si was only grafted on the surface of MSNs. For the MSNs-Azo/DOX/CD, the disappearance of the peak at $2\theta = 2^\circ$ in the XRD patterns confirmed the nanopores were loaded with DOX.

3.4 Red-light-induced drug release

The red-light-induced DOX release from the MSNs-Azo/DOX/CD was investigated using the “mini dialysis” setup (**Figure 3.5a**). Red light (625 nm)

triggered the opening of mAzo/ β -CD valves and the DOX release. The release kinetics under various irradiation conditions was quantified by UV/vis spectroscopy (**Figure S3.5**). Only $\sim 5\%$ of DOX was released from the MSNs-Azo/DOX/CD in the dark after 360 min, indicating that the drug leakage was minimized (**Figure 3.5b**). Approximately 13% of DOX was released after red light (625 nm, 15 mW/cm²) irradiating for 360 min. Red light with a higher intensity (60 mW/cm²) induced a faster release, and $\sim 38\%$ of DOX was released after irradiating for 360 min.

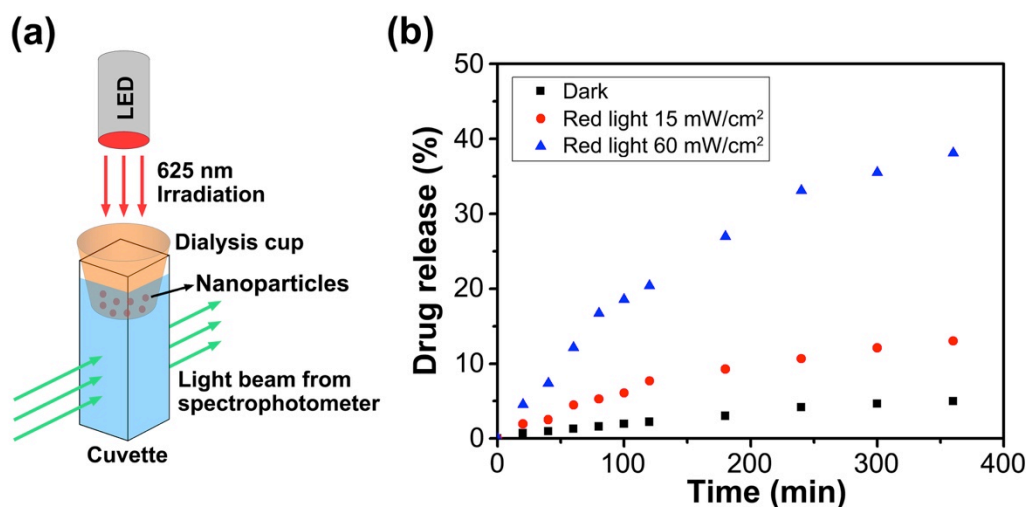


Figure 3.5 (a) Experimental setup for red-light-induced DOX release; (b) DOX release profiles for MSNs-Azo/DOX/CD in the dark and upon red light irradiation (625 nm, 15 mW/cm² or 60 mW/cm²).

Moreover, the photoresponsive drug release from the MSNs-Azo/DOX/CD in deep tissue was also investigated by placing a piece of 2 mm thick pork tissue between the light source and sample (**Figure 3.6a**). Red light still induced DOX release from the MSNs-Azo/DOX/CD after passing through the tissue. Approximately 8% and 23% of DOX were released from the MSNs-Azo/DOX/CD after red light (15 and 60 mW/cm²) irradiating for 360 min (**Figure 3.6b**). The lower released rate and amount might be attributed to the scattering and absorption of the tissue to the incident red light. Importantly, the light intensity used in this study was much lower than that required by the photoresponsive drug delivery systems designed

via upconversion process. Moreover, the light intensity was an order of magnitude lower than the maximum permissible exposure of skin at 625 nm (200 mW/cm^2).^{32, 33} Therefore, photodamage to skin and tissue during phototherapy can be prevented.

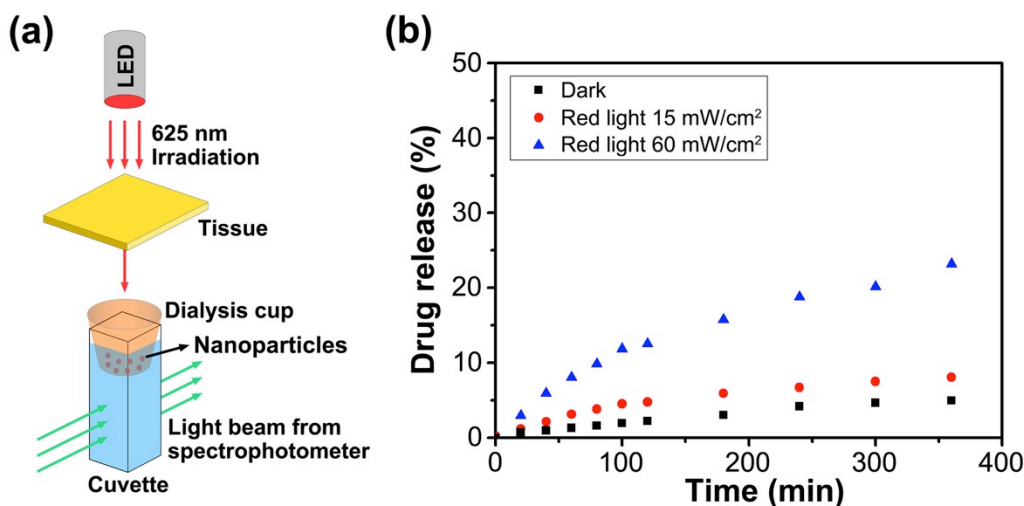


Figure 3.6 (a) Experimental setup for red-light-induced DOX release with a piece of tissue between light source and sample; (b) DOX release profiles for MSNs-Azo/DOX/CD in the dark and upon red light irradiation (625 nm, 15 mW/cm^2 or 60 mW/cm^2) in the presence of tissue.

3.5 Conclusion

In conclusion, we designed red-light-responsive MSNs using mAzo/ β -CD supramolecular valves for drug delivery. MSNs were used as the drug carriers, red-light-responsive supramolecular valves constructed by mAzo/ β -CD were grafted on the MSNs surface. A model drug, DOX, could be released from the MSNs under red light irradiation even in deep tissue. Compared with simultaneous two-photon absorption and up-conversion processes, red-shifting the responsive wavelength of photoresponsive materials showed several advantages: (i) the light intensity required was much lower than that for two-photon absorption and upconversion processes; (ii) the system was simple and no upconverting nanoparticles or high-intensity lasers was needed. Therefore, red-shifting the responsive wavelength of photoresponsive

materials is a new way to design red- or NIR-light-responsive drug delivery systems.

References

1. Gohy, J.-F.; Zhao, Y. *Chem. Soc. Rev.*, **2013**, *42*, 7117-7129.
2. Kang, X.; Cheng, Z.; Yang, D.; Ma, P.; Shang, M.; Peng, C.; Dai, Y.; Lin, J. *Adv. Funct. Mater.*, **2012**, *22*, 1470-1481.
3. Dai, Y.; Yang, D.; Ma, P.; Kang, X.; Zhang, X.; Li, C.; Hou, Z.; Cheng, Z.; Lin, J. *Biomaterials*, **2012**, *33*, 8704-8713.
4. Zhao, Q.; Wang, Y.; Yan, Y.; Huang, J. *ACS Nano*, **2014**, *11*, 11341-11349.
5. Liang, P.; Liu, C. -J.; Zhuo, R. -X.; Cheng, S. -X. *J. Mater. Chem. B.*, **2013**, *1*, 4243-4250.
6. Yuan, Z.; Zhao, D.; Yi, X.; Zhuo, R.; Li, F. *Adv. Funct. Mater.*, **2014**, *24*, 1799-1807.
7. Ferris, D. P.; Zhao, Y. -L.; Khashab, N. M.; Khatib, H. A.; Stoddart, J. F.; Zink, J. I. *J. Am. Chem. Soc.*, **2009**, *131*, 1686-1688.
8. Tan, L.; Wu, H. -X.; Yang, M. -Y.; Liu, C. -J.; Zhuo, R. -X. *RSC Adv*, **2015**, *5*, 10393-10399.
9. Wu, S.; Butt, H. -J. *Adv. Mater.*, 10.1002/adma.201502843.
10. Vrouwe, M. G.; Pines, A.; Overmeer, R. M.; Hanada, K.; Mullenders, L. H. F. *J. Cell. Sci.*, **2010**, *124*, 435-446.
11. Banerjee, G.; Gupta, N.; Kapoor, A.; Raman, G. *Cancer. Lett.*, **2005**, *223*, 275-284.
12. Wang, Z.; Johns, V. K.; Liao, Y. *Chem. Eur. J.*, **2014**, *20*, 14637-14640.
13. Kalka, K.; Merk, H.; Mukhtar, H. *J Am. Acad. Dermatol.*, **2000**, *42*, 389-413.
14. Rajendran, M. *Photodiagn. Photodyn.*, j.pdpdt.2015.07.177.
15. Cheng, Z.; Lin, J. *Macromol. Rapid. Commun.*, **2015**, *36*, 790-827.
16. Álvarez, M.; Best, A.; Unger, A.; Alonso, J. M.; Campo, A. D.; Schmelzeisen, M.; Kyonov, K.; Kreiter, M. *Adv. Funct. Mater.*, **2010**, *20*, 4265-4272.
17. Álvarez, M.; Best, A.; Pradhan-Kadam, S.; Koynov, K.; Jonas, U.; Kreiter, M. *Adv. Mater.*, **2008**, *20*, 4563-4567.

18. Yang, D.; Ma, P.; Hou, Z.; Cheng, Z.; Li, C.; Lin, J. *Chem. Soc. Rev.*, **2015**, *44*, 1416-1448.
19. He, S.; Krippes, K.; Ritz, S.; Chen, Z.; Best, A.; Butt, H. -J.; Mailänder, V.; Wu, S. *Chem. Commun.*, **2015**, *51*, 431-434.
20. Chen, Z.; Sun, W.; Butt, H. -J.; Wu, S. *Chem. -Eur. J.*, **2015**, *21*, 9165-9170.
21. Yang, Y.; Yue, L.; Li, H.; Maher, E.; Li, Y.; Wang, Y.; Wu, L.; Yam, V. W. -W. *Small*, **2012**, *8*, 3105-3110.
22. Lin, Y.; Qiao, Y.; Tang, P.; Li, Z.; Huang, J. *Soft. Matter.*, **2011**, *7*, 2762-2769.
23. Samanta, S.; Beharry, A. A.; Sadoski, O.; McCormick, T. M.; Babalhavaeji, A.; Tropepe, V.; Woolley, G. A. *J. Am. Chem. Soc.*, **2013**, *135*, 9777-9784.
24. Bléger, D.; Schwarz, J.; Brouwer, A. M.; Hecht, S. *J. Am. Chem. Soc.*, **2012**, *134*, 20597-20600.
25. Wang, D.; Xie, D.; Shi, W.; Sun, S.; Zhao, C. *Langmuir*, **2013**, *29*, 8311-8319.
26. Wang, D.; Wagner, M.; Butt, H. -J.; Wu, S. *Soft. Matter.*, **2015**, *11*, 7656-7662.
27. Wei, J.; Liu, Y.; Chen, J.; Li, Y.; Yue, Q.; Pan, G.; Yu, Y.; Deng, Y.; Zhao, D. *Adv. Mater.*, **2014**, *26*, 1782-1787.
28. Liu, J.; Bu, J.; Bu, W.; Zhang, S.; Pan, L.; Fan, W.; Chen, F.; Zhou, L.; Peng, W.; Zhao, K.; Du, J.; Shi, J. *Angew. Chem.*, **2014**, *126*, 1-6.
29. Yang, J.; Shen, D.; Zhou, L.; Li, W.; Li, X.; Yao, C.; Wang, R.; El-Toni, A. M.; Zhang, F.; Zhao, D. *Chem. Mater.*, **2013**, *25*, 3030-3037.
30. Liu, R.; Zhang, Y.; Zhao, X.; Agarwal, A.; Mueller, L. J.; Feng, P. *J. Am. Chem. Soc.*, **2010**, *132*, 1500-1501.
31. Fang, W.; Yang, J.; Gong, J.; Zheng, N. *Adv. Funct. Mater.*, **2012**, *22*, 842-848.
32. American National Standard for Safe Use of Lasers, Laser Institute of America, Orlando, FL, 2000.
33. Laser Safety Handbook, Northwestern University, Evanston, IL, 2011.

Supporting Information

1. Materials

2,6-Dimethoxyaniline ($C_8H_{11}NO_2$, CAS No. 2734-70-5) and β -cyclodextrin (β -CD) ($C_{42}H_{70}O_{35}$, CAS No. 7585-39-9) were purchased from Alfa Aesar. 3,5-Dimethoxyaniline ($C_8H_{11}NO_2$, CAS No. 10272-07-8), sodium nitrite ($NaNO_2$, CAS No. 7632-00-0), hexadecyltrimethylammonium bromide (CTAB) ($C_{19}H_{42}BrN$, CAS No. 57-09-0), tetraethyl orthosilicate (TEOS) ($C_8H_{20}O_4Si$, CAS No. 78-10-4) and (3-isocyanatopropyl)triethoxysilane (3-ICPES) ($C_{10}H_{21}NO_4Si$, CAS No. 24801-88-5) were purchased from Sigma Aldrich. Doxorubicin hydrochloride (DOX) ($C_{27}H_{30}NO_{11}Cl$, CAS No. 25316-40-9) was used as the model drug and purchased from Sigma Aldrich. All the solvents (HPLC grade) were purchased from Sigma Aldrich and were directly used without any further purification. Milli-Q water (resistivity: $18.2\text{ M}\Omega\times\text{cm}$) provided by a Sartorius Arium 611 VF Purification System was used throughout the project.

2. Methods

^1H and ^{13}C nuclear magnetic resonance (NMR) spectra were recorded on a Bruker Avance 250 MHz spectrometer. The ^1H -NMR experiments were acquired with a 5 mm BBI z-gradient probe on the 700 MHz Bruker AVANCE III system. For a proton spectrum, 128 transients were used with a $10\text{ }\mu\text{s}$ long 90° pulse and a 12600 Hz spectral width together with a recycling delay of 5 s. The ^{13}C NMR (176 MHz) measurements were made with a J-modulated (coupling constant of $145\text{ Hz } ^1\text{H}-^{13}\text{C}$ was used) spin-echo for C-nuclei coupled to protons to determine the number of attached protons and proton decoupling during acquisition. The 90° pulse for carbon was $14.5\text{ }\mu\text{s}$ long and 16000 scans were taken with a relaxation delay of 2 s.

The temperature was regulated at 298.3 K and calibrated with a standard ^1H methanol NMR sample using the topspin 3.2 software (Bruker). The control of the temperature was realized with a VTU (variable temperature unit) and an accuracy of

+/- 0.1 K.

Before Fourier transformation, the data were zero filled to 1024 points in f_1 and multiplied by a window function (q-sine bell or sine bell) in both dimension. The spectral widths were 30000 Hz (236 ppm) for ^{13}C and 9000 Hz (18 ppm) for ^1H , both nuclei with a relaxation delay of 2.5 s. Proton and carbon spectra were referenced using the solvents signals (DMSO- d_5H =2.49 ppm and ^{13}C : DMSO- d_6 =39.5 ppm) as an internal standard.

Mass spectra (MS) were obtained using a VG instrument ZAB 2-SE-FPD. UV/Vis absorption spectra were measured on a Lambda 900 spectrometer (Perkin Elmer).

Transmission electron microscopy (TEM) images were measured on a JEOL JEM1400 system. To prepare the TEM samples, a drop of the particle suspension in water was placed onto a 200-mesh copper TEM grid and dried at room temperature.

Nitrogen adsorption-desorption isotherms were measured at 77 K on a Micromeritics Tristar II surface area and pore size analyzer.

X-ray diffraction (XRD) patterns were recorded on a Fine focus anode system with Cu $\text{K}\alpha$ line ($\lambda=0.15418$ nm).

Photoisomerization was induced by the LEDs with the wavelengths of 470 and 625 nm (device types LCS-0470-03-22 and LCS-0625-03-22, Mightex Systems). The output intensities of the LEDs were controlled by an LED controller (device type SLC-MA04-MU, Mightex Systems) and were calibrated by an optical powermeter (Model 407A, Spectra-Physics Corporation).

3. Synthesis

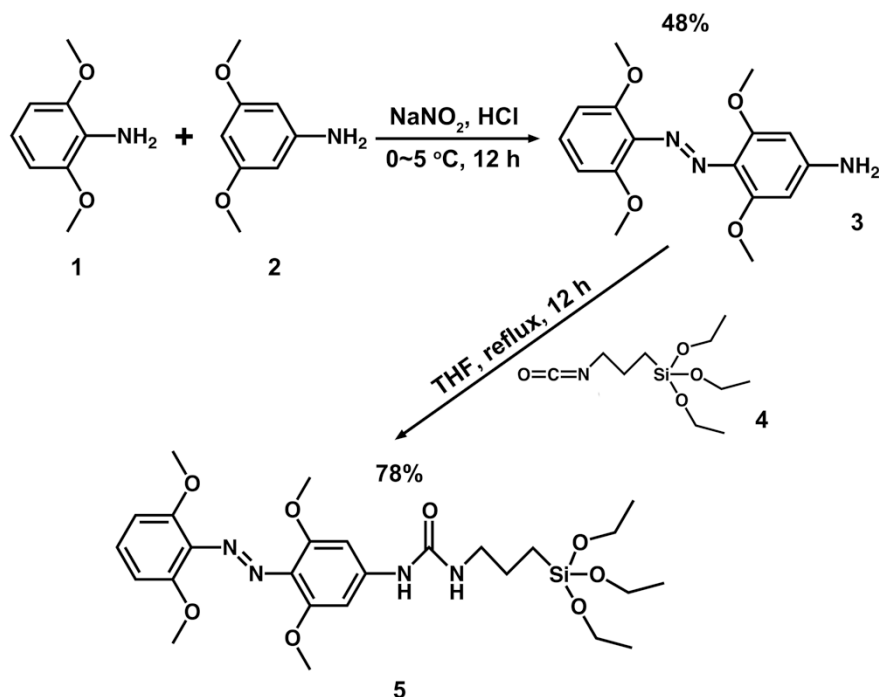


Figure S3.1 Route for the synthesis of 5 (mAzo-Si).

Synthesis of 3 (mAzo-NH₂) The synthesis of mAzo-NH₂ was as our previous work.¹ ¹HNMR (DMSO-*d*₆, 250 MHz): $\delta=7.15$ (t, $J=8.3$ Hz, 1H; Ar-H), $\delta=6.71$ (d, $J=8.4$ Hz, 2H; Ar-H), $\delta=5.99$ (s, 2H; Ar-NH₂), $\delta=5.94$ (s, 2H; Ar-H), $\delta=3.67$ (d, $J=1.7$ Hz, 12H; -OCH₃); ¹³CNMR (DMSO-*d*₆, 250 MHz): $\delta=156.1$ (Ar-C), $\delta=153.4$ (Ar-C), $\delta=151.0$ (Ar-C), $\delta=126.6$ (Ar-C), $\delta=123.4$ (Ar-C), $\delta=105.3$ (Ar-C), $\delta=89.9$ (Ar-C), $\delta=55.9$ (-OMe), $\delta=55.4$ (-OMe); MS $m/z=316.3$.

Synthesis of 5 (mAzo-Si) The synthesized 3 (0.032 g, 0.10 mmol) was mixed with 3-ICPES (4 in **Figure S3.1**) (0.018 g, 0.11 mmol) in 6 mL of THF. The mixture was heated under reflux and an atmosphere of N₂ overnight. After removal of the solvent, the residue was recrystallized in hexane/THF to get the mAzo-Si. Yield: 78%. ¹HNMR (DMSO-*d*₆, 250 MHz): $\delta=8.86$ (s, 1H; Ar-NH-CO), $\delta=7.27$ (t, $J=8.4$ Hz, 1H; Ar-H), $\delta=6.96$ (s, 2H; Ar-H), $\delta=6.80$ (d, $J=8.4$ Hz, 2H; Ar-H), $\delta=6.36$ (t, $J=5.7$ Hz, 1H;

C-NH-CO), $\delta=3.83$ (t, $J=8.4$ Hz, 6H; -OCH₂-), $\delta=3.72$ (s, 12H; -OCH₃), $\delta=3.14$ (q, $J=6.6$ Hz, 2H; N-CH₂-), $\delta=1.63$ - 1.48 (m, 2H; -CH₂-), $\delta=1.21$ (t, $J=7.0$ Hz, 9H; -CH₃), $\delta=0.70$ - 0.55 (m, 2H; -CH₂-Si). ¹³CNMR (DMSO-*d*₆, 250 MHz): $\delta=154.8$ (C=O), $\delta=153.6$ (Ar-C), $\delta=151.0$ (Ar-C), $\delta=143.5$ (Ar-C), $\delta=134.5$ (Ar-C), $\delta=128.0$ (Ar-C), $\delta=127.1$ (Ar-C), $\delta=105.3$ (Ar-C), $\delta=93.9$ (Ar-C), $\delta=57.7$ (-O-CH₂), $\delta=56.0$ (-OCH₃), $\delta=55.7$ (-OCH₃), $\delta=41.7$ (-N-CH₂-), $\delta=23.3$ (-CH₂-), $\delta=18.2$ (-CH₃), $\delta=7.2$ (-CH₂-Si).

4. Photoisomerization of mAzo-Si

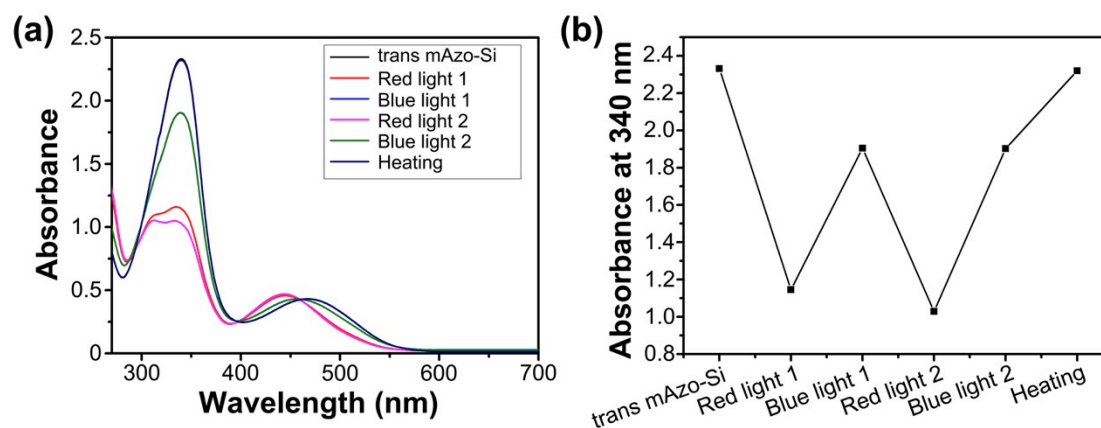


Figure S3.2 UV/vis spectra (a) of the mAzo-Si (1.3 mg in 15 mL DMSO) after treating with a sequence of red/blue light (60 mW/cm^2 , 30 min) and heating (60°C , 600 min), the absorbance at 340 nm is also showed (b).

5. Synthesis of mesoporous silica nanoparticles (MSNs)

The MSNs were synthesized as the reported procedures.¹ In a typical synthesis, CTAB (1.000 g, 3.00 mmol) was added to 480 mL of H₂O. Then 3.5 mL of NaOH (2 M) aqueous solution was added and induced the complete dissolving of the CTAB. The solution was then heated to 80 °C under stirring. TEOS (5.000 mL, 23.0 mmol) was added to the solution slowly over several minutes, during the adding the precipitate could be observed. The reaction was kept at 80 °C for 2 h under vigorous stirring. Then the solution was filtered while hot using a fritted funnel, the white solid was washed with H₂O and MeOH for several times. Then the solid was dried in an oven at 100 °C for over 24h to get the MSNs.

6. Photoresponse of MSNs-Azo

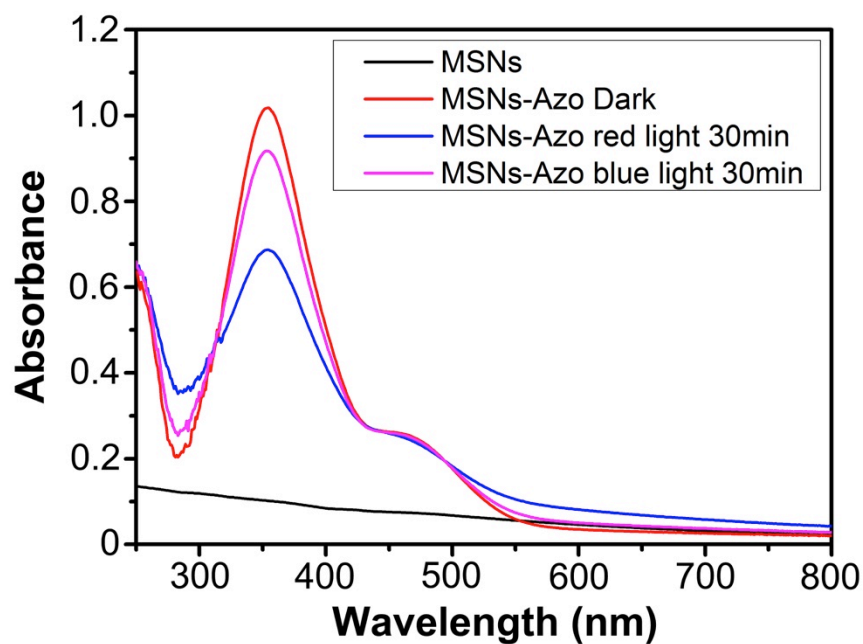


Figure S3.3 UV/vis spectra of MSNs (5 mg in 1 mL PBS pH=7.4) and MSNs-Azo (5 mg in 1 mL PBS pH=7.4) before and after red and blue light irradiating (60 mW/cm², 30 min).

7. DOX loading capacity of MSNs-Azo/DOX/CD

The loading capacity of the DOX in the nanoparticles was calculated as our previous work.² After the loading of DOX, the nanoparticles were collected by centrifugation, and the DOX concentration of the residual solution was measured via the UV/vis spectrophotometer. The nanoparticles were washed for three times to remove the adsorbed DOX on surface, and the DOX concentrations in the eluted solutions were measured. The loading capacity of the DOX in the nanoparticles could be calculated by the followed equation:

$$LC_{DOX} = \frac{C_{loading}V_{loading} - C_{residual}V_{residual} - C_1V_1 - C_2V_2 - C_3V_3}{m}$$

where LC_{DOX} is the DOX loading capacity (wt. %); m is the weight of the nanoparticles (mg); $C_{loading}$, $C_{residual}$, C_1 , C_2 and C_3 are the concentrations of the DOX in the original loading solution, residual solution and the eluted solutions for the 1st, 2nd and 3rd time, respectively (mg/mL); $V_{loading}$, $V_{residual}$, V_1 , V_2 and V_3 are the volumes of the original loading solution, residual solution and the eluted solutions for the 1st, 2nd and 3rd time, respectively (mL).

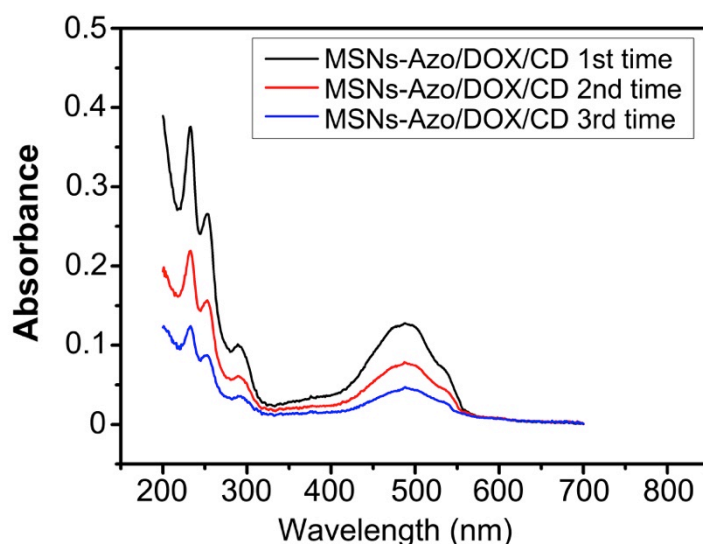


Figure S3.4 UV/vis spectra of the eluted solutions for MSNs-Azo/DOX/CD. The DOX loading capacity of the MSNs-Azo/DOX/CD was calculated to be 3.21 wt.%.

8. Red light induced DOX release

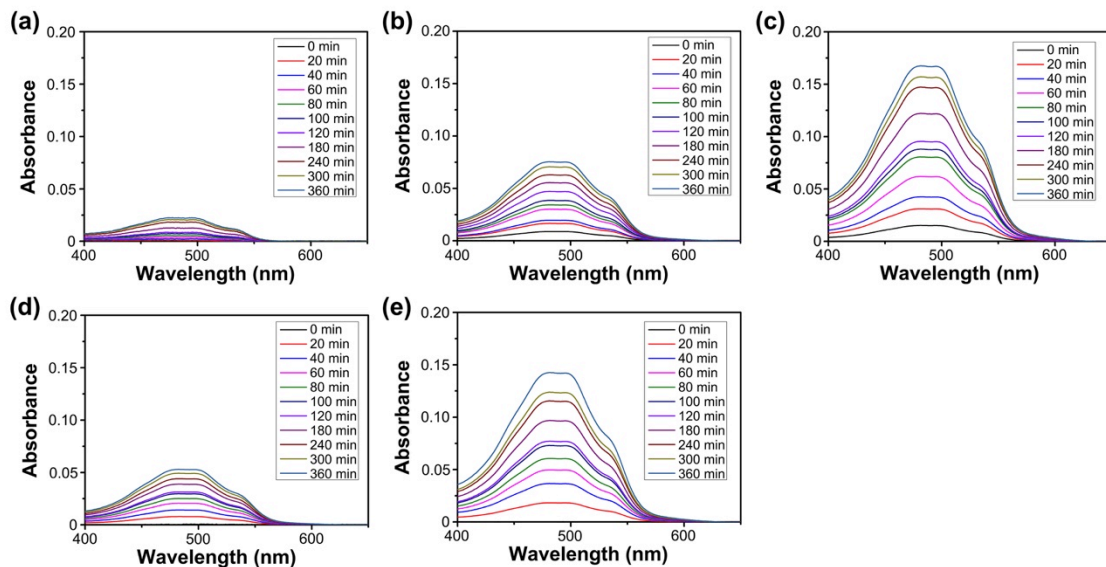


Figure S3.5 UV/vis spectra of the MSNs-Azo/DOX/CD in the dark (a), under 15 mW/cm² red light (b) and 60 mW/cm² red light (c) irradiation for different time. UV/vis spectra of the MSNs-Azo/DOX/CD under 15 mW/cm² red light (d) and 60 mW/cm² red light (e) irradiation for different time when a piece of tissue was placed between the sample and LED. The amount of released DOX is shown in **Figure 3.5(b)** and **Figure 3.6(b)** in the main manuscript.

The chemical structure of compound 1 is shown above the ¹H NMR spectrum. The structure is a 4,4'-dimethoxyazobenzene derivative. The left benzene ring has methoxy groups at positions 2 and 6 (labeled 'k' and 'l' in the spectrum). The right benzene ring has methoxy groups at positions 2 and 6 (labeled 'c' and 'b' in the spectrum). The azo group (-N=N-) connects the two rings. The right ring is substituted with a hydrazide group (-NH-C(=O)-NH-) at position 1, which is further substituted with a propyl chain (-CH₂-CH₂-CH₂-) at position 2. The propyl chain is labeled 'f', 'g', and 'h' in the spectrum. The propyl chain is attached to a silicon atom, which is also bonded to two ethoxy groups (labeled 'i' and 'j' in the spectrum) and a methyl group (labeled 'h' in the spectrum).

The ¹H NMR spectrum (DMSO-d₆) shows the following peaks (ppm):

- 9.1 (s, 1H, d)
- 7.4 (s, 1H, a)
- 7.1 (s, 1H, c)
- 6.9 (s, 1H, b)
- 6.6 (s, 1H, e)
- 3.8 (s, 3H, k+l)
- 3.7 (s, 3H, i)
- 3.3 (s, 3H, f)
- 2.5 (s, 3H, g)
- 1.5 (s, 3H, h)
- 1.2 (s, 3H, j)

The spectrum is recorded in DMSO-d₆ at 400 MHz. The x-axis is labeled 'f1 (ppm)' and ranges from 1.0 to 10.0. The y-axis represents intensity. The solvent peak for H₂O is visible at approximately 3.3 ppm.

Chemical structure of compound 10 is shown above the ^1H NMR spectrum. The structure is a 1,1'-diaryl-1,1'-diazene derivative. The left phenyl ring has a methoxy group at position 4 (protons *a*, *b*, *c*, *d*). The right phenyl ring has a methoxy group at position 4 (protons *e*, *f*, *g*, *h*). The central diazene group is at position 1 of both rings. The right ring is also substituted with a 2-ethyl-1H-imidazole-5-carboxamide group at position 2 (protons *i*, *j*, *k*, *l*, *m*, *n*, *o*, *p*). The NMR spectrum is recorded in $\text{DMSO}-d_6$ and shows peaks corresponding to the labeled protons. The x-axis is labeled f_1 (ppm) and ranges from 0 to 10. The solvent peak is at 4.0 ppm.

Figure S3.7 ^{13}C NMR spectrum of the mAzo-Si

Reference

1. Ferris, D.P.; Zhao, Y.-L.; Khashab, N. M.; Khatib, H. A.; Stoddart, J. F.; Zink, J. I. Light-Operated Mechanized Nanoparticles. *J. Am. Chem. Soc.* **2009**, *131*, 1686-1688.
2. He, S.; Krippes, K.; Ritz, S.; Chen, Z.; Best, A.; Butt, H.-J.; Mailänder, V.; Wu, S. Ultralow-intensity near-infrared light induces drug delivery by upconverting nanoparticles. *Chem. Commun.* **2015**, *51*, 431-434.

A photoresponsive orthogonal supramolecular complex based on host-guest interactions

Reprinted with permission from:

Wang, D.; Wagner, M.; Saydjari, A. K.; Mueller, J.; Winzen, S.; Butt, H.-J.; Wu, S. *Chem. Eur. J.*, **2017**, *23*, 2628-2634. Copyright (2017) by the Wiley-VCH Verlag GmbH & Co. KGaA, Weinheim.

Statement of Contribution

D. Wang convinced the idea of photoresponsive orthogonal supramolecular system.

led this work.

and D. Wang designed the experiment.

did the NMR measurements.

did the DFT calculations.

did the ITC measurements.

D. Wang did the synthesis and other measurements.

D. Wang and wrote the manuscript.

Abstract

We synthesized a novel green-light-responsive tetra-ortho-isopropoxy-substituted azobenzene (ipAzo). *Cis* ipAzo forms a strong host-guest complex with γ -cyclodextrin (γ -CD) whereas *trans* ipAzo binds weakly. This new photoresponsive host-guest interaction is reverse to the well-known azobenzene (Azo)/ α -cyclodextrin (α -CD) complex, which is strong only between *trans* Azo and α -CD. By combining the UV-light-responsive Azo/ α -CD and greenlight-responsive ipAzo/ γ -CD host-guest complexes, a photoresponsive orthogonal supramolecular system is developed.

Chapter 4

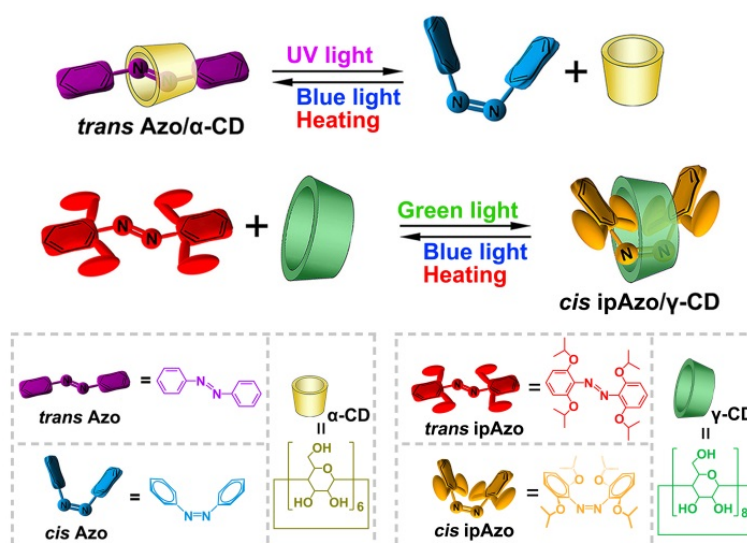
A photoresponsive orthogonal supramolecular complex based on host-guest interactions

4.1 Introduction

Light as a clean, efficient and precise external stimulus has been extensively used to control processes and functions in chemistry, biology and materials science.^[1-6] Photoresponsive supramolecular materials obtain plenty of attention due to the multi-functionality and efficient reactivity.^[7-11] Photoresponsive materials develop more complex recently. More than one chromophore is included, and multiple sources of light with various wavelengths can be applied to control the systems orthogonally in several independent states, which make the photoresponsive orthogonal materials able to react to complex external irradiations and show various properties.^[12-14] However, most of the photoresponsive chromophores have significantly overlapping absorption bands in the UV-visible region, which limit the targeted excitation.^[6, 12]

Azobenzene (Azo), well-known for UV light induced *trans*-to-*cis* isomerization and blue light or heating induced *cis*-to-*trans* isomerization, has been widely investigated for its photoresponsive host-guest supramolecular interaction with α -cyclodextrin (α -CD).^[15-21] Generally, *trans* Azo is able to enter the hydrophobic cavity of α -CD in water environment to form a 1:1 host-guest complex.^[22-24] In

contrast, *cis* Azo does not fit α -CD cavity and is more hydrophilic than *trans* Azo, which slides out of the hydrophobic cavity and further induces disassembly of the host-guest complex (**Scheme 5.1**). Photoresponsive supramolecular materials based on the Azo/ α -CD host-guest interaction have been constructed for various applications, including supramolecular hydrogels, drug delivery systems, photoresponsive surfaces, and macroscopic self-assemblies.^[25-28]



Scheme 4.1 Schematic illustration of the photoresponsive host-guest interaction between Azo and α -CD, and between ipAzo and γ -CD. Blue light or heating induces the assembly of the Azo/ α -CD complex, while UV light irradiation induces the disassembly of the complex. Green light irradiation induces the assembly of the ipAzo/ γ -CD complex, while blue light or heating induces the disassembly of the complex.

To realize the photoresponsive orthogonal supramolecular system, another host-guest complex responsive to irradiation with the wavelength far from UV light is needed. Incorporation of electron-donating groups ortho or para to the Azo moiety red-shifts the photoswitching wavelength for the *trans*-to-*cis* isomerization.^[29-31] In our previous work, by modifying the Azo moiety with methoxy groups, the synthesized tetra-ortho-methoxy-substituted Azo (mAzo) shows red light induced

trans-to-*cis* isomerization and different supramolecular properties compared with normal Azo.^[32, 33] Neither *trans* nor *cis* mAzo can form host-guest complex with α -CD. However, strong host-guest complex is formed between *trans* mAzo and β -cyclodextrin (β -CD), while the host-guest interaction between *cis* mAzo and β -CD is weak. The observed supramolecular properties of mAzo likely derive from the bulky substituent groups and the larger hydrophobic cavity of β -CD as compared to α -CD. However, while *trans* Azo has been reported to form strong host-guest complex with β -CD, the mAzo/ β -CD complex is not suitable to be applied for the photoresponsive orthogonal supramolecular system.^[34, 35] Another photoresponsive host-guest complex is still needed.

Here, we synthesized green-light-responsive tetra-ortho-isopropoxy-substituted Azo (ipAzo) with four larger substituent groups than mAzo. Interestingly, a strong host-guest complex was observed between *cis* ipAzo and γ -cyclodextrin (γ -CD), while the host-guest interaction between *trans* ipAzo and γ -CD was weak (**Scheme 4.1**). The result was the reverse of the Azo/ α -CD complex. The potential application to fabricate photoresponsive orthogonal supramolecular systems was investigated by combining the green-light-responsive ipAzo/ γ -CD complex with the known UV-light-responsive Azo/ α -CD host-guest complex.

4.2 Photoisomerization of ipAzo-Py

However, the solubility of ipAzo in water was poor, which hindered supramolecular investigations. To increase the hydrophilicity, ipAzo-Py was synthesized by grafting pyridine to ipAzo (Experimental Section). Due to the amphiphilicity, ipAzo-Py may form aggregates in water (**Figure S4.1-S4.3**).

The photoisomerization of ipAzo-Py was investigated by UV/vis absorption spectroscopy and ^1H NMR (**Figure 4.1**). After green light irradiation, *trans* ipAzo-Py switched to the *cis* form, inducing a decrease in the π - π^* transition band and an

increase in the $n\text{-}\pi^*$ transition band (**Figure 4.1a**). The $n\text{-}\pi^*$ transition band of *trans* ipAzo-Py was separated from that of *cis* ipAzo-Py in the green-light region. Thus, green light could excite the *trans* ipAzo-Py $n\text{-}\pi^*$ transition and induce the *trans*-to-*cis* isomerization.^[36, 37] Approximately 80% of *trans* ipAzo-Py switched to *cis* ipAzo-Py after 530 nm green light irradiation for 30 min (40 mW/cm²) (**Figure 4.1b**). The *cis* ipAzo-Py could be switched back to the *trans* form by heating or blue light irradiation (470 nm) (**Figure S4.4-S4.7**).

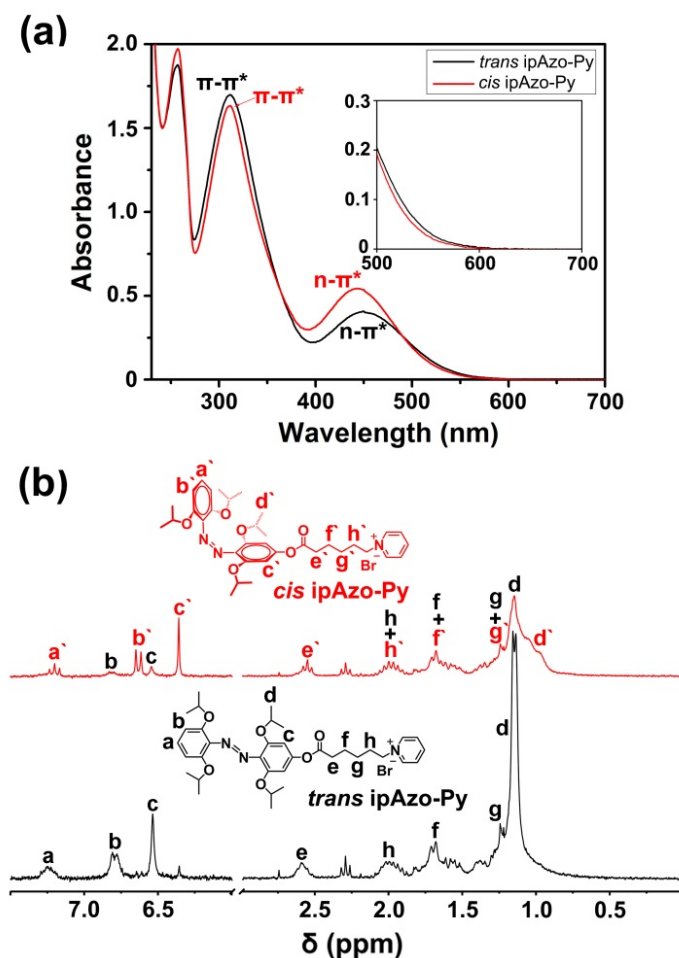


Figure 4.1 UV/vis (a) ([ipAzo-Py]=0.4 mM in H₂O/methanol, v:v=9:1) and ¹H NMR (b) (250 MHz in D₂O at 298 K, [ipAzo-Py]=1 mM) spectra of ipAzo-Py before (black lines) and after (red lines) green light irradiation (530 nm, 40 mW/cm², 30 min). The inset in (a) shows the enlarged absorption spectra of ipAzo-Py in the green light region. The signal at δ=2.25 may come from impurity, and will not affect the host-guest interaction.

4.3 Host-guest Interaction between ipAzo-Py and γ -CD

To investigate the supramolecular interaction between ipAzo-Py and γ -CD, *trans* ipAzo-Py in D₂O was irradiated with green light (20 mW/cm²) for 30 min to obtain ~50% *cis* ipAzo-Py ([*trans* ipAzo-Py]:[*cis* ipAzo-Py]≈1:1). ¹H NMR spectra were recorded for the *trans* ipAzo-Py/*cis* ipAzo-Py mixture before and after adding γ -CD, respectively (**Figure 4.2**). No obvious shift of the proton signals in the aromatic region of *trans* ipAzo-Py could be observed after adding γ -CD, suggesting no supramolecular complex was formed between *trans* ipAzo-Py and γ -CD. However, after adding γ -CD, significant shifts of *cis* ipAzo-Py proton signals in the aromatic region could be observed, due to the host-guest complex formation between *cis* ipAzo-Py and γ -CD. ¹H NMR and UV/vis titration results further supported that the *cis* ipAzo-Py could form a 1:1 host-guest complex with γ -CD, while no supramolecular complex was formed between *trans* ipAzo-Py and γ -CD (**Figure S4.8-S4.13**).

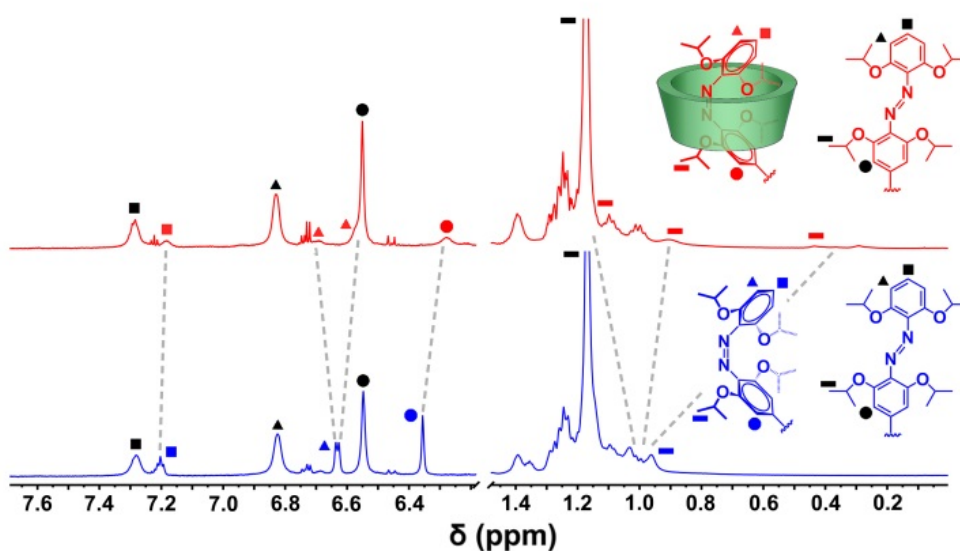


Figure 4.2 ¹H NMR spectra (700 MHz in D₂O at 298K) of *trans/cis* ipAzo-Py mixture before (blue) and after (red) adding of γ -CD. ([*trans* ipAzo-Py]:[*cis* ipAzo-Py]≈1:1, [ipAzo-Py]=1 mM, [ipAzo-Py]:[γ -CD]=1:1)

The green-light-responsive host-guest interaction between ipAzo-Py and γ -CD was further confirmed by two-dimensional nuclear Overhauser effect spectroscopy (2D NOESY) and electrospray ionization mass spectrometry (ESI-MS) (**Figure 4.3, S4.15, S4.16**). No correlation could be observed between the protons of *trans* ipAzo-Py and γ -CD, indicating that *trans* ipAzo-Py does not form a complex with γ -CD (**Figure 4.3, left**). After irradiation with green light, strong correlation between the protons of *cis* ipAzo-Py (proton a', b', c' and d') and the inner protons of γ -CD could be observed. These results indicated that *cis* ipAzo-Py entered the hydrophobic cavity of γ -CD deeply to form the host-guest complex (**Figure 4.3, S4.14**). The 2D NOESY results were in good accordance with the ESI-MS spectra. A strong peak at $m/z=1902.71$ corresponding to the singly charged host-guest complex *cis* ipAzo-Py/ γ -CD could be observed, which was weak for the mixture of *trans* ipAzo-Py and γ -CD. (**Figure S4.15, S4.16**).

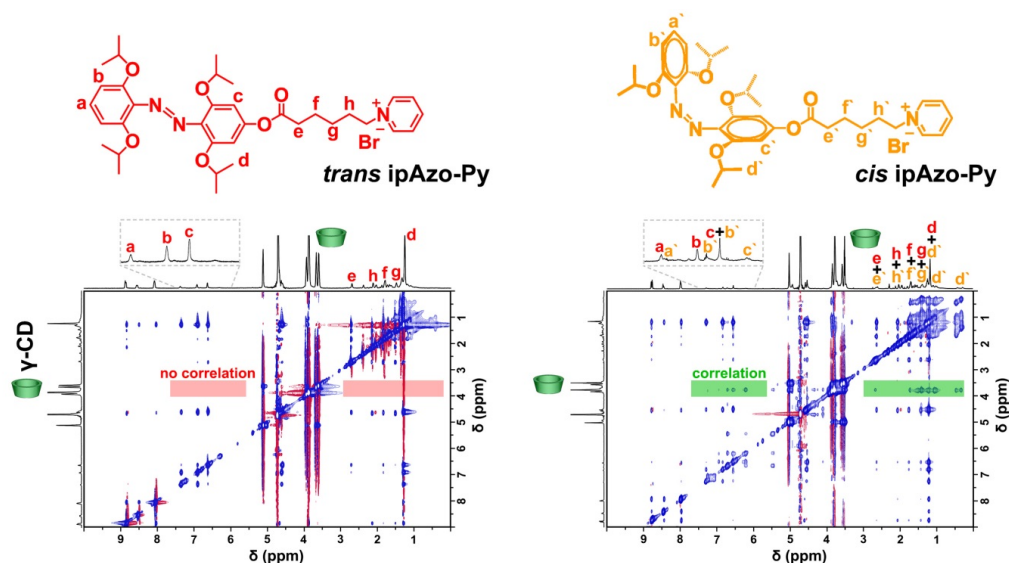


Figure 4.3 2D NOESY spectra (700 MHz in D₂O at 298 K) of *trans* ipAzo-Py/ γ -CD (left) and *cis* ipAzo-Py/ γ -CD (right). The red/green rectangles in the spectra show whether there are correlations between the protons of ipAzo-Py and the protons of γ -CD. ([ipAzo-Py]=2 mM, [ipAzo-Py]:[γ -CD]=1:1)

These results were also well supported by DFT calculated molecular models of

trans ipAzo and *cis* ipAzo (**Figure 4.4**). Both *trans* ipAzo and *cis* ipAzo showed highly nonplanar structures due to sterics of the grafted isopropoxy groups. In contrast to the reported Azo/ α -CD system, the calculated width of *trans* ipAzo was larger than the hydrophobic cavity of γ -CD while the calculated width of *cis* ipAzo was smaller than the hydrophobic cavity of γ -CD. Thus, the surprising behavior of ipAzo/ γ -CD system derives from a different mechanism of disassembly; instead of the guest width being too small for the host cavity, the guest width is too large.

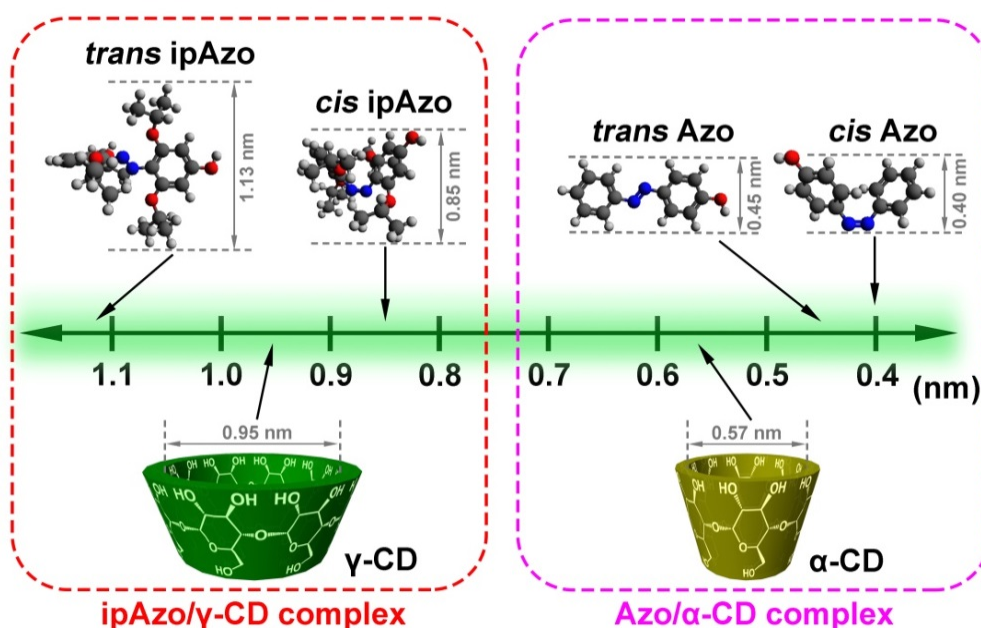


Figure 4.4 DFT calculated molecular models of Azo molecules. CD cavity sizes were from literature.^[40]

4.4 Photoresponsive orthogonal supramolecular system

Combining the widely-reported UV-light-responsive Azo/ α -CD host-guest complex with this novel green-light-responsive ipAzo/ γ -CD host-guest complex, we foresaw the potential for photoresponsive orthogonal supramolecular systems.

The light used to induce *trans*-to-*cis* photoisomerization of Azo and ipAzo were orthogonal to each other with respect to wavelength (**Figure S4.17, S4.18**). Then, to design an orthogonal supramolecular system using the Azo/ α -CD and ipAzo/ γ -CD

host-guest complexes, *trans* Azo should only combine with α -CD rather than γ -CD, while *cis* ipAzo should only combine with γ -CD rather than α -CD.^[38, 39] The host-guest interactions between Azo/ipAzo and α -CD/ γ -CD were therefore quantified by measuring the association constants (K_a) of the host-guest complexes (Supporting Information, **Figure S4.19-S4.30**). The association constants are listed in **Table 4.1**, where Azo-Py and ipAzo-Py were used as the guest molecules, and a modified Benesi-Hildebrand equation was used for the calculation of the association constants between Azos and CDs. *Trans* Azo-Py showed a high association constant with α -CD, while the association constant between *cis* Azo-Py and α -CD was low, in accordance with reported results.^[25, 28] Both *trans* and *cis* Azo-Py showed low association constants with γ -CD, indicating weak host-guest interactions between Azo-Py and γ -CD. The results were further consistent with calculated molecular models (**Figure 4.4**). Because the hydrophobic cavity of γ -CD is too large for both *trans* and *cis* Azo, *trans* Azo-Py may enter the hydrophobic cavity of γ -CD to form a weak supramolecular complex. However, the *trans* Azo-Py/ γ -CD complex is unstable and can be disassembled in the presence of α -CD (**Figure S4.32**). In the mixture of *trans* Azo-Py, α -CD, and γ -CD ([Azo-Py]:[α -CD]:[γ -CD]=1:1:1), ~80% of *trans* Azo-Py formed host-guest complex with α -CD, while only ~10% of *trans* Azo-Py/ γ -CD complex could be formed (SI). For ipAzo-Py, γ -CD showed a much higher association constant with *cis* ipAzo-Py compared to the *trans* isomer, while very low association constants were shown for both *trans* and *cis* ipAzo-Py with α -CD. These results were attributed to the hydrophobic cavity size of α -CD being smaller than the width of ipAzo (**Figure 4.4**).

From the above results, the photoresponsive orthogonal supramolecular system could be described as in **Figure 4.5a**. Strong host-guest complexes could only be formed between *trans* Azo and α -CD, and between *cis* ipAzo and γ -CD, which were UV/blue-light-responsive and green/blue-light-responsive, respectively. After heating or blue light irradiation, the system of Azo, ipAzo, α -CD, and γ -CD was in the

thermodynamic “single open” state (I). Green light irradiation transformed the system to the “both closed” state (II) while UV irradiation transformed the system to the “both open” state (III). Each of these state were easily obtained from any other by the application of heat or blue light (I, “single open”), green light (II, “both closed”), or UV light (III, “both open”).

Table 4.1 Association constants (K_a) between α -CD or γ -CD and ipAzo or Azo.^a

K _a (M ⁻¹)		Guest			
		<i>trans</i> ipAzo	<i>cis</i> ipAzo	<i>trans</i> Azo	<i>cis</i> Azo
Host	α-CD	26.4±8.0	28.3±6.9	1340.0±510.0	25.4±9.4
	γ-CD	25.9±5.1	1659.0±57.0	149.0±1.2	16.0±20.0

[a] The details for measuring K_a are provided in Supporting Information (Equation S1 and **Figure S4.19-S4.30**). Error bars represent one standard deviation as calculated from orthogonal distance regression.

2D NOESY was used to confirm the formation of the orthogonal supramolecular system in the mixture of *trans* Azo-Py, *cis* ipAzo-Py, α -CD, and γ -CD (II, “both closed” state) (**Figure 4.5b, left**). In the 2D NOESY spectrum, the proton signals of α -CD and γ -CD overlapped heavily. However, the signal at $\delta=3.8$ (belonging to the inner protons of γ -CD) displayed strong correlation with the protons of *cis* ipAzo-Py (yellow rectangle), while the correlation between the protons of *trans* Azo-Py and the inner protons of γ -CD was relatively weak (green rectangle). Thus, correlation of *trans* Azo-Py and the overlapped region of α -CD and γ -CD (purple rectangle) consisted mostly of signal from a strong *trans* Azo-Py/ α -CD complex. The 2D NOESY results indicated that a majority of *trans* Azo-Py/ α -CD and *cis* ipAzo-Py/ γ -CD complexes, in other words, the orthogonal supramolecular system, could be formed from the mixture of *trans* Azo-Py, *cis* ipAzo-Py, α -CD, and γ -CD (II,

“both closed” state). After blue light or UV light irradiation, the “single open” (I) or “both open” (III) states of the orthogonal supramolecular system could be obtained (Figure 4.5b, middle, right).

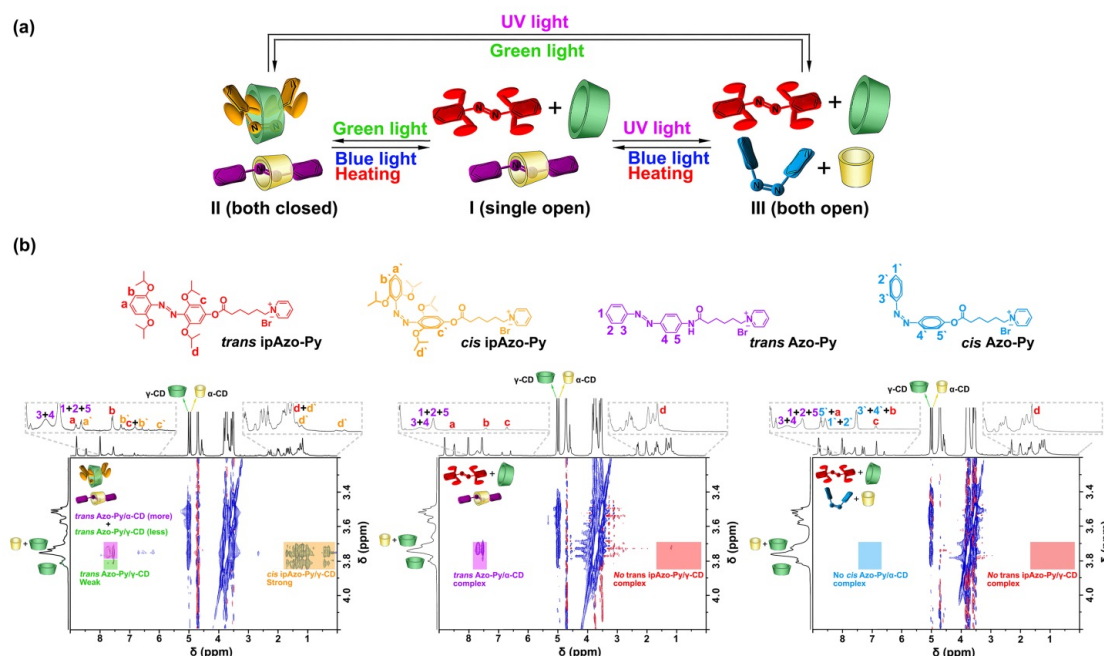


Figure 4.5 (a) Schematic illustration of the photoresponsive orthogonal supramolecular system formed by Azo/ α -CD and ipAzo/ γ -CD host-guest complexes. (b) 2D NOESY spectra (700 MHz in D₂O at 298 K) of the photoresponsive orthogonal supramolecular system in “both closed” state (II, left), “single open” state (I, middle), and “both open” state (III, right). The green rectangle shows the correlation between the protons of *trans* Azo-Py and the protons of γ -CD, the purple rectangle shows the correlation between the protons of *trans* Azo-Py and the protons of α -CD, the yellow rectangle shows the correlation between the protons of *cis* ipAzo-Py and the protons of γ -CD. ([Azo-Py]=2 mM, [Azo-Py]:[ipAzo-Py]:[α -CD]:[γ -CD]=1:1:1:1)

4.5 Conclusions

In the present research, a novel photoresponsive host-guest interaction between

ipAzo and γ -CD was demonstrated. Opposite of the known interaction between Azo and α -CD, *trans* ipAzo was unable to form supramolecular complex with γ -CD. However, after green light irradiation, a strong 1:1 host-guest complex could be formed between *cis* ipAzo and γ -CD. With the UV-light-responsive Azo/ α -CD and green-light-responsive ipAzo/ γ -CD host-guest complexes, the potential to design photoresponsive orthogonal supramolecular systems was confirmed. As a new photoresponsive host-guest interaction, the ipAzo/ γ -CD complex has potential to construct green-light-responsive supramolecular colloids, polymers, surfaces, and gels. We also expect that more interesting photoresponsive orthogonal supramolecular structures could be realized by combining the UV-light-responsive Azo/ α -CD and green-light-responsive ipAzo/ γ -CD host-guest complexes, including photoresponsive hierarchical self-assemblies, dual-drug release systems, and photoresponsive interpenetrating polymer network hydrogels.^[41-43]

References

1. Ichimura, K.; Oh, S. K.; Nakagawa, M. *Science*, **2000**, 288, 1624-1626.
2. Lv, J.; Liu, Y.; Wei, J.; Chen, E.; Qin, L.; Yu, Y. *Nature*, **2016**, 537, 179-184.
3. Mitrano, M.; Cantaluppi, A.; Nicoletti, D.; Kaiser, S.; Perucchi, A.; Lupi, S.; DiPietro, P.; Pontiroli, D.; Riccò, M.; Clark, S. R.; Jaksch, D.; Cavalleri, A. *Nature*, **2016**, 530, 461-464.
4. Jia, K.; Zhang, F.; Huang, H.; Chen, Y. *J. Am. Chem. Soc.*, **2016**, 138, 1514-1517.
5. Russew, M. M.; Hecht, S. *Adv. Mater.*, **2010**, 22, 3348-3360.
6. Ercole, F.; Davis, T. P.; Evans, R. A. *Polym. Chem.*, **2010**, 1, 37-54.
7. Moratz, J.; Samanta, A.; Voskuhl, J.; Nalluri, S. K. M.; Ravoo, B. J. *Chem. Eur. J.*, **2015**, 21, 3271-3277.
8. Yu, G.; Jie, K.; Huang, F. *Chem. Rev.*, **2015**, 115, 7240-7303.
9. Bisoyi, H. K.; Li, Q. *Acc. Chem. Res.*, **2014**, 47, 3184-3195.
10. Kamiya, Y.; Asanuma, H. *Acc. Chem. Res.*, **2014**, 47, 1663-1672.
11. Ma, X.; Tian, H. *Acc. Chem. Res.*, **2014**, 47, 1971-1981.
12. Lerch, M. M.; Hansen, M. J.; Velema, W. A.; Szymanski, W.; Feringa, B. L. *Nat. Commun.*, **2016**, 7, 12054.
13. García-Fernández, L.; Herbivo, C.; Arranz, V. S. M.; Warther, D.; Donato, L.; Specht, A.; del Campo, A. *Adv. Mater.*, **2014**, 26, 5012-5017.
14. Hansen, M. J.; Velema, W. A.; Lerch, M. M.; Szymanski, W.; Feringa, B. L. *Chem. Soc. Rev.*, **2015**, 44, 3358-3377.
15. Hartley, G. S. *Nature*, **1937**, 140, 281.
16. Dhammika Bandara, H. M.; Burdette, S. C. *Chem. Soc. Rev.*, **2012**, 41, 1809-1825.
17. Blasco, E.; Schmidt, B. V. K. J.; Barner-Kowollik, C.; Piñol, M.; Oriol, L. *Macromolecules*, **2014**, 47, 3693-3700.
18. Harada, A.; Takashima, Y.; Nakahata, M. *Acc. Chem. Res.*, **2014**, 47, 2128-2140.
19. Liao, X.; Chen, G.; Liu, X.; Chen, W.; Chen, F.; Jiang, M. *Angew. Chem. Int. Ed.*,

- 2010**, *49*, 4409-4413.
20. Samanta, A.; Stuart, M. C. A.; Ravoo, B. J. *J. Am. Chem. Soc.*, **2012**, *134*, 19909-19914.
21. Zhou, Y.; Wang, D.; Huang, S.; Auernhammer, G.; He, Y.; Butt, H.-J.; Wu, S. *Chem. Commun.*, **2015**, *51*, 2725-2727.
22. Zheng, X.; Wang, D.; Shuai, Z.; Zhang, X. *J. Phys. Chem. B*, **2012**, *116*, 823-832.
23. Tomatsu, I.; Hashidzume, A.; Harada, A. *Angew. Chem. Int. Ed.*, **2006**, *45*, 4605-4608.
24. Schmidt, B. V. K. J.; Hetzer, M.; Ritter, H.; Barner-Kowollik, C. *Prog. Polym. Sci.*, **2014**, *39*, 235-249.
25. Tamesue, S.; Takashima, Y.; Yamaguchi, H.; Shinkai, S.; Harada, A. *Angew. Chem. Int. Ed.*, **2010**, *49*, 7461-7464.
26. Xiao, W.; Chen, W.; Xu, X.; Li, C.; Zhang, J.; Zhuo, R.; Zhang, X. *Adv. Mater.*, **2011**, *23*, 3526-3530.
27. Wan, P.; Jiang, Y.; Wang, Y.; Wang, Z.; Zhang, X. *Chem. Commun.*, **2008**, *44*, 5710-5712.
28. Yamaguchi, H.; Kobayashi, Y.; Kobayashi, R.; Takashima, Y.; Hashidzume, A.; Harada, A. *Nat. Commun.*, **2012**, *3*, 603.
29. Dong, M.; Babalhavaeji, A.; Samanta, S.; Beharry, A. A.; Woolley, G. A. *Acc. Chem. Res.*, **2015**, *48*, 2662-2670.
30. Beharry, A. A.; Sadovski, O.; Woolley, G. A. *J. Am. Chem. Soc.*, **2011**, *133*, 19684-19687.
31. Samanta, S.; Beharry, A. A.; Sadovski, O.; McCormick, T. M.; Babalhavaeji, A.; Tropepe, V.; Woolley, G. A. *J. Am. Chem. Soc.*, **2013**, *135*, 9777-9784.
32. Wang, D.; Wagner, M.; Butt, H.-J.; Wu, S. *Soft. Matter.*, **2015**, *11*, 7656-7662.
33. Wang, D.; Wu, S. *Langmuir*, **2016**, *32*, 632-636.
34. Wang, D.; Xie, D.; Shi, W.; Sun, S.; Zhao, C. *Langmuir*, **2013**, *29*, 8311-8319.
35. Zhu, L.; Yan, H.; Ang, C. Y.; Nguyen, K. T.; Li, M.; Zhao, Y. *Chem. Eur. J.*,

- 2012**, *18*, 13979-13983.
36. Bléger, D.; Schwarz, J.; Brouwer, A. M.; Hecht, S. *J. Am. Chem. Soc.*, **2012**, *134*, 20597-20600.
37. Bushuyev, O. S.; Tomberg, A.; Frišćić, T.; Barrett, C. J. *J. Am. Chem. Soc.*, **2013**, *135*, 12556-12559.
38. Wang, W.; Zhang, Y.; Sun, B.; Chen, L.; Xu, X.; Wang, M.; Li, X.; Yu, Y.; Jiang, W.; Yang, H. *Chem. Sci.*, **2014**, *5*, 4554-4560.
39. Yan, X.; Cook, T. R.; Pollock, J. B.; Wei, P.; Zhang, Y.; Yu, Y.; Huang, F.; Stang, P. J. *J. Am. Chem. Soc.*, **2014**, *136*, 4460-4463.
40. Crini, G. *Chem. Rev.*, **2014**, *114*, 10940-10975.
41. Yan, X.; Li, S.; Cook, T. R.; Ji, X.; Yao, Y.; Pollock, J. B.; Shi, J.; Yu, G.; Li, J.; Huang, F.; Stang, P. J. *J. Am. Chem. Soc.*, **2013**, *135*, 14036-14039.
42. Li, X.; Zhou, L.; Wei, Y.; El-Toni, A. M.; Zhang, F.; Zhao, D. *J. Am. Chem. Soc.*, **2014**, *136*, 15086-15092.
43. Li, C.; Rowland, M. J.; Shao, Y.; Cao, T.; Chen, C.; Jia, H.; Zhou, X.; Yang, Z.; Scherman, O. A.; Liu, D. *Adv. Mater.*, **2015**, *27*, 3298-3304.

Supporting Information

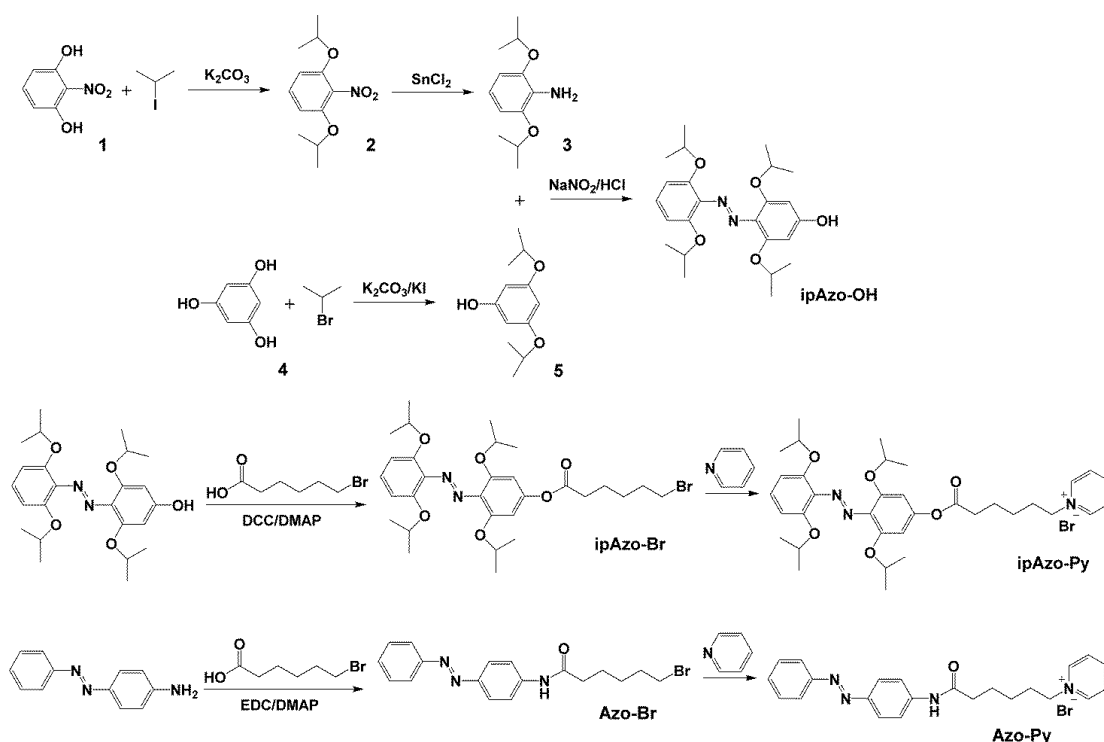
1. Materials and Reagents

2-nitroresorcinol ($C_6H_5NO_4$, CAS No. 601-89-8), 2-iodopropane (C_3H_7I , CAS No. 75-30-9), 6-bromohexanoic acid ($C_6H_{11}BrO_2$, CAS No. 4224-70-8), phloroglucinol ($C_6H_6O_3$, CAS No. 108-73-6), 2-bromopropane (C_3H_7Br , CAS No. 75-26-3), pyridine (C_5H_5N , 110-86-1), and tin (II) chloride dihydrate ($SnCl_2 \cdot 2H_2O$, CAS No. 10025-69-1) were purchased from Alfa Aesar. 4-Aminoazobenzene ($C_{12}H_{11}N_3$, CAS No. 60-09-3), N, N'-dicyclohexylcarbodiimide (DCC) ($C_{13}H_{22}N_2$, CAS No. 538-75-0), 4-(dimethylamino)pyridine (DMAP) ($C_7H_{10}N_2$, CAS No. 1122-58-3), and sodium nitrite ($NaNO_2$, CAS No. 7632-00-0) were purchased from Sigma Aldrich. α -Cyclodextrin (α -CD) ($C_{36}H_{60}O_{30}$, CAS No. 10016-20-3), γ -cyclodextrin (γ -CD) ($C_{48}H_{80}O_{40}$, CAS No. 17465-86-0), and N-(3-dimethylaminopropyl)-N'-ethylcarbodiimide hydrochloride (EDC) ($C_8H_{18}N_3Cl$, CAS No. 25952-53-8) were purchased from Acros Organics. All the solvents (HPLC grade) were purchased from Sigma Aldrich and were directly used without any further purification. Milli-Q water (resistivity: $18.2\text{ M}\Omega \times \text{cm}$) provided by a Sartorius Arium 611 VF Purification System was used throughout the project.

2. Methods

^1H and ^{13}C nuclear magnetic resonance (NMR) spectra were recorded on a Bruker Avance 250 MHz spectrometer. The 2D ^1H , ^1H -NOESY spectra were recorded on a Bruker Avance 700 MHz spectrometer. Mass spectra (MS) were obtained using a VG instrument ZAB 2-SE-FPD. Electrospray ionization mass spectra (ESI-MS) were obtained using a Waters instrument Q-ToF Ultima 3 micromass. UV/vis absorption spectra were measured on a Lambda 900 spectrometer (Perkin Elmer). ITC experiments were performed with a NanoITC Low Volume from TA Instruments (Eschborn, Germany). The reported DFT calculations were performed without any symmetry constraints, using 6-311G(d,p) basis set, and B3LYP functional in Gaussian09. Optimized geometries for trans and cis isomers were easily obtained by initializing the dihedral angle about the nitrogen-nitrogen double bond at 0 or 180° respectively. Photoisomerization was induced by the LEDs with the wavelengths of 365, 470 and 530 nm (device types LCS-0365-03-22, LCS-0470-03-22 and LCS-0530-03-22, Mightex Systems). The output intensities of the LEDs were controlled by an LED controller (device type SLC-MA04-MU, Mightex Systems) and were calibrated by an optical power meter (Model 407A, Spectra-Physics Corporation).

3. Synthesis



Scheme S4.1 Route for the synthesis of the chemicals.

The route for the synthesis of the chemicals is shown in **Scheme S4.1**.

Synthesis of 2. 2-nitroresorcinol (1 in **Scheme S4.1**, 1550 mg, 10 mmol), 2-iodopropane (3910 mg, 23 mmol) and K_2CO_3 (4140 mg, 30 mmol) were dissolved into 100 mL of DMF. After stirring under 90 °C for 16 h, the DMF was removed by rotating evaporation. The residue was washed by ethyl acetate (EA) 3 times to obtain the rough product. The black solid was further purified by chromatography using dichloromethane as eluent to obtain product 2. Yield: 75%. 1H NMR (DMSO- d_6 , 250 MHz): δ =7.40 (t, J =8.5 Hz, 1H), δ =6.87 (d, J =8.6 Hz, 2H), δ =4.73 (hept, J =6.1 Hz, 2H), δ =1.24 (d, J =6.1 Hz, 12 H). ^{13}C -NMR (DMSO- d_6 , 63 MHz): δ =153.5, δ =138.2, δ =121.3, δ =108.9, δ =70.0, δ =22.0. MS cal: m/z =239.1 found: m/z =239.3.

Synthesis of 3. 2 (2300 mg, 10 mmol) and excess of $SnCl_2 \cdot 2H_2O$ (4500 mg, 20 mmol) were dissolved into 30 mL of EA. The mixture was kept stirring under 60 °C for 20 h.

Then the mixture was poured into excess saturated Na_2CO_3 aqueous solution and a copious white precipitate was formed immediately. The precipitate was filtrated and the clear solution was washed with EA 3 times to obtain the rough product. The oil-like product was further purified by chromatography using dichloromethane as eluent to obtain the product 3. Yield: 85%. ^1H NMR ($\text{DMSO}-d_6$, 250 MHz): $\delta=6.87$ (s, 3H), $\delta=4.48$ (hept, $J=6.0$ Hz, 2H), $\delta=4.05$ (s, 2H), $\delta=1.28$ (d, $J=6.1$ Hz, 12H). ^{13}C NMR ($\text{DMSO}-d_6$, 63 MHz): $\delta=144.8$, $\delta=128.7$, $\delta=115.4$, $\delta=107.4$, $\delta=70.1$, $\delta=22.0$. MS cal: $m/z=209.1$ found: $m/z=209.2$

Synthesis of 5. The synthesis of 5 was followed previous literature.^[1] 4 (1260 mg, 10 mmol), 2-bromopropane (7320 mg, 60 mmol), K_2CO_3 (8280 mg, 60 mmol) and KI (400 mg, 2.4 mmol) were dissolved into 100 mL of DMF. The reaction was kept stirring under 90 °C for 48 h. Then the DMF was removed by rotating evaporation and the residue was washed by EA 3 times to obtain the rough product. The black oil-like rough product was further purified by chromatography using dichloromethane/methanol (1:5) as eluent to obtain product 5. Yield: 28%. ^1H NMR ($\text{DMSO}-d_6$, 250 MHz): $\delta=6.03$ (s, 1H), $\delta=5.86$ (s, 2H), $\delta=5.61$ (s, 1H), $\delta=4.46$ (m, 2H), $\delta=1.31$ (d, $J=6.1$ Hz, 12H). ^{13}C NMR ($\text{DMSO}-d_6$, 63 MHz): $\delta=159.7$, $\delta=157.8$, $\delta=96.9$, $\delta=96.2$, $\delta=71.3$, $\delta=20.9$. MS cal: $m/z=210.1$ found: $m/z=210.3$

Synthesis of ipAzo-OH. The synthesized 3 (823 mg, 3.9 mmol) was dissolved in the mixture of 0.75 mL of H_2O and 0.97 mL of HCl (37 wt.%). After the solution was cooled to 0~5 °C, NaNO_2 (276 mg, 4 mmol) in 4 mL H_2O was added quickly. The solution was stirred for 20 min and the temperature of the solution was kept at 0~5 °C. The synthesized 5 (823 mg, 3.9 mmol) and NaOH (300 mg, 7.5 mmol) were dissolved in 3 mL of H_2O and then the mixture was added slowly in the diazonium salt solution at 0~5 °C. After stirring overnight the dark red solid was collected and purified by chromatography using EA/THF (1:1) as eluent to get the product ipAzo-OH. Yield: 50%. ^1H NMR ($\text{MeOD}-d_4$, 250 MHz, with ~5 mg of NaOH, 298K): $\delta=7.06$ (t, $J=8.3$ Hz, 1H), $\delta=6.67$ (d, $J=8.4$ Hz, 2H), $\delta=5.96$ (s, 2H), $\delta=4.55$ (m, 4H), $\delta=1.27$ (dd,

$J=21.8, 6.0$ Hz, 24H). ^{13}C NMR (MeOD- d_4 , 176 MHz, with ~ 5 mg of NaOH, 243K): $\delta=173.1, \delta=155.0, \delta=150.1, \delta=137.6, \delta=126.1, \delta=125.0, \delta=107.7, \delta=98.2, \delta=70.5, \delta=21.1$. MS cal: $m/z=430.3$ found: $m/z=430.2$

Synthesis of ipAzo-Br. 6-bromohexanoic acid (246 mg, 1.3 mmol), DCC (268 mg, 1.3 mmol), DMAP (20 mg, 0.2 mmol) and ipAzo-OH (568 mg, 1.3 mmol) were dissolved in 60 mL of dichloromethane, the mixture was kept stirring under room temperature for 72 h. After removing the precipitate and solvent by filtration and roto-evaporation, the rough product was further purified by chromatography using dichloromethane as eluent to obtain the product of ipAzo-Br. ^1H NMR (DMSO- d_6 , 250 MHz): $\delta=7.21$ (t, $J=8.4$ Hz, 1H), $\delta=6.77$ (d, $J=8.5$ Hz, 2H), $\delta=6.58$ (s, 2H), $\delta=4.54$ (p, $J=5.8$ Hz, 4H), $\delta=2.62$ (t, $J=7.2$ Hz, 2H), $\delta=2.24$ (t, $J=7.2$ Hz, 2H), $\delta=1.89\text{--}1.47$ (m, 6H), $\delta=1.18$ (d, $J=6.0$ Hz, 24 H). ^{13}C NMR (DMSO- d_6 , 63 MHz): $\delta=171.57, \delta=150.77, \delta=150.39, \delta=149.77, \delta=136.56, \delta=133.60, \delta=128.48, \delta=71.25, \delta=35.10, \delta=33.30, \delta=31.83, \delta=26.92, \delta=23.34, \delta=21.73$. MS cal: $m/z=606.2$ found: $m/z=606.2$

Synthesis of ipAzo-Py. ipAzo-Br (97 mg, 0.16 mmol) was dissolved in THF (20 mL). Then, pyridine (20 mL) was added. The mixture was stirred overnight at 60°C under Ar. The solvents were removed by roto-evaporation. The obtained dark red solid was dissolved in methanol. The solution was added slowly to plenty of petroleum ether under stirring, and the red precipitate was filtered and dried under vacuum to obtain ipAzo-Py. Yield: 90%. ^1H NMR (D_2O , 250 MHz): $\delta=8.53$ (d, $J=5.6$ Hz, 2H), $\delta=8.21$ (t, $J=8.1$ Hz, 1H), $\delta=7.73$ (t, $J=7.0$ Hz, 2H), $\delta=6.99$ (t, $J=8.4$ Hz, 1H), $\delta=6.54$ (d, $J=8.5$ Hz, 2H), $\delta=6.29$ (s, 2H), $\delta=4.31$ (m, 2H), $\delta=2.34$ (t, $J=7.2$ Hz, 2H), $\delta=1.75\text{--}1.23$ (m, 6H), $\delta=0.90$ (d, $J=5.7$ Hz, 24H). ESI-MS cal: $m/z=604.3$ found: $m/z=605.3$

Synthesis of Azo-Br. 6-bromohexanoic acid (246 mg, 1.3 mmol), EDC (248 mg, 1.3 mmol), DMAP (20 mg, 0.2 mmol) and 4-aminoazobenzene (256 mg, 1.3 mmol) were dissolved in 60 mL of dichloromethane, the mixture was kept stirring under room temperature for 72 h. After the reaction, the solvent was removed by roto-evaporation.

The rough product was further purified by chromatography using dichloromethane as eluent to get the product of Azo-Br. ^1H NMR ($\text{DMSO}-d_6$, 250 MHz): $\delta=10.34$ (s, 1H), $\delta=7.94\text{--}7.79$ (m, 6H), $\delta=7.65\text{--}7.47$ (m, 3H), $\delta=3.52$ (t, $J=7.4$ Hz, 2H), $\delta=2.35$ (t, $J=7.2$ Hz, 2H), $\delta=1.82$ (t, $J=7.3$ Hz, 2H), $\delta=1.62$ (t, $J=7.2$ Hz, 2H), $\delta=1.42$ (t, $J=7.3$ Hz, 2H). ^{13}C NMR ($\text{DMSO}-d_6$, 63 MHz): $\delta=171.53$, $\delta=151.96$, $\delta=147.32$, $\delta=142.36$, $\delta=131.0$, $\delta=129.39$, $\delta=123.62$, $\delta=122.25$, $\delta=119.12$, $\delta=39.31$, $\delta=33.72$, $\delta=30.49$, $\delta=24.93$, $\delta=24.22$. MS cal: $m/z=375.1$ found: $m/z=375.2$

Synthesis of Azo-Py. Azo-Br (60 mg, 0.16 mmol) was dissolved in THF (20 mL) and pyridine (20 mL) was added. The mixture was stirred overnight at 60°C under Ar and solvents were removed by roto-evaporation. The obtained yellow solid was dissolved in methanol and the solution was added slowly to excess petroleum ether under stirring. The yellow precipitate was filtered and dried under vacuum to obtain the Azo-Py. ^1H NMR (D_2O , 250 MHz): $\delta=8.73$ (d, $J=5.9$ Hz, 2H), $\delta=8.34$ (t, $J=8.1$ Hz, 1H), $\delta=7.94$ (t, $J=7.1$ Hz, 2H), $\delta=7.76$ (m, 4H), $\delta=7.50$ (m, 5H), $\delta=4.53$ (t, $J=7.3$, 2H), $\delta=2.29$ (t, $J=7.2$ Hz, 2H), $\delta=1.96$ (q, $J=7.1$ Hz, 2H), $\delta=1.60$ (t, $J=7.4$ Hz, 2H), $\delta=1.29$ (m, 2H). ^{13}C NMR ($\text{DMSO}-d_6$, 63 MHz): $\delta=171.53$, $\delta=151.96$, $\delta=147.32$, $\delta=145.44$, $\delta=144.72$, $\delta=142.36$, $\delta=131.00$, $\delta=129.39$, $\delta=128.04$, $\delta=123.62$, $\delta=122.25$, $\delta=119.12$, $\delta=60.50$, $\delta=36.03$, $\delta=30.37$, $\delta=24.93$, $\delta=23.71$. ESI-MS cal: $m/z=373.2$ found: $m/z=374.2$

4. Aggregation of ipAzo-Py in water

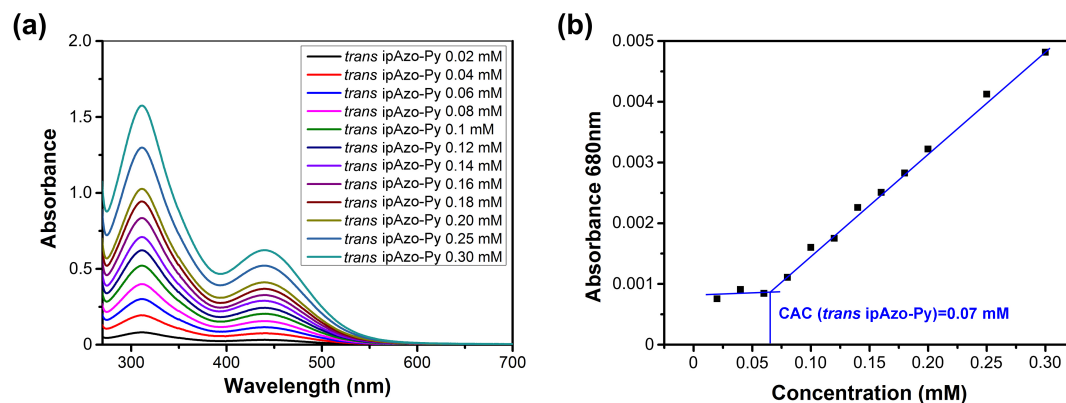


Figure S4.1 (a) UV/vis spectra of *trans* ipAzo-Py with various concentrations in H₂O.

(b) Dependence of absorbance at 680 nm on *trans* ipAzo-Py concentration.

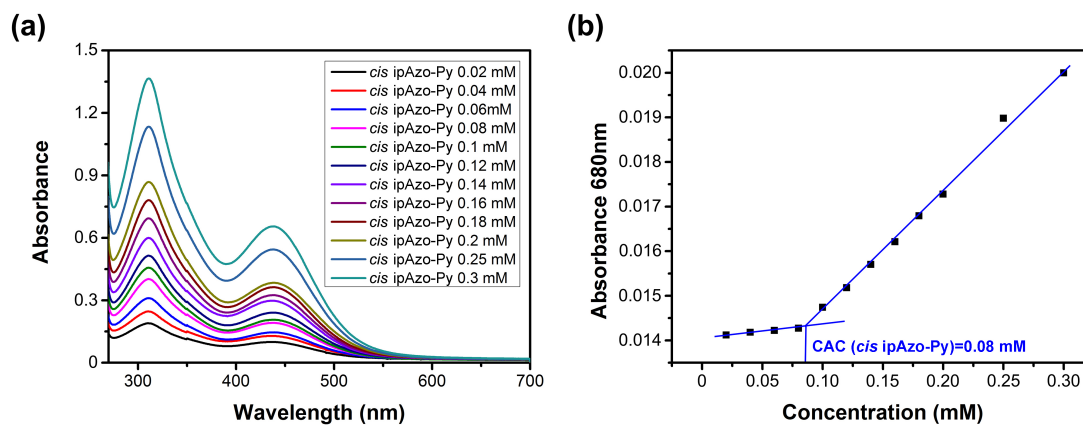


Figure S4.2 (a) UV/vis spectra of *cis* ipAzo-Py with various concentrations in H₂O.

(b) Dependence of absorbance at 680 nm on *cis* ipAzo-Py concentration.

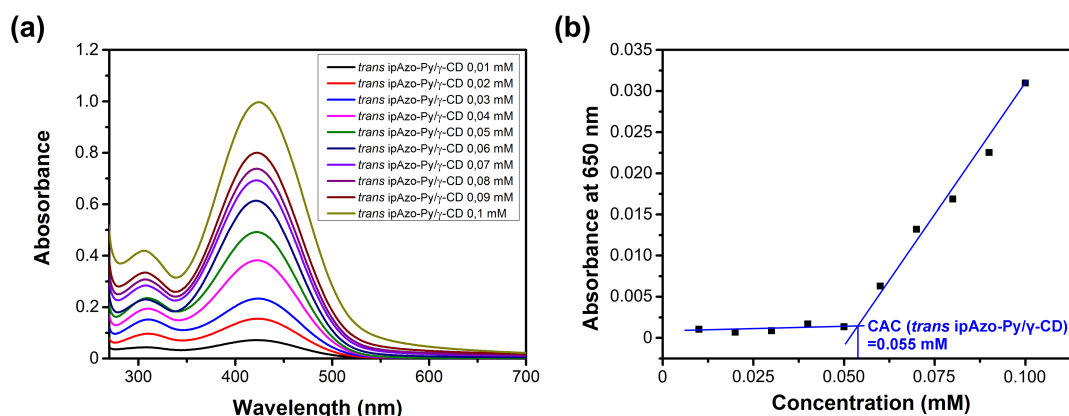


Figure S4.3 (a) UV/vis spectra of *trans* ipAzo-Py/ γ -CD with various concentrations in H₂O. (b) Dependence of absorbance at 680 nm on *trans* ipAzo-Py/ γ -CD concentration. ($[trans\ ipAzo-Py]:[\gamma-CD]=1:1$)

Aggregates could be formed by *trans* or *cis* ipAzo-Py in water due to the amphiphilicity of ipAzo-Py. The critical aggregation concentration (CAC) of *trans* and *cis* ipAzo-Py in water were 0.07 and 0.08 mM respectively. A lower CAC was found for *trans* ipAzo-Py/ γ -CD ($[trans\ ipAzo-Py]:[\gamma-CD]=1:1$), which was 0.055 mM, indicating γ -CD might form co-assemblies with *trans* ipAzo-Py (**Figure S4.1-S4.3**). Initially, this could appear to be a host-guest interaction between *trans* ipAzo-Py and γ -CD; however, no correlation was present in ¹H NMR and 2D NOESY spectra. Instead, strong host-guest interactions between *cis* ipAzo-Py and γ -CD were confirmed by ¹H NMR, 2D NOESY, and ESI-Mass spectra. Therefore, the aggregates formed between *trans* ipAzo-Py and γ -CD were not host-guest interactions. However, the aggregation of ipAzo-Py or between ipAzo-Py and γ -CD affected the UV/vis spectra. Thus, to prevent the aggregation, in this project UV/vis spectra were measured in the mixed solvent of H₂O and methanol (v/v=9:1)

5. Photoisomerization of ipAzo-Py

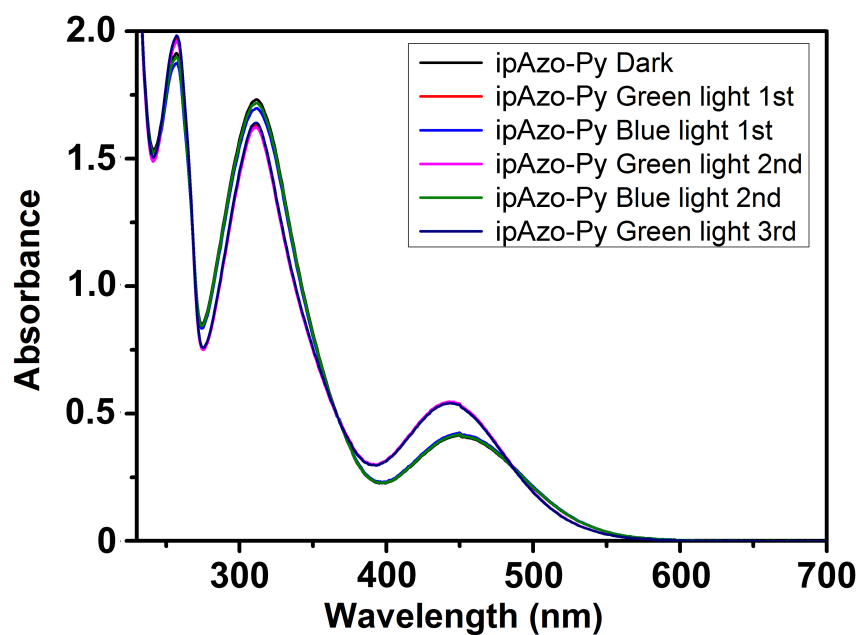


Figure S4.4 UV/Vis absorption spectra of *trans* ipAzo-Py (0.27 mg/mL in H₂O/methanol, v:v=9:1) after alternate green/blue light irradiation (40 mW/cm², 20 min).

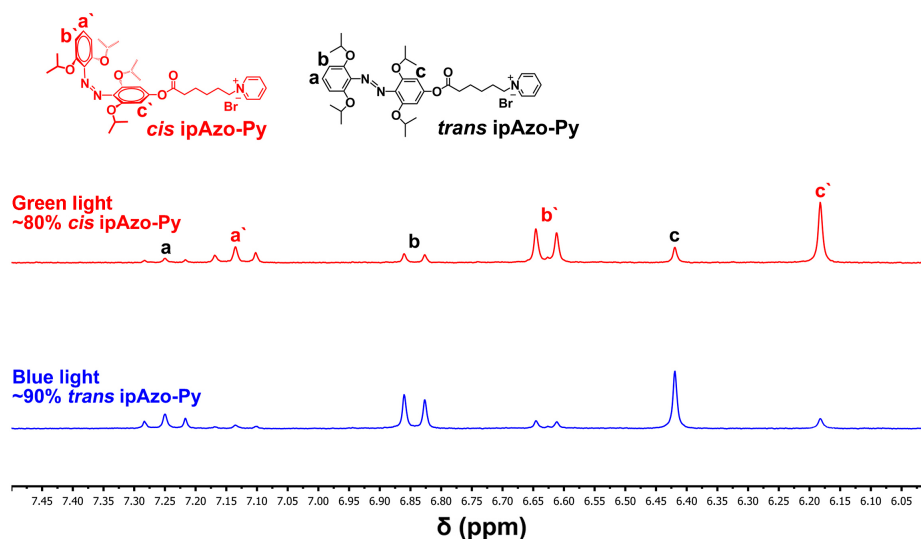


Figure S4.5 ¹H NMR spectra (250 MHz at 298K in DMSO-*d*₆) of ipAzo-Py after green and blue light irradiation.

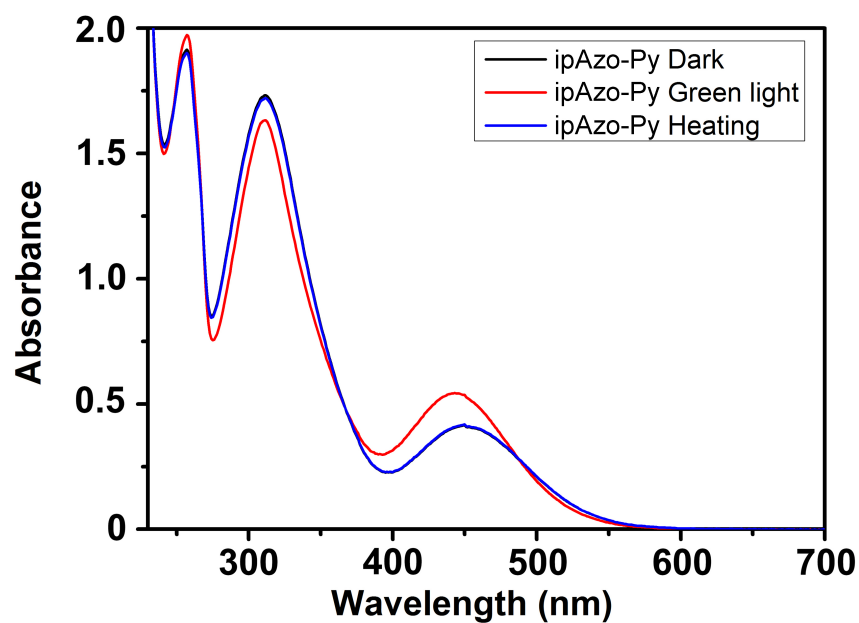


Figure S4.6 UV/Vis absorption spectra of *trans* ipAzo-Py (0.27 mg/mL in H₂O/methanol, v:v=9:1) after green light irradiation (40 mW/cm², 20 min) and heating (60 °C, 600 min).

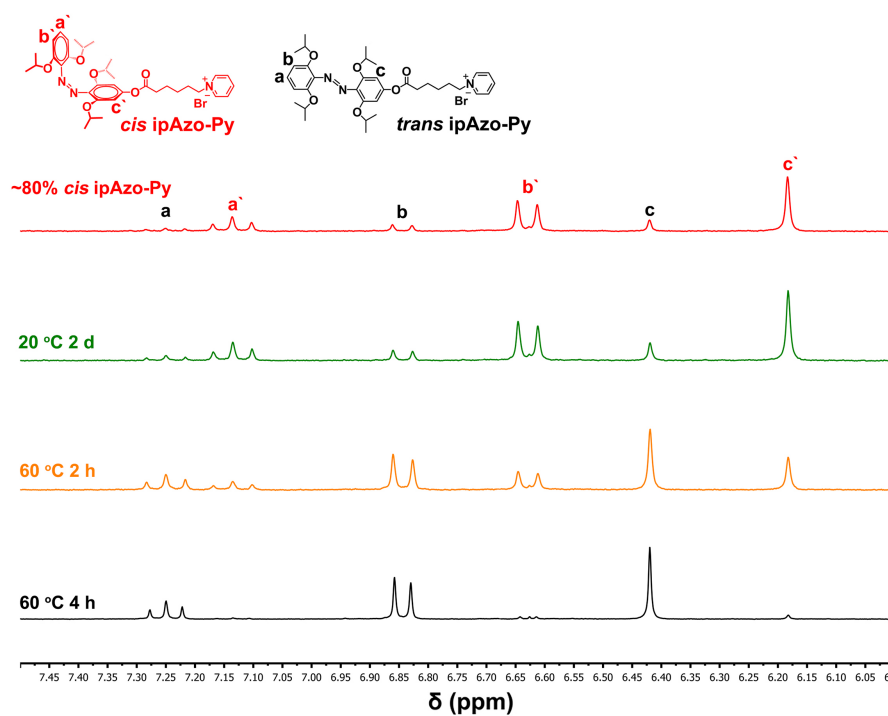


Figure S4.7 ^1H NMR spectra (250 MHz at 298K in $\text{DMSO-}d_6$) of ipAzo-Py after long time green light irradiation (~80% *cis* ipAzo-Py), 20 °C for 2 d, 60 °C for 2 h and 60 °C for 4 h.

6. Photoresponsive host-guest interaction between ipAzo-Py and γ -CD

^1H NMR titration

The molar ratio between *trans* or *cis* ipAzo-Py and γ -CD in the host-guest complex was determined by ^1H NMR titration. *Trans* or *cis* ipAzo-Py was dissolved into D_2O (1.0 mM) and γ -CD was stepwise added into the solution with concentrations ranging from 0 mM to 2.5 mM.

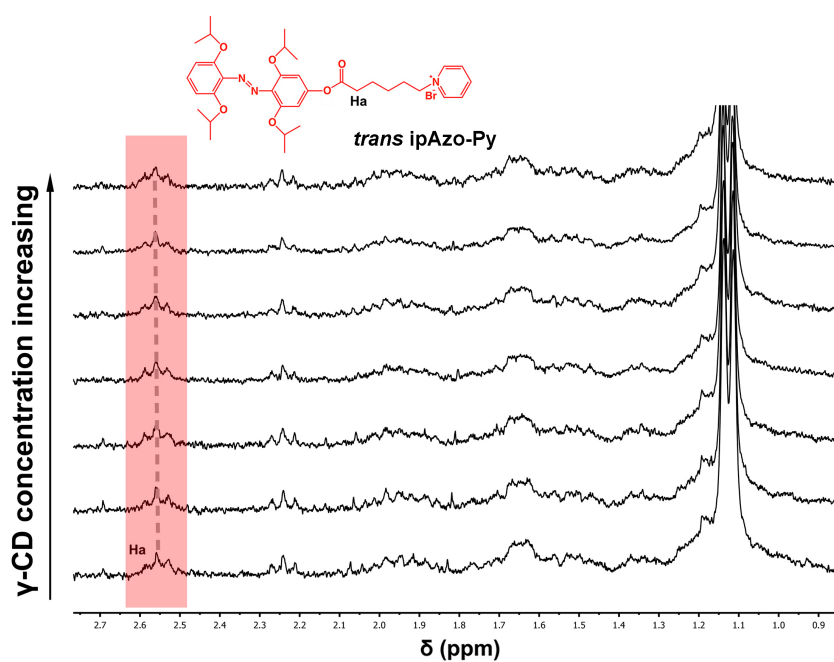


Figure S4.8 ^1H NMR spectra (250 MHz in D_2O at 298 K) of *trans* ipAzo-Py with various concentrations of γ -CD, [*trans* ipAzo-Py]=1.0 mM. The signal at $\delta=2.25$ may come from impurity.

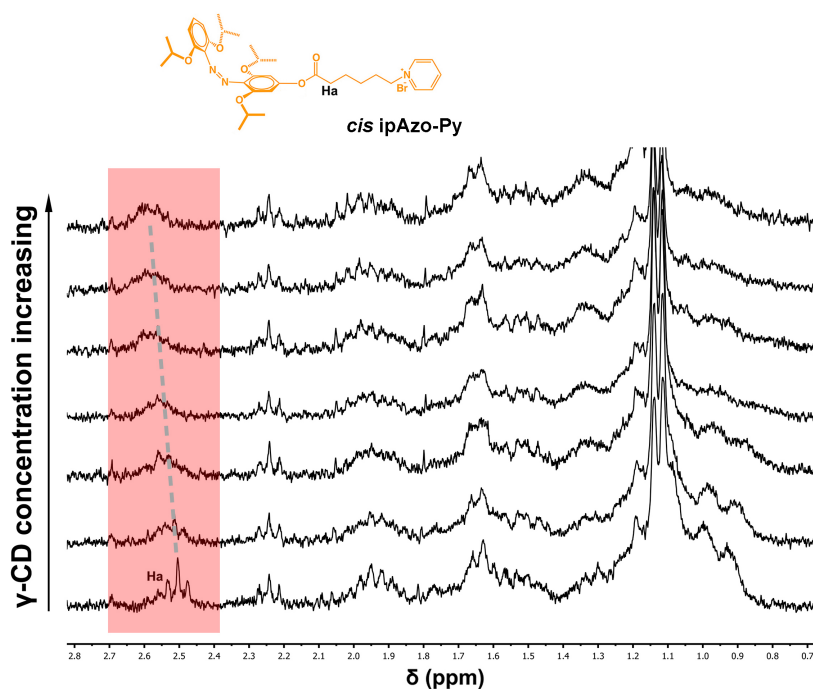


Figure S4.9 ^1H NMR spectra (250 MHz in D_2O at 298 K) of *cis* ipAzo-Py with various concentrations of γ -CD, $[\text{cis ipAzo-Py}] = 1.0 \text{ mM}$. *Cis* ipAzo-Py was obtained by irradiating *trans* ipAzo-Py with green light (40 mW/cm^2) for 60 min. The signal at $\delta = 2.25$ may come from impurity.

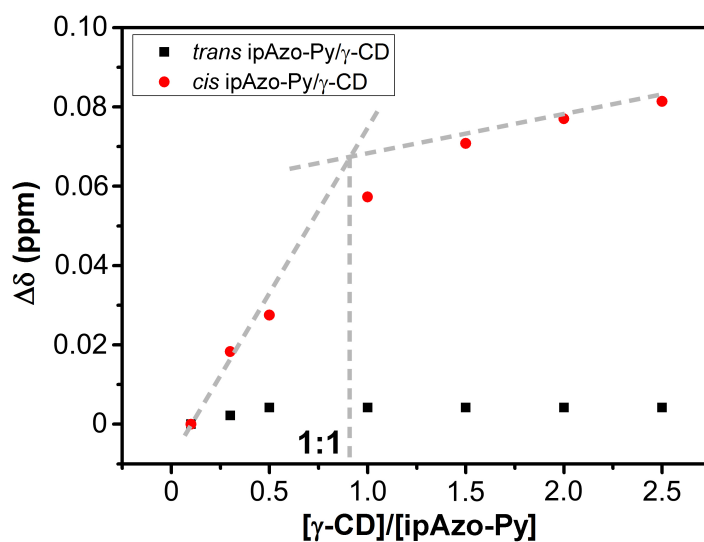


Figure S4.10 Dependence of pick shifting (Ha) on $[\gamma\text{-CD}]/[\text{ipAzo-Py}]$.

With the increasing γ -CD concentrations in *trans* ipAzo-Py solution, no obvious pick shift of Ha was observed. However, for the *cis* ipAzo-Py solution, with the increasing γ -CD concentrations, the Ha peak displayed an obvious down-field shift. The critical point of this peak shift for Ha could be found at $[\gamma\text{-CD}]:[\text{ipAzo-Py}]=1:1$, indicating that a 1:1 host-guest complex was formed between *cis* ipAzo-Py and γ -CD, while no supramolecular complex was formed between *trans* ipAzo-Py and γ -CD [2].

UV/vis titration

Trans or *cis* ipAzo-Py was dissolved in H₂O/methanol (0.08 mM) and γ -CD was stepwise added into the solution with concentrations ranging from 0 mM to 0.24 mM. The UV/vis spectra were recorded to determine the molar ratio between ipAzo-Py and γ -CD in the host-guest complex.

The results of UV/vis titration were in accordance with the ¹H NMR titration; *cis* ipAzo-Py could form a 1:1 host-guest complex with γ -CD, while no supramolecular complex was formed between *trans* ipAzo-Py and γ -CD.

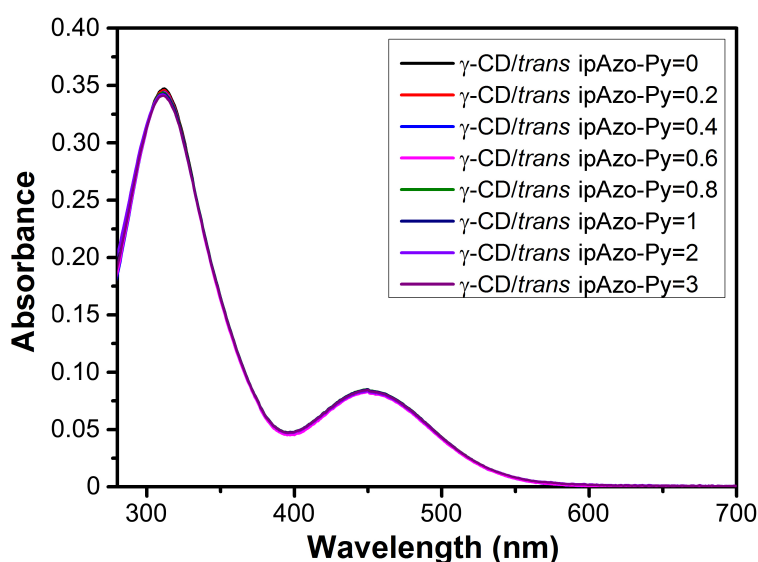


Figure S4.11 UV/vis spectra of *trans* ipAzo-Py with various concentrations of γ -CD, [*trans* ipAzo-Py]=0.08 mM in H₂O/methanol, v:v=9:1. H₂O/methanol was used to prevent the aggregation.

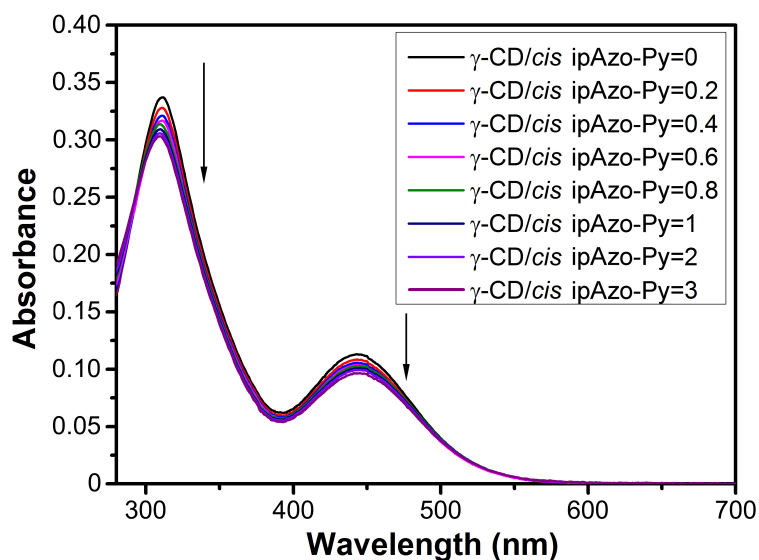


Figure S4.12 UV/vis spectra of *cis* ipAzo-Py with various concentrations of γ -CD, [*cis* ipAzo-Py]=0.08 mM in H₂O/methanol, v:v=9:1. H₂O/methanol was used to prevent the aggregation.

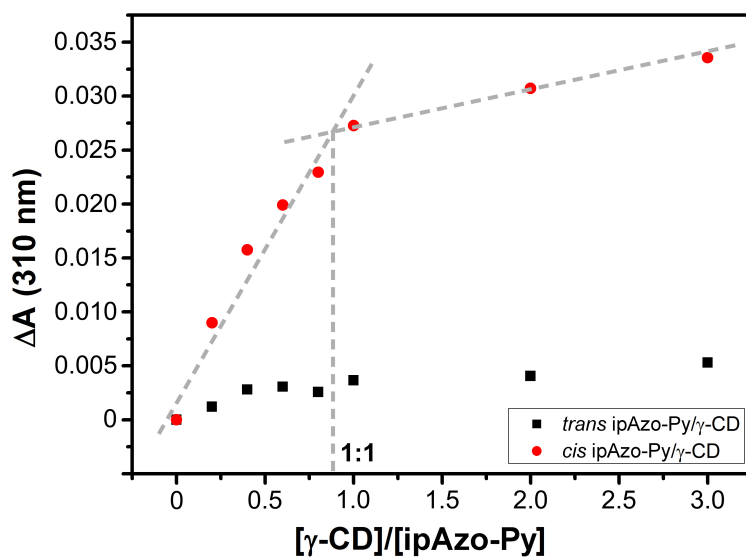


Figure S4.13 Dependence of absorbance change at 310 nm (ΔA) on $[\gamma\text{-CD}]/[\text{ipAzo-Py}]$.

Relative position of *cis* ipAzo-Py and γ -CD in host-guest complex

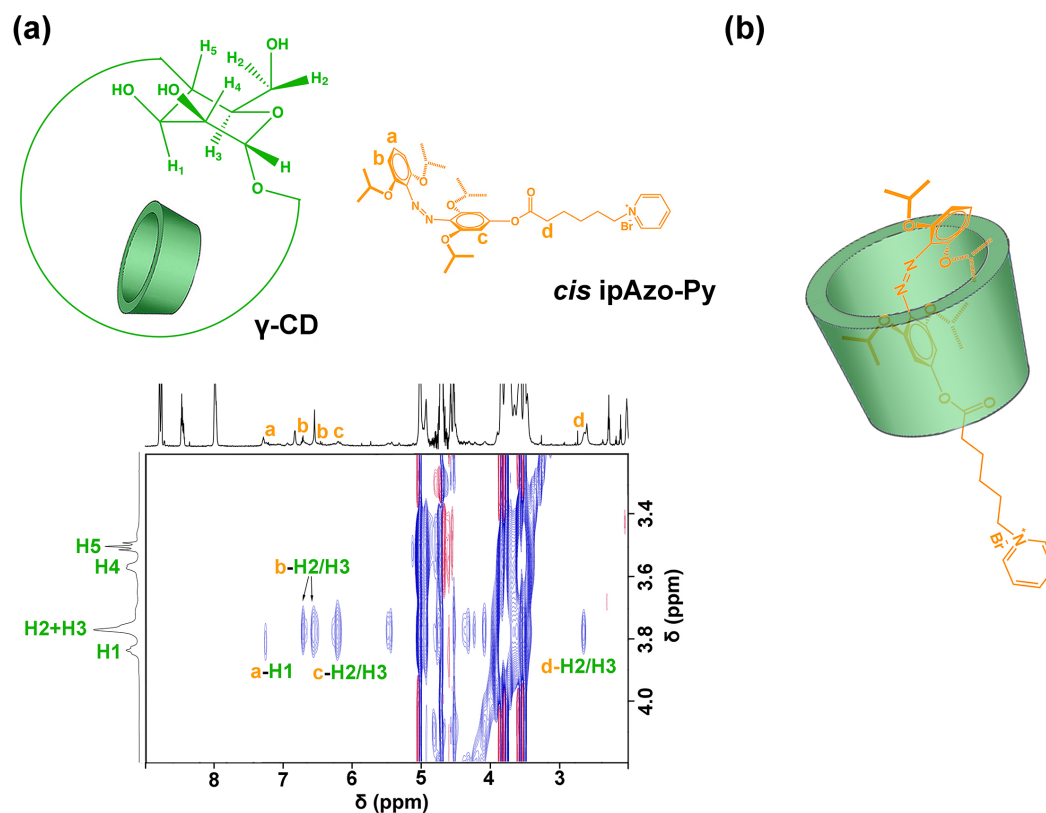


Figure S4.14 (a) 2D NOESY spectra (700 MHz in D₂O at 298 K) of *cis* ipAzo-Py/γ-CD ([ipAzo-Py]=2 mM, [ipAzo-Py]:[γ-CD]=1:1). (b) Estimated relative position of *cis* ipAzo-Py and γ-CD in host-guest complex. Correlation between proton a (*cis* ipAzo-Py) and H1 (γ-CD) was observed, while protons b, c, and d (*cis* ipAzo-Py) were correlated with H2 and H3 (γ-CD). These correlations indicated that *cis* ipAzo-Py sit deeply in the hydrophobic cavity of γ-CD with the Py tail oriented to extend through the narrower end of the CD cavity. No correlation between the protons on *cis* ipAzo-Py and H4 or H5 was observed, because H4 and H5 sit forward and to the outside of the hydrophobic cavity of γ-CD.

ESI-Mass Spectra

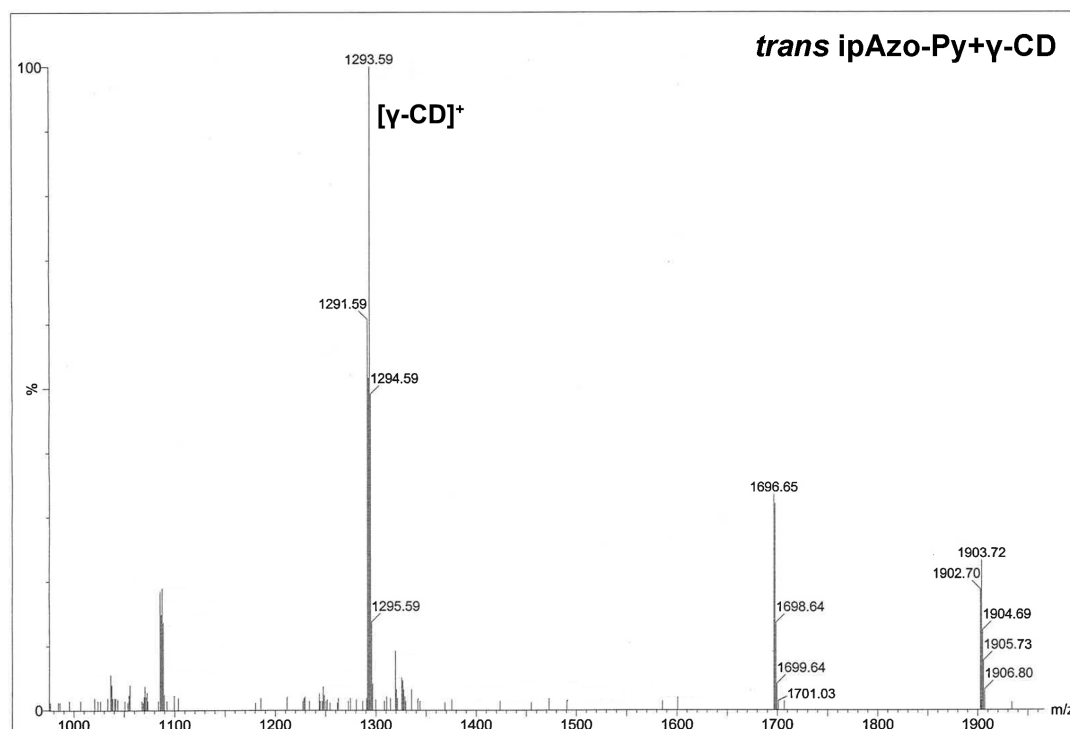


Figure S4.15 ESI-MS spectrum of mixture of *trans* ipAzo-Py and γ -CD in H_2O ($[\textit{trans} \text{ ipAzo-Py}]:[\gamma\text{-CD}]=1:1$). The weak peak at $m/z=1903.72$ could be attributed to the inclusion of alkyl chain of *trans* ipAzo-Py in γ -CD [3].

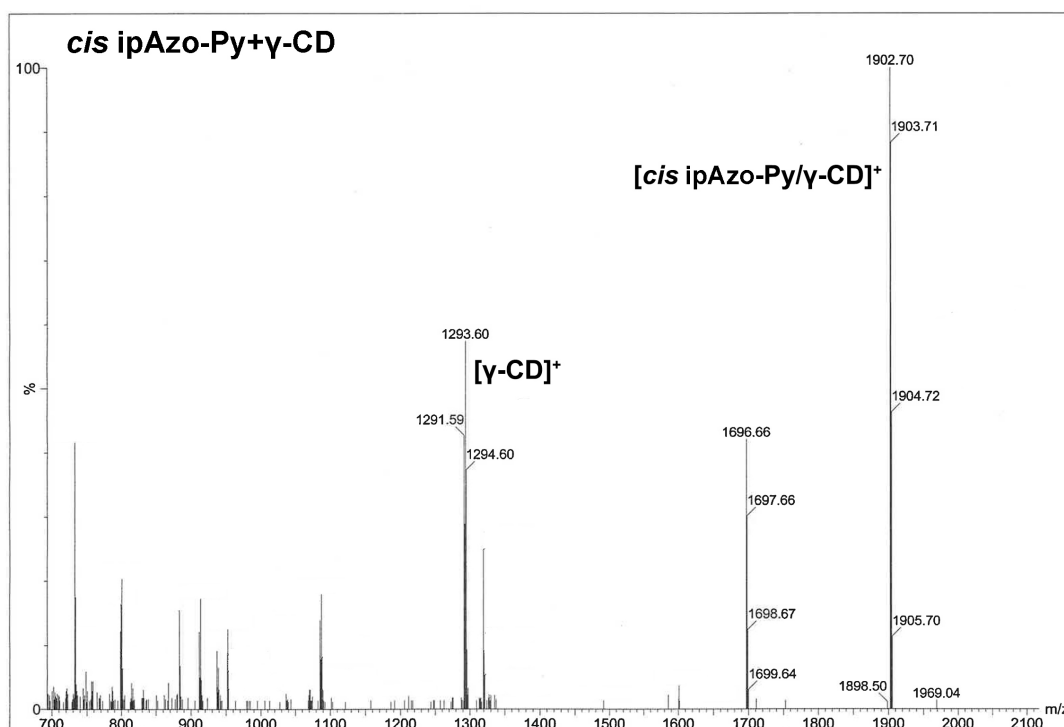


Figure S4.16 ESI-MS spectrum of mixture of *cis* ipAzo-Py and γ -CD in H₂O ($[cis\ ipAzo-Py]:[\gamma-CD]=1:1$). *cis* ipAzo-Py+ γ -CD was obtained by irradiating *trans* ipAzo-Py+ γ -CD with green light.

7. Photoresponsive orthogonal supramolecular system

DFT calculation of Azos

Trans Azo-OH

C 4.9973000000 0.1507640000 -0.0000010000
C 4.4566330000 -1.1358440000 0.0001430000
C 3.0736090000 -1.3075890000 0.0000880000
C 2.2236340000 -0.1938000000 -0.0000520000
C 2.7695280000 1.1015080000 -0.0002130000
C 4.1494880000 1.2656220000 -0.0001910000
N 0.8354350000 -0.4875970000 -0.0001080000
N 0.0820180000 0.5253460000 0.0002430000
C -1.3012840000 0.2413380000 0.0001140000
C -2.1544060000 1.3557700000 0.0001150000
C -3.5336700000 1.1995660000 0.0000020000
C -4.0793100000 -0.0897110000 -0.0000520000
C -3.2352130000 -1.2128470000 0.0000030000
C -1.8583580000 -1.0492750000 0.0000790000
O -5.4372100000 -0.1967300000 -0.0001380000
H 6.0746330000 0.2885460000 0.0000130000
H 5.1106740000 -2.0027260000 0.0002800000
H 4.5728740000 2.2660880000 -0.0003350000
H -4.2025770000 2.0531870000 -0.0000250000
H -3.6668070000 -2.2119350000 0.0000100000
H -5.6838980000 -1.1313630000 -0.0001190000
H 2.6240790000 -2.2954510000 0.0001670000
H 2.0966620000 1.9510600000 -0.0003500000
H -1.7052730000 2.3436540000 0.0001900000
H -1.1925760000 -1.9044700000 0.0001140000

Cis Azo-OH

N 1.2213780000 1.9628010000 -0.1351130000
N -0.0128540000 2.1237600000 -0.0895660000
C -0.9735250000 1.0625400000 -0.0895140000
C -2.1484010000 1.3199300000 0.6236470000
C -3.1927140000 0.4051110000 0.6279830000
C -3.0987330000 -0.7580320000 -0.1410490000
C -1.9521430000 -0.9945320000 -0.9071850000
C -0.8953640000 -0.0994350000 -0.8734350000
O -4.0943130000 -1.6857040000 -0.2019800000
C 3.4451930000 -1.5895320000 0.3522690000
C 2.4663980000 -1.2612610000 1.2900830000
C 1.6782450000 -0.1280620000 1.1200340000
C 1.8807440000 0.6972700000 0.0073730000
C 2.8968570000 0.3978190000 -0.9053840000
C 3.6563920000 -0.7564980000 -0.7460010000
H -4.0902700000 0.6053230000 1.2056130000
H -1.9109950000 -1.8854910000 -1.5216150000
H -4.8281370000 -1.4055000000 0.3550790000
H 4.0509600000 -2.4781590000 0.4864510000
H 2.3134320000 -1.8928170000 2.1581000000
H 4.4277280000 -0.9956840000 -1.4694280000
H -0.0166760000 -0.2932170000 -1.4735660000
H -2.2223590000 2.2485950000 1.1768800000
H 3.0749640000 1.0777850000 -1.7303690000
H 0.9184830000 0.1269670000 1.8485200000

Trans ipAzo-OH

C 4.8021510000 -0.6391050000 -0.0561870000
C 4.3217240000 0.3362830000 -0.9213090000
C 2.9823400000 0.7201940000 -0.8535950000
C 2.1035670000 0.1024700000 0.0570330000
C 2.6189330000 -0.8528390000 0.9653950000
C 3.9651830000 -1.2205440000 0.8920300000
O 1.7856820000 -1.3150580000 1.9333670000
O 2.5024580000 1.7178590000 -1.6624600000
N 0.7621450000 0.5610960000 0.0681820000
N -0.0985670000 -0.3489660000 0.1411210000
C -1.4394230000 0.0802720000 0.2183460000
C -2.4022820000 -0.7767880000 -0.3798010000
C -3.7568180000 -0.4498210000 -0.3597670000
C -4.1703200000 0.7091370000 0.2952200000
C -3.2575900000 1.5396280000 0.9383950000
C -1.8941060000 1.2277300000 0.9071920000
O -0.9907070000 1.9438310000 1.6149220000
O -1.9020700000 -1.8803090000 -0.9867860000
C 1.8191710000 -2.7111320000 2.3143930000
C 2.4177990000 1.4488210000 -3.0834960000
C -1.0264870000 3.3932440000 1.6004980000
C -2.7691050000 -2.8258140000 -1.6488850000
C 2.4204790000 -2.8376150000 3.7108400000
C 0.3848430000 -3.2204880000 2.2352750000
C 1.2391740000 0.5286470000 -3.3866980000
C 2.3027030000 2.8067690000 -3.7590150000
C -1.4686540000 3.8957190000 2.9715230000

C 0.3709020000 3.8655200000 1.2176940000
C -3.1120420000 -2.3400310000 -3.0557040000
C -2.0067220000 -4.1439000000 -1.6545040000
O -5.5097320000 0.9712570000 0.2851420000
H 5.8454960000 -0.9308040000 -0.0981620000
H 4.9770720000 0.8255160000 -1.6314700000
H 4.3638770000 -1.9381390000 1.5975000000
H -4.5085170000 -1.0574920000 -0.8391360000
H -3.6037680000 2.3983270000 1.5013800000
H 2.4377310000 -3.2502800000 1.5891870000
H 3.3500430000 0.9624800000 -3.3972680000
H -1.7429630000 3.7085810000 0.8345670000
H -3.6813230000 -2.9456520000 -1.0545860000
H 2.4119960000 -3.8810690000 4.0392610000
H 3.4509460000 -2.4767210000 3.7384140000
H 1.8361770000 -2.2475080000 4.4215650000
H 0.3467260000 -4.2931820000 2.4476720000
H -0.0242610000 -3.0294190000 1.2423820000
H -0.2406350000 -2.6995600000 2.9650520000
H 1.1902880000 0.3182320000 -4.4592690000
H 1.3329700000 -0.4216400000 -2.8568880000
H 0.3027790000 0.9981770000 -3.0764830000
H 2.2581790000 2.6913140000 -4.8450690000
H 3.1605310000 3.4338320000 -3.5078470000
H 1.3950470000 3.3172790000 -3.4270970000
H -1.4529490000 4.9889640000 3.0016960000
H -2.4779040000 3.5589750000 3.2196340000
H -0.7890550000 3.5200380000 3.7405670000

H 0.3902680000 4.9550660000 1.1196940000
H 0.6824780000 3.4081860000 0.2783390000
H 1.0906100000 3.5735670000 1.9868620000
H -3.7672930000 -3.0592770000 -3.5549410000
H -3.6185800000 -1.3736970000 -3.0377170000
H -2.1984820000 -2.2362870000 -3.6467230000
H -2.5982640000 -4.9214980000 -2.1445050000
H -1.7858060000 -4.4639550000 -0.6347240000
H -1.0622180000 -4.0326570000 -2.1923890000
H -5.6738100000 1.7966140000 0.7526630000

Cis ipAzo-OH

N 0.8445770000 -0.4498170000 0.9935350000
N -0.2198770000 0.1678390000 1.1828150000
C -1.0123030000 0.7222550000 0.1288230000
C -2.3826290000 0.4147650000 0.1417880000
C -3.2508870000 0.9631210000 -0.7990480000
C -2.7635260000 1.8656580000 -1.7436210000
C -1.4225290000 2.2386580000 -1.7267970000
C -0.5510360000 1.6835670000 -0.7941480000
O 0.7491400000 2.1149880000 -0.8015070000
O -2.8280850000 -0.5242390000 1.0386600000
C 1.1665550000 3.0103880000 0.2748450000
C -3.8094200000 -0.0950860000 2.0185020000
C 2.6114860000 3.3610680000 -0.0383270000
H 1.1166050000 2.4503370000 1.2149540000
C -4.3715710000 -1.3675190000 2.6331870000
C -3.1717480000 0.8329610000 3.0473560000

O -3.5610290000 2.4276310000 -2.7003930000
C 2.6109460000 -1.8834410000 -2.5580620000
C 1.2626190000 -2.1345890000 -2.3398040000
C 0.6225270000 -1.6250530000 -1.2067130000
C 1.3455660000 -0.8394400000 -0.2856760000
C 2.7230310000 -0.6362200000 -0.5024650000
C 3.3462360000 -1.1364310000 -1.6416120000
O 3.4023200000 0.1248560000 0.4146460000
O -0.6995640000 -1.8770100000 -0.9734060000
C -1.1098130000 -3.2640300000 -0.8190580000
C -0.8243130000 -3.7249810000 0.6064860000
C -2.5860160000 -3.3113870000 -1.1809170000
C 4.5470910000 -0.4758790000 1.0737450000
C 4.0906750000 -1.5450970000 2.0611530000
C 5.2944200000 0.6693640000 1.7393300000
H -4.2904290000 0.6529120000 -0.8119020000
H -1.0501740000 2.9687060000 -2.4325980000
C 0.2746140000 4.2448020000 0.3686680000
H -4.6109260000 0.4396120000 1.4933970000
H 2.6698800000 3.9011340000 -0.9874710000
H 3.2110600000 2.4544900000 -0.1047810000
H 3.0220230000 3.9981330000 0.7499160000
H 0.6351680000 4.8909090000 1.1739340000
H -0.7627760000 3.9847720000 0.5866460000
H 0.2997140000 4.8134430000 -0.5652060000
H -5.1362300000 -1.1231920000 3.3747810000
H -4.8206560000 -2.0034660000 1.8674600000
H -3.5774730000 -1.9312200000 3.1290260000

H -3.9184550000 1.1517850000 3.7804990000
H -2.7623530000 1.7252970000 2.5693020000
H -2.3570940000 0.3230060000 3.5652060000
H -4.4590060000 2.0968800000 -2.5973050000
H 3.0907160000 -2.2611580000 -3.4536150000
H 0.6846510000 -2.7063160000 -3.0555110000
H 4.3925960000 -0.9198750000 -1.8175480000
H -0.5353930000 -3.8739230000 -1.5250150000
H -1.1195820000 -4.7705960000 0.7348890000
H 0.2401680000 -3.6418940000 0.8379280000
H -1.3797300000 -3.1074240000 1.3148220000
H -2.9688840000 -4.3303890000 -1.0793460000
H -2.7397750000 -2.9813190000 -2.2105720000
H -3.1487230000 -2.6531200000 -0.5160750000
H 5.1879720000 -0.9325930000 0.3103690000
H 4.9555390000 -1.9904960000 2.5614220000
H 3.5463660000 -2.3421790000 1.5503540000
H 3.4281650000 -1.1089860000 2.8114240000
H 6.1810390000 0.2929940000 2.2556790000
H 5.6097270000 1.4082540000 0.9999010000
H 4.6512580000 1.1647960000 2.4707640000

Orthogonal photoresponse between Azo-Py and ipAzo-Py

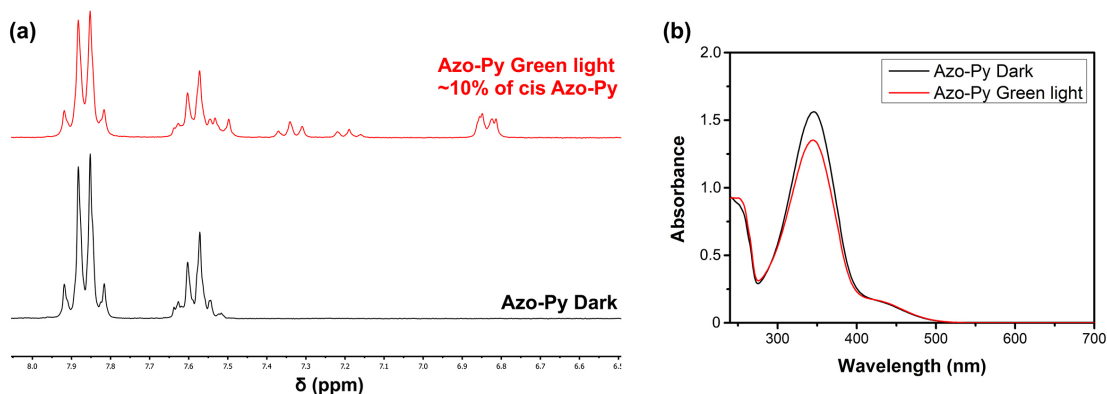


Figure S4.17 ^1H NMR (250 MHz at 298K in $\text{DMSO-}d_6$) (a) and UV/vis (b) spectra of Azo-Py in dark and after 530 nm green light irradiation (40 mW/cm^2 , 30 min). Only ~10% of cis Azo-Py could be obtained after green light irradiation. (Azo-Py is 0.075 mg/mL in H_2O)

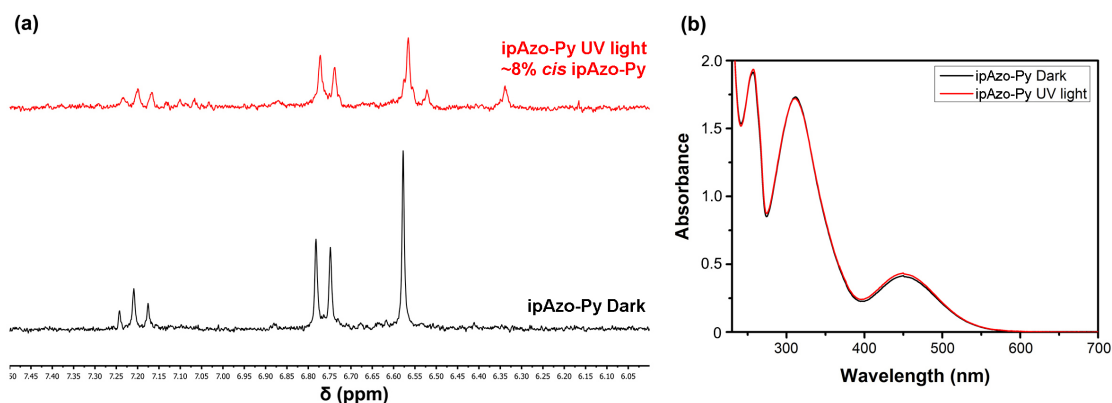


Figure S4.18 ^1H NMR (250 MHz at 298K in $\text{DMSO-}d_6$) (a) and UV/vis (b) spectra of ipAzo-Py in dark and after 365 nm UV light irradiation (40 mW/cm^2 , 30 min). Only ~8% of cis ipAzo-Py could be obtained after UV light irradiation. (ipAzo-Py is 0.075 mg/mL in H_2O /methanol, v:v=9:1)

The photoresponsive host-guest complex formed between ipAzo and γ -CD has potential applications for the designing of photoresponsive orthogonal supramolecular systems.

It has been reported that *trans* Azo can form very strong host-guest complex with α -CD. After UV light irradiation, due to the decreased molecular size, the *cis* Azo slips out from the hydrophobic cavity of α -CD, which further induces disassembly of the host-guest complex [4].

For the host-guest supramolecular systems with more than one host (guest) molecule, the host (guest) molecules compete for the guest (host) molecules. The association constants (K_a) between the host molecules (α -CD or γ -CD) and guest molecules (Azo or ipAzo) were therefore determined to investigate the possibility of photoresponsive orthogonal supramolecular systems designed by Azo/ α -CD and ipAzo/ γ -CD complexes.

Azo-Py and ipAzo-Py were synthesized as in **Scheme S4.1** and used as guest molecules. The light to induce *trans*-to-*cis* photoisomerization of Azo-Py and ipAzo-Py were orthogonal with respect to wavelength (**Figure S4.17, S4.18**). Using α -CD and γ -CD as the host molecules, ^1H NMR was used to measure the association constants between Azos and CDs. Azos and CDs were dissolved in D_2O and the concentrations of Azos were kept at 1.0 mM. The concentrations of CDs were 5, 10, 15 and 20 mM. Due to the host-guest interaction between Azos and CDs, a shift in Azo protons was observed. A modified Benesi-Hildebrand equation was used for the calculation of the association constants between Azos and CDs [5]:

$$\frac{1}{\Delta\delta_{\text{obs}}} = \frac{1}{K_a\Delta\delta C_{\text{CD}}} + \frac{1}{\Delta\delta}$$

where $\Delta\delta_{\text{obs}}$ is the observed shifts of the peaks; K_a is the association constant; $\Delta\delta$ is a constant correlated to the concentration of the Azos; C_{CD} is the CDs concentrations.

When possible, multiple proton peaks were fit and the reported K_a was a weighted average of these values. In all cases, the 90% confidence intervals from each proton overlapped with the weighted average. Further, the 90% confidence intervals for the K_a associated with strong host-guest complexation (*trans* Azo/ α -CD, *cis* pAzo/ γ -CD) do not overlap with the 90% confidence intervals for the K_a associated with weak host-guest complexation.

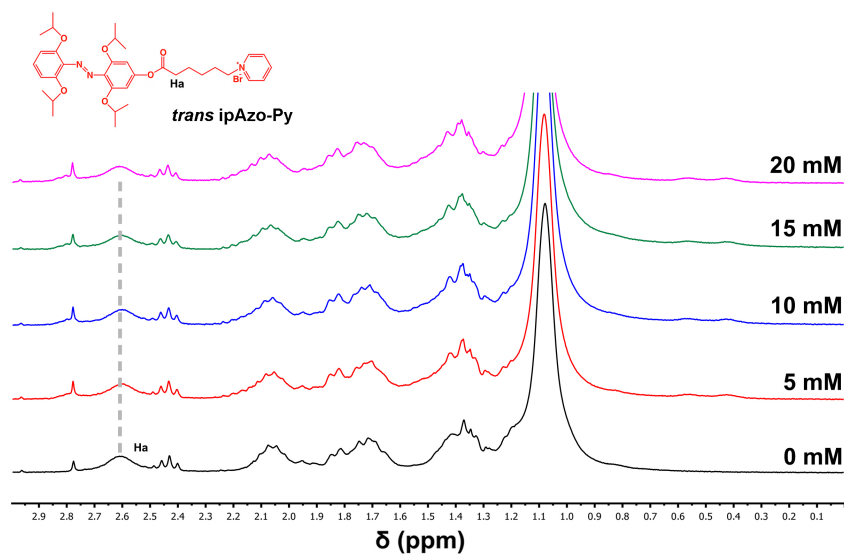
Association constants between ipAzo-Py and α/γ -CD

Figure S4.19 ^1H NMR (250 MHz, 298K) spectra of *trans* ipAzo-Py with different concentrations of γ -CD (0, 5, 10, 15 and 20 mM) in D_2O . The concentration of ipAzo-Py is 1 mM. The signal at $\delta=2.41$ may come from impurity.

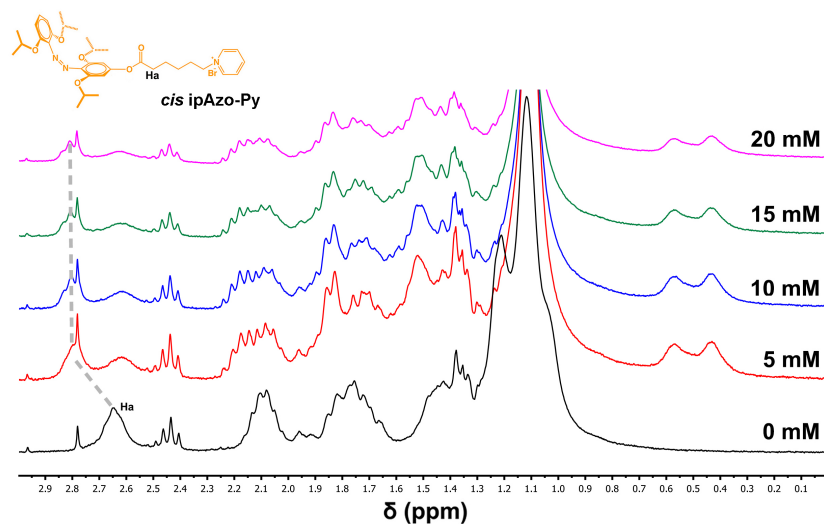


Figure S4.20 ^1H NMR (250 MHz, 298K) spectra of *cis* ipAzo-Py with different concentrations of γ -CD (0, 5, 10, 15 and 20 mM) in D_2O . The concentration of ipAzo-Py is 1 mM. The signal at $\delta=2.41$ may come from impurity.

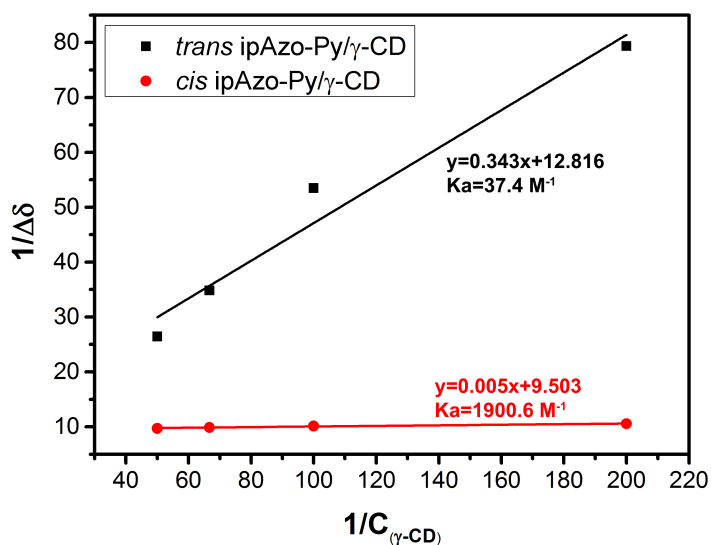


Figure S4.21 Association constants (K_a) between ipAzo-Py and γ -CD. The data for calculating the association constants were obtained from **Figure S4.19** and **S4.20**. The K_a in **Table 4.1** is the average of K_a s calculated by choosing different protons on ipAzo-Py.

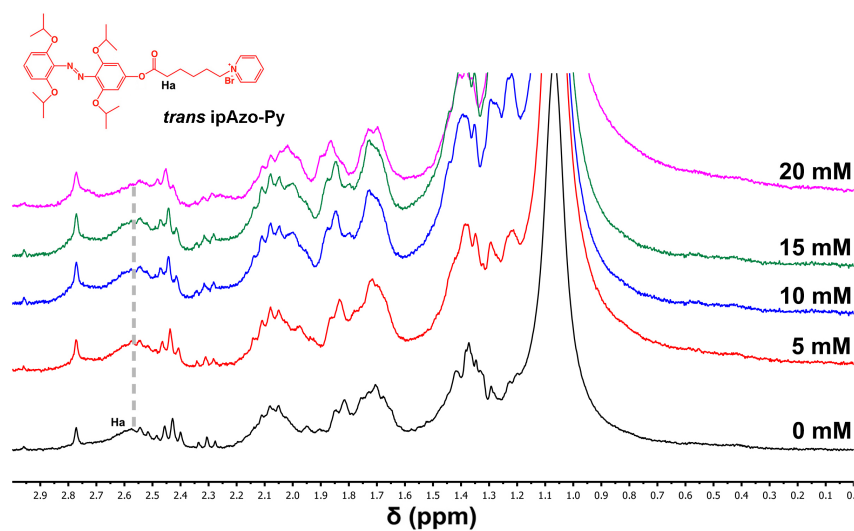


Figure S4.22 ^1H NMR (250 MHz, 298K) spectra of *trans* ipAzo-Py with different concentrations of α -CD (0, 5, 10, 15 and 20 mM) in D_2O . The concentration of ipAzo-Py is 1 mM. The signal at $\delta = 2.41$ may come from impurity.

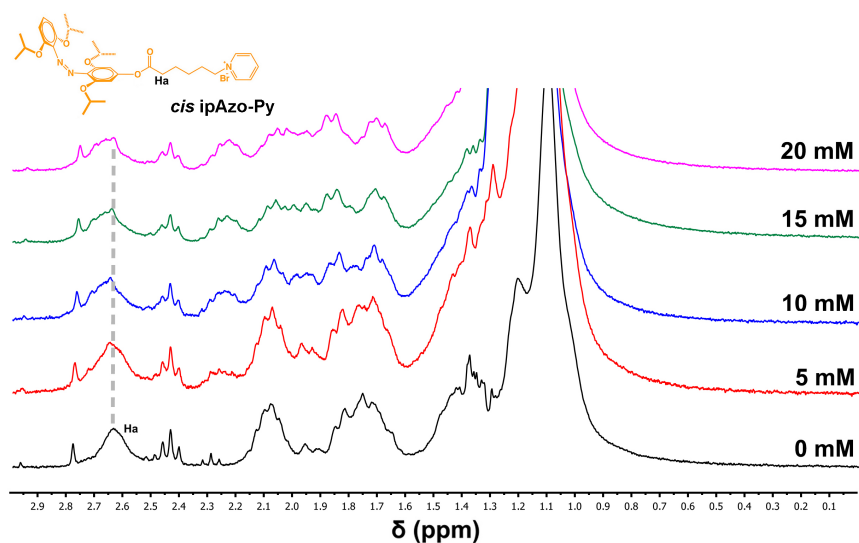


Figure S4.23 ^1H NMR (250 MHz, 298K) spectra of *cis* ipAzo-Py with different concentrations of α -CD (0, 5, 10, 15 and 20 mM) in D_2O . The concentration of ipAzo-Py is 1 mM. The signal at $\delta=2.41$ may come from impurity.

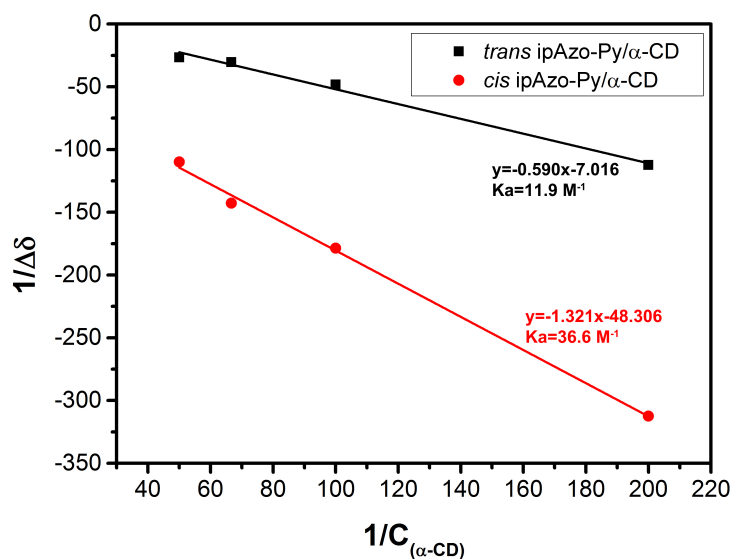


Figure S4.24 Association constants (K_a) between ipAzo-Py and α -CD. The data for calculating the association constants were obtained from **Figure S4.22** and **S4.23**. The K_a in **Table 4.1** is the average of K_a s calculated by choosing different protons on ipAzo-Py.

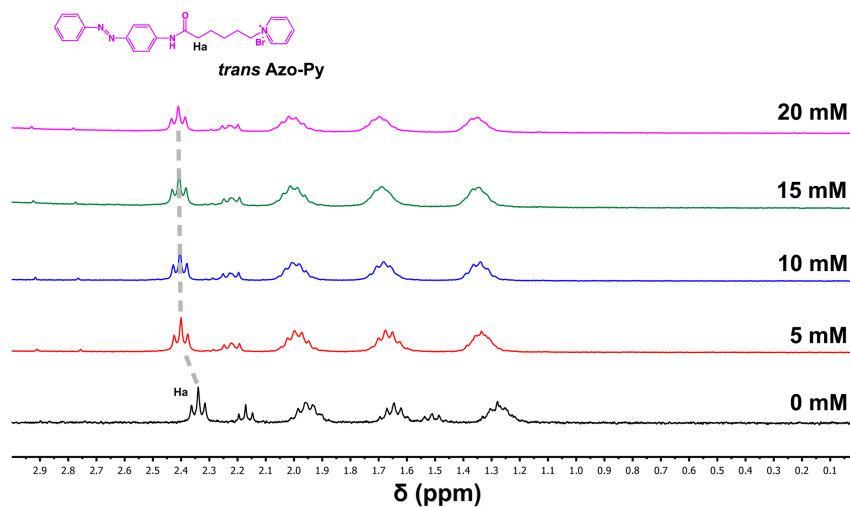
Association constants between Azo-Py and α/γ -CD

Figure S4.25 ¹H NMR (250 MHz, 298K) spectra of *trans* Azo-Py with different concentrations of α -CD (0, 5, 10, 15 and 20 mM) in D₂O. The concentration of Azo-Py is 1 mM. The signal at $\delta=2.21$ may come from impurity.

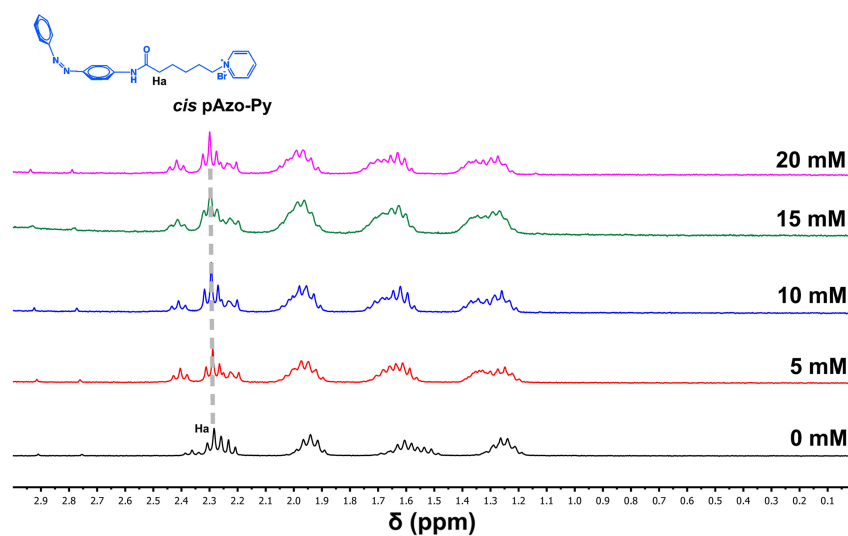


Figure S4.26 ¹H NMR (250 MHz, 298K) spectra of *cis* Azo-Py with different concentrations of α -CD (0, 5, 10, 15 and 20 mM) in D₂O. The concentration of Azo-Py is 1 mM. The signal at $\delta=2.21$ may come from impurity.

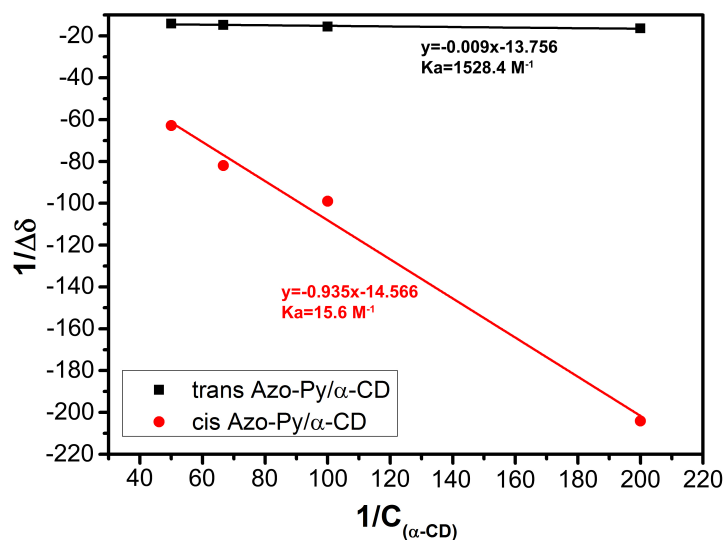


Figure S4.27 Association constants (K_a) between Azo-Py and α -CD. The data for calculating the association constants were obtained from **Figure S4.25** and **S4.26**. The K_a in **Table 4.1** is the average of K_a s calculated by choosing different protons on Azo-Py.

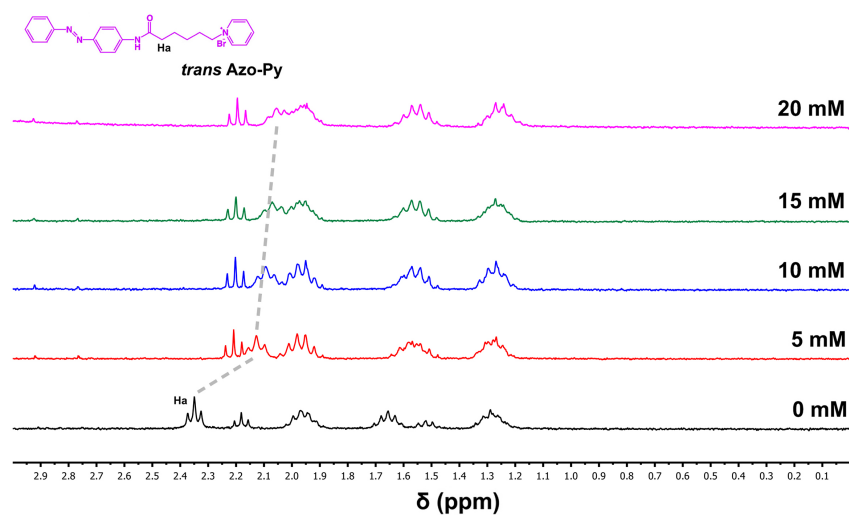


Figure S4.28 ^1H NMR (250 MHz, 298K) spectra of *trans* Azo-Py with different concentrations of γ -CD (0, 5, 10, 15 and 20 mM) in D_2O . The concentration of Azo-Py is 1 mM. The signal at $\delta=2.21$ may come from impurity.

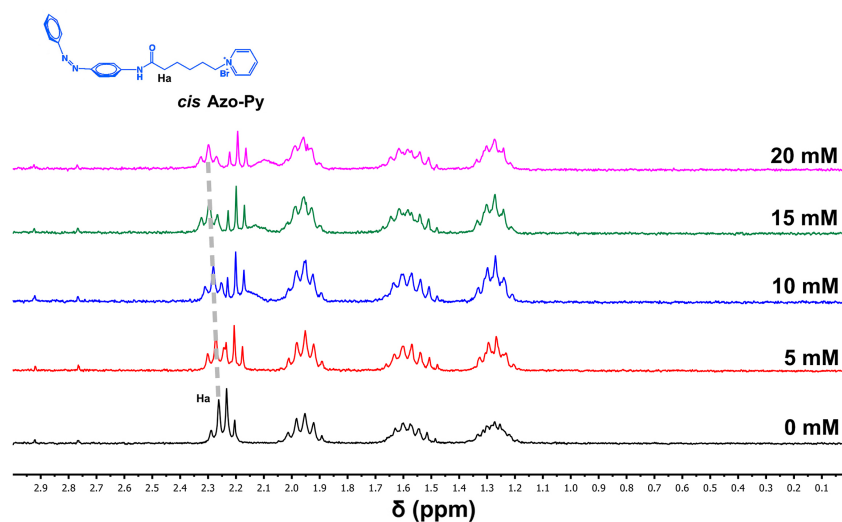


Figure S4.29 ^1H NMR (250 MHz, 298K) spectra of *cis* Azo-Py with different concentrations of γ -CD (0, 5, 10, 15 and 20 mM) in D_2O . The concentration of Azo-Py is 1 mM. The signal at $\delta=2.21$ may come from impurity.

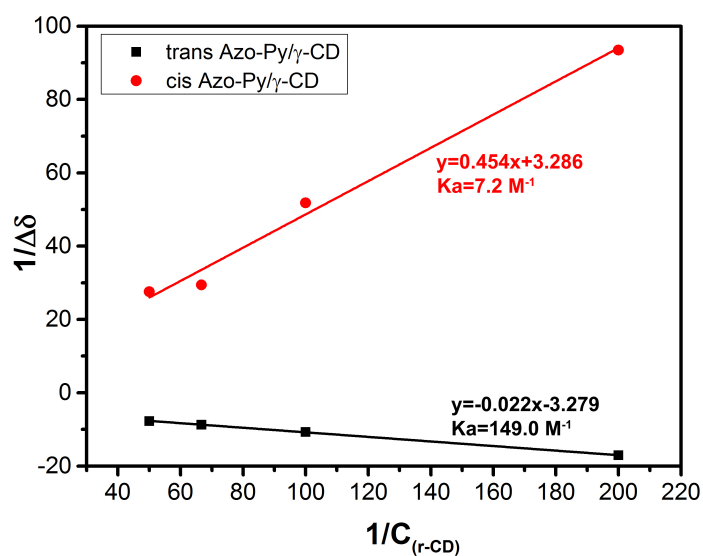


Figure S4.30 Association constants (K_a) between Azo-Py and γ -CD. The data for calculating the association constants were obtained from **Figure S4.28** and **S4.29**. The K_a in **Table 5.1** is the average of K_a s calculated by choosing different protons on Azo-Py.

ITC measurements

ITC was investigated for the *trans* ipAzo-Py/ γ -CD and *cis* ipAzo-Py/ γ -CD.

ITC experiments were performed with a NanoITC Low Volume from TA Instruments (Eschborn, Germany). The effective cell volume was 170 μ L, the temperature was set to 25 $^{\circ}$ C and a stirring rate of 350 rpm was maintained for all experiments. To correct the data by the heat of dilution, the titrant was titrated into water and the resulting heats were subtracted from each titration of NPs with the corresponding titrant. The same was done for the inverse way of dilution: the syringe was filled with water and titrated to the probed compound, the resulting heats were subtracted likewise.

An aqueous solution of each of the ipAzo-Py isomers with a concentration of 3.5 g/L was titrated with 46.4 μ L of an aqueous solution of γ -CD at a concentration of 26 g/L (20 mM). The titration was carried out in 40 steps of 1.16 μ L each.

In order to consider the remaining fraction of 20 % *trans* isomer in the solution of *cis* ipAzo-Py, a solution of 0.7 g/L *trans* ipAzo-Py was titrated with a solution of γ -CD at 26 g/L and the resulting heats were subtracted from the corresponding measurement with *cis* ipAzo-Py.

Due to the amphiphilicity of *trans* or *cis* ipAzo-Py, it could form aggregates in water, which might affect the ITC data. The ITC data between *trans* ipAzo-Py/ γ -CD and *cis* ipAzo-Py/ γ -CD were observed to be very different (**Figure S4.31**). More heat was released during the titrating process between *cis* ipAzo-Py and γ -CD, the thermodynamic data was shown in Table R1. The fitted binding constants (K_a) might be affected by the aggregation of ipAzo-Py in water, however, *cis* ipAzo-Py still showed a higher K_a with γ -CD compared with *trans* ipAzo-Py. The fitted stoichiometric number n was 0.82 for *cis* ipAzo-Py and γ -CD, which was close to 1, indicating that *cis* ipAzo-Py formed a strong 1:1 host-guest complex with γ -CD. The data were in accordance with the ^1H NMR and UV/vis titration results.

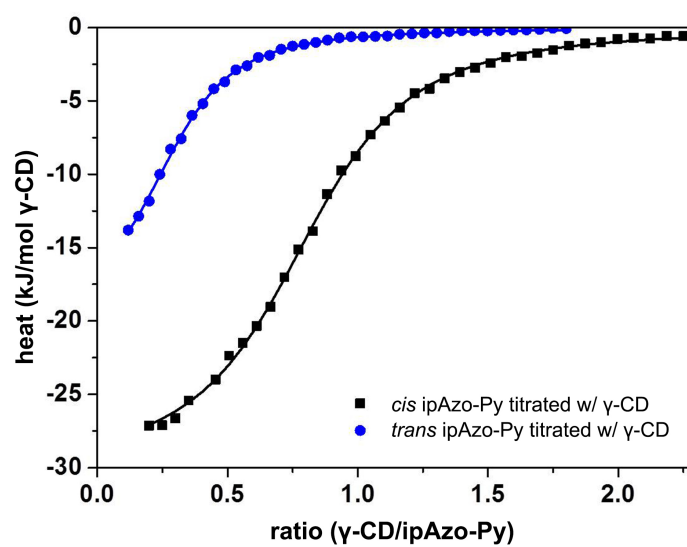


Figure S4.31 ITC data corresponding to the host-guest interaction between ipAzo-Py and γ -CD.

Table S4.1 Thermodynamic data for the host-guest interaction between ipAzo-Py and γ -CD

Host	Guest	K_a [M^{-1}]	n	ΔH [kJ/mol]	ΔS [J/K mol]	ΔG [kJ/mol]
γ -CD	<i>trans</i> ipAzo-Py	4.68×10^3	0.31	-19.8	4.0	-20.9
γ -CD	<i>cis</i> ipAzo-Py	5.58×10^3	0.82	-30.9	-31.8	-21.5

Competition between *trans* Azo-Py/ α -CD and *trans* Azo-Py/ γ -CD complexes

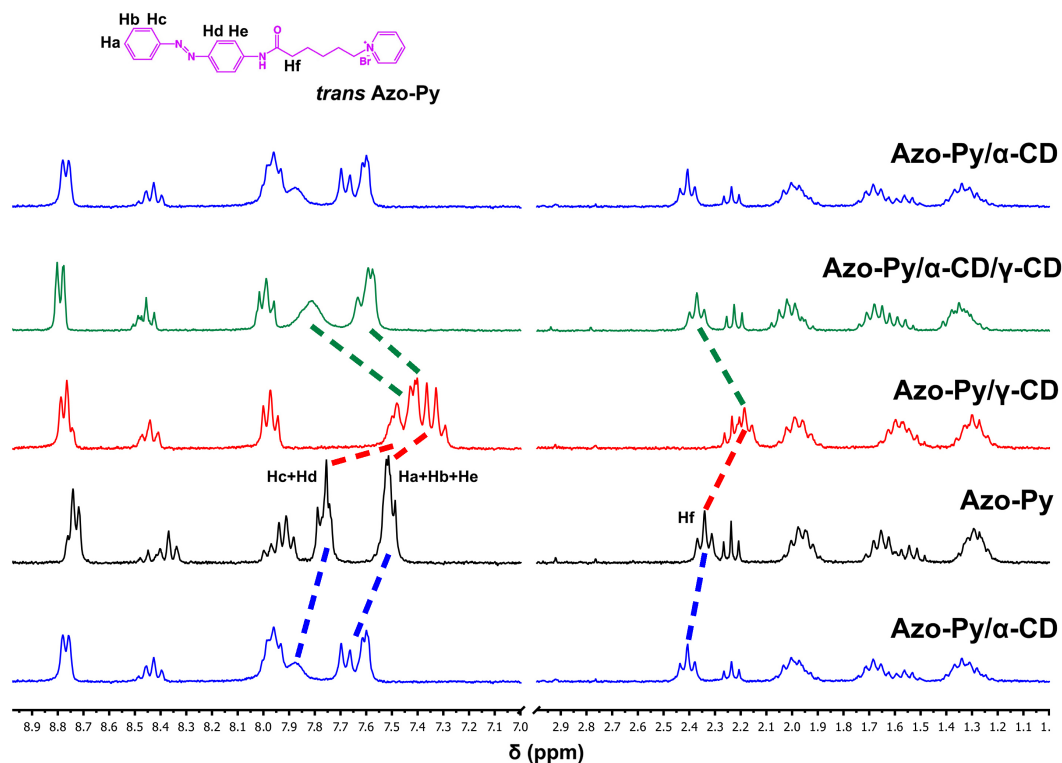


Figure S4.32 ^1H NMR spectra (250 MHz, 298K) of *trans* Azo-Py (black), *trans* Azo-Py/ γ -CD (red), *trans* Azo-Py/ α -CD (blue) and *trans* Azo-Py/ α -CD/ γ -CD (green) in D_2O . The concentration of Azo-Py in all the samples was 1.5 mM. For the samples of *trans* Azo-Py/ γ -CD and *trans* Azo-Py/ α -CD, the molar ratios between *trans* Azo-Py and CDs were 1:1. For the *trans* Azo-Py/ α -CD/ γ -CD, the molar ratio of the three components was 1:1:1. The signal at $\delta=2.21$ may come from impurity.

Azo and Azo/CD complex are fast exchanging in aqueous solution. Therefore, an average Hf signal can be observed in ^1H NMR spectrum for the mixture of Azo and CD (**Figure S4.32**). The chemical shift of the average Hf signal is determined by the fraction of Azo/CD complex.

$$\begin{cases} f_{\text{Azo}}\delta_{\text{Azo}} + f_{\text{Azo/CD}}\delta_{\text{Azo/CD}} = \delta_{\text{observed}} \\ f_{\text{Azo}} + f_{\text{Azo/CD}} = 1 \end{cases} \quad (\text{S2})$$

where f_{Azo} and $f_{\text{Azo/CD}}$ are the fractions of Azo and Azo/CD complex, δ_{Azo} and $\delta_{\text{Azo/CD}}$

are the chemical shifts of Hf on Azo and Azo/CD complex, δ_{observed} is the chemical shift of the average Hf signal of the mixture of Azo and CD.

In our case, $\delta_{\text{Azo-Py}}$ was observed at $\delta=2.34$. $\delta_{\text{Azo}/\alpha\text{-CD}}$ and $\delta_{\text{Azo}/\gamma\text{-CD}}$ were determined by Benesi-Hildebrand equation (**Figure S4.27** and **S4.30**).

$$\begin{cases} \delta_{\text{AzoPy}} = 2.34 \\ \delta_{\text{AzoPy}/\alpha\text{CD}} = 2.41 \\ \delta_{\text{AzoPy}/\gamma\text{CD}} = 2.04 \end{cases} \quad (\text{S3})$$

For the mixture of *trans* Azo-Py and γ -CD (1:1 molar ratio), the δ_{observed} is at $\delta=2.19$. From the equation S2, only half of *trans* Azo-Py could form host-guest complex with γ -CD.

$$\begin{cases} f_{\text{AzoPy}} = 50\% \\ f_{\text{AzoPy}/\gamma\text{CD}} = 50\% \end{cases} \quad (\text{S4})$$

For the mixture of *trans* Azo-Py and α -CD, (1:1 molar ratio), the δ_{observed} is at $\delta=2.40$. Most of *trans* Azo-Py could form host-guest complex with α -CD.

$$\begin{cases} f_{\text{AzoPy}} = 50\% \\ f_{\text{AzoPy}/\alpha\text{CD}} = 50\% \end{cases} \quad (\text{S5})$$

For the mixture of *trans* Azo-Py, α -CD, and γ -CD (1:1:1 molar ratio), the δ_{observed} is at $\delta=2.37$. In this case, $f_{\text{Azo-Py}}$ must be in the range of $0\% < f_{\text{Azo-Py}} < 14\%$. Therefore, the fractions of *trans* Azo-Py/ α -CD and *trans* Azo-Py/ γ -CD complexes can be calculated by the equation S2.

$$\begin{cases} 14\% > f_{\text{AzoPy}} > 0\% \\ 78\% < f_{\text{AzoPy}/\alpha\text{CD}} < 89\% \\ 8\% < f_{\text{AzoPy}/\gamma\text{CD}} < 11\% \end{cases} \quad (\text{S6})$$

The fraction of *trans* Azo-Py/ α -CD complex is always much higher than the *trans* Azo-Py/ γ -CD complex in the mixture of *trans* Azo-Py, α -CD, and γ -CD. Therefore, the orthogonal supramolecular system could be formed.

Orthogonality between *trans* Azo-Py/ α -CD and *cis* ipAzo-Py/ γ -CD

For the mixture of *trans* Azo-Py, *cis* ipAzo-Py, α -CD, and γ -CD ($[trans \text{ Azo-Py}] = 1 \text{ M}$, $[trans \text{ Azo-Py}]:[cis \text{ ipAzo-Py}]:[\alpha\text{-CD}]:[\gamma\text{-CD}] = 1:1:1:1$). The equilibrium could be written as follow.



The equilibrium concentrations of the host-guest complexes could be calculated by the equation set,

$$\begin{cases} \frac{a}{(1-a-b)(1-a-c)} = K_a(trans \text{ Azo}/\alpha\text{CD}) \\ \frac{b}{(1-a-b)(1-b-d)} = K_a(trans \text{ Azo}/\gamma\text{CD}) \\ \frac{c}{(1-c-d)(1-a-c)} = K_a(cis \text{ ipAzo}/\alpha\text{CD}) \\ \frac{d}{(1-c-d)(1-b-d)} = K_a(cis \text{ ipAzo}/\gamma\text{CD}) \end{cases} \quad (S7)$$

where a is $[trans \text{ Azo}/\alpha\text{-CD}]$, b is $[trans \text{ Azo}/\gamma\text{-CD}]$, c is $[cis \text{ ipAzo}/\alpha\text{-CD}]$, and d is $[cis \text{ ipAzo}/\gamma\text{-CD}]$.

The calculated result is:

$$\begin{cases} [trans \text{ Azo}/\alpha\text{CD}] = 0.95 \text{ M} \\ [trans \text{ Azo}/\gamma\text{CD}] = 0.02 \text{ M} \\ [cis \text{ ipAzo}/\alpha\text{CD}] = 0.01 \text{ M} \\ [cis \text{ ipAzo}/\gamma\text{CD}] = 0.96 \text{ M} \end{cases} \quad (S8)$$

indicating the *trans* Azo/ α -CD and *cis* ipAzo/ γ -CD are orthogonal each other.

No interaction between pyridinium and CD

The possibility of the interaction between pyridinium and CD in this system could be excluded by 2D NOESY spectrum (**Figure S4.33**). No correlation signal between pyridinium part on Azo-Py or ipAzo-Py and α -CD or γ -CD could be found, indicating the interaction between pyridinium and CD is weak in this system.

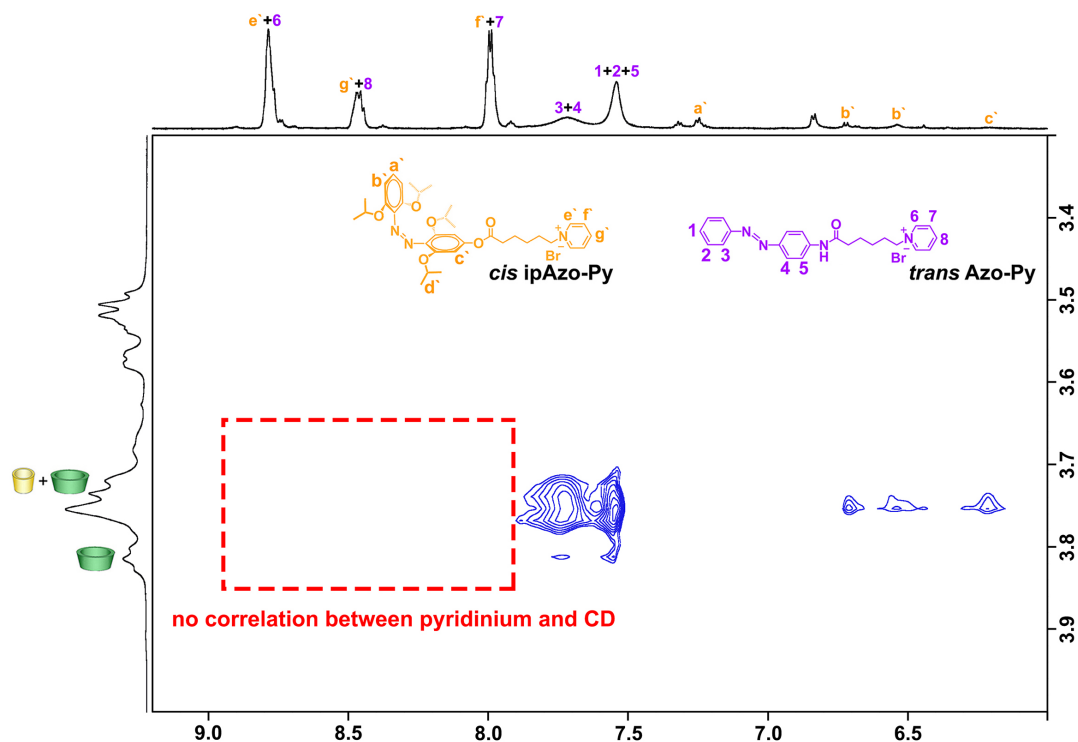


Figure S4.33 2D NOESY spectrum (700 MHz in D₂O at 298 K) of the photoresponsive orthogonal supramolecular system in “both closed” state ([Azo-Py]=2 mM, [Azo-Py]:[ipAzo-Py]:[α -CD]:[γ -CD]=1:1:1:1).

8. NMR of new Chemicals

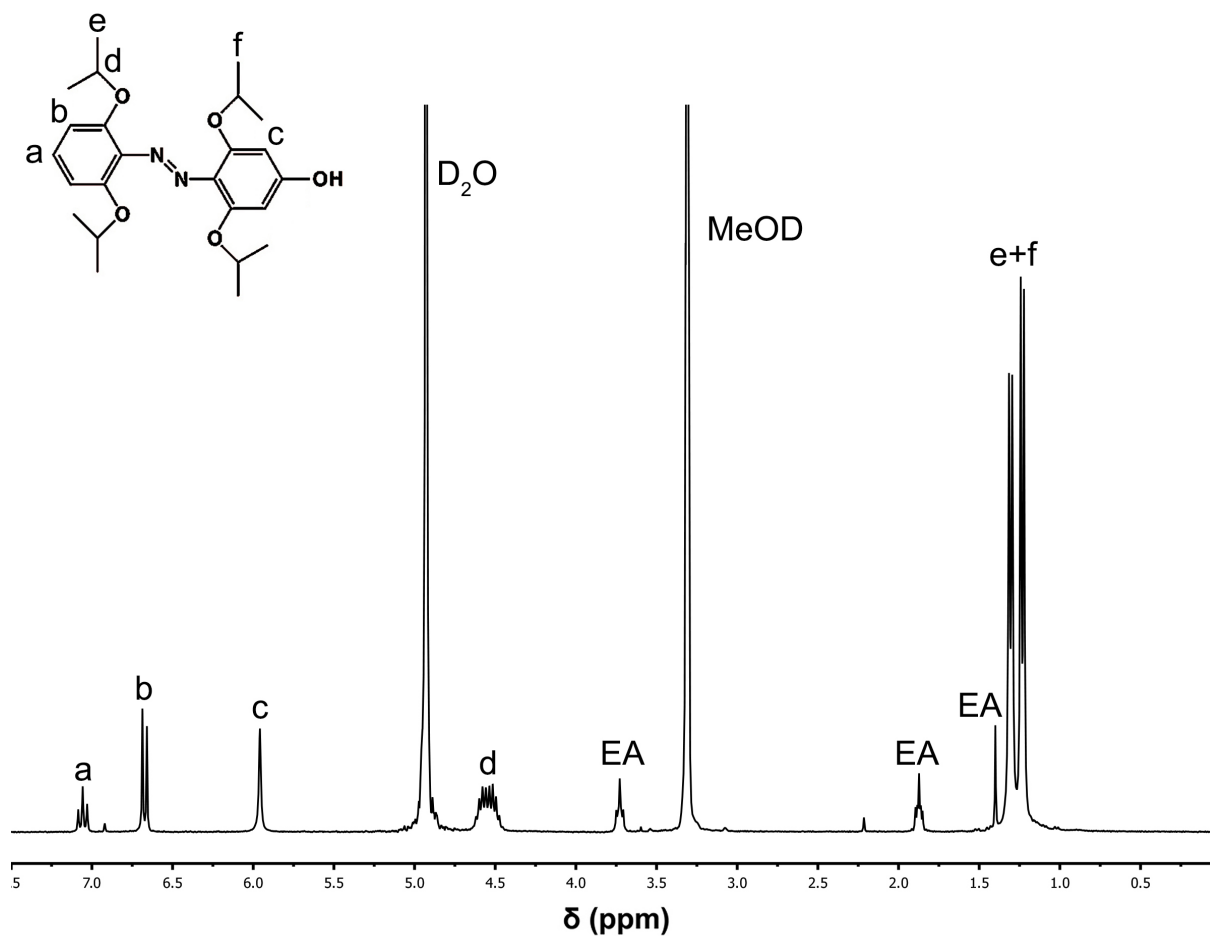


Figure S4.34 ^1H NMR spectrum of ipAzo-OH. (250 MHz, 298 K, MeOD, with ~5mg of NaOH)

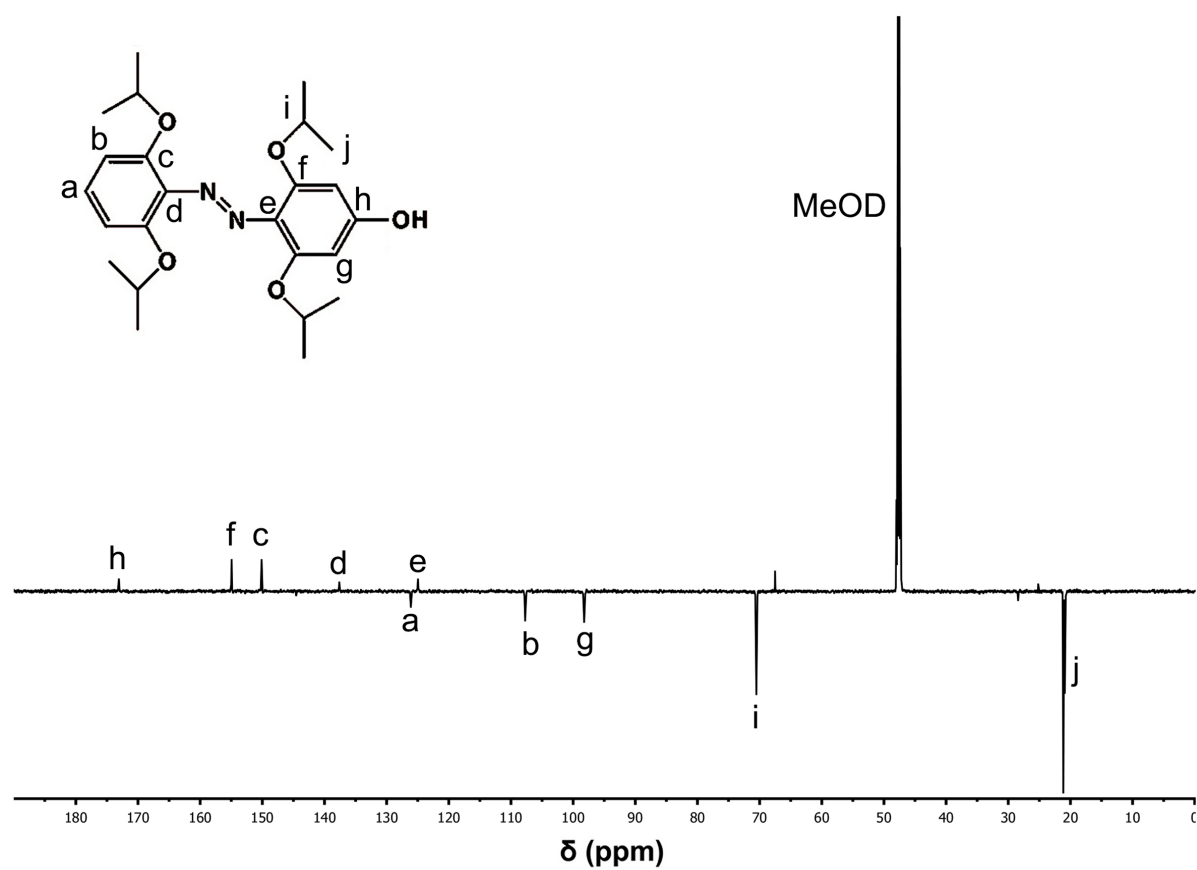


Figure S4.35 ^{13}C NMR of spectrum of ipAzo-OH. (176 MHz, 243 K, $\text{MeOD}-d_4$, with ~5mg of NaOH)

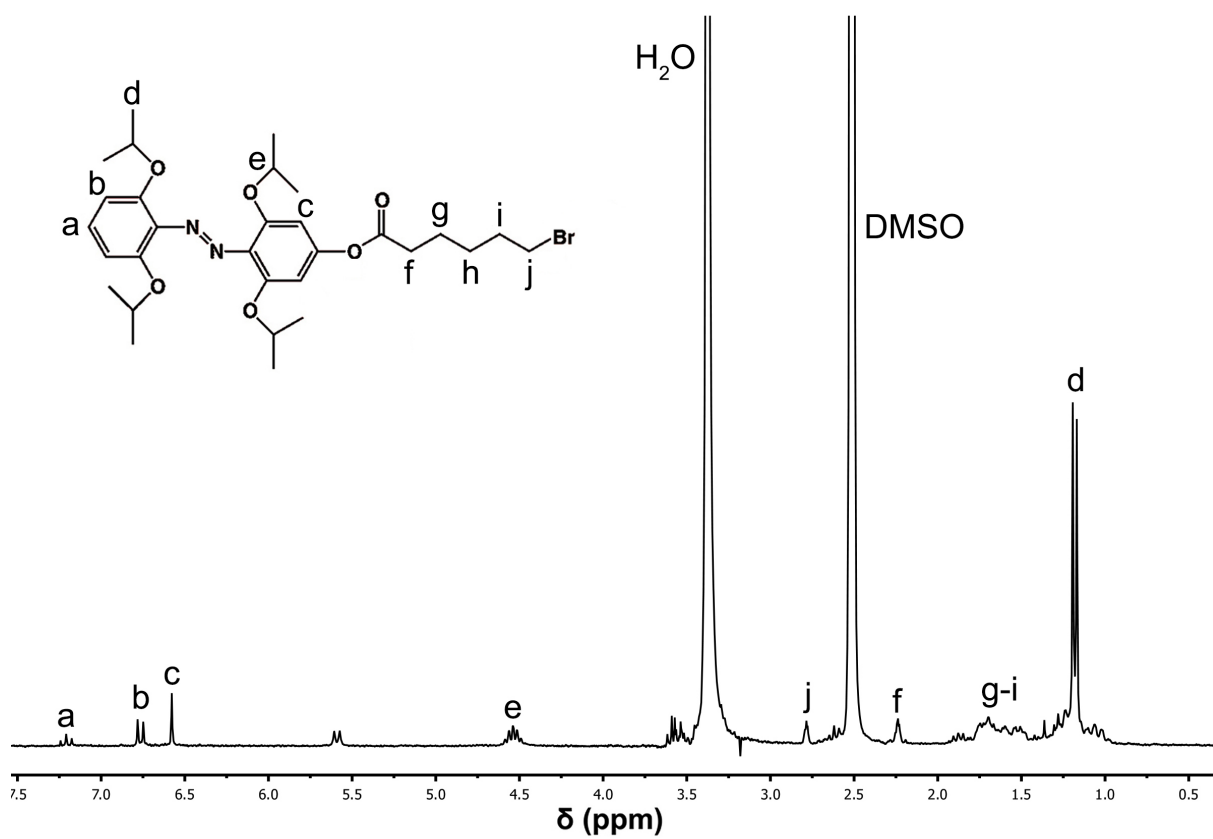


Figure S4.36 ^1H NMR spectrum of ipAzo-Br. (250 MHz, 298 K, $\text{DMSO}-d_6$)

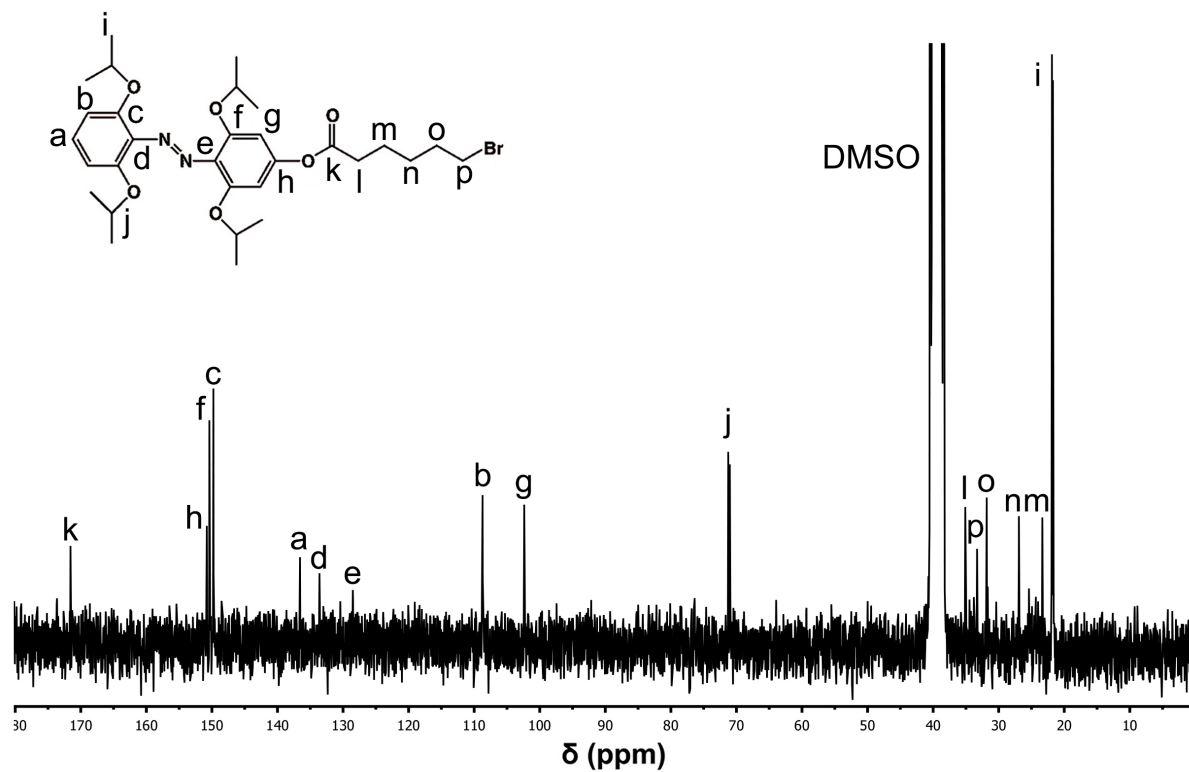


Figure S4.37 ^{13}C NMR spectrum of ipAzo-Br. (63 MHz, 298 K, $\text{DMSO-}d_6$)

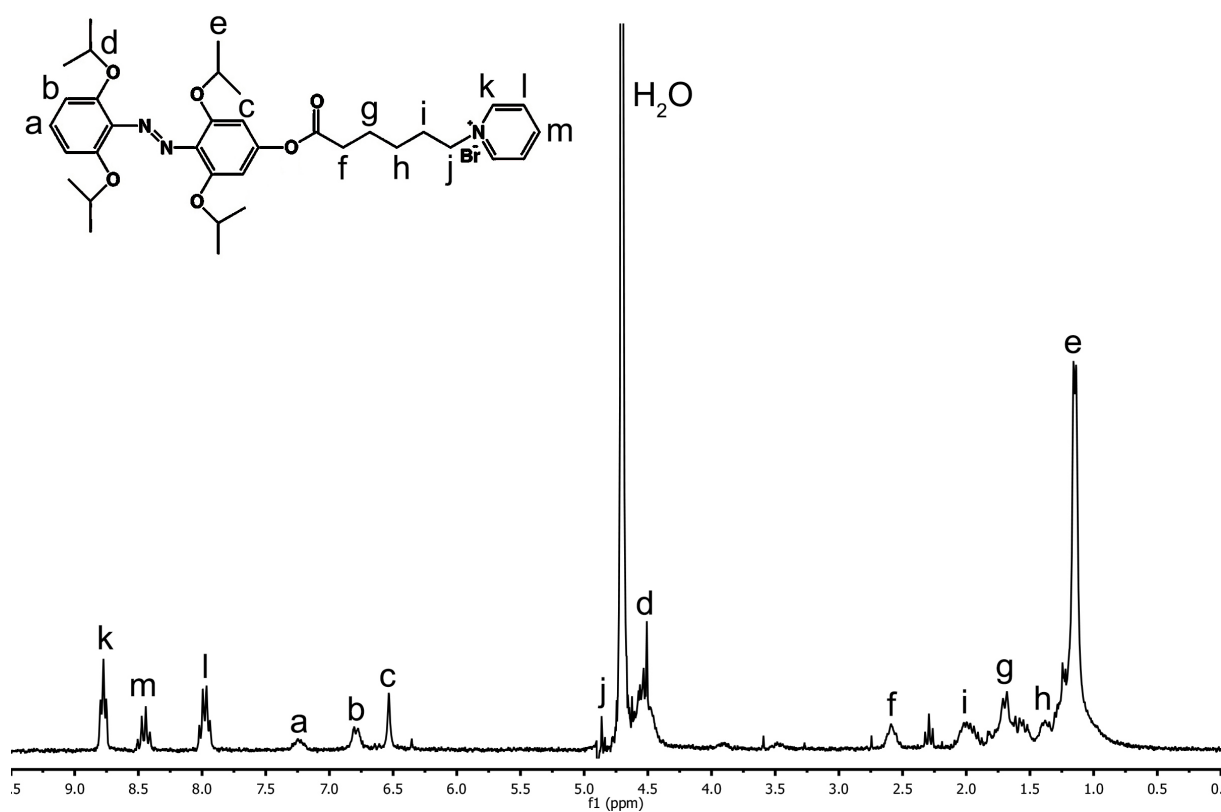


Figure S4.38 ^1H NMR spectrum of ipAzo-Py. The signal at $\delta=2.25$ may come from impurity. (250 MHz, 298 K, D_2O)

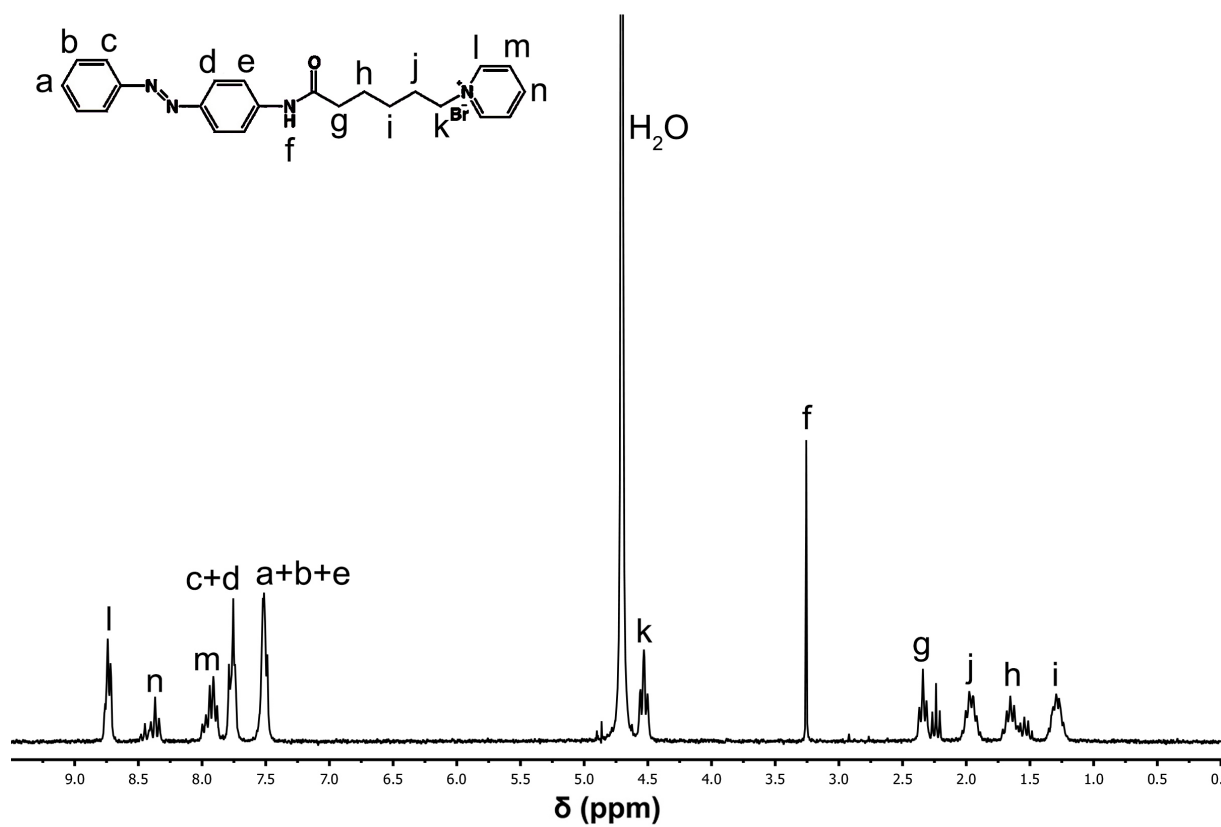


Figure S4.39 ^1H NMR spectrum of Azo-Py. The signal at $\delta=2.25$ may come from impurity. (250 MHz, 298 K, D_2O)

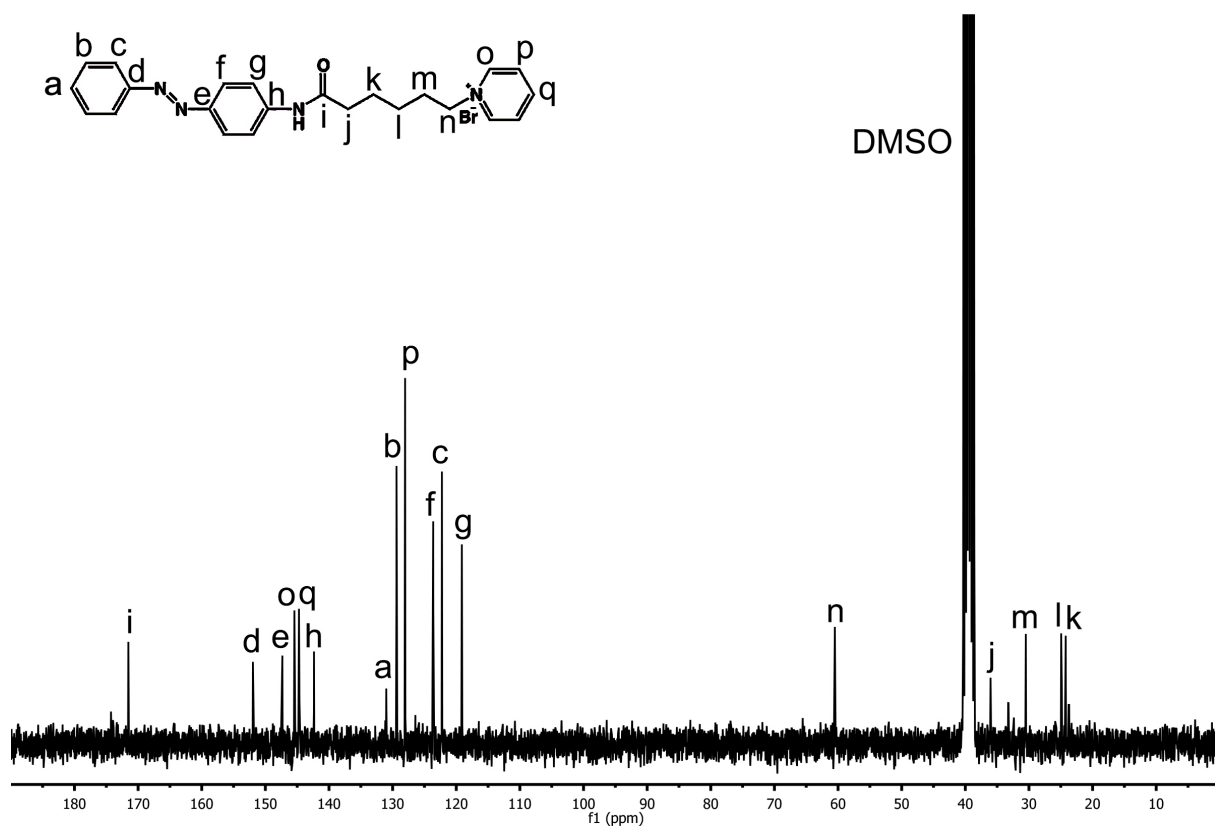


Figure S4.40 ^{13}C NMR spectrum of Azo-Py. (63 MHz, 298 K, $\text{DMSO}-d_6$)

9. Possible impurities

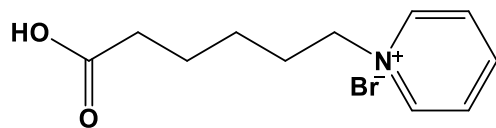


Figure S4.41 Chemical structure of the possible impurity in Azo-Py and ipAzo-Py. No correlation could be found between the impurity and CDs in 2D NOESY spectra. The impurity shows low host-guest interaction with CDs, and does not affect the host-guest interaction between Azo-Py or ipAzo-Py and α -CD or γ -CD [6].

References

1. Jayasundera, K. P.; Watson, A. J.; Taylor, C. M. *Tetrahedron. Lett.*, **2005**, *46*, 4311-4313.
2. Zhao, H.; Guo, D.; Liu, Y. *J. Phys. Chem. B*, **2013**, *117*, 1978-1987.
3. Wang, Y.; Ma, N.; Wang, Z.; Zhang, X. *Angew. Chem.*, **2007**, *119*, 2881-2884.
4. Zheng, X.; Wang, D.; Shuai, Z.; Zhang, X. *J. Phys. Chem. B*, **2012**, *116*, 823-832.
5. Tamesue, S.; Takashima, Y.; Yamaguchi, H.; Shinkai, S.; Harada, A. *Angew. Chem. Int. Ed.*, **2010**, *49*, 7461-7464.
6. Harada, A.; Takashima, Y.; Nakahata, M. *Acc. Chem. Res.*, **2014**, *47*, 2128-2140.

Chapter 5

Conclusion and Outlook

We successfully designed visible-light-responsive supramolecular host-guest systems between mAzo or ipAzo and CDs, and developed the applications in biomedicine and orthogonal photoswitching. Actually, compared with the normal UV-light-responsive Azo/CD host-guest complex, the visible-light-responsive host-guest systems are better suited to be applied in biomedical field, especially for the photoresponsive materials used in deep tissue. Besides the *in vivo* applications, the visible-light-responsive supramolecular systems can find applications in tissue engineering and cell culture. As a clean and cell friendly stimulus, visible light can precisely and efficiently control the cell growth, orientation, and shape by switching the supramolecular complexes.

However, visible-light-responsive supramolecular host-guest systems are not only playing on the stage of biomedicine. By combining the UV-light-responsive Azo/ α -CD and red-light-responsive ipAzo/ γ -CD host-guest complexes, we designed a photoresponsive orthogonal supramolecular system. Different with the traditional photoresponsive system, the orthogonal supramolecular system can be controlled by up to 4 different light and show up to 4 photostationary states, which is intelligent and multifunctional under complex external stimuli.

After winning the Nobel Prize of 2016, molecular machine is supposed to be the future of supramolecular systems. Under triggering of the specific external stimuli (input), the molecular machine can produce quasi-mechanical movements (output).

By applying the photoresponsive orthogonal supramolecular systems, it is possible to design composite molecular machines, which are responsive to different light and show various functions and movements. As the system grows, the molecular machines are required to be intelligent and multifunctional. Orthogonal switching is therefore an important point for the developing of intelligent molecular machines. We are looking forward of the fabricating of composite molecular machines or even molecular robots in the future by photoresponsive orthogonal supramolecular systems.

Acknowledgement

Curriculum vitae

Personal Information

Name: Dongsheng Wang

Date of Birth: 27.10.1988

Nationality: China

Sexual: Male

Education

Since 09.2013: PhD candidate in Max Planck Institute for Polymer Research, Germany

Major: Chemistry

Supervisor: Prof. Dr. Hans-Jürgen Butt

09.2010-06.2013: Master of Science in College of Polymer Science and Engineering, Sichuan University, China.

Major: Biomedical Engineering

Supervisor: Prof. Dr. Changsheng Zhao

09.2006-06.2010: Bachelor of Science in College of Polymer Science and Engineering, Sichuan University, China.

Major: Polymer Materials and Engineering

Supervisor: Prof. Dr. Changsheng Zhao

Publications

Dongsheng Wang, Manfred Wagner, Andrew K. Saydjari, Hans-Jürgen Butt and Si

Wu*, A photoresponsive orthogonal supramolecular complex based on host-guest interactions. *Chemistry-A European Journal*. **2017**, *23*, 2628-2634

Dongsheng Wang and Si Wu*, Red-Light-Responsive Supramolecular Valves for Photocontrolled Drug Release from Mesoporous Nanoparticles. *Langmuir*. **2016**, *32*, 632-636.

Dongsheng Wang, Manfred Wagner, Hans-Jürgen Butt and Si Wu*, Supramolecular Hydrogels Constructed by Red-Light-Responsive Host-guest Interactions for Photo-Controlled Protein Release in Deep Tissue. *Soft Matter*. **2015**, *11*, 7656-7662.

Ying Zhou, **Dongsheng Wang**, Shilin Huang, Guenter Auernhammer, Yujian He, Hans-Jürgen Butt and Si Wu*, Reversible Janus particle assembly via responsive host-guest interactions. *Chemical Communications*. **2015**, *51*, 2725-2727.

Philipp Weis, **Dongsheng Wang** and Si Wu*, Visible light responsive azopolymers with inhibited π - π stacking enable fully reversible photopatterning. *Macromolecules*. **2016**, *49*, 6368-6373.

Conferences

2016:

30th Conference of The European Colloid and Interface Society, Rome, Italy.

2015:

15th Conference of the International Association of Colloid and Interface Scientists, Mainz, Germany.

Affidavit

I hereby declare that I wrote the dissertation submitted without any unauthorized external assistance and used only sources acknowledged in the work. All textual passages which are appropriated verbatim or paraphrased from published and unpublished texts as well as all information obtained from oral sources are duly indicated and listed in accordance with bibliographical rules. In carrying out this research, I complied with the rules of standard scientific practice as formulated in the statutes of Johannes Gutenberg-University Mainz to insure standard scientific practice.

(Place, Date)

(Signature)